The Formation of Acetate Corrosion on Bronze Antiquities: Characterisation and Conservation

by
Alice Boccia Paterakis

A thesis presented to UCL in fulfillment of the requirements for the degree of Doctor of Philosophy

University College London
Institute of Archaeology

2010

I, Alice Boccia Paterakis, confirm that the work presented in this thesis is my own. Where information has been derived from other sources, I confirm that this has been indicated in the thesis.

Abstract

This project reveals the proliferation in the awareness of acetate and other carbonyl corrosion on bronze artifacts in archaeological collections. Blue and blue-green carbonyl corrosion of bronze is a recent discovery in part due to its mistaken attribution over the years to bronze disease, chalconatronite, and azurite.

This project examines sources of acetic acid, and evaluates the environmental conditions in which acetate corrosion develops and the influence of alloyed lead and sodium contaminants in this process. Case studies identifying corrosion by XRD on predominantly Egyptian archaeological bronzes, with a focus on Saqqara, revealed a preponderance of a sodium copper carbonate acetate and copper sodium formate acetate. These were identified on the majority of Saqqara bronzes sampled in the Fitzwilliam Museum, Ashmolean Museum, Liverpool Museum, Petrie Museum and British Museum. Unknown compounds not included in the International Centre for Diffraction Data (ICDD) catalogue were also discovered.

Due to the novelty of this discovery, the conservation of bronze with carbonyl corrosion is as yet an unexplored area. This project examines passive and active means of conservation. Solubility and cleaning tests were carried out on the Saqqara bronzes. Solubility of carbonyl corrosion is discussed in terms of removability, influence on cleaning methods, and stabilization of corrosion by means of environmental control. Two coatings, the acrylate Incralac®, and the polyethylene wax emulsion Poligen® ES 91009, underwent corrosion testing on leaded and unleaded bronze with promising results as protective coatings against attack by volatile acetic acid.

Table of Contents

List of Tables

List of Figures

Acknowledgements

I wish to thank the Getty Conservation Institute, specifically Giacomo Chiari, Cecily Grzywacz, Joy Mazurek, David Carson, Karen Trentelman, Eric Doehne, Jim Druzik, and Michael Schilling for their generous assistance with the analytical work in this project. I also wish to thank David Scott and Karen Trentelman for their support and guidance in this research, Lorraine Gibson and David Thickett for their helpful responses to my queries, my supervisors John Merkel, Dafydd Griffith, and Cliff Price. I appreciate the assistance of Ashley Cooke, Helen Whitehouse, and Karen Loven. Dr. Emilio Cano and Diana LaFuente of the Centro Nacional de Investigaciones Metalúrgicas (CENIM), CSIC, Madrid, Spain, provided indispensable assistance with part of the analytical work for which I am very grateful. I wish to acknowledge the Samuel H. Kress Foundation for a Travel Fellowship in the History of Art awarded in 2006-2007 and UCL for a Graduate School Research Fund Grant awarded in 2007. My friends Susi Pancaldo and Michael Turoff greatly facilitated my success in completing this degree for which I am very grateful. Finally, I wish to express my appreciation for all the encouragement I have received from Hillary Kapan, Edward and Madeleine Boccia, and Jennifer Pateraki.

Chapter 1 Introduction

This project focuses on the corrosion of copper-tin and copper-tin-lead alloys, materials widely used for the ancient manufacture of metal objects throughout Europe and the Mediterranean world starting from the Bronze Age. Wood and other organic materials, commonly used for the storage and display of bronze antiquities, are known to emit acetic acid, formic acid, and other organic vapours, commonly referred to as carbonyl compounds (Cruz *et al.* 2008; Dubus and Laurent 2009; Gibson and Watt 2010; Giorgi *et al.* 2009; Hodgkins 2008). The acid readily attacks the surface of bronze causing it to corrode forming acetates and other compounds of blue, blue-green, and sometimes white colors. Other sources of acetic acid include conservation and patination chemicals, wood from original manufacture (e.g. wooden statue bases of bronze statues) or associated burial context. The first cases of acetate corrosion on artistic and functional bronze objects were confirmed by XRD in museum collections in Europe in the 1990s. Bronze objects from all periods and provenances are susceptible to this form of deterioration. Ancient bronze alloys of copper-tin and copper-tin-lead present more complex corrosion phenomena. Archaeological pieces seem especially sensitive to attack (Thickett and Odlyha 2000; Thicket 2008).

Acetate compounds form a corrosion layer on the surface of the objects disfiguring the artifacts, obscuring important information, decreasing the aesthetic quality of the metals, and subjecting the objects to further physical and chemical deterioration. The depth of corrosion penetration into the object may depend on various factors, two of which are the composition and method of manufacture. The identity and concentration of alloyed elements will influence the susceptibility of the bronze to corrosion. Until the 1990s and the discovery of acetate on bronze, this blue and blue-green corrosion on copper alloys had been commonly identified as azurite (copper carbonate), chalconatronite (sodium copper carbonate) and the very common corrosion product copper chloride, often called “bronze disease”, upon examination with the naked eye. White corrosion has often been identified as tin oxide and benzotriazole. None of these compounds derive from exposure to volatile acetic acid and, consequently, the conservation measures necessary to address the challenges of acetate corrosion have not been identified. They are both new and specific to acetate corrosion. Since the causes of acetate corrosion on metal are completely different from those giving rise to the previously named corrosion products, the correct identification of corrosion is of the

utmost importance. An understanding of the true nature of the corrosion products and the causes of formation is absolutely critical for the prevention of ongoing deterioration and for the protection of bronze collections.

The research presented in this thesis is unique as it examines the corrosion behavior of bronze exposed to acetic acid emissions in museum and archaeological collections. A literature survey revealed numerous studies for acetates and formates on pure copper and copper-zinc. These metal compounds have undergone corrosion testing with acetic acid mostly for industrial purposes largely neglecting ancient, corroded bronze that makes up a considerable portion of our cultural heritage. Only two projects addressed the corrosive influence of acetic acid on modern bronze with a focus on the protective qualities of a copper sulphide patina (Bastidas *et al.* 1995, López-Delgado *et al.* 1997). This project presents original research in the study of acetic acid corrosion on leaded and unleaded bronze and fills a void in our knowledge of the behavior of copper alloys.

Based on the findings presented in this thesis, the likelihood of the extensive occurrence of acetate corrosion on copper alloy collections throughout the world is great since the majority of collections are stored in wood boxes, trays, and cabinets in uncontrolled climatic conditions and a high percentage of objects have undergone chemical treatments. Now that the causes are known, such damage to bronze cultural objects in storage and display can be significantly decreased or prevented if acetic acid vapours are excluded.

Aims of the Project

The driving force of this doctoral thesis is the protection of collections and the cultural heritage. The means I have chosen to promote the protection and sustainability of our cultural heritage are innovative research, scientific experimentation, and the identification of suitable storage environments.

Research Questions:

1. How and why does acetate corrosion form on bronzes in museums and archaeological collections?

2. What compounds form in addition to acetates on ancient bronzes?
3. What are the factors that contribute to acetate corrosion on bronzes in museums and archaeological collections?
4. How can the formation of acetate corrosion on bronzes be prevented?
5. What are the most suitable conservation treatments for bronzes contaminated with acetate corrosion?
6. Do acetate compounds tend to form on ancient bronzes from certain parts of the world, such as Greece and Egypt?

Research Objectives:

1. Provide an understanding of the process of acetate formation on bronze
2. Identify the contributing factors so that they may be regulated to control and prevent corrosion
3. Determine the influence of alloy elements in the corrosion process
4. Determine the influence of relative humidity on acetate corrosion
5. Determine the influence of acid vapour levels on corrosion
6. Determine the influence of patina (pre-existing corrosion) on corrosion
7. Determine the influence of conservation materials and treatments on corrosion
8. Provide guidelines for conservators and curators for the treatment of contaminated objects and for prevention of corrosion
9. Compile a database of acetate corrosion products (with conservation treatments and storage history) that other researchers, conservators, abd conservation scientists may refer to and build upon as a tool for the identification of carbonyl corrosion in collections.

The Structure of this Thesis

The research methods by which I have answered these questions and attained these objectives can be presented as a sequence of steps and chapters. Chapter 2 presents the groundwork for the thesis by discussing the carboxylic acids and focusing on acetic acid and formic acid. After examining the sources of acetic acid an historical survey of occurrences of acetate corrosion on museum objects is included. The published case studies are presented in chronological sequence of discovery of materials affected in museum collections. This sequence begins with shell and calcareous materials eventually

moving to the metals. The metal objects are covered in more detail with emphasis on bronze and lead. These are listed by museum as a catalogue. Concentrations of acetic and formic acid vapour in museum cases are reported where available. These figures are used for comparison with the published acceptable levels of volatile carbonyl compounds in Chapter 7.

In the third chapter, Corrosion and Corrosion Testing in Archaeological Conservation, a comprehensive literature survey of all published studies on the scientific testing and experimentation of the effects of acetic acid on metal is presented. Since my literature survey revealed limited testing of bronze exposed to volatile acetic acid, it was necessary to study the corrosion tests of other researchers on the individual components, copper, tin and lead. It is vital to examine the reaction of the copper and its alloy components with acetic acid in order to understand the corrosion behavior of ancient bronze compositions. This gap in the testing of bronze is the reason for the experimental program in Chapter 4. The results of corrosion testing carried out by other researchers on copper and its alloy components form a basis for interpretation of my test results in Chapter 4.

In Chapter 4, Experimental Methods for Corrosion Testing, testing and experimentation were designed to address the various questions I am posing. One aim of the experimental work is to provide conservators, for the first time, with a clear understanding of the chemical origin of the corrosion products on susceptible copper alloys held in contaminated environments. Moreover, a rigorous experimental design has been implemented to identify better the factors that initiate, or exacerbate, corrosion so that advice can be given to museum personnel in order to prevent degradation of similar artifacts in their collections. This experimentation consisted of establishing controlled environments in which new bronze standards and ancient, archaeological bronze artifacts were assessed.

My extensive involvement with archaeological bronze collections as Head of Conservation for the Agora Excavation, American School of Classical Studies in Athens, Greece, indicated that several factors may be involved in the formation of acetate corrosion on bronze. Since the influence of conservation materials on the corrosion of bronze by acetic acid has not been tested, this has been included as an experimental

variable in my project. A conservation material that has been used for the stabilization of bronze for decades, sodium sesquicarbonate, was selected for testing.

In summary, the five experimental variables of most relevance to my project are copper alloy composition, relative humidity, acetic acid vapour concentration, patina (pre-existing corrosion), and past conservation materials. These variables have been tested with the aim of determining acceptable exposure levels to relative humidity and acetic acid vapour concentration, as well as the effects of alloy composition, patina and conservation treatments on corrosion. The bronzes that I am studying are predominantly of alloy mixtures: copper-tin and copper-tin-lead.

My experimental work in Chapter 4 consisted of two test series, I and II. Test Series I comprised corrosion testing on modern and ancient, archaeological bronze and Test Series II involved exposing bronze corrosion products (removed from the objects) and a conservation chemical to accelerated corrosive conditions.

Test Series I consisted of two parts. In Part One I carried out in-house testing in microenvironments using Tedlar® bags at the Getty Conservation Institute during my 9-month fellowship as Conservation Guest Scholar. Part Two was carried out in a certified laboratory in Madrid for the purpose of confirming my results from Part One. By the time I was in a position to carry out Part Two I was no longer associated with the Getty Conservation Institute in an official capacity, therefore I was not authorized to use acetic acid in their laboratory. For this reason I was obliged to find another testing facility. I developed my experimental design for Part Two based on my own experiments in Part One. My experimental design proved interesting to Dr. Emilio Cano of the Centro Nacional de Investigaciones Metalúrgicas (CENIM), CSIC, in Madrid, Spain, as Dr. Cano had carried out similar corrosion testing of metals exposed to carbonyl acids. Part two testing was carried out in an environmental chamber in the laboratory in Madrid following ASTM testing procedures. Part Two tested the procedure using microclimates in the Getty Conservation Institute in Part One that I substituted for standard testing procedures. I carried out all corrosion tests, analysed the corrosion by X-ray Diffraction at the Getty Conservation Institute and at the University of California at Los Angeles (UCLA), and compiled all the results in Part One. Dr. Cano carried out the corrosion tests, identified the corrosion by XRD analysis, and compiled the results in Part Two as indicated in Chapter 4.

Test series II of my experimental work in Chapter 4 consisted of exposing two corrosion products commonly found on archaeological bronze, malachite and chalconatronite, and the conservation chemical sodium sesquicarbonate, to high levels of acetic acid and relative humidity. The goal of this test series was to recreate the formation of the carbonyl compounds identified on bronzes in Chapters 4 and 5 of this study thereby simulating the corrosion processes that occur on the objects in wooden storage cabinets. This was accomplished by subjecting the copper corrosion products, sodium sesquicarbonate, and a mixture of these to the accelerated corrosive conditions.

Another component of my thesis consists of case studies involving the identification of acetate corrosion on bronzes in several museum collections in Chapter 5. Objects were selected on the basis of the tentative detection or suspicion of acetates on bronze that warranted further study and confirmation. Suspect corrosion was targeted on bronze objects from Saqqara, Egypt, that were excavated from 1964 to 1976 and distributed among several museum collections in the UK. I selected Saqqara bronzes from several museum collections including the Petrie Museum, the Ashmolean Museum, the British Museum, the Liverpool Museum and the Fitzwilliam Museum, that comprised 52% of the total number of objects in my case studies. The remaining 48% of objects selected in the case studies were predominantly Egyptian from other sites. The history of the objects was researched in terms of provenance, date of excavation, alloy composition, past conservation treatments, construction materials used in storage or display cases, concentration of acetic acid vapour exposure and climatic conditions. Suspect corrosion was sampled and analysed by X-ray Diffraction at the Getty Conservation Institute and at the University of California at Los Angeles (UCLA) by the author.

Previous research at the British Museum indicated a substantial presence of carbonyl corrosion compounds on the Egyptian bronze collection. My results from the Saqqara bronzes bolstered the existing analytical evidence regarding this corrosion problem in the British Museum and prompted the Conservation Department and Conservation Science staff at the British Museum to carry out further analysis of the Saqqara bronzes (Wang *et al.* 2009). One of the objects I tested was selected for analysis by the British Museum (Wang *et al.* 2009). The British Museum Saqqara bronze analytical project served to confirm my analytical results presented in Chapter 5.

I intend to contribute the diffraction patterns from my XRD results to an international database of case studies of bronze objects with carabonyl corrosion and to include pertinent information including conservation treatment and storage history where available. Researchers, conservation scientists, conservators, and curators may utilize this database as a diagnostic tool for identification of mixed corrosion products and may contribute information from their collections. The dissemination of the results of this project through publication and the internet is of the utmost importance to provide those curators and conservators responsible for the preservation of bronze collections around the world with detailed information of this widespread corrosion phenomenon and means of mitigation and prevention.

Chapter 6, Protective Coatings, presents the initial results on the use of protective coatings for bronze against the corrosive effects of acetic acid vapour. With the relatively recent discovery of acetate corrosion on bronze it is vital to determine and possibly recommend suitable conservation coatings that may provide protection. This can only be accomplished through testing under controlled, measured conditions. I have carried out a corrosion test of two coatings: an acrylate solution (Incralac®); a polyethylene emulsion (Poligen® ES 91009). Incralac® has been used successfully for decades as a coating for bronze that continues in use today and for this reason it is important to determine its suitability as a protection against acetic acid attack. Poligen® was recently introduced as a coating with potential application for the conservation of metals (Siatou *et al.* 2007). Based on the promising results obtained with Poligen® in corrosion tests on copper, brass, and steel, and considering the hydrophobic properties of this coating, I decided to test Poligen® on bronze (Cano *et al.* 2007; Cano *et al.* 2010). The experimental variables were purposely selected to replicate those in Chapter 4 to facilitate quantitative comparison between coated and uncoated bronze: copper alloy compositions, relative humidity, acetic acid concentration, and duration of corrosion test. Both coatings performed admirably during the 8-week accelerated corrosion test preventing corrosion of the underlying metal. Recommendations are made for the further testing and characterization of Poligen® ES 91009 prior to its adoption as a conservation material.

Chapter 7 provides recommendations for the prevention and treatment of corrosion by acetic acid. Preventive conservation to combat the corrosive influence of acetic acid on bronze artifacts in storage or display begins with (1) monitoring volatile acetic acid concentrations and determining the sources of carbonyl emissions, followed

by (2) selecting suitable materials for storage and display to eliminate carbonyl emissions and/or (3) controlling levels of relative humidity and oxygen and/or (4) applying protective coatings to bronze artifacts. Conservation treatment measures include various approaches to cleaning. To date only one published study exists that includes active conservation measures for ancient bronze corroded by acetic acid (Wang *et al.* 2009). By carrying out solubility and cleaning tests on bronze with acetate corrosion I have addressed this gap in our knowledge. The conservation treatments considered in this study are based on the identification and solubility characteristics of the corrosion. After identification of the corrosion was carried out by XRD, solubility testing was performed with four solvents. Mechanical (dry), chemical (wet), and a combination of the two cleaning methods were tested on bronzes from the case studies in the Petrie Museum (Chapter 5).

Chapter 2 Organic Acids and Metal Corrosion

2.1 Carboxylic Acids

The organic acids of interest in this study are carbonyl compounds. The carbonyl compounds are simple organic (carboxylic) acids and aldehydes that contain the carbonyl group >C=O. The carbonyl compounds consist of acetic (ethanoic) acid, formic (methanoic) acid, acetaldehyde (ethanal) and formaldehyde (methanal). "All four organic carbonyl pollutants are primary pollutants off-gassed from a source. In addition, acetic acid and formic acid can be secondary pollutants formed from the oxidation of acetaldehyde and formaldehyde, respectively." (Grzywacz 2006, 3). Aldehydes are oxidized to carboxylic acids through hydrates in aqueous media. Aldehydes can also form carboxylic acids in the gas phase through photochemical or radically induced oxidation. Of the aldehydes formaldehyde is the most readily oxidized (Raychaudhuri and Brimblecombe 2000, 226).

Carboxylic acids are organic compounds characterized by one or more carboxyl groups (-COOH) (Figure 2.1) (Eagleson 1994, 180).

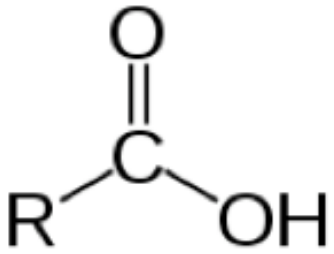

Figure 2.1 Structure of carboxylic acid (Considine 1984, 174)

The carboxyl group "is composed of a carbonyl group [C=O] and a hydroxyl group [-OH] bonded to a carbon atom." (Hawley 2001, 213). The number of carboxyl groups determines the classification: e.g. one carboxyl group is a monocarboxylic acid (Considine 1984, 174). They may be further classified according to the number of hydrogen atoms available for reaction. A carboxylic acid with one available hydrogen is monobasic (Considine 1984, 175). Carboxyl groups are prone to acidity based on their tendency to give up a hydrogen atom as an H+ ion (proton) forming carboxylic acid. The carboxyl group "…usually occupies the terminal position in the molecule and is capable

of assuming a negative charge, which makes the end of the molecule water soluble." (Hawley 2001, 212). Carboxylic acids often exist as dimeric pairs especially in the vapour phase at high temperatures (Figure 2.2).

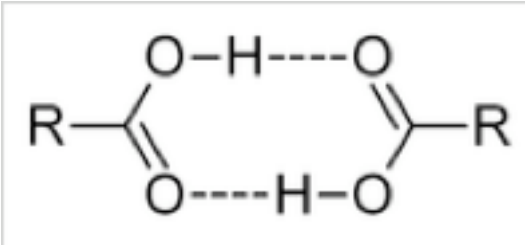

Figure 2.2 Carboxylic acid dimer (dashed lines represent hydrogen bonds) (Kirk-Othmer 2004, vol. 5, 38)

Carboxylic acids partially dissociate into H+ cations and RCOO- anions in aqueous solution forming weak acids (Eq. 1) (Kirk-Othmer 2004, vol. 1, 119).

Eq. 1 $RCOOH \leftrightarrow RCOO^- + H^+$

Those with fewer carbon atoms, e.g. acetic and formic acid, are miscible with water.

The carboxylate anion, RCO_2^-, forms "by the loss of a proton from the hydroxyl group of a carboxylic acid." (Orchin 2005, 168). Carboxylic acids react with bases (e.g. NaOH) and alkaline substances such as hydroxides, oxides, and carbonates of a strongly electropositive metal (e.g. Ca) forming a salt (Eq. 2) (Eagleson 1994, 180; Kirk-Othmer 2004, vol. 5, 40,41). Another way to express this is "alkali metal salts of carboxylic acids are readily obtained by neutralization." (Ullmann 2003, vol. 6, 494). Most of these salts are water-soluble.

Eq. 2 $RCOOH + MOH \rightarrow RCOO^- + M^+ + H_2O$

Formic acid (HCOOH) is the first member (1 carbon atom) of the carboxylic acid series and acetic acid (CH_3COOH) is the second member (2 carbon atoms) of the carboxylic acid series (Orchin 2005, 166,167).

2.2 Acetic and Formic Acid

Acetic acid, CH_3COOH, is also called ethanoic acid (Buckingham 1985, 2). It is classified as a weak, monobasic acid (Considine 1984, 3). Formic acid, HCOOH, is also called methanoic acid. Formic acid is present in the venomous stings of nettles, caterpillars, and ants. Both are monocarboxylic acids. Glacial acetic acid contains approximately 99.7% acetic acid with a water impurity (Considine 1984, 3). Acetic acid is polar, hygroscopic, and absorbs moisture from the atmosphere (Considine 1984, 3).

Acetic acid is monobasic because only one hydrogen atom can be involved in reactions (right side of compound structure). The three hydrogen atoms on the left side of the compound cannot be replaced by metals (Figure 2.3) (Considine 1984, 3).

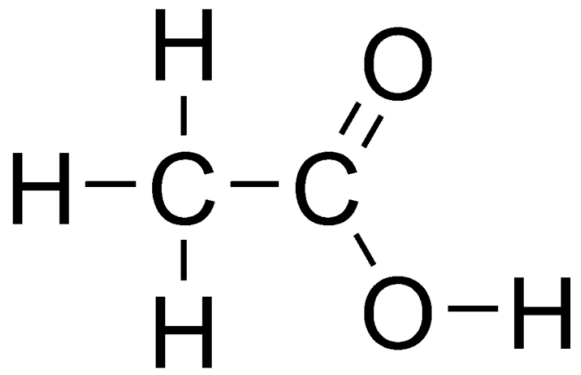

Figure 2.3 Structure of acetic acid (http://chemistry.about.com)

Formic acid is monobasic because only the hydrogen atom on the right side of the compound can be involved in reactions (Figure 2.4).

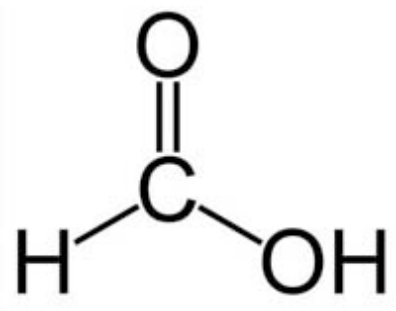

Figure 2.4 Structure of formic acid (http://course1.winona.edu/sberg/ChemStructures/Formic.gif)

The molecules of acetic and formic acid are linked into infinite chains by hydrogen bonds (Holtzberg 1953, 127; Jones and Templeton 1958, 484) (Figure 2.5). The molecular chains of formic acid can take two forms in the solid state, the α-type chain and the β-type chain (Ullman 2003, vol. 15, 50). Jones (1958, 484) and Holtzberg (1953, 130) suggest that bonding between chains in both acids is due to van der Waals forces, i.e. relatively weak molecular forces.

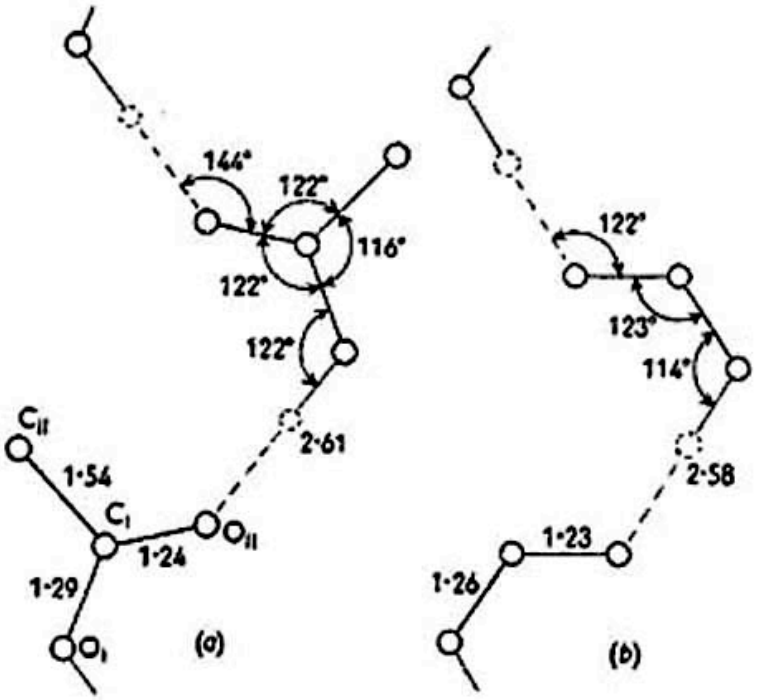

Figure 2.5 Molecular chain of acetic acid (a) and formic acid (b), bond lengths are in Angströms (from Jones 1958, 487)

The crystal structure of acetic and formic acid consists of an orthorhombic unit cell (Figure 2.6) (Holtzberg 1953, 127; Jones 1958, 484).

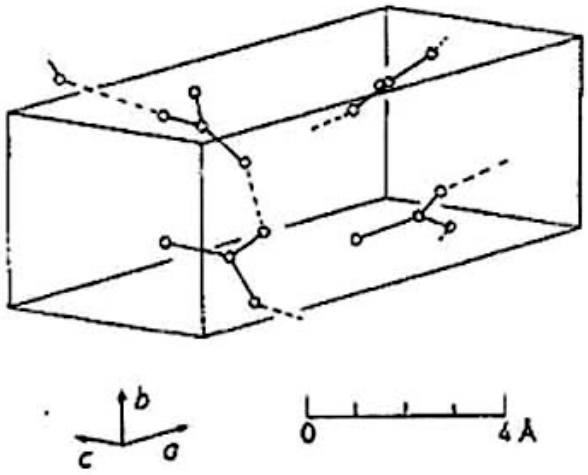

Figure 2.6 Crystal structure of acetic acid, dashed lines represent hydrogen bonds between oxygen atoms (Jones 1958, 486)

Acetic and formic acid consist of molecular chains made up of monomers and pairs of molecules, or dimers, connected by hydrogen bonds in the vapour and liquid phase (Figure 2.2) (Kirk-Othmer vol.1, 115). In the gas phase acetic acid exists for the most part in equilibrium between monomer and dimer and undergoes hydrolysis (Figure 2.7) (Ullmann 2003, vol. 1, 151).

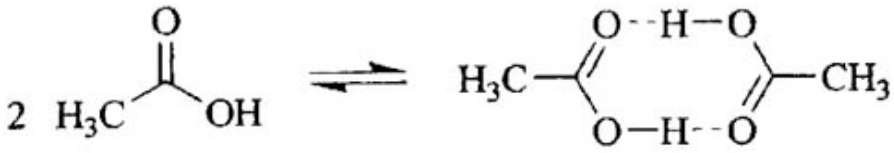

Figure 2.7 Monomeric (left) and dimeric (right) acetic acid (from Ullmann 2003, vol. 1, 151)

Acetic acid equilibrates between monomer and dehydrated dimer in solution (Ullmann 2003, vol. 1, 151). The equilibrium shifts to the right with increasing concentration of acid (favoring dimeric acetic acid) and to the left with increasing temperature (favoring monomeric acetic acid) (Ullmann 2003, vol. 1, 151).

When combined with water acetic acid forms a weak acid (CRC 1998, 8-46). Acetate can result from the reaction of hydrogen and carbon monoxide with acetic acid (Ullmann 2003, vol. 1, 169).

Acetates are “salts and esters of acetic acid with the general formula CH_3–$COOM^1$ or CH_3–COOR. M^1 symbolizes an ammonium residue or a monovalent metal, and R an aliphatic, aromatic or heterocyclic residue.” (Eagleson 1994, 4). Solutions of acetic acid form acetates by reaction with alkalis, oxides, hydroxides, carbonates and electropositive metals (Considine 1984, 3). “Acetic acid neutralizes the hydroxides of the alkali metals and the alkaline earths to form the corresponding acetates.” (Kirk-Othmer 2004, vol. 1, 119). Neutral and basic acetates are formed with multivalent metals (e.g. copper) (Eagleson 1994, 4). Neutral acetates are water-soluble, basic acetates are water-insoluble (Considine 1984, 3). Three neutral and five basic copper acetates (e.g. verdigris) have been indicated by Fourier Transform Infrared Analysis (FTIR) (Scott 2002, 271, 272).

When combined with water formic acid forms a weak acid (Ullmann 2003, vol. 15, 49). “Formic acid reacts differently from its higher homologues because it is both a carboxylic acid and an aldehyde.” (Ullmann 2003, vol. 15, 51). The decomposition of formic acid takes the form of dehydration (decomposes into CO and H_2O) or dehydrogenation (decomposes into CO_2 and H). Catalysts, temperature and concentration of the formic acid influence the nature and rate of this decomposition (Ullmann 2003, vol. 15, 52). Dehydrogenation is catalyzed by metals such as copper. Dehydration is promoted by mineral acids but inhibited by water (Ullmann 2003, vol. 15, 52).

Formate is a “salt or ester of formic acid; the general formula is H-$COOM^1$ or H-COOR, where M^1 is an ammonium ion or a monovalent metal cation, and R is an aliphatic, aromatic or heterocyclic group.”(Eagleson 1994, 424). Solutions of formic acid react with metal hydroxides, oxides and carbonates to form formates ($HCOO^-$) (Considine 1984, 404). Copper (II) hydroxide, copper (II) oxide, and copper (II) carbonate react with formic acid to form copper (II) formate (Ullmann 2003, vol. 15, 67).

2.3 Volatility of Acetic and Formic Acid

In this study the corrosive influence of carboxylic acids on bronze is examined in the dissolved and gaseous state and therefore it is important to examine the physical properties of these acids in the liquid and vapour state. Volatility is the tendency of a substance to vaporize which depends on vapour pressure. The higher the vapour pressure of a substance the more readily it will vaporize. Solvents are typically characterized

according to degree of volatility and may be divided into low-, medium-, and high-volatility groups (Horie 2003, 58). Vapour pressure may be thought of as "the driving force behind the … tendency for liquids and solids to disperse into the gaseous phase." (Considine 1984, 962). Vapour pressure is used to describe the tendency of a liquid to evaporate. The higher the vapour pressure of a liquid at a given temperature, the higher the volatility and the lower the normal boiling point of the liquid (Considine 1984, 963). There is a fundamental relationship between temperature and vapour pressure (Considine 1984, 963). The boiling point is defined as the temperature at which the vapour pressure of a liquid equals the atmospheric pressure (Redmore 1979, 275). Vapour pressure can be expressed in these units of measurement: mmHg, atmospheres, psi (lb/in^2), and kPa (kPa x 0.145 = psi) (Kirk-Othmer 2004, vol. 1, 116).

Heat of vaporization is the amount of heat needed to change the state from liquid to gas at the normal boiling point (Redmore 1979, 276). It is defined as "the enthalpy change (heat absorbed [ΔH or $kJ.mol^{-1}$]) when one mole (molar heat of vaporization) or one gram (specific heat of vaporization) of a substance is converted from the liquid to the vapour phase at a specified pressure (usually one atm.) and a specified temperature (usually the boiling point of the substance)." (Orchin 2005, 460). The heat of vaporization ΔH_v of acetic acid is 23.7 and of formic acid is 22.7 (at their respective boiling points) (Table 2.1) (Lange 2005, 2.561, 2.576).

Table 2.1 Vapour Pressure and Heat of Vaporization of Carboxylic Acids compared to Common Solvents

Organic compound	Vapour pressure (kPa) $_{at}$ 25° C	Vapour pressure mmHg	ΔH_v at respective boiling points
Acetic acid	2.07	11.25	23.36
Formic acid	3.74	34.5	20.10
Acetone	30.8	231	30.99
Ethanol	7.87	59.03	42.32
Water	3.169	23.77	43.99

(from CRC 1998-1999, 6-3, 6-8, 6-66, 6-104, 6-105, 15-14, 15-16)

It can be seen from the values in Table 2.1 that formic acid is slightly more volatile than acetic acid and has a lower ΔH_v. The volatility of the carboxylic acids, their versatility to react with alkalis, oxides, carbonates, and metals, and their miscibility with water account in large part for the corrosive threat they pose to artifacts.

The carboxylic acids are considered to be Volatile Organic Compounds (VOCs). VOCs are defined as organic chemical compounds with vapour pressures under normal conditions that are high enough to cause vaporization. They are described as "carbon-based compounds that become a gas or vapour at normal, ambient temperatures, or when heated, and have vapour pressures greater than 1 mm Hg." (Table 2.1) (Hatchfield 2002, 3). A wide range of carbon-based molecules qualify as indoor pollutants that pose as health hazards and threaten the preservation of collections. The aldehydes (acetaldehyde and formaldehyde), formic acid, and acetic acid are the organic carbonyl pollutants of primary concern in museums (Grzywacz 2006, 3). Threshold limit values (TLV's) are the highest levels of pollutants in air that adults can tolerate over an eight-hour period (Hatchfield 2002, 3). The TLV's based on an average 40-hour week are called the threshold limit value-time weighted average (TLC-TWA). The TLV's based on short-term exposures are called the threshold limit value-short term exposure limit (TLV-STEL) (Hatchfield 2002, 3). VOCs are quantified in parts per million (ppm), parts per billion (ppb), or in milligrams of substance per cubic meter of air (mg/m^3) (Hatchfield 2002, 3).

2.4 Sources of Acetic and Formic Acid

2.4.1 Museum Case Construction

Hundreds of VOCs may be detected inside buildings resulting from the off-gassing of many materials used in construction, exhibit preparation, and cleaners (Grzywacz 2006, 3). The most prevalent source in museum collections is wood and other organic materials used in the construction of display and storage cases (Gibson and Watt 2010, Werner 1987). Acetic acid (CH_3COOH) derives from the oxidation of acetaldehyde and formic acid (HCOOH) derives from the oxidation of formaldehyde (Evans 1961, 990). The aldehydes are oxidized by oxidants such as the peroxides or ozone forming acetic and formic acid (Grzywacz 2006, 11). Catalysts can play an important role in this oxidation process as exemplified by manganese that increases the rate of reaction (Ullmann 2003, vol. 1, 162) and by copper (Cu^{2+}) that oxidizes acetyl radicals rapidly (Ullmann 2003, vol. 1, 163).

Acetic and formic acid are contained in wood (Arni *et al.* 1961; Arni *et al.* 1965, 467). "The progressive hydrolysis of acetyl groups attached to hemicelluloses in the

wood produces free acid which evolves from the wood over an indefinite period of time." (Hatchfield 2002, 67). "Woods contain varying amounts of acetic acid and formic acid, either free or chemically combined in compounds that can release the acid during aging." (Hatchfield 2002, 67). Acetic acid can be recovered from wood distillate. The distillation of lumber woods yields pyroligneous acid that contains 5 to 8% acetic acid (Kirk-Othmer 2004, vol. 1 p. 126). The pH of wood can indicate degree of volatility (Hatchfield 2002, 68).

Other sources of acetic and formic acid in the museum environment include construction materials made from wood products such as particle board. Acetic acid can derive from adhesives, sealants, and the degradation of cellulose acetate films (Hatchfield 2002, 21). Other sources of acetic acid include vinyl acetate and polyvinyl acetate polymers applied as adhesives or in paint for the construction of cases (Donovan and Stringer 1971, 539). Formic acid can derive from drying oil paints and alkyd resin paints (Hatchfield 2002, 21). Formic acid also derives from polyesters, polyformaldehyde, nonvulcanized rubber, polysulfide rubber, oleo-resinous type paints and lacquers, elastomeric adhesives and rot/moth-proofed fabrics (Donovan 1986, 79; Donovan and Stringer 1971, 539,540).

2.4.2 Conservation Materials and Treatments

The following chemicals and conservation materials have been used for the treatment of artifacts that can introduce acetic acid contamination and cause the formation of acetates. Acetic acid was recommended for cleaning archaeological bronzes in the first half of the 20th century (Fink and Eldridge 1925). Vinyl acetate, polyvinyl acetate and cellulose acetate polymers have also been widely used as adhesives, consolidants and lacquers for the conservation of artifacts (Down 1996; Fink and Eldridge, 1925, 45; Paterakis 1998, 257). Testing at the Canadian Conservation Institute found that polyvinyl acetate (PVAC) adhesives release acetic acid (Down 1996). Na-EDTA (ethylene diamine tetraacetic acid) used for cleaning bronze can leave acetic acid contaminants (Stambolov 1985, 105).

Another source of acetic acid is the patination of chemically stripped copper alloys. Several recipes have been published over the years that incorporate ammonium acetate and/or acetic acid (Fink and Eldridge, 1925, 17, 39; Hemming 1977, 94).

2.4.3 Bacterial Action

Acetic acid is produced and excreted by certain bacteria, the Acetobacter and the Clostridium acetobutylicum, found in food, water, and soil. Vinegar is made by the Acetobacter. 2 to 12% acetic acid solutions (vinegar) are obtained from fermented fruit and vegetable juices (Kirk-Othmer 2004, vol. 1, 115). The oxidative reaction is as follows (Eq. 5) (Hromatka and Ebner 1959; Kirk-Othmer 2004, vol. 1, 127):

Eq. 5 $C_2H_5OH + O_2 \rightarrow CH_3COOH + H_2O$

Members of the genus Clostridium of anaerobic bacteria can convert sugars to acetic acid directly without ethanol or oxygen. The overall chemical reaction is (Eq. 6) (Sim *et al.* 2007):

Eq. 6 $C_6H_{12}O_6 \rightarrow 3\ CH_3COOH$

2.5 History of Damage to Artifacts by Carboxylic Acids

The earliest identification of acetate on an object stored in a museum collection was made in 1899 on shells (Byne 1899). For some time thereafter identifications were made on calcareous objects of various sorts such as shell, stone and ceramics (Fitzhugh and Gettens 1971; Nicholls 1934; Taboury 1931; Tennent and Baird 1985; Van Tassel 1945; Wheeler and Wypyski 1993). As of 1992 one or a combination of the following acetate compounds have been identified on shells (Mollusca): calcium acetate hydrate, calcium hemihydrate, calcium acetate formate hydrate (Tennent *et al.* 1992, 874). It was found that the shells with a higher chloride content were more likely to have the acetate corrosion. The explanation according to Tennent *et al.* (1992, 875) was the hygroscopicity of the salt that can modify the local moisture content of the shell, facilitating attack by acetic acid. A similar finding with regard to acetic acid was made on marble containing sodium bromide (Padfield *et al.* 1982). The formation of calcium acetate chloride nitrate hydrate, thecotrichite, $[Ca_3(CH_3COO)_3Cl(NO_3)_2 \cdot 7H_2O]$ occurred on an Egyptian limestone relief that was stored in a wood cabinet for 6 years where the levels of acetic acid vapour were estimated to be about 0.14 to 0.32 ppm (Tennent *et al.* 1992, 875). Sodium formate was found on a 16th c. enamel triptych in the Walters Art Gallery, Baltimore (Fitzhugh and Gettens 1971), and on glass lids of storage boxes for

10th c. archaeological textiles from Birka, Sweden (Nockert and Wadsten, 1978). In all these cases the objects had been stored in wood or cardboard. It was not until 1951 that corrosion due to acetic acid was reported on copper alloys (Evans 1951).

Acetic acid has been used for many centuries to manufacture lead white (lead carbonate) and verdigris (copper acetate) by combining it with lead and copper. Lead is first converted to lead acetate that readily converts to lead carbonate. Dioscorides was the first to record the manufacture of verdigris (copper acetate) for use as a pigment in the 1st century (Scott 2002, 268). Theophrastos recorded the manufacturing process of lead white using acetic acid in 450 BC (Donovan 1986, 78). In spite of the fact that the corrosive effects of acetic acid on metals have been known for centuries and that acetic acid, at one time, was produced commercially by the distillation of hardwoods, the hazards of storing metal in wood were not recognized by collection managers until relatively recently.

In the 18th century the damaging effects of volatile acids from wood were first reported on lead. Lead roofs of churches corroded as a consequence of their proximity to the wooden structure (Watson 1789, 365). Apparently the warning issued in 1932 regarding the dangers of storing lead in wood in the book entitled Antiques: Their Restoration and Preservation did not reach many collection managers since wood was still used for the storage of lead well into the latter part of the 20th century (Lucas 1932, 115). In 1967 volatile organic acids were identified as the cause of damage to lead in the British Museum and their source was traced to wood and adhesives in closed wooden cases (Werner 1967, 96).

In a study by Arni (Arni *et al.* 1965, 463) freshly felled oak and chestnut were found to contain considerable free acid whereas other types of wood did not: in the latter the acetyl groups bound to the hemicellulose were readily hydrolyzed in high humidities and temperatures between 30° and 48° C (smaller amounts of formic acid were detected) (Donovan and Stringer 1971, 132). Other variables that affect acidic emissions are type of wood, season of felling, sapwood or heartwood, ageing, and microbiological action (Donovan and Stringer 1971, 132, 137). Therefore storeroom and exhibition environmental parameters of temperature and relative humidity (RH) play a direct role in volatile acid emissions from wood storage cupboards and cases.

In 1995 while the author was serving as Head of Conservation of the Agora Excavation and Museum in Athens, Greece, for the American School of Classical Studies, a survey revealed the prevalence of blue corrosion on one particular group of bronze artifacts (Paterakis 2003). This group consisted of coins and a variety of objects recovered from the North Slope of the Acropolis that had been stored in closed wooden cupboards since the 1930s. Approximately 20% of the coins and 40% of other objects from this group were found with blue corrosion. At the time the North Slope bronzes constituted approximately 3.5% of the entire bronze collection of 72,000 objects. The predominance of blue corrosion on these objects recovered from one particular area of the excavation during a relatively short time span (less than 10 years) triggered several questions: What in particular caused the abundance of blue corrosion on this particular group of bronzes? What was the identity of the corrosion? Did burial conditions or conservation treatments influence the development of the blue corrosion? This blue corrosion was not restricted to the North Slope bronzes but was found on bronzes in the rest of the collection (less than 20%). A search into the Agora conservation treatment archives by conservators revealed two sodium-based chemicals that were frequently used in the 1930s: sodium sesquicarbonate and sodium hydroxide (Agora Excavations, undated).

My analytical investigation of the blue corrosion in the Athenian Agora collection began in 1997 in collaboration with Dr. George Wheeler of the Metropolitan Museum of Art (currently with Columbia University). By 2002 a blue sodium copper carbonate acetate compound and white sodium acetate trihydrate were identified on Agora bronzes by Dr. David Thickett at the British Museum (currently with English Heritage) (Paterakis 2003). The sodium present in the Agora corrosion indicates contamination from conservation chemicals applied in the 1930s based on the old conservation notes found in the files (Agora Excavation, undated). The sampling of corrosion in this analytical campaign was not restricted to the North Slope bronzes but represented a large area of the excavation. In 2004 I carried out scientific examination and testing to delve further into the problem of acetate corrosion on bronze while a Conservation Guest Scholar at the Getty Conservation Institute (Chapter 4).

2.6 Case Studies: Corrosion on Copper Alloy and Lead Artifacts in Museums by Acetic and Formic Acid Volatile Emissions

2.6.1 Copper Alloys

2.6.1.1 Acetic Acid

In 1993 a large survey was carried out in metal collections in several European museums (Grzywacz and Tennent 1994). The concentration of volatile acetic acid was found to range from 25 to 750 ppb, formic acid <0.3 to 60 ppb, formaldehyde 10 to 380 ppb, and acetaldehyde 5 to 85 ppb (Grzywacz andTennent 1994, 164). Acetic acid was found to surpass the other carbonyl compounds in concentration. Numerous cases of corrosion caused by acetic and formic acid have been reported on copper alloys. These are listed in Table 2.2 for acetic acid.

Table 2.2 Acetic Acid (ppb) and Acetate Compounds on Copper Alloys

Institution	Acetate compound	Acetic acid ppb	References	Analytical Technique
Liverpool Museum	nd	600 - 700	Lang 1995, 1996	IR
Fitzwilliam Museum	nd		Evans 1961	Micro-chemical
Burrell Collection	Sodium acetate trihydrate; unidentified copper acetate; formate	140 - 320	Tennent and Baird 1992; Tennent *et al.* 1993a; Tennent *et al.* 1992	XRD, IC, FAAS, IR, TGA, NMR, micro-chemical
British Museum	Copper chloride acetate; sodium copper carbonate acetate; sodium acetate trihydrate	439 - 1181	Thickett and Lee 1996; Thickett *et al.* 1998; Thickett 1998; Thickett and Odlyha 2000	XRD, SEM-EDXA, FTIR, AAS, IC, TGA, micro-chemical
Athenian Agora Excavations	sodium copper carbonate acetate; sodium acetate trihydrate	426 - 519	Paterakis 2003	XRD, FTIR, SEM-EDS, IC
Detroit Institute of Art	Copper sodium formate acetate	nm	Trentelman *et al.* 2002	XRD, XPS, WDS, RS

nd = not determined; nm = not measured
XRD= x-ray diffraction; IC = ion chromatography; IR = infra red specttrosocpy; FAAS = flame atomic absorption spectrometry; TGA = thermogravimetric analysis; NMR = nuclear magnetic resonance; SEM-EDXA = scanning electron microscopy-energy dispersive x-ray; FTIR = fourier transform infrared spectroscopy; AAS = atomic absorption spectroscopy; SEM-EDS = scanning electron microscopy-energy dispersive; XPS = x-ray photoelectron spectroscopy ; WDS = wavelength dispersive x-ray spectroscopy ; RS = raman microspectroscopy

The first publication that indicated acetic acid as the source of the deterioration of bronze was in 1951 from the collection of the Fitzwilliam Museum, Cambridge (Evans

1951, Evans 1961). Bronze artifacts were stored in wood shavings from 1939 to 1945 during World War II. When they were returned to museum cases at end of the war corrosion soon started (Evans 1961, 492). According to the author, acetic acid penetrated through cracks in corrosion layer (in this case basic copper chloride) and attacked the copper, producing soluble copper acetate (Evans 1961, 492).

Since 1961 numerous other cases have been identified and reported. Most of these have occurred in the United Kingdom, one in Greece and one in the United States. Bright blue-green corrosion was found to contain acetate by infrared spectroscopy on bronzes that had been stored in wood since the 1960s in the Liverpool Museum, UK (Lang 1995; Lang 1996, 57). The exact identity of the compound(s) was not investigated. Most of the artifacts affected were Egyptian and Near Eastern copper alloys that had not been chemically cleaned. The acetate corrosion formed on top of the primary corrosion layers resulting from burial. Passive monitors developed at Strathclyde University were used to measure acid levels in boxes (Gibson *et al.* 1997a). The level of acetic acid was found to be 600 to 700 ppb and that of formic acid 150 to 200 ppb.

In the Burrell Collection, Glasgow, acetates formed on Egyptian and other bronze antiquities that were re-housed in new wooden storage cabinets (Tennent and Baird 1992; Tennent *et al.* 1992, 87). In this case white crystalline sodium acetate trihydrate was identified in association with a blue crystalline copper acetate. On some objects the white crystals formed over a three-year period whereas the blue corrosion formed over a few weeks. The formation of the blue corrosion was observed to precede the white crystals. The blue corrosion was analysed by X-ray Diffraction (XRD), Ion Chromatography (IC), Flame Atomic Absorption Spectrometry (FAAS) and found to contain acetate and formate; a complete identification was not carried out (Tennent *et al.* 1993a). The concentrations of acetic acid vapour in the new storage ranged from 0.14 to 0.32 ppm. Identification of sodium acetate trihydrate was made with Infrared Analysis (IR), X-ray Diffraction (XRD), Thermogravimetric Analysis (TGA), Nuclear Magnetic Resonance (NMR) and microchemical elemental analysis. XRD and Infrared analysis are the most useful analytical techniques for identifying compounds. Materials used in the construction of the storage cabinets included spruce, cedar, ramin, birch/spruce plywood, polyvinyl acetate and phenolic-type adhesives, and polyurethane varnish (Tennent and Baird 1992, 41).

Ion chromatography was investigated as a means of detecting acetates and formates on artifacts. Acetate was found by ion chromatography on a bronze object from the British Museum that had been stabilized with sodium sesquicarbonate (Tennent *et al.* 1992, 878). The object was soaked in water to extract the contaminants for analysis. The object showed the blue-green surface typical of the sesquicarbonate treatment but didn't show any signs of deterioration in terms of crystallization and efflorescence. No acetates were found in another bronze of the same provenance that hadn't been treated with sodium sesquicarbonate (Tennent *et al.* 1992, 878). It is hypothesized that residues of the sodium sesquicarbonate in the object reacted with acetic acid in the air forming an acetate such as sodium acetate trihydrate (Tennent *et al.* 1992, 878). Three bronzes from the Burrell Collection, that had been stored in wood for 9 years at 0.14 to 0.32 ppm acetic acid, were soaked in distilled water and the diluent analysed by IC. They contained considerable amounts of acetate and formate even though there was no evidence of efflorescence on the surface of the object (Tennent *et al.*1992, 878). Ion chromatography has been shown to be a sensitive means of detecting low concentrations of acid on artifacts.

In 1996 the British Museum began investigating the blue corrosion on the Egyptian antiquities collection and measuring volatile acid levels in the cases. Blue, green and white corrosion on four Egyptian copper alloy objects in the British Museum were analysed by XRD, SEM-EDXA (energy dispersive x-ray analysis) and FTIR. No conservation treatment records for these objects were available. A copper acetate was found on three of the objects that could not be identified with precision as to exact composition since several neutral and basic copper acetates exist that have not been differentiated by their diffraction pattterns (Scott 2002; Thickett and Lee 1996, 2). It was found coexisting with chalconatronite ($Na_2(Cu(CO_3)_2.3H_2O$) by XRD. Chalconatronite can form naturally in soils or it can derive from chemical cleaning with products containing basic carbonates such as sodium sesquicarbonate. The acetates could have derived from conservation treatment or from storage in wooden cupboards. The green and blue corrosion products on a copper alloy dagger in the British Museum were analysed by XRD and FTIR. The dagger appeared to have been chemically stripped. The green was identified as copper chloride hydroxide (atacamite) and the blue was found to contain copper chloride acetate (Thickett 1996, 1). The exact composition could not determined due to the presence of other compounds not included in the international diffraction or spectroscopy analytical databases.

Further analytical work was carried out on the Egyptian bronze collection at the British Museum in which white and blue acetates were identified (Thickett and Odlyha, 2000; Thickett 1998; Thickett *et al.* 1998). A survey of the Egyptian bronze objects revealed that 6.7 % of the collection showed blue corrosion (Thickett and Odlyha 2000, 63). The blue corrosion was found in cracks in objects that had been chemically stripped and at breaks in a pale green corrosion layer high in sodium and chloride. Chemical agents that had been used in cleaning were alkaline Rochelle salt or alkaline glycerol; sodium sesquicarbonate had been used for stabilization (Thickett *et al.* 1998, 261). High concentrations of sodium hydroxide were found in the cracks of the chemically stripped objects. Most of the collection had been stored in wooden cabinets since the 1930s (Thickett *et al.* 1998, 261). The pale green corrosion layer was identified as malachite or atacamite on several objects. White crystalline corrosion was associated with the blue corrosion on most of the objects. This collection was housed in wooden cupboards with a RH from 35 to 45 %. Levels of acetic acid vapour ranged from 1071 to 2880 $\mu g/m^3$ (439 - 1181 ppb). Levels of other carbonyl pollutants were very low. The RH and acetic acid levels were fairly stable over a four-year period. White crystalline sodium acetate trihydrate was identified by XRD and FTIR (Thickett and Odlyha 2000, 64). The blue corrosion was identified as copper chloride acetate $CuCl(CH_3CO_2)$ (ICDD file 31-453) in a few instances (Thickett and Odlyha 2000, 63), whereas the corrosion on the majority of samples was identified as a sodium copper carbonate acetate with the stoichiometric ratio 1:1:1:1, $NaCu(CO_3)(CH_3COO)$ (Thicket and Odlyha 2000, 65).

The sodium copper carbonate acetate was characterized at the British Museum by the analysis of numerous (approximately 30) pale blue corrosion samples removed from Egyptian bronze objects. The pale blue corrosion was analysed by XRD, FTIR, Ion Chromatography (IC), Atomic Absorption Spectroscopy (AAS), Scanning Electron Microscopy with Energy Dispersive Analysis (SEM-EDS), Thermogravimetric Analysis (TGA), and microchemical tests (Thickett and Odlyha 2000, 65). Thermogravimetric analysis was carried out on a physical mixture of malachite, copper acetate, sodium acetate, and sodium carbonate to verify the ratio of acetate to carbonate. “This was just used as a confirmatory technique for the stoichiometry and agreed exactly with ion chromatography/colourmetric testing (for carbonate).” (D. Thickett pers comm. 2009). Thickett distinguished two sodium copper carbonate acetate compounds, Type A and Type B. “I believe both A and B are single unique compounds and not mixtures, the XRDs are identical for all instances as are the FTIRs, not only the peak positions but

their intensities … all FTIR absorption bands are within 5% of area of each other, (one) would expect (this) to vary if a mixture (were present). The ion ratios are also very steady." (D. Thickett pers comm. 2009). Thickett believes Type B to have similar stoichiometry to Type A but a different structure with different XRD and FTIR spectrum (D. Thickett pers comm. 2009). Regarding the submission of the sodium copper carbonate acetate compound(s) to the International Centre for Diffraction Data (ICDD), a structural analysis must first be carried out to characterize the crystallographic structure of the compound (D. Thickett pers comm. 2009).

Sodium acetate trihydrate ($CH_3COONa.3H_2O$) and a sodium copper carbonate acetate compound [$NaCu(CO_3)(CH_3COO)$] were identified on archaeological bronzes of various periods in the Ancient Athenian Agora (Paterakis 2003; Paterakis 2004). The analyses were carried out by XRD, FTIR, SEM-EDS, and IC. Most of the objects analysed had been chemically cleaned. The objects had been stored in storage cabinets constructed from softwood and plywood since their excavation between 1936 and 1981. Storage periods ranged from18 to 63 years. The level of acetic acid concentration in the storage cabinets in 1998 was found to range from 1039 to 1267 $\mu g/m^3$ (426 to 519 ppb at 25° C) (Paterakis 2003, 321). These levels are similar to those in the British Museum, 1071 to 2880 $\mu g/m^3$ (439 to 1181 ppb) (Thicket *et al.* 1998). The stoichiometric ratio of a sodium copper carbonate acetate compound has not been established and for this reason it is not known if this compound matches the compound(s) found in the British Museum (Thickett and Odlyha, 2000). The occurrence of this blue corrosion product was considerably more pronounced from one specific area of the excavation (North Slope) (Paterakis 2003, 315). The white sodium acetate trihydrate was found closely associated with the blue corrosion, as was the case in the Burrell Collection and the British Museum (Paterakis 2003, 317).

2.6.1.2 Formic Acid

The published cases of corrosion caused by formic acid are reported in Table 2.3. A corrosion compound containing acetate and formate was found on ancient Egyptian, Greek, Assyrian and Chinese copper alloys (Trentelman *et al.* 2002, 217). It was also found on non-archaeological and non-ancient objects such as a 15th century AD leaded copper tin in the Detroit Institute of the Arts (Trentelman *et al*. 2002, 222). Analyses used were XRD, XPS (x-ray photoelectron spectroscopy), WDS (Wavelength dispersive

x-ray spectroscopy), and Raman microspectroscopy. The compound found was copper sodium formate acetate, $CuNaC_xH_yO_6$, with a ratio of copper : sodium : formate : acetate 1:1:1:2 (x=5, y = 9) or 1:1:2:1 (x = 4, y = 6) (Trentelman *et al*. 2002, 217).

Table 2.3 Formic Acid (ppb) and Formate Compounds on Copper Alloys

Institution	Formate compound	Formic acid concentration - ppb	References	Analytical techniques
Burrell Collection	nd	nm	Tennent *et al*. 1993a; Tennent *et al*. 1992	
Detroit Institute of Art	Copper sodium formate acetate	nm	Trentelman *et al*. 2002	XRD, XPS, WDS, RS
Liverpool Museum	nd	150 - 200 ppb	Lang 1995, 1996	

nd = not determined; nm = not measured
XRD= x-ray diffraction; IC = ion chromatography; IR = infra red spectroscopy; FAAS = flame atomic absorption spectrometry; TGA = thermogravimetric analysis; NMR = nuclear magnetic resonance; FTIR = fourier transform infrared spectroscopy; XPS = x-ray photoelectron spectroscopy; WDS = wavelength dispersive x-ray spectroscopy; RS = raman microspectroscopy

In all the aforementioned case studies, storage in wood and wood products is identified as the main source of acetic and formic acid contaminant. Overall conclusions of these investigations indicated that a combination of factors contributed to the formation of acetate and formate corrosion on bronze: mainly wooden storage materials and, in some cases, sodium-based chemicals used in conservation treatments or sodium from burial.

2.6.2 Lead

2.6.2.1 Acetic Acid

Numerous cases of lead corrosion caused by acetic acid are reported in Table 2.4. The deleterious effects of volatile organic acids on lead have been analysed in several collections. The acetic acid in the atmosphere condenses on the surface, neutralizes the carbonates and forms very soluble lead acetates (Degrigny *et al*. 1996, 867). The lead acetates react with moisture and carbon dioxide to form hydrocerussite and acetic acid. The acetic acid in turn reacts with moisture and oxygen to form more lead acetates and water. A cyclical process of corrosion is set in motion (Degrigny *et al.* 1996, 867).

Table 2.4 Acetic Acid Concentration and Corrosion Compounds on Lead

Institution	Corrosion compound	Acetic acid concentration - ppb	Reference	Analytical techniques
Burrell Collection	nd	100 - 3000	Tennent *et al.* 1993b	
Science Museum London	hydrocerussite	nm	Tanter and Jull 1987	IR
Glasgow Museums & Art Galleries	nd		Tennent *et al.* 1993b	
St. Andrews University Library	nd		Tennent *et al.* 1993b	
Athenian Agora	hydrocerussite	nm	Paterakis 1998	XRD, FTIR
Musée du Conservatoire National des Arts et Métiers, Paris	Lead acetate	nm	Degrigny *et al.* 1996	XRD
British Museum	hydrocerussite		Lane 1975; Oddy 1975	
National Museum of Scotland	nd		Weierter and Tate 1993	

nd = not determined; nm = not measured
XRD = x-ray diffraction; IR = infrared spectroscopy; FTIR = fourier transform infrared spectroscopy

The effects of VOCs on lead were analysed by XRD at the British Museum. The VOCs studied were known to derive from wood and adhesives used in storage materials (Werner 1967, 96). Lead corrosion and the formation of lead carbonate hydroxide ($Pb_2(OH)_2CO_3$) (hydrocerussite) in the British Museum were attributed to the off gassing of acetic acid from wood storage cupboards and cardboard boxes, specifically oak and chipboard (Lane 1975, 215; Oddy 1975, 235). This organic acid was claimed to be the most commonly found organic acid in museum storage (Lane 1975, 215). The corrosive effects of acetic acid on lead weights in the Musée du Conservatoire National des Arts et Métiers de Paris and on lead tokens in the Ancient Agora of Athens were analysed by X-ray diffraction and FTIR (Degrigny *et al.* 1996; Paterakis 1998, 257). Corrosion on lead was identified by Infrared Spectroscopy at the Science Museum in London (Tanter and Jull 1987). In all cases but one hydrocerussite, lead carbonate hydroxide, was found resulting from attack by acetic acid. A unique case of lead acetate was detected at the Musée du Conservatoire National des Arts et Métiers de Paris. The detection of lead acetate is uncommon since it readily converts to hydrocerrusite.

Lead objects from the 12th to the 14th century AD, stored in wooden cabinets in three collections in France, were examined (Harch *et al.* 1993). The state of preservation was characterized as two main types: 1) original surface is preserved, 2) surface displays different alteration morphologies such as pustules, efflorescence, and fissures (Harch *et*

al. 1993, 18). The deterioration is attributed to a combination of high and fluctuating RH, storage in wood, and galvanic corrosion (Harch *et al.* 1993, 21).

In the National Museums of Scotland, Edinburgh, lead communion tokens were stored in oak and mahogany cupboards on felt pads, materials that off-gas harmful vapours (Weierter and Tate 1993, 57). They were analysed by X-ray fluorescence (XRF) for elemental composition on the surface to determine the relationship between composition and corrosion. The most severely corroded tokens had Pb content greater than 98.8%. Those with minor corrosion had between 96.7% and 98.8%. This work supports the findings of Tennent *et al.* (1993b) that pure lead is more severely attacked by acid than alloyed lead (Weierter and Tate 1993, 59).

Lead objects from three collections in Scotland were stored in wood cabinets (Tennent *et al.* 1993b, 8). Many had suffered deterioration by acetic acid attack. The objects in question were lead Beggar's Badges from Glasgow Museums & Art Galleries, lead cames from stained glass windows in the Burrell Collection, Glasgow, and lead communal tokens at St. Andrew's University Library in St. Andrews. The wood cabinets in the Burrell Collection contained acetic acid vapour levels of 0.1 to 3.0 ppm (Tennent *et al.* 1993b, 9). The composition of these objects was analysed by energy dispersive X-ray fluorescence (XRF) and inductively coupled plasma optical emission spectroscopy (ICP-OES). A concordance between composition and corrosion was found. Objects consisting of greater than 98.5% Pb tended to be much more prone to corrosion than less pure lead. Lead alloyed with greater than 1.5% Sn, such as pewter, was found to have corrosion resistance.

2.6.2.2 Formic Acid

Cases of lead corrosion by formic acid are reported in Table 2.5. Lead formate was identified on a 16th c. AD lead medal in the National Gallery of Art, Washington D.C., that resulted from storage in wood and other organic materials in the case (Fitzhugh and Gettens 1971, 93). Lead formate was identified on the lead portion of an American Indian pipe in the Brooklyn Museum of New York. In this case it was postulated to result from a conservation material (Fitzhugh and Gettens 1971, 97).

Corrosion on lead artifacts in new gallery space in the British Museum was identified as lead formate (Thickett *et al.* 1998, 262). The formic acid derived from paint used in the display case and measured 156 ppb to 247 ppb in concentration (Thickett *et al.* 1998, 262). Lead artifacts were found to have lead formate and basic lead carbonate in varying proportions in the Science museum in London (Tanter and Jull, 1987).

Table 2.5 Formic Acid (ppb) and Corrosion Compounds on Lead

Institution	Formate compound	Formic acid concentration - ppb	Reference	Analytical technique
British Museum	Lead formate	156-247 ppb	Thickett *et al.* 1998	XRD
Science Museum, London	Lead formate	nm	Tanter and Jull 1987	IR
Bayerischen Nationalmuseums, Munich	Lead formate	nm	Brunnert 1985	XRD
National Gallery of Art, Wash.D.C.	Lead formate	nm	Fitzhugh and Gettens 1971	XRD
Brooklyn Museum	Lead formate	nm	Fitzhugh and Gettens 1971	XRD

nm = not measured
XRD = x-ray diffraction; IR = infrared spectroscopy

Lead artifacts in the Bayerischen Nationalmuseums of Munich developed white efflorescence that was identified as basic lead carbonate by XRD. This corrosion is said to have occurred by the reaction of formaldehyde from wood products that oxidized to formic acid. The formic acid reacted with the lead forming
lead formate that subsequently reacted with carbon dioxide in the atmosphere to form lead carbonate (Brunnert 1985, 161).

2.7 Research Issues and Questions

Although the majority of references cited in this chapter pertain to collections in North America and Europe, the phenomenon of the attack by VOC's on collections is worldwide since wood and organic materials are the most commonly used materials for storage. The transmission of these findings proceeds slowly through publications, lectures, and the internet requiring some years yet for many collections in various parts of the world to receive these updates.

Regarding the identification of corrosion resulting from attack by acetic and formic acid, there are an unknown number of compounds that have yet to be

characterized and submitted to the international reference databases such as the International Centre for Diffraction Data® (ICDD®) and the FDM Reference Spectra Databases of infrared spectra. Once the compounds caused by VOCs are registered the identification of corrosion by XRD and FTIR can be made around the world.

After the causes of deterioration and the identity of corrosion are brought to the attention of curators and collections managers any mitigation process itself can be slow since it is reliant on the financial health of the respective organization. Replacing storage furniture can be costly in proportion to the size of the collection and more economic means of reducing VOC emissions, such as sealing interior surfaces of cases with barrier films, require considerable time and labor.

Chapter 3 Corrosion and Corrosion Testing in Archaeological Conservation

3.1 Introduction

Knowledge of chemistry is fundamental for the understanding of the corrosion and conservation of metals. The field of Conservation Science links chemistry with conservation. In most cases the Conservation Scientist is armed with a more in-depth understanding of science and chemistry than is the Conservator and provides a much-needed service to conservators by facilitating their investigation of corrosion mechanisms and increasing their understanding of the processes involved in material science, corrosion, and analytical techniques. Conservation science is a very specialized field as it addresses the state of preservation of art and antiquities, unlike other fields in science such as engineering and chemistry that address industrial or commercial purposes. In addition to the assistance from Conservation Scientists, a basic understanding of the mechanisms involved is required for the conservator to be able to approach cleaning and stabilization (anti-corrosion) issues of metals. To aid in this understanding of the application of science to conservation in general a three volume series entitled *Science for Conservators*, as part of the Conservation Science Teaching Series, was published by The Conservation Unit of the Museums and Galleries Commission, London, in 1987 (Ashley-Smith (ed.) 1987). Several publications on conservation science include *Conservation Science in the U.K.* (Tennent (ed.) 1993), *Conservation Science 2002: papers from the Conference held in Edinburgh, Scotland,* 22-24 May 2002 (Townsend (ed.) 2002), *Conservation Science* (Bisht 2003), *Conservation Science: Heritage Materials* (May and Jones (eds.) 2006), and *Conservation Science 2007: papers from the Conference held in Milan, Italy 10-11 May 2007* (Townsend (ed.) 2008).

One of many textbooks on the corrosion of metals of use to conservators is *Principles and Prevention of Corrosion* by Jones (1996). A specialized publication on metal corrosion with application to the conservation of metals is *Metals and Corrosion: a Handbook for the Conservation Professional* published by the Canadian Conservation Institute (Selwyn 2004). Another conservation institution that has contributed to the metals conservation literature is the Getty Conservation Institute with *Ancient and Historic Metals: Conservation and Scientific Research* (Scott (ed.) 1994) and *Copper and Bronze in Art: Corrosion, Colorants, Conservation* (Scott 2002).

Several texts have been published dealing with this subject for the conservation scientist and conservator of metal objects and antiquities with an emphasis on archaeological materials. These include *Corrosion and Metal Artifacts: a Dialogue between Conservators and Archaeologists and Corrosion Scientists* (Brown (ed.) 1977), *The Conservation & Restoration of Metals: Proceedings of the Symposium held in Edinburgh 30-31 March 1979* (Tennent (ed.) 1979), *The Corrosion and Conservation of Metallic Antiquities and Works of Art* (Stambolov 1985), and *Corrosion of Metallic Heritage Artefacts: Investigation, Conservation and Prediction for Long-term Behaviour* (Dillmann (ed.) 2007).

To lay the foundation for this research project it is important to examine the corrosion mechanisms of copper and copper alloys from archaeological context prior to discussing the corrosive influence of acetic acid. The corrosion mechanisms produced by moisture will be examined before the additional variables of acetic acid and other carbonyl compounds are considered. The alloy constituents lead and tin, will also be examined.

"The corrosion of metals is an electrochemical process with the anodic reaction, metal dissolution, and the cathodic reaction, oxygen reduction or hydrogen evolution, occurring at separate sites on the metal surface. The circuit is completed by flow of electrons within the metal and of ions in solution." (Turgoose 1985, 16) (Figure 3.1).

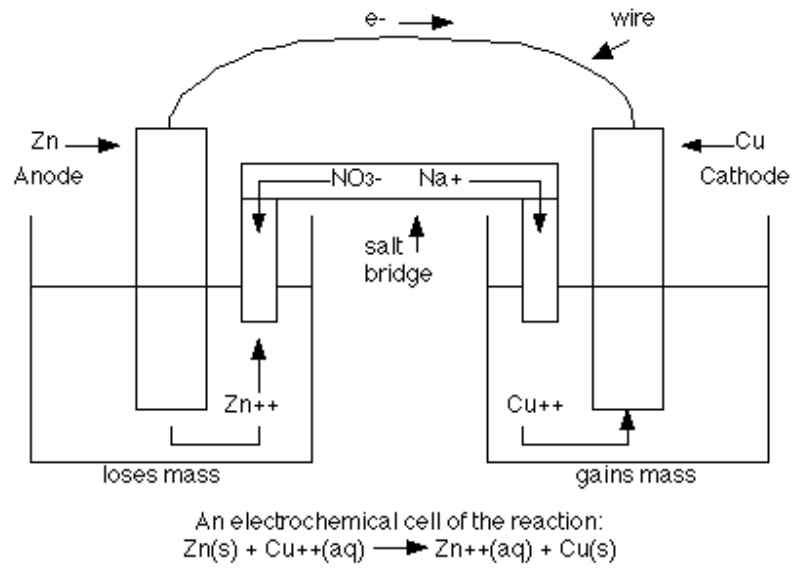

Figure 3.1 Electrochemical cell using a sodium nitrate electrolyte (from http://www.shodor.org/appstchem/advanced/redox/index.html)

3.2 Copper

3.2.1 Properties of Copper and Copper Alloys

3.2.1.1 Copper

The principal oxidation states of copper are +1(Cu^{+}) and +2 (Cu^{2+}). Copper corrodes in moisture according to the following electrochemical reactions:

Anodic half-reaction: $Cu(s) \rightarrow Cu^{+} + e^{-}$

Cathodic half-reaction: $1/4O_2(g) + 1/2H_2O + e^{-} \rightarrow OH^{-}$

Net reaction: $Cu(s) + 1/4O_2(g) + 1/2H_2O \rightarrow Cu^{+} + OH^{-}$

Standard electrode potentials for copper are

$Cu^{2+} + 2e \Leftrightarrow Cu$ +0.34V

$Cu^{+} + e \Leftrightarrow Cu$ +0.52 V

$Cu^{2+} + e \Leftrightarrow Cu^{+}$ +0.17V (Shreir 1978, 4:37).

The equilibrium potential (Eh) occurs "when the electrode potential of an isolated half-reaction at equilibrium with no current flowing is determined at non-standard conditions (e.g. other temperatures, other ion concentrations)…" (Selwyn 2004, 23). Stability, Pourbaix, or potential-pH diagrams can be used to determine the potential and pH at which a metal will be immune to corrosion, actively corroding, or passivated (Pourbaix 1974; Selwyn 2004, 24). Referring to Figure 3.2 and Figure 3.3 the "horizontal line … represents the equilibrium potential for the half-reaction $Cu(s) \Leftrightarrow Cu^{2+} + 2e^{-}$" (Selwyn 2004, 26). Acid-base equilibrium reactions at a specific pH are represented by the vertical lines (Selwyn 2004, 26). Equilibrium reactions involving electrons and H^{+} ions are represented by the sloped lines (Selwyn 2004, 26). Water is stable between the lines (a) and (b). Water at and above line (b) can be oxidized to oxygen gas and at and below line (a) can be reduced to hydrogen gas.

Figures 3.2 and 3.3 show the conditions in which copper, copper compounds, and copper ions are stable. The upper left corner region labeled Cu^{2+} (defined by solid lines) indicates that Cu^{2+} ions are stable and copper metal is unstable and will corrode forming Cu^{2+} ions in these conditions of pH and Eh (Figure 3.2) (Selwyn 2004, 26). The passive

and immune areas in Figure 3.3 correspond to the stable copper metal Cu(s) and stable copper oxides Cu_2O(s) and CuO(s) within solid lines in Figure 3.2.

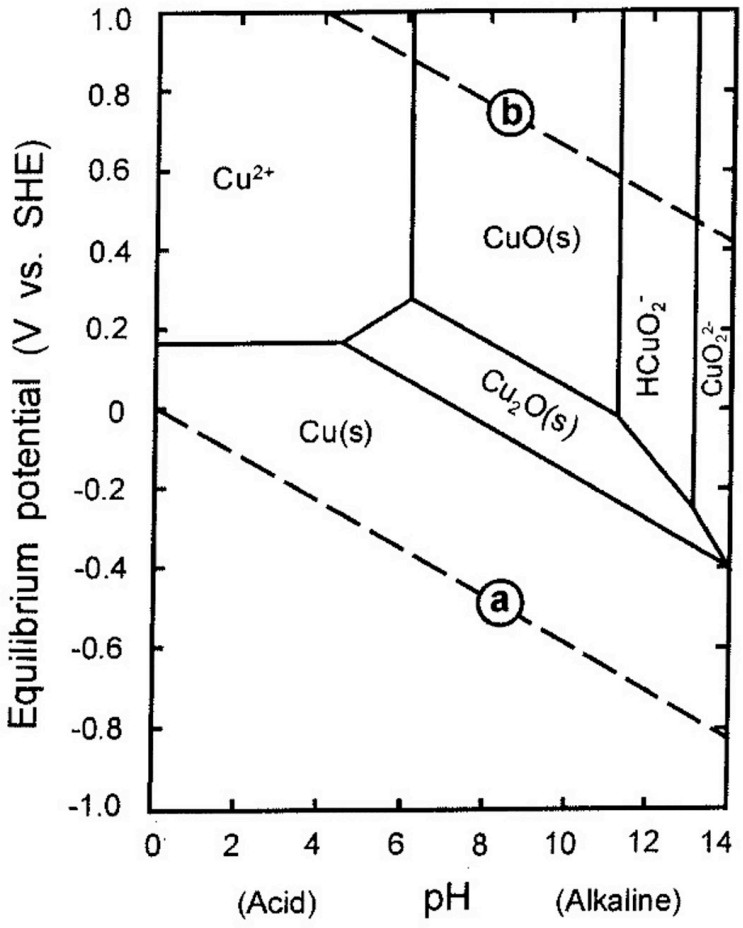

Figure 3.2 Potential–pH diagram for a copper-water system at 25 C, 1 atm., Cu^+ concentration 10^{-6} M. The areas are labeled with the most thermodynamically stable species (Pourbaix 1974; Selwyn 2004, 25)

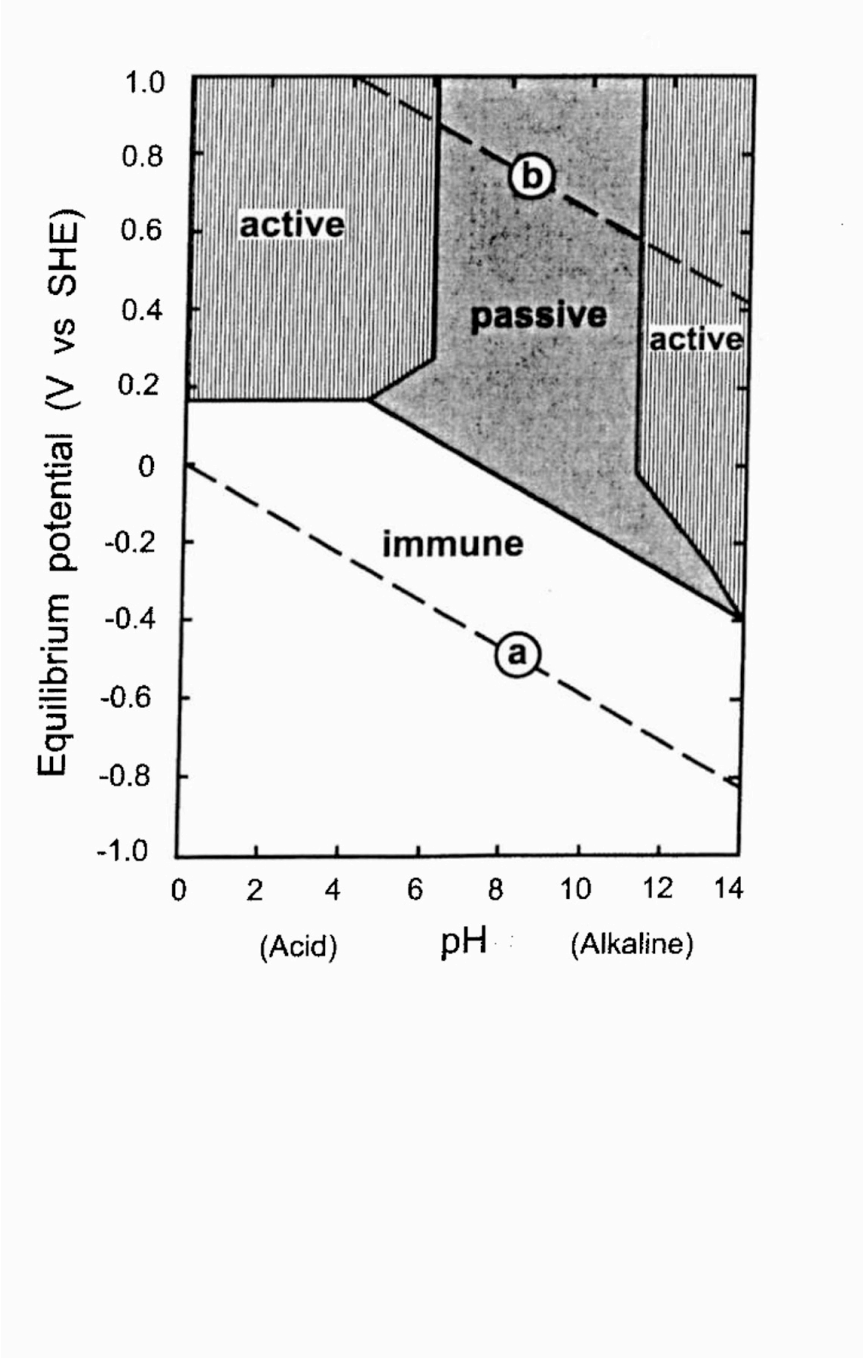

Figure 3.3 Same potential-pH diagram for a copper-water system as in Fig. 3.2 showing immunity, activity, passivity (Pourbaix 1974; Selwyn 2004, 25)

Areas with fresh water tend to be acidic (pH <7) whereas areas with marine water are alkaline (pH>7). The higher the potential (Eh), the lower the pH. A comparison of Figure 3.4 with Figure 3.5 reveals that the copper sulphates, carbonates, and oxides are

formed in well-aerated soils, whereas the sulfides are formed in soil isolated from the atmosphere (Schweizer 1994, 44). The pH and potentials of natural environments can be seen in Figure 3.4.

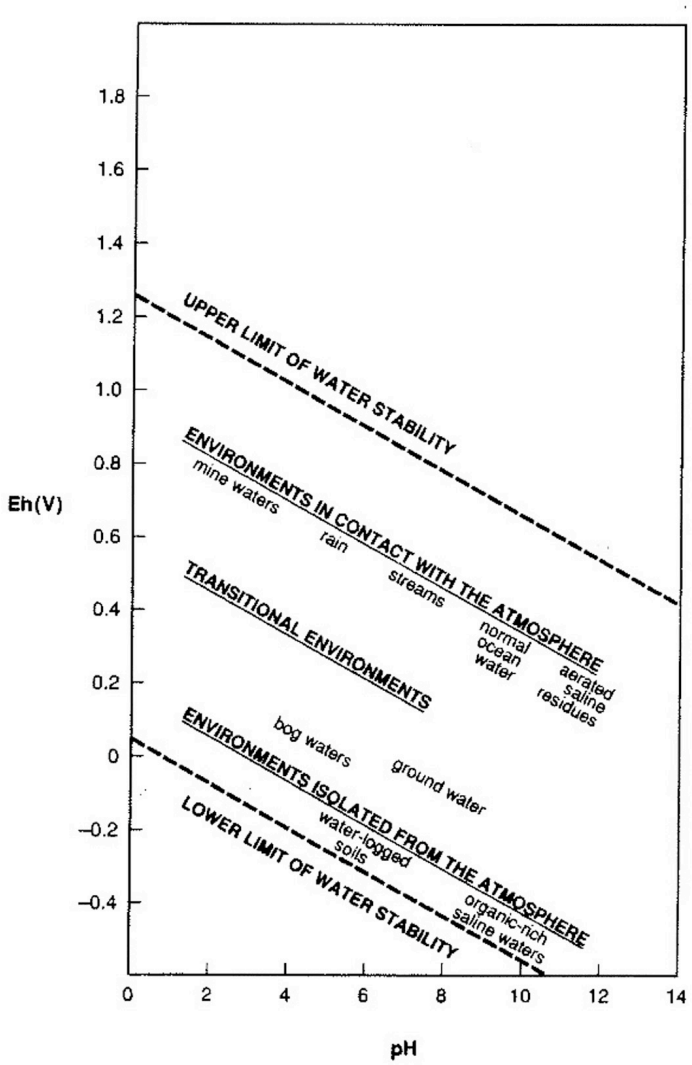

Figure 3.4 Approximate position of some natural environments as characterized by pH and potential (Eh) (after Garrels and Christ 1965, from Schweizer 1994, 45)

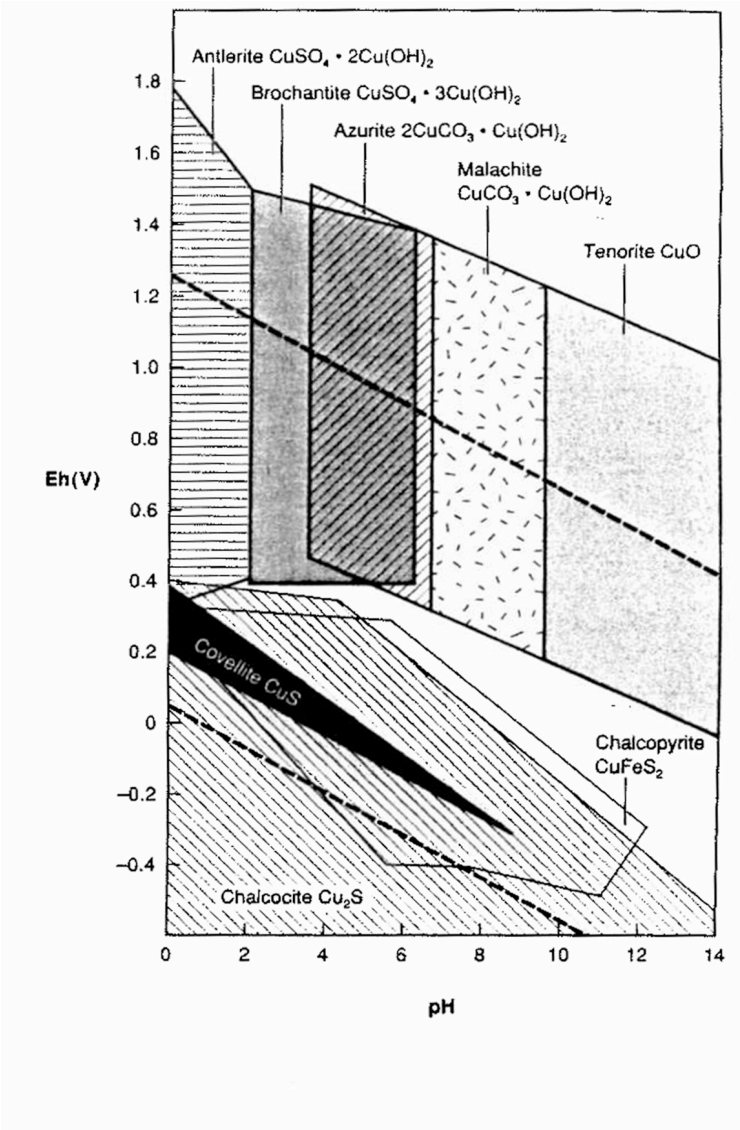

Figure 3.5 Simplified pH-Eh diagram for the ternary systems Cu-CO_2-H_2O and Cu-S-H_2O (Pourbaix 1974; Schweizer 1994, 45)

3.2.1.2 Copper-Tin Binary Alloys

Low-tin and high-tin are the two main categories of copper-tin bronze. Low-tin contains less than 17% tin, the high-tin more than 17% (Scott 2002, 401). Most ancient bronzes contain less than 17% tin as this permits cold-working and annealing. A typical cast tin bronze structure consists of cored dendritic growth with alpha + delta eutectoid surrounding the dendrites. The dendrites are copper-rich and may contain different amounts of tin depending on the cooling rate. Working by hammering and annealing causes annealing twins, strain lines, flattened and finer grains. Alpha + delta eutectoid is found between recrystallized grains of the alpha solid solution. Four characteristic structures of low-tin bronze are:

1.all tin has dissolved with the copper,

2.cored structure in which there is unequal distribution of copper and tin, the eutectoid phase is absent,
3.alpha phase and eutectoid phase are present (typical of most ancient bronzes),
4.extensive coring in alpha phase, eutectoid phase is present (Scott 2002, 401).

The copper-tin bronze used in corrosion experiments in Chapter 4 qualifies as a low-tin bronze as it contains 16% tin, ASTM B584 (Chapter 4, Table 4.1). Metallographic examination of this copper-tin bronze revealed an alpha phase and a eutectoid phase (Appendix 2.1). The tin content of the ancient coins used in corrosion testing ranged from 1.3% to 17% (Chapter 4, Table 4.2).

3.2.1.3 Copper-Tin-Lead Ternary Alloys

In low-tin bronzes lead does not alloy with the copper or the tin, it forms globules randomly throughout the metal that range from a few microns to 30 - 200 μm in diameter (Scott 2002, 403). At higher tin contents the structure is finer grained. The Widmanstättten structure is a morphology formed by “the continuous precipitation of plate or lathlike structures” that can occur in quickly cooled bronze (Vander Voort 2004, 137). The copper-tin-lead alloy used in corrosion experiments in Chapter 4 contains 8% tin and 8% lead and therefore qualifies as a low-tin bronze, ASTM B505 (Chapter 4, Table 4.1).

The ancient coins used in corrosion testing ranged from 1% to 23% lead (Chapter 4, Table 4.2). Therefore, all bronze used in corrosion testing contained less than 30% lead. "Cu-Sn-Pb ternary alloys with Pb less than 30%: first a Cu-Sn solid solution solidifies while Pb remains in liquid state. Pb solidifies once the temperature falls below the eutectic temperature (326° C in the Cu-Pb system). The distribution of Pb in the solidified material depends to a large extent on the formation of the growing Cu-Sn crystals (slow cooling = dendrites; fast cooling = equiaxed grains. A globular dissemination of Pb indicates fast cooling. The precipitation of Pb as an intergranular phase indicates relatively slow cooling. Because lead collects along the grain boundaries, it acts like a lubricant and improves the fluidity of the melt (facilitates casting)" (Klein 1999, 1080).

3.2.2 Corrosion Mechanisms of Archaeological Bronze

Perhaps the most extensive study of corrosion on Greek archaeological bronzes has been carried out by Earle Caley. Reporting on several bronzes of high tin and low lead content from Corinth, the principal corrosion products found were cuprous oxide (cuprite), tin oxide, and basic cupric chloride (atacamite) (Table 3.1) (Caley 1941). Among those objects analysed by Caley were a 5^{th}-6^{th} century BC strigil blade and a 5^{th} century BC strigil handle. The analysis of the corrosion on a Greek strigil handle is claimed to be "the first complete quantitative analysis of the patina of any sort of a Greek bronze object." (Caley 1941, 697). The strigil blade contained 82% copper, 10% tin, and no lead (Caley 1941, 694). The strigil handle contained 82% copper, 14% tin, and 0.02% lead (impurity). The major difference between the two objects is that the strigil blade was completely mineralized whereas the strigil handle preserved a metal core (Caley 1941, 696). On the handle the innermost layer of corrosion next to the metal core contained mostly cuprous oxide (cuprite) with considerable stannic oxide (casiterite) and some basic cupric chloride (atacamite) (Caley 1941, 695). The outermost layer of corrosion consisted mainly of basic cupric chloride (atacamite) with some basic cupric carbonate (malachite) and a trace of basic cupric carbonate (azurite) (Caley 1941, 695). Cuprous oxide (cuprite) was found as an intergranular corrosion product (Caley 1941, 696). Silica was also found in the corrosion of the blade. A comparison of the corrosion on the strigil handle with that on the strigil blade reveal similarities: Cuprite represented 85% of the corrosion on the handle and 82% on the blade; cassiterite made up 9% of the corrosion on the handle and10% on the blade; atacamite represented 2% of the corrosion on the handle and 4% on the blade (Caley 1941, 697). There was no loss of lead from the corrosion on the strigil handle, i.e. the proportion of lead in the corrosion matched that in the metal core (Caley 1941, 698). The ratio of tin to copper was found to be lower in the corrosion than in the metal core, as is typical of ancient bronzes (Caley 1941, 693). This is attributed to the fact that the soluble tin corrosion products are lost by diffusion, by mechanical means or by movement of the water during burial (Caley 1941, 730).

Corrosion of the Corinth bronzes is attributed to the formation of an electrochemical cell on the heterogeneous metal (heterogeneity established by tin-rich delta phase) in the presence of an electrolyte (chloride solution in this case from ground water) (Caley 1941, 717). "The more heterogeneous the metal the greater will be the number of local [electrical] currents, and the greater will be the rate of corrosion if other

conditions remain constant." (Caley 1941, 718). Large differences in potential (Eh) exist between the areas of tin–rich delta phase and the mass of alpha phase bronze (Caley 1941, 719). Fink and Polushkin found that the copper-rich alpha phase in cast bronze can corrode before the tin-rich delta phase which contradicts the rule that less noble metals (tin in the case of a copper-tin bronze) corrode first (Fink and Polushkin 1936). This discrepancy is attributed to "the intermetallic compound of copper and tin contained in the eutectoid [that] caused the grains composed of this solid solution to be more electronegative in character than the grains composed of the alpha solid solution so that the latter were anodic and were therefore corroded by the action of the electrolyte." (Caley 1941, 722 [from Fink and Polushkin 1936]). Fink and Polushkin found corrosion to follow the rules of electronegativity of the metals present in wrought bronze for the most part (Caley 1941, 722; Fink and Polushkin 1936). Cuprous chloride is less likely to be found (usually next to the core metal) as it readily converts to basic cupric chloride in the presence of oxygen and moisture (Caley 1941, 706).

Table 3.1 Corrosion Products that form on Archaeological Bronze

Compound	Formula	Mineral name	Color
Copper (I) oxide	Cu_2O	Cuprite	Red
Copper (II) oxide	CuO	Tenorite	Black
Copper (II) hydroxide	$Cu(OH)_2$	Spertinite	Blue
Copper (II) carbonate hydroxide	$Cu_2CO_3(OH)_2$	Malachite	Green
Copper (II) carbonate hydroxide	$Cu_2CO_3(OH)_2$	Georgeite	Blue
Copper (II) carbonate hydroxide	$Cu_3(CO_3)_2(OH)_2$	Azurite	Blue
Copper (II) sodium carbonate trihydrate	$CuNa_2(CO_3)_2.3H_2O$	Chalconatronite	Blue
Copper (I) chloride	CuCl	Nantokite	Pale grey
Copper (II) chloride dihydrate	$CuCl_2.2H_2O$	Eriochalcite	Blue-green
Copper (II) chloride hydroxide	$Cu_2Cl(OH)_3$	Atacamite	Green
Copper (II) chloride hydroxide	$Cu_2Cl(OH)_3$	Clinoatacamite	Green
Copper (II) chloride hydroxide	$Cu_2Cl(OH)_3$	Paratacamite	Green
Copper (II) chloride hydroxide	$Cu_2Cl(OH)_3$	Botallackite	Green
Copper (I) sulphide	Cu_2S	Chalcocite	Black
Copper iron (II) sulphide	$CuFeS_2$	Chalcopyrite	Yellow
Copper iron (II) sulphide	Cu_5FeS_4	Bornite	Red-brown
Copper (I,II) sulphide	$Cu_{1.6}S$	Geerite	Black
Copper (I,II) sulphide	$Cu_{1.8}S$	Digenite	Blue-black
Copper (I,II) sulphide	$Cu_{1.96}S$	Djurleite	Black
Copper (I,II) sulphide	CuS	Covellite	Dark blue
Copper (II) sulphate pentahydrate	$CuSO_4.5H_2O$	Chalcanthite	Blue
Copper (II) hydroxide sulphate	$Cu_4(OH)_6SO_4$	Brochantite	Green
Copper (II) hydroxide sulphate	$Cu_3(OH)_4SO_4$	Antlerite	Green
Copper (II) hydroxide sulphate monohydrate	$Cu_4(OH)_6SO_4.H_2O$	Posnjakite	Light blue
Copper (II) iron (III) hydroxide sulphate tetrahydrate	$CuFe(OH)(SO_4)_2.4H_2O$	Guildite	Yellow-brown
Calcium copper (II) sodium chloride phosphate pentahydrate	$CaCu_5NaCl(PO_4)_4.5H_2O$	Sampleite	Blue-green
Copper (II) hydroxide phosphate	$Cu_2(OH)(PO_4)$	Libethenite	Green
Copper (II) chloride hydroxide sulphate trihydrate	$Cu_{19}Cl_4(OH)_{32}(SO_4).3H_2O$	Connellite	Blue
Copper (II) hydroxide nitrate	$Cu_2NO_3(OH)_3$	Gerhardtite	Green

(from Selwyn 2004, 60)

The metallographic examination of the handle of a bronze strigil shows homogenized and twinned crystals of small size indicating the mechanical working of a wrought object (Caley 1941, 709). Annealing bands indicated the application of heat during manufacture (Caley 1941, 709). The microstructure reveals that the corrosion of the strigil handle did not proceed from its surface inward but rather along grain boundaries within the object in a non-uniform fashion (Caley 1941, 711).

Caley found the corrosion on some archaeological metals in the Athenian Agora to be misleading regarding the identity of the core metal. Copper corrosion resulted from the corrosion of a thin plating of copper on pure lead weights (Caley 1964). Silver coins were found covered with copper corrosion products, masking their true composition (Caley 1964).

The technology of manufacture and corrosion morphology was examined on a gilded bronze Hellenistic equestrian statue from the Athenian Agora (Paterakis 2000a). Corrosion products found on archaeological bronzes in Greece were summarized and attributed to various burial conditions (Paterakis 2000b). A condition survey of the Bronze age bronzes in the collection of the Ancient Athenian Agora revealed bronze disease in approximately 4% of the these objects (Paterakis 1999).

A sodium copper carbonate acetate, sodium acetate trihydrate, copper (II) hydroxide, tin dioxide, and cuprous oxide have been identified on archaeological bronzes with a blue patina in the Ancient Athenian Agora (Paterakis 2003; Paterakis 2004; Paterakis 2007).

Two corrosion morphologies have been distinguished based on the analysis of archaeological bronzes dating from 1500 BC to 750 BC (Robbiola *et al.* 1998). The bronzes analysed were binary copper-tin alloys (Sn content ranges 4-23% wt., Pb less than 0.3% wt., minor impurities) from France. The binary alloys consisted of an α-phase (Sn is less than 14% wt.) and a δ-phase (Sn is greater than 14% wt.). The alloy composition was determined with UV Emission Spectrometry and the corrosion by SEM-EDS (Energy Dispersive Spectrometry), XRD and Infrared Spectrometry. Two categories of corrosion were identified based on analysis by SEM-EDS, XRD, and Infrared Spectroscopy: Type I and Type II (Robbiola *et al.* 1998).

Type I preserves the surface detail. A passivating layer of Sn oxide formed on the surface that retarded decuprification, defined as the selective dissolution of copper from the alloy. XRD and IRS showed that the corrosion was amorphous to a large extent (Robbiola *et al*. 1998, 2092). The tin oxide becomes hydrated forming gel-like amorphous compounds that are chemically inert and stable over a wide range in pH (Robbiola *et al*. 1998, 2105). These form the passive barrier layer. Patina may be defined as the corrosion on the surface. In the Type I model the patina grows into the alloy by replacing the alloy with minerals during the process of corrosion. This preserves the surface detail. The rate of patina growth at the alloy core /corrosion interface exceeds the rate of dissolution of the patina at the corrosion layers/environment interface. The rate of dissolution of copper slows down until an equilibrium in copper content between the alloy and the outer corrosion layer is reached (Robbiola *et al*. 1998, 2105). The tin content of the alloy is related to the tin content in the patina. It was found that soil and minor alloying elements do not play a major role in the selective dissolution of copper (Robbiola *et al*. 1998, 2106). The minor alloying elements do not modify the ratio between Cu and Sn in the alloy and in the outer corrosion layer or patina (Robbiola *et al.* 1998, 2107). In Type I the corrosion stabilizes (i.e. ceases) once the Cu and Sn content in the metal and in the corrosion reach equilibrium during the replacement of the original surface metal by corrosion.

In Type II corrosion the surface detail is damaged or lost. The inner corrosion layer was low in Cu, high in Sn, and contains copper oxide. Decuprification occurs in this type of corrosion. The middle corrosion layer was red cuprous oxide that functions as an electrolytical membrane, allowing the transport of anions inward and cuprous ions outward (Robbiola *et al*. 1998, 2100). The outer corrosion layer consisted of the precipitation of copper compounds such as malachite, atacamite, and paratacamite. Hydroxysilicates and/or hydroxyphosphates, together with silica or aluminosilicates from the soil, were also found. A layer of CuCl was often found between the inner and middle corrosion layers (Robbiola *et al*. 1998, 2100). In Type II the corrosion does not stabilize on account of a cuprite layer that forms permitting the continuous dissolution of copper resulting in a loss of surface detail.

This study concludes that Type I and Type II Corrosion Models can be applied to most ancient archaeological bronzes, with or without lead (Robbiola *et al*. 1998, 2109).

Since lead is not miscible in the alloy it does not modify the α-phase or the δ-phase (Robbiola *et al*. 1998, 2087). Tin plays a passivating role in both models.

3.2.3 Accelerated Corrosion Tests on New Copper Alloys to reproduce the Effects of Burial Conditions on Archaeological Bronzes

Preventing and controlling the corrosion of archaeological copper alloy objects continues to represent a major challenge to conservators. In an attempt to find corrosion inhibitors that are effective in preventing bronze disease numerous analytical projects have been carried out. Two such projects testing several corrosion inhibitors on new and archaeological copper alloys were carried out at the Institute of Archaeology, University College London (Faltermeier 1995; Golfomitsou 2006).

In an attempt to understand the processes involved in the corrosion of archaeological bronzes during burial and to discover conservation treatments successful for combating corrosion many studies have been carried out. One such study succeeded in replicating a passivating SnO_2 layer on the surface of a copper tin alloy. Copper tin binary alloy of 16% Sn was subjected to accelerated corrosion by anodic polarization testing in a 0.01M sodium sulphate solution of pH 5.8 (Mabille *et al*. 2003). Composition of the corrosion layer that formed was monitored by SEM-EDS. It was expected that the less noble metal, Sn in this case, would dissolve first. Instead selective dissolution of copper occurred which is attributed to the formation of a passive oxide film (SnO_2) on the tin that acted as a protective layer. This inhibited dissolution of the copper (Mabille *et al*. 2003, 863). The accelerated corrosion testing resulted in cracking along the axes of the dendrites. The rate of dissolution of copper differed between the dendrites and the bulk matrix. This is due to the heterogeneous composition of the alloy, the dendrites were enriched with copper from the casting process that became depleted during testing (Mabille *et al*. 2003, 864). Thicker corrosion formed on the dendritic zones. Cracks in the corrosion layer resulted from the decuprification process (causing internal stresses), allowing access of the electrolyte to the metal core and further corrosion (Mabille *et al*. 2003, 864). The structure and composition of the resulting corrosion was similar to the Type I corrosion identified on archaeological bronzes (Robbiola *et al*. 1998). This corrosion structure consists of a Sn-enriched passivating layer that preserves the original surface.

IMMACO (Improvement of Means of Measurement on Archaeological Copper-Alloys for Characterization and Conservation) was a project coordinated by the Institut Français d'Archéologie Orientale of the European Commission. It was supported by seven laboratories in France, Belgium and Germany (European Commission 1998). “One of the aims of this project was to study copper alloy compositions of European objects dating from the Bronze Age to Roman times. This work has revealed that five types of alloy seem to be particularly representative of what was produced in Europe during this period. These alloy compositions will be certified as reference materials by the European Union. In the second part of the project, artificial patinas have been made on the different bronze alloys using electrochemical polarizations as the surface modification techniques. The characterization of the corrosion surfaces and interfaces formed during the treatment with light microscopy (LM) and scanning electron microscopy (SEM-EDX, x-ray mapping) have shown that the artificial patinas seem to be very close to those from excavations. As a consequence, the patinated specimens can be used as a substitute for genuine artifacts in the future to improve conservation techniques.” (Beldjoudi *et al.* 2001a, 803).

The five bronze standards produced by IMMACO consist of a quaternary bronze (7% Sn, 9% Pb, 6% Zn), an arsenic copper, a tin bronze (7% Sn), a leaded tin bronze (10% Pb, 10% Sn), and brass (15% Zn, 2% Sn) (Beldjoudi *et al.* 2001b, 233).
As part of the IMMACO project 3 copper alloys were electrochemically corroded to reproduce archaeological bronze: a tin bronze (7% Sn), a leaded bronze (10% Sn, 10% Pb), and a quaternary bronze (7% Sn, 9 % Pb, 6% Zn) (Beldjoudi *et al*. 2001b). The copper alloys were subjected to the electrolytes Na_2SO_4, NaCl, and $NaHCO_3$ that formed oxides (Cu_2O, SnO_2), chlorides, carbonates ($PbCO_3$, $Cu_2(CO_3)(OH)_2$), and sulphates. Enrichment of tin compounds occurred at the metal/corrosion interface and in the surface layers of the binary and quaternary bronzes, faithfully reproducing the corrosion structure of archaeological quaternary bronze (Beldjoudi *et al*. 2001b, 234). These findings regarding tin enrichment are in agreement with those of Mabille *et al*. (2003).

Critical Review of Section 3.2.3 Accelerated Corrosion Tests on New Copper Alloys to reproduce the Effects of Burial Conditions on Archaeological Bronzes

The study of corrosion has sometimes involved the artificial patination of test coupons that are used as a substitute for naturally corroded, archaeological bronze. “Patinated specimens can be used as a substitute for genuine artifacts…” (Beldjoudi

2001a, 803). How representative is this patination compared to authentic archaeological patina (i.e. corrosion)? Attempts have been made by Mabile (Mabile *et al.* 2003) and Beldjoudi (Beldjoudi *et al.* 2001b) to simulate the corrosion of archaeological bronze on lab coupons with partial success. There are certain limitations in using artificially corroded bronze in place of archaeological bronze that has corroded naturally during burial. A bronze object is exposed to many uncontrollable variables such as pH, temperature, moisture, and contaminants during burial. For this reason artificial patination in the laboratory cannot accurately reproduce the corrosion on archaeological bronzes. In the experimental work in Chapter 4 the new bronze test coupons were not artificially patinated prior to corrosion testing. The intent was to avoid the creation of an unnatural patina to enable the comparison between the reaction of non-corroded bronze test coupons with naturally corroded archaeological bronze artifacts exposed to volatile organic acids.

The limitations of the use of accelerated corrosion testing in artificial laboratory conditions as a substitute for real time corrosion in real life museum conditions have to be considered. We cannot delude ourselves in thinking that the controlled test conditions in the laboratory simulate actual display and storage conditions since many of the variables and contaminants at play in the museum are excluded. Another disadvantage of accelerated corrosion testing is the inducement of stress that can cause the physical alteration of the metal, setting up new avenues of corrosion that may not occur under normal conditions of burial or museum storage/display.

Advantages of accelerated corrosion testing include the capability of monitoring the corrosion process, i.e. the dissolution of the metal, preferential corrosion, and the influence of composition on the corrosion process(es). By exposing test pieces to a few specific and controlled variables during laboratory corrosion testing we are able to focus on the corrosion mechanisms specific to these variables, without interference from uncontrolled variables such as fluctuating temperature/relative humidity or contaminants such as sulphur dioxide (Wadsak *et al.* 2002). Accelerated corrosion testing can elucidate certain aspects of corrosion processes that take place in archaeological metals to provide an understanding of the vulnerabilities and reactivity of the metal in the attempt to protect and conserve artifacts. Studies of the corrosion characterization and morphology of naturally corroded archaeological bronze, such as those by Robbiola (Robbiola *et al.* 1998) and Caley (Caley 1964), are of the utmost importance for comparison with bronze

that has undergone artificial patination and/or accelerated corrosion testing. They serve as a qualitative guide to the reliability of corrosion reproduction or simulation.

For these reasons the corrosion testing implemented in Chapter 4 includes accelerated as well as non-accelerated conditions. Elevated levels of acetic acid and relative humidity (e.g. 40 ppm and 86% RH) that far exceed those commonly found in museums create accelerated test conditions. The exposure of authentic, naturally corroded archaeological bronze to acid and moisture levels commonly found in museums (e.g. 0.4 ppm and 52% RH) in Chapter 4 was to promote "real conditions" of corrosion testing. It is important to carry out experimentation on naturally corroded archaeological artifacts in addition to test coupons for a more representative picture. For this reason authentic, archaeological bronzes corroded from burial were included in the experimental work in Chapter 4. It is acknowledged that the conditions during corrosion testing in Chapter 4 did not include all environmental variables and contaminants that can occur in the museum environment.

3.2.4 Corrosion Tests on Pure Copper and Copper Alloys exposed to Water Vapour

It is important to review the corrosion behavior of metals exposed to moisture before examining the effects of the addition of acid to the exposure tests. This lays the foundation for an understanding of the mechanisms of attack by acid and will help distinguish the corrosion processes due to moisture from those caused by atmospheric contaminants.

3.2.4.1 Pure Copper exposed to Water Vapour

Pure copper was exposed to three levels of Relative Humidity (RH), 43%, 58% and 78%, in an uncontaminated atmosphere in an airtight chamber for 21 days at 30° C (Cano *et al*. 2001a, E26). The purpose of this study was to determine the composition of the corrosion as a function of RH. The resulting corrosion was analysed by X-ray Photoelectron Spectroscopy (XPS) (Cano *et al.* 2001a, E26). The components at the beginning of the corrosion test were found to be: at 78% RH copper hydroxide (major component, cuprite (minor component); at 58% RH copper hydroxide and cuprite were present in equal amounts; at 43% cuprite major, copper hydroxide minor. The formation of an oxide film on the surface occurs by the establishment of local anodic and cathodic

areas under the adsorbed water layer on the metal (Cano *et al*. 2001a, E26). The X-rays of XPS caused the removal of the outer layer of copper hydroxide and its decomposition to cuprite (Cano *et al*. 2001a, E28). The reduction of cupric hydroxide that occurred may more likely be an effect of the ultra high vacuum (UHV) conditions in XPS (Wu *et al.* 2006). Mixed layers of cuprite and copper hydroxide form a more adherent corrosion layer than cuprite on its own which is porous and allows the diffusion of copper ions from the metal to the outer corrosion layer (Cano *et al*. 2001a, E30). Corrosion layers combining cuprite and copper hydroxide tend to retard the diffusion of copper to the surface. A parallel is drawn between the amount of copper hydroxide present and the corrosion rate; the higher the copper hydroxide content the lower the corrosion rate (Cano *et al*. 2001a, E30). The thickest corrosion layer(s) formed at the lowest RH whereas the thinnest corrosion layer(s) formed at the highest RH. The success of these layers as passivation layers will be determined in part by their thickness.

Another study of copper exposed to humidified air used three analytical means to examine the metal-atmosphere interface (Aastrup *et al*. 2000). The copper test pieces that were examined by infrared reflection absorption spectroscopy (IRAS) and quartz crystal microbalance (QCM) were artificially corroded to form cuprous oxide before exposing to RH 40%, 60% and 80%. The copper test pieces examined with atomic force microscopy (AFM) were untarnished when exposed to these RH levels. It was determined that "copper exposed to humidified air forms Cu_2O with an aqueous adlayer adsorbed on the surface. The formation of Cu_2O at 80% RH has a corrosion rate 1.5 to 2 times faster than at 60% RH. The growth of Cu_2O follows a logarithmic rate law and is enhanced by an increased RH." (Aastrup *et al*. 2000, 962). Changes in mass resulted from physisorbed water (reversible change), an aqueous adlayer adsorbed on the surface, and the formation of copper (I) oxide (irreversible change) (Aastrup *et al*. 2000, 961). At 80% RH the random formation of round features was observed (Aastrup *et al*. 2000, 964) in the scratches left from polishing. They are attributed to the formation of cuprous oxide grains and occurred more slowly at the lower RH levels. "The Cu_2O formed as grains with a diameter of around a few tens of nannometer and with a nucleation rate enhanced by RH" (Aastrup *et al*. 2000, 964). “The enhanced nucleation rate (contributes to) the increased oxidation rate at higher RH.” (Aastrup *et al*. 2000, 965). “Three effects of increased RH could be identified in this study” (Aastrup *et al*. 2000, 965):
(1)“The increase in number of physisorbed water clusters with relative humidity.” (Aastrup *et al*. 2000, 965):

Water is just as likely to bond with a clean metal surface as with other water since both have equal binding energies. Water tends to adsorb onto clean metal surfaces in clusters forming a heterogeneous aqueous adlayer (Figure 6.1 in Chapter 6). These water clusters may act as nucleation sites for Cu_2O grains. The higher the RH the more prolific the number of water clusters.

(2)"A gradual change with relative humidity towards more bulk-like properties of the physisorbed water layer." (Aastrup *et al*. 2000, 965):

Increased RH results in a thicker water layer that facilitates the mobility of surface species and affects the solubility of gases, thereby resulting in an increased oxidation rate.

(3)"The effect of relative humidity on the mechanism of Cu_2O growth." (Aastrup *et al*. 2000, 965):

Hydrogen defects may be introduced into the Cu_2O when the physisorbed water interacts with the oxide. "Oxygen in the aqueous adlayer and defects in the oxide promote the dissociation of water." (Aastrup *et al*. 2000, 966). Oxygen released from dissociated water contributes to the Cu_2O.

To summarize, high RH promotes defects in the oxide that enhance the transport of copper in the oxide. Stated another way, the oxidation rate may be increased by the formation of defects in the oxide at higher RH. In this case the oxygen derives from dissociated water and dissolved oxygen gas.

Critical Review of Section 3.2.4.1 Pure copper exposed to water vapour

The results of corrosion testing of pure copper exposed to three levels of RH by Cano *et al.* (2001a) and Aastrup *et al.* (2000) are directly applicable to the experimental work in Chapter 4. These studies showed the influence of relative humidity levels and the mechanisms of corrosion. Both studies agreed on the formation of an adsorbed water layer on the surface and the formation of cuprite as the initial corrosion compound. The XPS analysis by Cano *et al.* provided quantitative elemental composition whereas the analysis with AFM (atomic force microscopy) by Aastrup *et al.* was carried out with nanoscale resolution providing a close look at corrosion mechanisms. These studies lay the groundwork for the corrosion of copper and copper alloys in elevated levels of RH that can be directly applied to the examination of the role of acetic acid vapour when introduced in the experimental work in Chapter 4. The role that moisture plays on its

own is critical in the understanding of the reactions that take place when acetic acid is introduced. The studies confirm the function of cuprite as allowing the diffusion of copper ions from the metal to the outer corrosion layer, a vehicle that is enhanced by elevated RH.

3.2.4.2 Copper Alloys exposed to Water Vapour

This section examines the role alloying elements play in the corrosion of copper and copper alloys exposed to moisture. Quaternary bronze from the IMMACO Project was used to test the atmospheric corrosion of copper alloy exposed to moisture (Wadsak *et al*. 2002, 793). IMMACO is the Improvement of Means of Measurements on Archaeological Copper Alloys for characterisation and conservation. The composition of the bronze was Cu 76.5%, Sn 7.0%, Pb 9.0%, Zn 6.0% (Ni 0.10%, Fe 0.20%, As 0.20%, Sb 0.50%, S 0.30%). The copper alloy was prepared as a single-phase solution with lead precipitates not larger than 500 nm. The test pieces were exposed to 80% RH. X-ray Photoelectron Spectroscopy (XPS) and atomic force microscopy (AFM) showed that the copper in the bronze was present in the valence state 0 and 1 before testing, this corresponds to pure copper and cuprous oxide. Lead, zinc and tin were present in the oxidized state and lead was enriched on the surface before testing (Wadsak *et al*. 2002, 799). During exposure to 80% RH small features formed all over the surface but much more slowly than on pure copper in the study by Aastrup *et al*. (2000). They could not be identified (Wadsak *et al*. 2002, 799). A thicker layer of adsorbed water formed on the surface of the bronze (2 $\mu g\ cm^{-2}$) than on the pure copper (0.5 $\mu g\ cm^{-2}$). Infrared reflection absorption spectroscopy (IRAS) found lead oxide or hydroxide that could have formed during preparation of the test pieces. This could have protected the copper in the bronze and prevented the formation of copper oxide and could explain the lower corrosion rate and lower formation rate of features on the bronze compared to pure copper (Wadsak *et al*. 2002, 799). It was found that the introduction of SO_2 destroyed the protective layer of lead oxide/hydroxide.

Copper alloy containing more than 9% lead was found to be more protected from corrosion by a lead oxide layer (Wadsak *et al*. 2002, 801). It was concluded that corrosion processes on bronze are much more complex than corrosion on pure copper when exposed to high humidity. The only similarity was the roughness of the surface expressed as the root mean square (rms-roughness) that remained unchanged for the

duration of the tests on bronze (Wadsak *et al*. 2002, 795) and pure copper (Aastrup *et al*. 2000, 963). To summarize, the corrosion of a quaternary bronze (leaded brass) was similar to that of pure copper in the unchanging rms-roughness of surface and the formation of round elements on the surface but differed by a lower corrosion rate and lower formation rate of the round features on account of a protective layer of oxides from the alloyed elements.

Two copper binary alloys, bronze (Cu 92%, Sn 8%) and brass (Cu 90%, Zn 10%), were exposed to 80% RH to determine the influence of Sn and Zn on corrosion behavior (Kleber and Schreiner 2003, 294). The thickness of the water film that formed on each of the polished metals depended on the 1) chemical composition of the metal, 2) roughness of surface, 3) ambient RH, and 4) ambient temperature. Both developed round features on the metal surface that were inhomogeneous on the bronze and homogeneous on the brass. The rate of corrosion of bronze was found to be double that on brass. On the bronze the corrosion began in the scratches left from polishing (Kleber and Schreiner 2003, 298). Root mean square (rms)-roughness was measured with tapping mode atomic force microscopy (TM-AFM). Eventually a homogenous corrosion covering was achieved. Brass developed corrosion first in the scratches, spreading across the surface in a homogeneous fashion and attaining a constant rms-roughness.

To summarize, the corrosion of tin bronze and brass showed similarities with copper and quaternary bronze in the formation of round features on the surface, brass was similar to copper in the constant rms-roughness, and tin bronze was found to corrode faster and in a less uniform fashion than brass. It could be inferred that tin was less protective than zinc in these tests.

Critical Review of Section 3.2.4.2 Copper alloys exposed to water vapour

The studies by Wadsak (Wadsak *et al.* 2002) and Kleber and Schreiner (Kleber and Schreiner 2003) are extremely useful to this thesis as they comprised the corrosion testing of three copper alloys in 80% RH and facilitated their comparison with the same analytical technique, atomic force microscopy (AFM). AFM images and quantifies on the nanoscale as well as providing 3D surface profiling. The studies show the reaction of lead and the protective role of a lead corrosion layer that lowers the corrosion rate on leaded bronze compared to unleaded bronze and pure copper. These findings encouraged

the inclusion of leaded bronze test pieces in the experimental work in Chapter 4. The degree to which the lead content protects the copper component from corroding is an important aspect that is examined in Chapter 4.

3.2.4.3 Comparison of the Corrosion of Copper and Coppers Alloys by Water Vapour

To summarize this section on the corrosion of copper and copper alloys exposed to moisture, corrosion started in scratches on all metals and round features formed on all copper and copper alloys (binary and quaternary) that were identified as cuprite on the copper samples. A lead content of at least 9% can afford protection against corrosion. In general the alloyed elements tin, zinc and lead protected the copper from corrosion. Quaternary bronze corroded more slowly than pure copper; tin bronze corroded faster than brass.

3.2.5 Corrosion of Copper, Copper Alloys, and Other Metals exposed to Organic Acid Vapours

Copper and copper alloys have a high degree of resistance to atmospheric corrosion, due to the development of protective layers (Shreier 1978, 4:39). Copper doesn't usually displace hydrogen from acid solutions and is not attacked in non-oxidizing solutions (Shreier 1978, 4:53). Acetic and formic acids are not oxidizing and do not readily attack copper. Tin-bronzes are one of the copper alloys most resistant to acids. Brass is the least resistant of the copper alloys.

Exposure Levels of Acids

Aqueous solutions of acid that are in equilibrium with the air space in a closed container will have known vapour concentrations. There is a 1:50 relationship between the vol. % of acetic acid in aqueous solution and the concentration of acid vapour (ppm) and a 1:60 relationship between the vol. % formic acid in aqueous solution and the concentration in acid vapour (ppm). For example, a 1.0% vol. aqueous acetic acid solution is in equilibrium with 50 ppm acid vapour and a 1.0 % vol. aqueous formic acid solution is in equilibrium with 60 ppm acid vapour at 30° C (Donovan and Stringer 1971, 136, Fig. 1). These figures are based on acids as monomers that can be applied accurately to concentrations below 1 ppm. Above 1 ppm dimers are present (Donovan and Stringer, 1971, 133).

3.2.5.1 Acetic Acid

3.2.5.1.1 Corrosion Tests on Pure Copper exposed to Acetic Acid

The corrosive behavior of acetic acid will be examined on pure copper before proceeding to the more complex reactions resulting on copper alloys. The extent of corrosion is expressed in different forms: as quantification based on weight change or loss of surface; or in terms of corrosion rate. Results are presented in Table 3.2 (Appendix 1.1).

Table 3.2 Copper Exposed to Acetic Acid - Corrosion Results

ppm	ppm yr	ºC	RH%	Days	Compound description	Formula	Type of analysis	Reference
0.005	0.0002	30	100	21	No tarnish			Clarke & Longhurst 1961
0.05	0.002	30	100	21	No tarnish			Clarke & Longhurst 1961
0.5	0.02	30	100	21	Brown, blue spots		NA	Clarke & Longhurst 1961
0.5	0.02	30	100	21	Not provided		NA	Donovan & Stringer 1971
0.5	0.1	19	50	120	Not provided	Not provided	XRD	Thickett 1997
0.5	0.1	19	100	120	Dark brown, green, copper, unidentified compound	Cu	XRD	Thickett 1997
0.5	0.04	60	100	30	Mostly green, some white		NA	Thickett 1997
5	0.2	30	100	21	Black, blue crystals, dark green liquid		NA	Clarke & Longhurst 1961
5	0.2	30	100	21	Black, blue crystals, dark green liquid		NA	Clarke & Longhurst 1961
5	0.2	30	100	21	Not provided		NA	Donovan & Stringer 1971
5	1.6	19	50	120	Dark brown, copper, cuprite	Cu, Cu_2O	XRD	Thickett 1997
5	1.6	19	100	120	Dark brown, mostly green, Copper, unidentified compound	Cu	XRD	Thickett 1997
5	0.4	60	100	30	Mostly green,		NA	Thickett 1997

					some white			
10	0.5	30	40	21	Cuprite, copper hydroxide dihydrate, copper acetate dihydrate (minor)	Cu_2O, $Cu(OH)_2.2H_2O$, $Cu(CH_3COO)_2.2H_2O$	XRD XPS SEM	Cano & Bastidas 2002
10	0.5	30	80	21	Cuprite, copper hydroxide dihydrate, copper acetate dihydrate (minor)	Cu_2O, $Cu(OH)_2.2H_2O$, $Cu(CH_3COO)_2.2H_2O$	XRD XPS SEM	Cano & Bastidas 2002
10	0.5	30	100	21	Copper, cuprite	Cu, Cu_2O	XPS, XRD, FTIR, SEM, gravimetric, electro-chemical	Lopez-Delgado *et al.* 1998, Lopez-Delgado *et al.* 2001, Cano & Bastidas 2002
25	1.4	30	75	21	Slight tarnish		NA	Clarke & Longhurst 1961
50	2.8	30	100	21	Black, blue crystals, dark green liquid		NA	Clarke & Longhurst 1961
50	0.8	30	100	6	Dark, blue/green spots, dark green crystals		NA	Clarke & Longhurst 1961
50	2.8	30	100	21	Black, blue crystals, dark green liquid		NA	Clarke & Longhurst 1961
50	2.8	30	100	21	Not provided		NA	Donovan & Stringer 1971
50	2.8	30	100	21	Cuprite, copper hydroxide acetate dihydrate, copper acetate dihydrate	Cu_2O, $Cu(OH)(CH_3COO)_2.2H_2O$, $Cu(CH_3COO)_2.2H_2O$	XPS, XRD, FTIR, SEM, gravimetric, electro-chemical	Lopez-Delgado *et al.* 1998, Lopez-Delgado *et al.* 2001, Cano & Bastidas2002
100	5.7	30	40	21	Cuprite, copper hydroxide dihydrate, copper acetate dihydrate	Cu_2O, $Cu(OH)_2.2H_2O$, $Cu(CH_3COO)_2.2H_2O$	XRD XPS SEM	Cano & Bastidas2002
100	5.7	30	100	21	Cuprite, copper hydroxide acetate dihydrate, copper acetate dihydrate	Cu_2O, $Cu(OH)(CH_3COO)_2.2H_2O$, $Cu(CH_3COO)_2.2H_2O$	XPS, XRD, FTIR, SEM, gravimetric, electro-chemical	Lopez-Delgado *et al.* 1998, Lopez-Delgado *et al.* 2001, Cano & Bastidas2002
200	11.5	30	100	21	Cuprite, copper acetate dihydrate	Cu_2O, $Cu(CH_3COO)_2.2H_2O$ main component,	XPS, XRD, FTIR, SEM, gravimetric, electro-chemical	Lopez-Delgado *et al.* 1998, Lopez-Delgado *et al.* 2001, Cano & Bastidas2002
300	17.2	30	40	21	Cuprite, copper	Cu_2O, $Cu(CH_3COO)_2.2H_2O$	XRD	Cano &

					acetate dihydrate		XPS SEM	Bastidas2002
300	17.2	30	80	21	Cuprite, copper acetate dihydrate	Cu_2O, $Cu(CH_3COO)_2.2H_2O$	XRD XPS SEM	Cano & Bastidas2002
300	17.2	30	100	21	Cuprite, copper acetate dihydrate	Cu_2O, $Cu(CH_3COO)_2.2H_2O$ main component,	XPS, XRD, FTIR, SEM, gravimetric, electro-chemical	Lopez-Delgado *et al.* 1998, Lopez-Delgado *et al.* 2001, Cano & Bastidas2002
500	28.7	30	100	21	Black, blue crystals, dark green liquid		NA	Clarke & Longhurst 1961

NA = not analysed

Exposure of 0.005 and 0.05 ppm acetic acid at 100% RH caused no tarnish or corrosion on pure copper (Clarke and Longhurst, 1961). Exposure tests using 0.5, 5, 50 and 500 ppm acetic acid produced brown and black coatings with blue corrosion (Table 3.2) (Clarke and Longhurst 1961, 436). Exposure of 50 ppm acetic acid at 100% RH at 30° C for 6 days caused patchy dark tarnish with blue/green spots and deep green crystals (Clarke and Longhurst 1961, 436). It was determined that a RH greater than 85% was required before acetic acid promoted corrosion of pure copper (Clarke and Longhurst 1961, 442). Two forms of corrosion were found: type I powdery corrosion made up of mostly hydroxide and oxide, occurs at low acid concentrations and at high acid concentrations when the RH is 100%; type II a deliquescent layer forms at high concentrations of acid and at intermediate concentrations when the RH is less than 100% (Clarke and Longhurst 1961, 442).

In other exposure testing, copper corroded 9 times as much in 5 ppm acetic acid compared to 0.5 ppm acetic acid, and 30 times as much in 50 ppm at 100% RH for 3 weeks (Donovan and Stringer 1971, 133, 135). In acetic acid vapour pure copper was found to corrode less than pure lead or pure zinc, in agreement with the preceding study (Clarke and Longhurst 1961, 438). The corrosive effects of acetic acid on pure copper tested at 100% RH and 30° C for three weeks are reported in μm of surface lost in Table 3.2 (Donovan and Stringer 1971, 135). Exposure to 0.5, 5, and 50 ppm acetic acid at 100% RH and 30º C for 3 weeks resulted in 0.02 g/dm^2, 0.18 g/dm^2, and 0.60 g/dm^2 of surface loss respectively. To summarize the amount of copper corrosion increases exponentially with increase in acetic acid concentration; pure copper is more resistant to corrosion than pure lead and pure zinc.

Test samples were exposed to 0.5 and 5 ppm acetic acid at 50% and 100% RH at 19° C for 120 days and 60° C for 30 days (Thickett 1997). XRD analysis was unable to identify the corrosion products that formed after 120 day exposure that were dark brown and green in color, only copper could be identified (Thickett 1997, 7). Corrosion from the 30-day test was not analysed.

Pure copper was exposed to 10, 50, 100, 200 and 300 ppm acetic acid concentrations at 100% RH for 21 days at 30° C (López-Delgado *et al*. 1998). In all tests blue crystals formed during the first week that were surrounded by corrosion free zones. Corrosion followed the orientation of the scratches left from polishing. Analysis of the corrosion was carried out with XRD, FTIR and SEM. Corrosion was monitored by gravimetric measurements and electrochemical studies by cathodic reduction (López-Delgado *et al*. 1998; López-Delgado *et al*. 2001, 5205). The copper corrosion rate increased in line with increasing concentration of acetic acid. The corrosion rate was found to stabilize above 200 ppm (López-Delgado *et al*. 2001, 5205). Amorphous cuprite (Cu_2O) formed first by the reaction of water with copper followed by crystalline cuprite. At 10 ppm acetic acid the first layer of corrosion, copper (I) oxide, is amorphous and therefore cannot be identified by XRD (López-Delgado *et al*. 2001, 5209). Copper acetate was the next compound to form that coexisted with the crystalline cuprite. Copper hydroxide acetate was also identified (López-Delgado *et al*. 1998, 4140). Cuprite served as the path through which acetic acid vapour reacted with copper. The 50, 100, 200, 300 ppm tests produced cuprite and copper acetate dihydrate (López-Delgado *et al*. 1998, 4143). Copper hydroxide acetate was found in the 50, 100, and 200 ppm tests. In the 300 ppm sample copper acetate dihydrate $Cu(CH_3COO)_2.2H_2O$ (JCPDS 27-145) was the principal component (95%) and cuprite Cu_2O (JCPDS 5-667) made up 5%. XPS indicated a layered structure from the metal to the atmosphere: $Cu_2O/CuO/Cu(OH)_2$ or $CuO.xH_2O$ in the first passivating layer (López-Delgado *et al*. 1998, 4143).

"The presence of hydroxide or hydrated oxide at the initially exposed copper surface provides a building block for the formation of basic copper acetate. The formation of copper hydroxide acetate dihydrate may be as follows

$$4CuO \cdot xH_2O + 7CH_3COOH \rightarrow Cu_4(OH) + (CH_3COO)_7 \cdot 2H_2O + (x + 1)\, H_2O \quad (1)$$

This copper hydroxide acetate evolves to form copper acetate under the atmospheric conditions of high concentration of acetic acid, by the reaction

$$Cu_4(OH)(CH_3COO)_7 \cdot 2H_2O + CH_3COOH \rightarrow 4Cu(CH_3COO)_2 \cdot 2H_2O + H_2O \qquad (2)$$

The final constituents of the patina being cuprite and copper acetate dihydrate. Thus, the presence of copper hydroxide acetate among the patina components could mean that the patination process has not yet finished." (López-Delgado *et al*. 2001, 5207, 5208).

Cathodic reduction curves in 10 ppm acetic acid showed the following: the first peak represented the reduction of amorphous cuprite, the second peak represented the reduction of crystalline cuprite on the amorphous cuprite, the third peak is attributed to copper acetate (López-Delgado *et al*. 2001, 5205).

Examination with the SEM revealed on the 50 ppm samples clear droplets containing cuprite crystals and dark droplets containing acetic acid (López-Delgado *et al*. 1998, 4145). In the dark droplets a dendritic growth of copper hydroxide acetate was found extending from the edge of the droplet (area of highest acetic acid concentration) to the interior of the droplet. The arborescent crystallizations of cuprite afford a path through which acetic acid vapour may travel to the copper core (López-Delgado *et al*. 1998, 4145). At 100 ppm cuprite crystals are observed (López-Delgado *et al*. 2001, 5210). On the 100 ppm samples the copper hydroxide acetate formed rectangular prismatic crystals, the copper acetate formed "irregular, plate-like crystals growing perpendicular to the copper hydroxide acetate phase…" (López-Delgado *et al*. 1998, 4146). The copper hydroxide acetate forms on top of the cuprite, then the copper acetate forms next to the copper hydroxide acetate, eventually forming over the top of it. At 200 ppm the "plate-like copper acetate crystals" formed over the cuprite (López-Delgado *et al*. 1998, 4146). The high concentration of acetic acid disrupted the copper oxide surface. Cuprite crystals occur between the copper acetate crystals in places at 300 ppm acetic acid vapour. At 300 ppm the copper acetate layer covers the entire metal surface (López-Delgado *et al*. 1998, 4146). Two corrosion processes may be distinguished according to the level of acetic acid concentration. In the lower concentrations the acetic acid is adsorbed onto the wetted copper surface from the gas phase. Corrosion occurs on the adsorbed film of water and begins in a uniform manner (López-Delgado *et al*. 1998, 4147). At higher levels of concentration the copper hydroxide acetate and copper acetate

develop locally “from droplets of acetic acid adsorbed on the surface.” (López-Delgado *et al*. 1998, 4147).

In similar tests copper was exposed to 10, 50, 100, 200 and 300 ppm acetic acid for 21 days in tests at 40% and 80% RH at 30° C (Cano and Bastidas, 2002). Results are presented in Table 3.2. The corrosion rate was similar at 40% RH from10 to 100 ppm acetic acid. At 200 and 300 ppm the corrosion rate increased (Cano and Bastidas 2002, 329). At 80% RH the corrosion rate increased with each increase in acetic acid concentration. XPS of the samples exposed to 40% and 80% RH showed cuprite, copper hydroxide, and copper acetate at 10 and 100 ppm and cuprite and copper acetate at 300 ppm (Cano and Bastidas 2002, 331).

Examination with the SEM found that the corrosion started in the scratches left from polishing where water was retained (Cano and Bastidas 2002, 330). At 80% RH in 100 ppm copper acetate and cuprite crystals were surrounded by uncorroded areas. The corrosion formed by acetic acid was non-uniform and porous (Cano and Bastidas 2002, 335).

Summary of Section 3.2.5.1.1 Pure copper exposed to acetic acid

Corrosion occurred on copper in all tests that were conducted in the RH levels of 40%, 50%, 80%, 100%, and in acetic acid vapour concentrations of 0.5, 5, 10, 50, 100, 200, and 300 ppm. Three studies did not identify the corrosion products. Two of these studies report similar colors of brown and green (Clarke and Longhurst; Thickett) and one reports the formation of blue corrosion at the low concentration of 0.5 ppm in 100% RH after 6 days (Clarke and Longhurst). Clarke and Longhurst claimed that a RH of greater than 85% was required for copper to corrode that was most likely a result of the short test duration of 6 days. Corrosion was also reported at 0.5 ppm in 50% RH by Thickett over a 30 day period at 60° C and over 120 days at 19° C. The concept of the overall dose (concentration x time) of acetic acid is important so that the results from the various tests can be directly compared. The lowest observed adverse effect level [LOAEL] of acid concentration is used to calculate LOAED, “the cumulative dose concentration [LOAEL x time] at which the first signs of adverse effects are observed.” (Tetreault 2003a, 23). LOAED is expressed as mg m^{-3} yr or μg m^{-3} yr that can be converted to ppm or ppb per year. The LOAED of acetic acid on copper is reported to be

1000 μg m^{-3} yr (0.4 ppm yr) at 50 to 60% RH (Tetreault 2003a, 26). It is important to report the RH levels with the dose as they directly influence the amount of corrosion.

Critical Review of Section 3.2.5.1.1 Pure copper exposed to acetic acid

Two studies with the same test variables of 10, 50, 100, 200, and 300 ppm acetic acid for 21 days at 30° C may be directly compared (Table 3.2) (Lopez-Delgado 1998, 2001; Cano and Bastidas 2002). These acetic acid levels equate to the overall concentration doses of 0.5, 2.8, 5.7, 11.5, and 17.2 ppm yr respectively. Cano and Bastidas tested the RH levels of 40% and 80% whereas Lopez-Delgado tested 100% RH. Blue corrosion in the first week formed at a higher dose (0.2 ppm yr) than the blue corrosion found by Clarke and Longhurst at 0.008 ppm yr. Two identical corrosion products, cuprite and copper acetate, were identified in the studies by Lopez-Delgado and Cano. A discrepancy was found in the identification of hydroxide compounds, however. Copper hydroxide acetate was found in 100% RH (Lopez-Delgado *et al.* 1998) but not in 40% or 80% RH (Cano and Bastidas 2002). This indicates that the increased moisture present at 100% RH contributes to the formation of an intermediate compound, copper hydroxide acetate, that is not required for the formation of copper acetate at lower relative humidities. Another explanation for the discrepancy may lie in the number and types of analytical techniques used for identification: Cano used XPS whereas Lopez-Delgado used XRD and FTIR. A second discrepancy was found at 10 ppm (0.5 ppm yr) acetic acid concentration: copper acetate was identified by Cano in 40% and 80% RH whereas it was not identified in 100% RH by Lopez-Delgado. A possible explanation may be attributed to different amounts of moisture. Lopez-Delgado *et al.* have shown that in lower concentrations acetic acid is adsorbed onto the metal surface wetted by moisture. It is conceivable that the high RH level of 100% and the resulting abundant wetting of the surface were great enough to dilute the effects of the lowest concentration level of 10 ppm (0.5 ppm yr). At higher acid concentration levels this dilution was overcome in 100% RH and copper acetate was formed.

While the corrosion rate was found to increase steadily with increasing acetic acid concentration at 100% RH (Lopez-Delgado *et al.* 1998; Donovan and Stringer 1971), at 40% RH the corrosion rate was found to be similar from 10 to 100 ppm (0.5 to 5.7 ppm yr) (Cano and Bastidas 2002). This may be attributed to reduced wetting of the metal surface in the lower RH.

These studies indicate that a dose concentration of acetic acid as low as 0.008 ppm yr in 100% RH can produce corrosion (Clarke and Longhurst 1961) and that 0.5 ppm yr in 40% RH will produce copper acetate corrosion (Cano and Bastidas 2002). These results were used as a guide in the selection of acetic acid concentrations in the experimental work in Chapter 4. The low dose concentrations of 0.046 ppm yr at 32% RH, 0.049 ppm yr at 52% RH, and 0.063 ppm yr at 86% RH were chosen to provoke copper corrosion and the high dose concentrations of 4.602 ppm at 32% RH, 4.931 ppm yr at 52% RH, and 6.356 ppm yr at 86% RH were chosen to produce acetate corrosion within the time limits of the tests (Table 4.6).

The early studies of Clarke and Longhurst (1961) and Donovan and Stringer (1971) provided an initial assessment of the corrosive influence of acetic acid and relative humidity on pure copper. Since then researchers have used XRD for the identification of corrosion with some shortcomings (Thickett 1997). XRD can indicate the presence of amorphous material by a halo in the data but cannot identify amorphous compounds. To compensate additional techniques have been added to the analytical repertoire for the identification of corrosion including FTIR, XPS, and SEM-EDS. Monitoring of corrosion in these studies was carried out gravimetrically, electrochemically, and with the SEM. Cuprite was found to be the first corrosion product to form on pure copper in volatile acetic acid as well as on pure copper in moisture. The development and growth of corrosion starting from cuprite to copper hydroxide acetate and copper acetate and was monitored with SEM imaging (Lopez-Delgado 1998, 2001).

The studies that traced the growth and morphology of corrosion caused by acetic acid vapour using the SEM have focused on pure copper (Lopez-Delgado *et al.* 2001). This study on pure copper cannot be directly applied to bronze on account of the influence of the alloyed elements on corrosion. In order to overcome this gap in our knowledge of the corrosion behavior of bronze two copper alloys were monitored with the SEM in Chapter 4 that proved extremely enlightening. The morphologies described by Lopez-Delgado *et al.* (1998, 2001) were used for comparison in the experimental work in Chapter 4. The formation of the intermediary corrosion product, copper hydroxide acetate, as determined by these researchers was also investigated in Chapter 4 on copper alloys.

The studies reviewed in this section corroborate each other by confirming that an increase in acetic acid concentration and/or RH level causes increased corrosion rate. The most interesting aspect of this section is the influence of acetic acid concentration on the role of moisture in the corrosion process. One of the goals of the experimental work in Chapter 4 was to determine the synergy of moisture and acetic acid vapour on copper alloys. The elevated levels of 11.5 ppm yr and 17.2 ppm yr acetic acid (Lopez-Delgado *et al.* 1998) were not included in the thesis experiments as they represent exaggerated conditions not found in museums and override much of the importance of the contribution of moisture to corrosion. The analytical techniques used by the researchers in this section, XRD, FTIR, SEM, and SEM-EDS, were adopted in the Chapter 4 experimental work to facilitate comparability of data from these studies.

3.2.5.1.2 Corrosion Tests on Copper Alloys exposed to Acetic Acid

Very little corrosion testing on bronze (copper-tin alloy) exposed to acetic acid has been published to date (Bastidas *et al*. 1995; López-Delgado *et al*. 1997). These studies concentrated on the protective effects of the bronze patina, copper sulphide, commonly formed on outdoor bronze sculpture from sulphur dioxide pollutants and occasionally on archaeological bronze objects from anoxic environments. Two copper alloys (leaded copper tin bronze (8% Sn, 5% Pb) and a leaded copper tin bronze with zinc (5% Sn, 5% Pb, 4% Zn), in a patinated (copper sulphide) and unpatinated state, were exposed to 25 (2 ppm yr), 83 (6.8 ppm yr), 225 ppm (18.4 ppm yr) of acetic acid vapour in 100% RH at 30° C for 30 days (Bastidas *et al*. 1995). The patinated copper-tin-lead alloy was found to corrode faster than the unpatinated test pieces and formed copper acetate. Patination did provide protection for the copper-tin-lead-zinc alloy, however (Bastidas *et al*. 1995, 517). A leaded copper-tin bronze (8% Sn, 5% Pb) was patinated (copper sulphide) and exposed to 225 ppm (12.9 ppm yr) acetic acid vapour at 100% RH for 21 days (López-Delgado *et al*. 1997). Copper acetate hydrate was identified by XRD (López-Delgado *et al*. 1997, 777). The overall conclusion may be drawn that copper sulphide patina does not protect leaded bronze from corroding in the acetic acid dose concentration of 2 ppm yr and may act as a catalyst in the formation of acetate.

Critical Review of Section 3.2.5.1.2 Copper alloys exposed to acetic acid vapour

The only studies that tested the corrosive effects of acetic acid on copper alloys focused on the protective qualities of a patinated surface consisting of copper sulphide (Bastidas *et al.* 1995, Lopez-Delgado *et al.* 1997). In these tests bronze was artificially patinated to form a copper sulphide coating. These results are not directly applicable to the experimental work in this thesis since artificial patination was not included although the acetic acid dose concentration that produced copper acetate in the Bastidas *et al.* tests falls within the range tested in Chapter 4. Although copper sulphide can form on archaeological bronzes in anoxic environments the more common corrosion products are oxides, carbonates, and chlorides. Since the focus of this thesis is the corrosion and protection of copper alloy archaeological objects from the volatile carbonyl compounds, naturally corroded archaeological artifacts with oxides, carbonates, and chlorides from burial, as well as uncorroded new bronze (avoiding interference from artificial patinas), were tested to address the issues of archaeological materials. The experimental work in Chapter 4 was designed to address this considerable gap in our knowledge.

3.2.5.2 Formic Acid and Other Variables

Formic acid is a simple organic molecule that can react by complete fragmentation, dehydrogenation, or dehydration:

Fragmentation: $C_{(a)} + H_{2\,(g)} + 2O_{(a)}$
Dehydrogenation: $CO_2 + H_2$
Dehydration: $CO + H_2O$

(Bowker *et al*. 1998b, 188).

3.2.5.2.1 Exposure and Adsorption of Formic Acid on Copper and Bronze

Adsorption of formic acid on metal surfaces takes place by dehydrogenation. Dehydrogenation is defined as "a reaction in which hydrogen is detached from a molecule" (Fulton 2002, 1). At room temperature formic acid dehydrogenates to give hydrogen and carbon dioxide by desorption and bonds with copper as formate (Section 3.2.5.2.2). A formate that is unstable at room temperature forms on late transition metals

(copper is a late transition metal), on IB metals (Cu, Ag, and Au) the formate is "stable to higher temperatures" (Bowker *et al*. 1998a, 77).

Because formic acid is involved in catalytic reactions including those in the synthesis of methanol it has been examined in great depth in many studies (Bowker *et al*. 1996; Bowker *et al*. 1998a; Bowker *et al*. 1998b; Hsu *et al*. 2003; Poulston *et al*. 1997).

When formic acid "dehydrogenates and bonds" with copper as formate "it produces a resistance change." (Hsu *et al*. 2003, 123). The two techniques used in the study of adsorption kinetics, dc resistance and nonresonant infrared reflectance measurements, are non-destructive (Hsu *et al*. 2003, 121). They can be carried out in real time while exposing the sample to gas. The resistance is suitable for studying the first chemisorbed layer whereas the reflectance is suited for studying the transition to the subsequent multilayers and these layers themselves. The two methods are complementary.

The adsorption of formic acid on Cu precoated with oxygen was studied by Scanning Tunnelling Microscopy (STM), a molecular beam system, Temperature-Programmed Desorption (TPD), and Low Energy Electron Diffraction (LEED) (Bowker *et al*. 1996, 97; Bowker *et al*. 1998b, 185; Poulston *et al*. 1997, 66; Stone *et al*. 1998, 71). The molecular beam reactor probes the kinetics of reaction and the STM examines the structural and dynanic aspects of reaction. The molecular beam provides macroscale kinetic information and the STM provides a link with the nanoscale events at atomic resolution. The thickness of the oxygen layer plays a major role in the corrosion. Less than 0.25 monolayers of oxygen results in no adsorption of oxygen on the surface since it is removed as water by the reaction with formic acid to produce formate according to this reaction: $2HCOOH_{(g)} + O_{(a)} \rightarrow H_2O_{(g)} + 2HCOO_{(a)}$ (Bowker *et al*. 1998b, 189). Thicker (0.5 monolayers) oxygen coverage results in coadsorption of oxygen and formate on the surface. From room temperature, 300 K (27° C), to 400 K (127° C) the oxygen and formate form separate islands in a reaction stoichiometry of 2:1 formic acid:oxygen atoms. Above 400 K (127° C) the formate is unstable and the reaction stoichiometry changes from 2:1 to 1:1. The structure of the formate was found to vary depending on temperature of the substrate, amount of oxygen precoverage, and formic acid exposure. The adsoprtion of formic acid on oxygen pre-dosed Cu below 400 K proceeds as follows:

$HCOOH_{(g)} + O_{(ads)} \rightarrow HCOO_{(ads)} + OH_{(ads)}$ (1)

$HCOOH_{(g)} + OH_{(ads)} \rightarrow HCOO_{(ads)} + H_2O_{(g)}$ (2)

Above 400 K:

$HCOO_{(ads)} + OH_{(ads)} \rightarrow CO_{2(g)} + H_2O_{(g)}$ (3)

(Stone *et al*. 1998, 71).

To summarize, the structure of the formate depends on temperature of the substrate, amount of oxygen precoverage, and formic acid exposure; the molecular beam reactor probes the kinetics of reaction and the STM examines the structural and dynanic aspects of reaction.

3.2.5.2.2 Corrosion Tests of Pure Copper exposed to Formic Acid and Formaldehyde

Numerous exposure tests of copper to formic acid have been carried out by several researchers. The results are presented in Table 3.3 (Appendix 1.2).

Table 3.3 Results of Corrosion Tests of Copper with Formic Acid and Formaldehyde

ppm	ppm yr	ºC	RH %	Days	Compound description	Formula		Author
FORMIC ACID								
0.2	0.07	23	75	135	Cuprite, tenorite or hydroxy-copper compound	Cu_2O, CuO	XRD	Tetreault *et al.* 2003
0.5	0.1	19	50	120	Not provided	Cu	XRD	Thickett 1997
0.5	0.1	19	100	120	Dark, green, cuprite, unidentified compound	Cu_2O	XRD	Thickett 1997
0.5	0.04	60	100	30	Black		NA	Thickett 1997
0.6	0.03	30	100	21	Not provided			Donovan & Stringer1971
5	1.6	19	50	120	Dark, cuprite	Cu_2O	XRD	Thickett 1997
5	1.6	19	100	120	Copper hydroxide hydrate (?), unidentified compound		XRD	Thickett 1997
5	0.4	60	100	30	Black		NA	Thickett 1997
6	0.3	30	100	21	Not provided		NA	Donovan &

								Stringer1971
8	2.9	23	75	135	Cuprite, tenorite or hydroxy-copper compound	Cu_2O, CuO	XRD	Tetreault *et al.* 2003
10	0.5	30	40	21	Cuprite, copper hydroxide monohydrate, copper formate ?	Cu_2O, $(Cu(OH)_2.H_2O)$, $Cu(HCOO)_2$	XPS	Cano *et al.* 2001b, Cano & Bastidas 2002
10	0.5	30	80	21	Cuprite, copper hydroxide monohydrate, copper formate ?	Cu_2O, $(Cu(OH)_2.H_2O)$, $Cu(HCOO)_2$	XPS	Cano *et al.* 2001b, Cano & Bastidas 2002
10	0.5	30	100	21	Copper (II) hydroxide monohydrate	$(Cu(OH)_2.H_2O)$	XRD	Lopez-DelGado *et al.* 2001, Bastidas 2000
14	5.1	23	54/ 75	135	Copper formate	$Cu(CHO_2)_2$	XRD	Tetreault *et al.* 2003
50	2.8	30	100	21	Cuprite, copper (II) hydroxide monohydrate	Cu_2O, $(Cu(OH)_2.H_2O)$	XRD	Lopez-DelGado *et al.* 2001, Bastidas 2000
60	3.4	30	100	21	Not provided		NA	Donovan & Stringer 1971
100	5.7	30	40	21	Cuprite, copper hydroxide monohydrate, copper formate	Cu_2O, $(Cu(OH)_2.H_2O)$, $Cu(HCOO)_2$	XPS	Cano *et al.* 2001b, Cano & Bastidas 2002
100	5.7	30	80	21	Cuprite, copper hydroxide monohydrate, copper formate	Cu_2O, $(Cu(OH)_2.H_2O)$, $Cu(HCOO)_2$	XPS	Cano *et al.* 2001b, Cano & Bastidas 2002
100	5.7	30	100	21	Cuprite, copper (II) hydroxide monohydrate, copper formate	Cu_2O, $(Cu(OH)_2.H_2O)$ $Cu(HCOO)_2$	XRD	Lopez-DelGado *et al.* 2001, Bastidas 2000
140	51.7	23	54/ 75	135	Copper formate dihydrate	$Cu(CHO_2)_2.2H_2O$	XRD	Tetreault *et al.* 2003
200	11.5	30	100	21	Cuprite, Copper hydroxide formate, Copper formate	Cu_2O, Cu(OH)HCOO $Cu(HCOO)_2$	XRD	Lopez-DelGado *et al.* 2001, Bastidas 2000
300	17.2	30	40	21	Cuprite, copper hydroxide monohydrate, copper formate	Cu_2O, $(Cu(OH)_2.H_2O)$, $Cu(HCOO)_2$	XPS	Cano *et al.* 2001b, Cano & Bastidas 2002
300	17.2	30	80	21	Cuprite, copper hydroxide monohydrate, copper formate	Cu_2O, $(Cu(OH)_2.H_2O)$, $Cu(HCOO)_2$	XPS	Cano *et al.* 2001b, Cano & Bastidas 2002
300	17.2	30	100	21	Copper hydroxide formate, Copper formate	Cu(OH)HCOO $Cu(HCOO)_2$	XRD	Lopez-DelGado *et al.* 2001, Bastidas 2000
FORMALDEHYDE								
0.5	0.1	19	50	120	Dark	Cu	XRD	Thickett 1997
0.5	0.1	19	100	120	Dark	Cu	XRD	Thickett 1997
0.5	0.04	60	100	30	Dark, black		NA	Thickett 1997
5	1.6	19	50	120	Black, cuprite	Cu, Cu_2O	XRD	Thickett 1997
5	1.6	19	100	120	Dark	Cu	XRD	Thickett 1997
5	0.4	60	100	30	Dark, black		NA	Thickett 1997

NA = not analysed

Examination of the reaction of formic acid oxidation with Cu was carried out with Scanning Tunnelling Microscopy (STM) with a molecular beam reactor (Bowker *et al*. 1998a). "2D crystallisation" occurs when the adsorbate coverage exceeds a critical level. This involves precipitation of the adsorbate from the surface solvent and its crystallisation (Bowker *et al*. 1998a, 82). Images show the beginning of the formation of formate islands between oxygen islands on the surface of the copper. These copper

formate islands are the "2D crystallisation" of the adsorbate. "For formic acid on Cu(110), the reaction of formic acid to produce formate by reduction of surface oxygen to liberate gas-phase water results in mass migration of surface Cu atoms, which diffuse to their most stable sites." (Bowker *et al*. 1998a, 83). Below the 2D solubility limit, the adsorbate is mobile and unstructured. The crystals resulting from 2D crystallisation are in dynamic equilibrium with the inter-island solution on the metal surface (Bowker *et al*. 1998a, 83).

Another study of the reaction of formic acid on pre-oxidized copper was carried out using the surface science techniques of temperature programmed desorption (TDP) and X-ray photoelectron spectroscopy (XPS) (Carley *et al*. 1998). Copper formate decomposes on copper at 440 K to give hydrogen and carbon dioxide by desorption in a 1:2 ratio (Carley *et al*. 1998, 401). Carbonates form on copper from the oxidation of carbon dioxide. The oxidation of formic acid can also produce carbonates on the surface of copper (Carley *et al*. 1998, 409). The formation of carbonate involves one formic acid molecule whereas the formation of formate involves two formic acid molecules. For this reason carbonate can form from a single adsorption site and therefore may form more easily than formate. Carbonate can be hydrogenated to formate (Carley *et al*. 1998, 411).

The corrosive effects of formic acid on pure copper tested at 100% RH and 30° C for three weeks are reported in μm of surface lost. Copper loss ranged from 0.15 to 0.71 g/dm^2 from 0.6 to 6 ppm formic acid (Donovan and Stringer 1971, 135). Copper was exposed to formic acid vapour at 54% and 75% RH for 135 days (Tetreault *et al*. 2003). Formic acid concentration ranged from 0.6 - 40 ppm at 54% RH and from 0.2 - 140 ppm at 75% RH. Results showed that above 0.4 ppm the copper began to react significantly and the surface turned brown-green. Above 14 ppm white corrosion appeared. A formic acid concentration greater than 2 ppm was found to contribute to a significant weight gain. At 14 ppm copper formate ($Cu(CHO_2)_2$) formed and at 140 ppm copper formate dihydrate ($Cu(CHO_2)_2.2H_2O$) was identified (Tetreault *et al*. 2003, 239)

In another set of tests exposing copper to formic acid (0.2 and 8 ppm) at 75% RH for 135 days produced mainly cuprite (Tetreault *et al*. 2003, 244). An inner layer of cuprite and an outer layer of tenorite or hydroxy-copper compound formed. These serve as the foundation for the formation of formates (Tetreault *et al*. 2003, 244).

Corrosion of copper was tested by exposing copper to formic acid vapour concentrations of 10, 50, 100, 200 and 300 ppm at 100% for 21 days (Bastidas *et al*. 2000; López-Delgado *et al*. 2001). Corrosion was monitored by gravimetric measurements, electrochemical studies by cathodic reduction, SEM, XRD and FTIR. XRD identified copper, copper (II) hydroxide monohydrate ($Cu(OH)_2.H_2O$) (JCPDS 42-746) at 10 ppm formic acid. Copper (II) hydroxide monohydrate and cuprite (JCPDS 5-667), and possibly copper hydroxide formate (Cu(OH)(HCOO) (maybe a tetrahydrate), were found at 50 and 100 ppm formic acid. It was determined that copper hydroxide formate formed from copper hydroxide and started to appear in 200 ppm formic acid. Copper hydroxide disappeared at 300 ppm (López-Delgado *et al*. 2001, 5207).

Cathodic reduction curves from tests in 10 ppm formic acid showed the following: the first peak represented the reduction of amorphous cuprite, the second peak represented the "reduction of copper (II) hydroxide monohydrate", the third peak represented the "reduction of amorphous copper formate on the … amorphous cuprite", the fourth peak is attributed to copper formate (López-Delgado *et al*. 2001, 5205).

At low concentrations of formic acid, cuprite and copper hydroxide formed. From 100 to 300 ppm these two components decreased and copper formate increased around droplets of formic acid adsorbed on the surface that "originated by a dissolution-precipitation reaction mechanism" (Bastidas *et al*. 2000, 1004; López-Delgado *et al*. 2001, 5211).

The corrosion of copper exposed to formic acid proceeds as follows (López-Delgado *et al*. 2001, 5208):

"Exposed first to 100% RH:

$4Cu + O_2 + 4H^+ \rightarrow 4Cu^+ + 2H_2O$

first solid corrosion product formed is copper hydroxide monohydrate. The Cu (I) becomes oxidized:

$4Cu^+ + O_2 + 4H^+ \rightarrow 4Cu^{2+} + 2H_2O$

this reaction is favored by formic acid on account of its higher value of the dissociation constant.

Cathodic reaction:

$O_2 + 2H_2O + 4e^- \rightarrow 4OH^-$

produces hydroxyl ions that can form copper hydroxide during or after drying. Hydroxide or hydrated oxide forms the building blocks for copper formate.
Formation of copper formate from copper hydroxide monohydrate $Cu(OH)_2.H_2O$:
$Cu(OH)_2.H_2O + 2HCOOH \rightarrow Cu(HCOO)_2 + 3H_2O$
Alternatively, in low formic acid concentrations copper hydroxide formate forms as an intermediate product prior to copper formate:
$Cu(OH)_2.H_2O + HCOOH \rightarrow Cu(OH)(HCOO) + 2H_2O$
Formic acid forms a complex with cuprous ions:
$8Cu^+ + 8HCOOH + O_2 \rightarrow 4Cu(HCOO)_2 + 2Cu_2O + 8H^+$
in this reaction both cuprite and cupric formate are formed." (López-Delgado *et al*. 2001, 5208).

SEM shows that corrosion develops locally from droplets of formic acid adsorbed on the surface. The acid reacts with the metal once it is incorporated in water droplets. At 10 ppm formic acid concentration crystalline copper hydroxide formed in the areas of droplets. At 50 ppm the surface was covered by corrosion and corrosion precipitated in ring shapes from droplets. Concentrations of 100 ppm and greater of formic acid caused the formation of porous, non-passive and non-protective corrosion (López-Delgado *et al*. 2001, 5209). At 200 ppm copper hydroxide and cuprite crystals co-existed. Rapid drying of the samples may have been responsible for the wave-like and smooth surface morphologies of the corrosion. At 300 ppm the corrosion has taken on the morphology of smooth bubbles (López-Delgado *et al*. 2001, 5210).

Copper was exposed to 10, 50, 100, 200 and 300 ppm formic acid for 21 days in tests at 40% and 80% RH at 30° C (Cano *et al*. 2001b; Cano and Bastidas 2002). The corrosion rate increased with an increase in formic acid concentration at both RH levels (Cano and Bastidas 2002, 329). At 10 ppm cuprite and copper hydroxide were the main corrosion compounds formed. Copper hydroxide was formed during or after the dry-out of the adsorbed layer of water or the droplets of formic acid vapour on the surface. Copper formate formed from formic acid vapour droplets (Cano *et al*. 2001b, 675).

X-ray photoelectron spectroscopy (XPS) was used with the argon-ion sputtering technique to characterize the element composition of the surface as a function of depth. It was found that copper formate and copper hydroxide are not stable to Ar^+-ion bombardment and that copper hydroxide decomposed to cuprite. Charging of copper

hydroxide and copper formate occurred at 40% RH whereas it did not at 80% RH. The X-rays charged the compounds causing the peaks in the XPS spectra to split. At 40% RH in all concentrations a thin layer of cuprite formed on the surface that was not charged by the x-rays. Copper hydroxide and copper formate formed in localized areas (Cano *et al.* 2001b, 671). At 80% RH, as formic acid concentration increases from 10 to 100 ppm, copper hydroxide decreased while cuprite and copper formate increased. Corrosion consisted of cuprite, copper hydroxide and copper formate. The corrosion formed a uniform layer in which no charging occurred (Cano *et al*. 2001b, 673; Cano and Bastidas 2002, 331). The chemical reduction of the compounds could be a result of the ultra high vacuum (UHV) conditions in XPS (Wu *et al.* 2006). XPS was found not to be a suitable analytical technique at 40% RH.

Summary

Corrosion occurred on copper in all tests that were conducted in formic acid vapour concentrations ranging from 0.04 ppm yr to 52 ppm yr at 40% to 100% RH. Corrosion was found to increase with increasing acid concentration from 0.3 to 3 ppm yr (100% RH) by Donovan and Stringer and from 0.5 ppm yr to 17 ppm yr (40% and 80% RH) by Cano (2001b) and Cano and Bastidas (2002). 5.1 ppm yr (54%/75% RH) was required for copper formate to form (Tetreault 2003a). The three research teams that identified corrosion on copper found the same three corrosion products from 3.6 ppm yr to 51.7 ppm yr: cuprite, copper hydroxide, and copper formate (Tetreault 2003a; Lopez-Delgado *et al.* 2001 and Bastidas *et al.* 2000; Cano *et al.* 2001b and Cano and Bastidas 2002).

Two of these studies that tested the same variables of 10, 50, 100, 200, and 300 ppm (0.5, 2.8, 5.7, 11.5, and 17.2 ppm yr) formic acid for 21 days at 30° C may be directly compared (Lopez-Delgado 2001 and Bastidas *et al.* 2000; Cano *et al.* 2001b and Cano and Bastidas2002). Cano tested the RH levels of 40% and 80% whereas Lopez-Delgado tested 100% RH. With increasing acid concentration from 0.5 ppm yr to 5.7 ppm yr copper hydroxide was found to decrease while cuprite and copper formate increased in 80% RH which did not occur in 40% RH (Cano *et al.* 2001b, Cano and Bastidas 2002). The increased concentrations of formic acid and the increased moisture in 80% RH reacted with copper hydroxide forming copper formate. A discrepancy was found in the identification of hydroxide compounds: copper hydroxide formate was

found in the 100% RH tests (Lopez-Delgado) and not in the tests at 40% and 80% RH (Cano *et al.* 2001b and Cano and Bastidas2002). This discrepancy parallels that of copper hydroxide acetate found on copper in acetic acid vapour in section 3.2.5.1.1. This indicates that the increased moisture present in 100% RH contributes to the formation of an intermediate compound, copper hydroxide formate, that is not required for the formation of copper formate at lower relative humidities (that occurs directly from copper hydroxide). Another explanation for the discrepancy may lie in the analytical techniques used for identification. The use of FTIR in addition to XRD by the Lopez-Delgado team may have aided in the identification of copper hydroxide formate.

Critical Review of Section 3.2.5.2.2 Corrosion Tests of Pure Copper exposed to Formic Acid and Formaldehyde

The effects of formic acid on pure copper have been studied extensively. Many of the researchers who tested pure copper in acetic acid also tested pure copper in formic acid using the same analytical techniques. Quantitative studies began with weight loss by Donovan and Stringer and proceeded to analytical identification of corrosion with XRD by Tetreault. Examination progressed to techniques using nanoscale resolution such as Scanning Tunnelling Microscopy (STM) Bowker 1998a). XPS can pose difficulties in the examination and analysis of corrosion causing decomposition of some corrosion products. Cano *et al.* (2001b) claim that the x-rays charged the corrosion causing its decomposition whereas it may more likely be an effect of the ultra high vacuum (UHV) conditions (Wu *et al.* 2006). The transformation of carbonate compounds into formate compounds on copper has been studied by Carley (1998). This knowledge, combined with evidence pointing to the conversion of carbonate compounds into acetate and formate compounds on archaeological bronzes (Paterakis 2003), inspired the conversion tests carried out in Chapter 4 (Section 4.3).

3.2.5.2.3 Corrosion Tests on Pure Copper exposed to Mixtures of Acetic Acid, Formic Acid and Formaldehyde

Experiments combining formic acid, acetic acid, and formaldehyde on pure copper were run for 135 days at 75% RH (Table 3.4, Appendix 1.3) (Tetreault *et al*. 2003). An inner layer of cuprite and an outer layer of tenorite or hydroxy-copper compound formed. These serve as the foundation for the formation of acetates and formates (Tetreault *et al*. 2003, 244). Formaldehyde and acetic acid were not found to participate in a significant way to the corrosion of copper. Cuprite was identified in all

test pieces analysed and hydroxy-copper compounds were indicated. Copper acetate (hydrate) was produced in only one test, that with acetic acid, formaldehyde and formic acid at high concentration levels (11 ppm acetic acid, 3 ppm formaldehyde, 8 ppm formic acid) (Tetreault *et al.* 2003, 241). The copper reacted mostly with formic acid. Copper formate dihydrate formed in all tests of mixed carbonyls with 8 ppm formic acid except where acetic acid was present at 11 ppm. It is interesting to note that of the two tests with 11 ppm acetic acid, the one with formaldehyde (3 ppm) produced copper acetate hydrate whereas the test without formaldehyde produced formate. Apparently the formaldehyde did not oxidize to increase the formic acid concentration in this test.

Table 3.4 Copper Corrosion that formed in Experiments of Mixed Organic Acids in 135 days at 75% RH

Acetic Acid		Formic Acid		Formal-dehyde ppm	Compound	Formula	ICDD #	Colour
ppm	ppm yr	ppm	ppm yr					
0.2	0.07	0.2	0.07		cuprite	Cu_2O	5-0667	red
11	4.0	0.2	0.07					
		0.2	0.07	0.6				
		0.2	0.07	3				
0.2	0.07	0.2	0.07	0.6				
11	4.0	0.2	0.07	3				
0.2	0.07	8	2.9		cuprite, copper formate dihydrate	Cu_2O, $Cu(CHO_2)_2.2H_2O$	5-0667 16-0954	
11	4.0	8	2.9					
		8	2.9	0.6				
		8	2.9	3				
0.2	0.07	8	2.9	0.6				
11	4.0	8	2.9	3	copper acetate hydrate	$Cu(CH_3CO_2)_2.H_2O$	27-0145	dark green

From (Tetreault *et al.* 2003, 240)

3.2.5.2.4 Corrosion Tests on Copper Alloys exposed to Formic Acid

Very little corrosion testing on bronze (copper-tin alloy) exposed to formic acid has been published to date (Bastidas *et al*. 1995; López-Delgado *et al*. 1997). These studies concentrated on the protective effects of the bronze patina, copper sulphide. Two copper alloys (leaded copper tin bronze (8% Sn, 5% Pb) and a leaded copper tin bronze with zinc (5% Sn, 5% Pb, 4% Zn), in a patinated (copper sulphide) and unpatinated state, were exposed to 50 ppm (4 ppm yr), 157 ppm (12.9 ppm yr), 314 ppm (25.8 ppm yr) of formic acid vapour in 100% RH at 30 C for 30 days (Bastidas *et al*. 1995). The patinated copper-tin-lead alloy was found to corrode faster than the unpatinated test pieces and produced copper formate. Patination did provide protection for the copper-tin-lead-zinc alloy however, at 157 and 314 ppm (Bastidas *et al*. 1995, 517). A leaded copper-tin

bronze (8% Sn, 5% Pb) was patinated (copper sulphide) and exposed to 314 ppm (18 ppm yr) formic acid vapour at 100% RH for 21 days (López-Delgado *et al*. 1997). Copper hydroxide was the principal component identified by XRD, copper formate was not found (López-Delgado *et al*. 1997, 778). The overall conclusion may be drawn that copper sulphide patina does not protect copper-tin-lead bronze from corroding in formic acid vapour but it does provide protection for copper-tin-lead-zinc bronze at concentrations ranging from 157 ppm to 314 ppm. These results are comparable with those from the same two copper alloys with copper sulphide patina tested in acetic acid vapour at slightly lower levels of acid concentration (Section 3.2.5.1.2).

Critical Review

The only studies that tested the corrosive effects of formic acid on copper alloys focused on the protective qualities of a patinated surface consisting of copper sulphide that can form on outdoor sculptures from sulphur dioxide air pollutant (Bastidas 1995, Lopez-Delgado 1997). In these tests bronze was artificially patinated to form a copper sulphide coating. For these reasons these studies are not directly applicable to the thesis topic, namely the protection of naturally corroded archaeological bronze from carbonyl compounds in museums.

3.2.5.3 Comparison of Copper Corrosion by Acetic and Formic Acid

In the comparative study of separate exposure tests of acetic acid and formic acid on copper the copper corrosion rate increased in line with increasing concentration of each acid. The corrosion rate was found to stabilize above 200 ppm for both acids. Although the dissociation constant in aqueous solution is higher for formic acid than for acetic acid, formic acid gave a lower copper corrosion rate (López-Delgado *et al*. 2001, 5205). At the lower concentrations this may be explained by protective qualities provided by the thicker, more compact and adherent corrosion layer formed by formic acid. The corrosion formed by acetic acid was non-uniform and porous. At low concentrations of acetic or formic acid (10 ppm), the corrosion process takes place on the adsorbed film and the corrosion products are initially developed in a uniform manner. As the acid concentration increases (100-300 ppm), the copper hydroxide and copper acetate or formate start to develop on local zones of the surface (Cano and Bastidas 2002, 336).

With high RH and high ppm the corrosion rate was influenced by the nature of the corrosion products of acetic and formic acid (Cano and Bastidas 2002, 335).

Summary

One major difference between formic and acetic acid in these studies is that copper formate formed at the expense of copper hydroxide whereas the formation of copper acetate did not. Copper hydroxide was found to coexist with copper acetate. This indicates “an acid-base reaction by means of a dissolution-precipitation mechanism” in the case of formic acid (López-Delgado *et al*. 2001, 5208). Another major difference is copper acetate started to form at 0.5 ppm yr acetic acid whereas copper formate required much higher concentration doses, 5.1 ppm yr formic acid. In these studies formic acid formed a protective corrosion layer causing a lower corrrosion rate while acetic acid formed a non-protective layer (Cano and Bastidas 2002; López-Delgado *et al*. 2001).

3.2.5.4 Corrosion Tests on Copper Alloys exposed to Acids Other than Acetic and Formic

Given the lack of published data pertaining to the corrosion of bronze by acetic acid and formic acids, two reports are presented on the effects of other acids that may be useful in the understanding of bronze corrosion by acids.

Two copper binary alloys, tin bronze (Cu 92%, Sn 8%) and brass (Cu 90%, Zn 10%), were exposed first to 80% RH, then to SO_2 to determine the influence of Sn and Zn on corrosion behavior (Kleber and Schreiner 2003, 294). Introduction to SO_2 after 80% RH caused an increase in corrosion rate on both metals. SO_2 is dissolved into the water and forms a bisulphite ion (HSO_3) by hydrolysis of SO_2. "The bisulphite ions produce metal-sulphito complexes through a liquid exchange mechanism with the hydroxylated metal oxide surface. These complexes $MeSO_3^{(n-1)+}$ then detach from the metal surface and precipitate as solid corrosion products." (Kleber and Schreiner 2003, 299). During exposure of brass to SO_2 new corrosion developed on top the corrosion layer from high humidity. Bronze developed new corrosion after the RH/ SO_2 tests were completed, accompanied by an increase in root mean square-roughness (Kleber and Schreiner 2003, 300).

Following is a report on the effects of acidic water (to mimic acid rain) and acidic gaseous pollutants (NOx and SO_2, 1 ppm and 10 ppm each) on bronze (Brunoro *et al*. 2001, 227). Two copper alloys were tested of the same composition, 94% Cu, 6% Sn, one (B6) was wrought and the other (G6) cast. B6 was a single-phase alloy. G6 was found to have $\alpha + \delta$ eutectoid in a dendritic α matrix. Both metals were subjected to acid rainwater test solution of sulphuric acid, ammonium sulphate, sodium sulphate, nitric acid, sodium nitrate, and sodium chloride with a pH adjusted to 2.7. Electrochemical tests (polarisation curves and electrochemical impedance) were used to analyse the corrosion mechanisms. Thin layer analysis (TLA) was used to monitor depth of corrosion and subsequent extent of loss (Brunoro *et al*. 2001, 229).

Polarisation curves (PC) show that the wrought bronze (B6) corroded less than the cast bronze (G6) on account of its lower anodic corrosion rate (it is single phase). Electrochemical impedance spectra (EIS) data agreed (Brunoro *et al*. 2001, 229). The first corrosion products that form usually on copper alloys in aqueous solutions are Cu(OH) and the more stable Cu_2O. This has been confirmed in the work by Wadsak *et al*. (2002) and Aastrup *et al*. (2000). It was found that in higher concentrations of pollutants more corrosion formed. As the corrosion layer forms in high levels of pollutants it takes on a protective function and slows down the rate of corrosion (Brunoro *et al.* 2001, 231). B6 exposed to wet-dry cycles without pollutants underwent discoloration, spot tarnishing, and was covered with interference colored oxidation films. When nitric and sulphuric acids were added to the wet-dry cycling CuO and gerhardtite ($Cu_2(OH)_3NO_3$) corrosion formed. It was determined that high chemical purity and fine microstructure improve the corrosion resistance of the bronze (Brunoro *et al*. 2001, 232). TLA was found to be an applicable method for monitoring corrosion.

In another study TLA was found to be a suitable technique to evaluate the degradation of bronze. This is attributed to its high sensitivity in measuring weight and depth loss (Laguzzi *et al*. 1999, 198). The copper alloy in this study, G6 (Cu 94% and Sn 6%), was exposed to nitrous oxide (1 ppm) and sulfur dioxide (1 ppm) gases for 60 and 130 days.

3.3 Tin

3.3.1 Characterization of Tin Corrosion

"The principal oxidation states of tin are +2 (Sn^{2+}) and +4 (Sn^{4+}).

The anodic half-reaction is $Sn(s) \rightarrow Sn^{2+} + 2e^-$

The cathodic half-reaction is $1/2\ O_2(g) + H_2O + 2e^- \rightarrow 2OH^-$

Net reaction is $Sn(s) + 1/2\ O_2(g) + H_2O \rightarrow Sn^{2+} + 2OH^-$"

(Selwyn 2004, 146).

The main cathodic reaction that occurs in aerobic conditions, even in highly acidic solutions, is oxygen reduction. Tin tends to form tin (IV) oxide, SnO_2. Sn(II) compounds oxidize to the Sn(IV) oxide, SnO_2. Often Sn(II) and Sn(IV) coexist in corrosion and for this reason tin is more similar to copper than is lead (Turgoose 1985, 16).

Tin is usually in the β phase (white tin) that exists between 13° C and 232° C. The α phase (gray tin) forms at low temperatures (below 13° C). The transformation from the α phase to the β phase causes expansion of the tin on account of the lower density of the α phase. This can be accompanied by the formation of local warts, cracking and eventual disintegration into powder. This form of deterioration is called "tin pest", "tin plague" or "tin disease" (Selwyn 2004, 141). Most cases are due to high RH and atmospheric pollutants (Selwyn 2004, 141).

Since tin is amphoteric it corrodes in low pH levels by dissolving as Sn^{2+} or Sn^{4+} ions and in high pH levels by dissolving as $Sn(OH)_6^{2-}$ or $Sn(OH)_3^-$ ions. In air with no moisture or pollutants tin forms a stable tin oxide layer. Tin is somewhat stable in aqueous solution in the range pH 3 to 10 although tin (II) oxide can be oxidized to tin (IV) oxide. Tin is not seriously affected by volatile organic acids although elements alloyed with tin, such as lead, can be. Chloride ions can promote local corrosion (Selwyn 2004, 146)

3.3.2 Corrosion of Archaeological Tin

The tendency for tin and lead to corrode is very similar and their oxides are soluble in acidic and alkaline conditions (Turgoose 1985). Corrosion products found on archaeological tin are listed in Table 3.5. SnO_2 (cassiterite) is the only stable corrosion

product in water between pH 3.5 and 9. Sn^{2+} is stable in "reducing acidic conditions" (Turgoose 1985, 16). Equilibrium potential - pH diagrams are very useful in determining the conditions in which corrosion products are stable. The initial corrosion product to form in aerobic conditions is SnO_2. Corrosion may be localized if oxygen access is restricted or the metal contains inhomogeneities. Reactions that occur near the metal surface are (Turgoose 1985, 19):

$Sn^{2+} + H_2O = SnOH^+ + H^+$
$SnOH^+ = SnO + H^+$

An increase in hydrogen concentration results at the metal surface that can lower the pH to a level at which basic salts (basic stannous compounds) are stable (Turgoose 1985, 19). Stannous ion in solution will be found in acidic conditions. Upon drying the pH will drop as the solution in the corrosion becomes more concentrated. With water and oxygen stannous ions oxidize causing more acidity on the surface (Turgoose 1985, 20):
$2Sn^{2+} + O_2 + 2\ H_2O = 2SnO_2 + 4H^+$

Table 3.5 Corrosion Products that Form on Archaeological Tin

Compound	Formula	Mineral name	Color
Stannic oxide - tin (IV) oxide	SnO_2	Cassiterite	White
Stannous oxide -tin(II) oxide	SnO	Romarchite	Black
Hydrated stannous oxide - tin (II) hydroxide oxide	$5SnO.2H_2O$	Hydroromarchite	White
Stannous chloride	$SnCl_2$		
Basic stannous chloride	Sn_2OCl_2		
Basic stannous sulphate	$Sn_3O_2SO_4$		
Tin (II) sulphide	SnS	Herzenbergite	Black
Tin (II,IV) sulphide	Sn_2S_3	Ottemannite	Gray
Tin(IV) sulphide	SnS_2	Berndtite	Yellow-brown
Magnesium tin(IV) hydroxide	$MgSn(OH)_6$	Schoenfliesite	White

from Selwyn 2004, 147, and Turgoose 1985, 15.

3.3.3 Corrosion of Tin exposed to Organic Acid Vapours

3.3.3.1 Acetic Acid

3.3.3.1.1 Adsorption of Acetic Acid on Tin

Thin-film tin oxide (SnO_2) was exposed to 10, 100, and 1000 ppm acetic acid, (as well as methanol, ethanol, isopropanol, and acetone) at elevated temperature (Gong *et al.* 1999). An acid-base interaction may be responsible for the adsorption of acetic acid

vapours on the tin oxide. Acetic acid dissociates its hydrogen atom when adsorbed on the oxide surface (Gong *et al*. 1999, 234).

3.3.3.1.2 Corrosion Tests on Tin exposed to Acetic Acid

Exposure to 50 ppm acetic acid solution (100% RH, 30° C, 6 days) produced no corrosion on tin (Clarke and Longhurst 1961, 436). Exposure tests at 100% RH and 30° C in 0.5 ppm, 5 ppm and 50 ppm acetic acid for 21 days resulted in corrosion on the 50 ppm test samples only (0.02 g/dm^2) (Donovan and Stringer 1971, 135).

The electrochemical behavior of tin was examined by chronopotentiometic analysis. Tin exposed to 0.4 M acetic acid solution and 0.02 M to 0.06 M acetic acid solutions at 25° C was found to form complexes by undergoing reductions and reoxidations in many steps (Elbourne and Buchanan 1970a, 497). Two tin acetates were formed from 0.0008M, 0.002 M and 0.004 M solutions of tin with 0.04 M acetic acid and a third intermediary complex was formed (Elbourne and Buchanan 1970b, 3566).

3.3.3.2 Formic Acid

3.3.3.2.1 Adsorption of Formic Acid on Tin

The adsorption and desorption of formic acid on reduced SnO_2 surfaces was examined by angle-resolved photoemission (ARPES), Auger electron spectroscopy (AES) and low energy electron diffraction (LEED) (Irwin *et al*. 1996). ARPES and LEED are used to monitor the surface symmetry and electronic structure. Formic acid was found to adsorb molecularly on both surfaces and was desorbed if heated to 375 K. Decomposition of formic acid on SnO_2 produces the desorption products CO_2, CO and H_2O (Irwin *et al*.1996, 481).

3.3.3.2.2 Corrosion Tests on Tin exposed to Formic Acid

Exposure of tin to 0.6, 6 and 60 ppm formic acid for 21 days at 100% RH and 30° C produced no corrosion (Donovan and Stringer 1971, 135).

3.3.3.3 Comparison of Tin Corrosion by Acetic and Formic Acid

Overall tin is very resistant to corrosion by acetic and formic acid and shows more susceptibility to acetic acid. Some loss of surface occurred with acetic acid (Donovan and Stringer 1971,135).

Critical Review of Sections 3.3.3.1.2/3.3.3.2.2 Tin exposed to acetic/formic acid

Very little testing of acetic acid on tin has been found in the literature. One study was by visual assessment, the other gravimetric, and the more recent study tested tin in solutions of acetic acid that has little relevancy for the current experimental project using volatile acid. Gravimetric monitoring determined that tin is quite resistant to both acetic and formic acid and most resistant to formic acid (Donovan and Stringer). For this reason lead was the alloy focused on in the experimental work in Chapter 4.

3.4 Lead

3.4.1 Characterization of Lead Corrosion

The principal oxidation states of lead are +2 (Pb^{2+}) and +4 (Pb^{4+}). Corrosion in aqueous solution occurs by:

Anodic half-reaction:	$Pb(s) \rightarrow Pb^{2+} + 2e$
Cathodic half-reaction:	$1/2O_2(g) + H_2O + 2e^- \rightarrow 2\ OH^-$
Net reaction:	$Pb(s) + 1/2O_2(g) + H_2O \rightarrow Pb^{2+} + 2OH^-$

Lead is amphoteric, its corrosion is accelerated by both alkalis and acids. The initial anodic product of lead is a 2+ cation and the standard electrode potential E° for the M^{2+}/M system is - 0.126 V (Turgoose 1985). The main cathodic reaction that occurs in aerobic conditions, even in highly acidic solutions, is oxygen reduction. The 2^+ cations react to form solid corrosion, the nature of which is influenced by the pH, solution redox potential and anions. The free energy of formation of Pb^{4+} is 302.5 kJ/mole for lead. The standard electrode potential is 1.69 V for lead. For these reasons lead tends to form Pb(II) compounds. Pb(II) compounds are stable in unpolluted atmosphere (Turgoose 1985, 16). Cerussite forms at a pH less than 11, hydrocerussite forms at pH 11 to 13, and plumbonacrite forms at pH greater than 13 (Selwyn 2004, 119).

3.4.2 Corrosion of Archaeological Lead

Lead carbonate ($PbCO_3$) (cerussite) and basic lead carbonate [$Pb_3(OH)_2(CO_3)_2$] (hydrocerussite) are the two most commonly found corrosion products on lead. The partial pressure of carbon dioxide will determine which of these will form. Above pH 7 and below pH 11 cerussite will form. It reduces the rate of corrosion by acting as a barrier to oxygen from reaching the metal surface and metal ions from escaping the metal. Cerussite is soluble in acidic conditions and corrosion can occur as long as anions such as lead chloride and lead sulphate are minimal (Turgoose 1985). The corrosion products that form on archaeological lead are listed in Table 3.6.

The relationship between composition and corrosion was investigated in archaeological lead from museum collections in Italy. The lead was analysed by microchemical analysis and scanning electron microscopy (SEM) (Mattias *et al*. 1984, 87). In the process described by Tetreault (Tetreault *et al*. 1998, 26) regarding the atmospheric corrosion of lead, non-metallic impurities (chlorine, sulphur) were found to contribute to corrosion. They form water-soluble salts that are extracted by atmospheric humidity via grain boundaries and appear on the surface. The resulting porous matrix is exposed to attack by atmospheric agents with the result that the oxidation products become hydrated and carbonated. The lead is transformed into a basic lead carbonate (Mattias *et al*. 1984, 90).

3.4.3 Atmospheric Corrosion of Lead

The atmospheric corrosion of lead depends on the type and concentration of the pollutants, RH, and the composition and morphology of the lead and lead surface (Tetreault *et al*. 1998, 28). In atmospheric corrosion humidity plays a major role by providing a water layer on the metal surface into which atmospheric gases may be deposited and in which the metal may dissolve (Graedel 1994, 922). Corrosion is not limited to oxidation. Oxidation-reduction reactions play a small role in atmospheric

Table 3.6 Corrosion Products that form on Archaeological Lead

Compound	Formula	Mineral name	Color
Lead (II) carbonate	$PbCO_3$	Cerussite	White
Lead (II) carbonate oxide hydroxide	$Pb_5O(OH)_2(CO_3)_3$	Plumbonacrite	White
Lead (II) carbonate hydroxide	$Pb_3(OH)_2(CO_3)_2$	Hydrocerussite	White
Lead (II) sulphate	$PbSO_4$	Anglesite	White
Lead (II) chloride	$PbCl_2$	Cotunnite	White
Lead (II) carbonate chloride	$Pb_2CO_3Cl_2$	Phosgenite	White
Lead sulphate carbonate hydroxide	$Pb_4SO_4(CO_3)_2(OH)_2$	Leadhilite	
Basic lead chloride	$Pb_2(OH)Cl_3$	Penfieldite	
Lead (II) chloride hydroxide	PbClOH	Laurionite	White
Lead (II) chloride phosphate	$Pb_5Cl(PO_4)_3$	Pyromorphite	Yellow
Lead (II) oxide	α-PbO	Litharge	Red
Lead (II) oxide	β-PbO	Massicot	Yellow
Lead (IV) oxide	PbO_2	Plattnerite	Dark grey
Lead (II) sulphide	PbS	Galena	Black

Table from Selwyn 2004, 118; Turgoose 1985, 16

corrosion since Pb^{+4} is unstable in most conditions. The corrosion of lead in the presence of water occurs by dissolution and crystallization. CO_2 and acidic gases are deposited in the water layer and lower the pH causing dissolution of lead. CO_2 at equilibrium can lower the pH to 5.6. Lead begins dissolving at a pH of 6 and attack increases with increasing acidity (decreasing pH). Lead acetate is very soluble and lead oxide is somewhat soluble (Graedel 1994, 923). Lead oxide is dissolved in atmospheric corrosion since it is usually occurs in acidic conditions (Graedel 1994, 923).

In leaded brass the lead corrodes, not copper or zinc (Graedel 1994, 924). In lead-tin alloys lead corrodes much the way it does in pure lead. A pit or groove in the surface tends to be the location where corrosion begins, the deposition of hygroscopic particles or condensed water on the surface is adequate (Graedel 1994, 925). Lead-rich alloys corrode faster than pure metals (Graedel 1994, 926).

3.4.4 Corrosion of Lead exposed to Organic Acid Vapours

3.4.4.1 Processes of Lead Corrosion by Acetic Acid

Lead is readily soluble in acetic acid on account of the high solubility of lead acetate (Selwyn 2004, 119) (Appendix 7.1). Lead with a purity greater than 98.8% (regardless of trace elements) is more prone to corrosion by acetic acid than less pure metal.

The reactions for the original manufacture of lead white (lead carbonate) that involved exposing lead to vinegar (acetic acid) proceed as follows:

"$2Pb + 4CH_3.CO_2H \rightarrow 2Pb(CH_3CO_2)_2$ (lead acetate) + $2H_2O$

$2Pb(CH_3CO_2)_2 + CO_2 + 3H_2O \rightarrow Pb(OH)_2.PbCO_3$(insoluble) + $4CH_3CO_2H$

anodic reaction: $Pb \rightarrow Pb^{2+} + 2e$

cathodic reaction: $O_2 + 2H_2O + 4e \rightarrow 4OH^-$

The lead ions from the acidic area of the anode diffuse toward the alkaline area of the cathode and CO_2 is absorbed from the atmosphere:

$2Pb^{2+} + 4OH^- + CO_2 \rightarrow Pb(OH)_2.PbCO_3$ (lead white) + H_2O

the lead white precipitates and the acetic acid is regenerated causing further attack." (Donovan 1986, 78).

Acetic acid condenses onto the surface of corroded lead and dissolves the lead carbonates. This neutralizes the acid and leaves acetate ions on surface. The acetate ions carry some of the ionic corrosion current and so carry the Pb^{2+} away from the surface to areas of high carbonate concentration and higher pH where it is precipitated as hydrocerussite (Turgoose 1985, 24). Hydrocerussite that is formed away from the surface does not have protective qualities.

The process of lead deterioration by acetic acid is explained as follows: "When exposed to acetic acid vapour, the acetic acid vapour can be dissolved in the water layer on the untarnished or lead oxide covered lead surface. The acetate ions produced can interact with lead oxide to form lead acetate oxide hydrate."(Tetreault *et al*. 1998, 24). When this compound is dissolved, it can migrate to where carbonates (dissolved carbon dioxide or precipitated carbonate compounds) are present, interact with the carbonate and release the acetate ion back into the water layer, and the corrosion cycle continues. The concentration of carbonate influences which type of lead carbonate compounds will be formed. Any migration of soluble lead compounds will provide a new source of lead ions for further reactions. Other “low molecular weight carboxylic acids, such as formic and propionic acids”, and “carbonyl compounds (excluding ketone compounds) that convert to carboxylic acids such as formaldehyde and acetaldehyde”, can promote similar reactions (Tetreault *et al*. 1998, 25).

The degree of protection provided by an oxide film on tarnished lead depends on the morphology and solubility of the lead compounds. Cracking or other alteration in the oxide film may allow the penetration by pollutants resulting in an increased corrosion rate. Pitting or efflorescence occurs preferentially at the sites of disruption in the tarnish layer (Tetreault *et al*. 1998, 26).

Water-soluble impurities in the lead, such as chloride and sulphur compounds, can dissolve and migrate along grain boundaries within the lead up to the surface. The porosity channel left behind allows penetration of acetic acid and other carbonyl compounds into the lead and further corrosion. This is one means by which purity of lead influences the corrosion rate. Traces of iron and zinc decrease resistance to corrosion whereas “traces of tin copper, silver and gold improve its resistance.” (Tetreault *et al*. 1998, 26). The atmospheric corrosion of lead is explained as follows by Niklasson *et al*. (2005):

"When lead is exposed to humid air containing acetic acid vapour, the acidification of the surface electrolyte results in dissolution of the native PbO film (reaction 11). This triggers an electrochemical corrosion process (reactions 2 and 3) generating lead ions and hydroxide that produce fresh lead oxide (reaction 4). The reaction of lead oxide with acetate and hydrogen carbonate ions produces a mixture of lead hydroxy acetate and lead hydroxy carbonate on the surface (reactions 6 and 8).” (Niklasson *et al*. 2005, B524).

The corrosion of lead first exposed to dry air, then to humid air, followed by acetic acid vapour at high humidity, is as follows (from Niklasson *et al*. 2005, B522):

"Lead forms oxide in dry air, mainly litharge (α-PbO):

$Pb(s) + 1/2O_2(g) \rightarrow PbO(s)$ (1)

Exposure to humid air causes electrochemical corrosion in an adsorbed aqueous film on the surface

the anodic reaction:

$Pb(s) \rightarrow Pb^{2+}(aq) + 2e^-$ (2)

the cathodic reaction is oxygen reduction:

$1/2O_2(g) + H_2O + 2e^- \rightarrow 2\ OH^-(aq)$ (3)

α-PbO precipitates:

$Pb^{2+}(aq) + 2\ OH^-(aq) \rightarrow PbO(s) + H_2O(l)$ (4)

Lead oxide reacts with carbon dioxide from the air forming lead hydroxy carbonate:

$CO_2(g) + H_2O(g) \rightarrow HCO_3^-(aq) + H^+(aq)$ (5)

$6HCO_3^-(aq) + 10PbO(s) + 6H^+(aq) \rightarrow$

$Pb_{10}O(OH)_6(CO_3)_6(s) + 3\ H_2O(g)$ (6)

Acetic acid deposition is subjected to gas-phase mass transfer limitations:

$PbO(s) + 2CH_3COOH(g) \rightarrow$

$Pb^{2+}(aq) + 2CH_3COO^-(aq) + H_2O$ (7)

PbO is completely consumed:

$2PbO(s) + Pb^{2+}(aq) + 2CH_3COO^-(aq) + H_2O \rightarrow$

$Pb(CH_3COO)_2.2PbO.\ H_2O(s)$ (8)

Acetic acid vapour dissolves easily in water:

$CH_3COOH(g) \Leftrightarrow CH_3COOH(aq)$ (9)

$CH_3COOH(aq) \Leftrightarrow CH_3COO^-(aq) + H^+(aq)$ (10)

Acidification of the electrolyte on the surface results in passive film dissolution:

$PbO(s) + 2CH_3COOH(aq) \rightarrow$
$Pb^{2+}(aq) + 2CH_3COO^-(aq) + H_2O$ (11)

Acetate forms complexes with divalent lead in aqueous solution:

$Pb^{2+}(aq) + CH_3COO^-(aq) \Leftrightarrow PbCH_3COO^+(aq)$ (12)

$Pb^{2+}(aq) + 2CH_3COO^-(aq) \Leftrightarrow Pb(CH_3COO)_2(aq)$ (13)

$Pb^{2+}(aq) + 3CH_3COO^-(aq) \Leftrightarrow Pb(CH_3COO)_3^-(aq)$ " (14)
(Niklasson *et al*. 2005, B522)

There is a linear relation between the corrosion of lead and exposure to acetic acid vapour (Niklasson *et al*. 2005, B523). "There is also a linear relation between the vapour pressure of acetic acid and corrosion rate … and the rate of acetic acid deposition during exposure is constant with time." (Niklasson *et al*. 2005, B523). Corrosive attack by acetic acid began at the edges of the samples (reaction 7) where consumption of lead oxide took place (reaction 8). Lead oxide was found only at a distance from the edges after exposure to 1100 ppb. This indicates that "acetic acid deposition is subjected to gas-phase mass transfer limitations." (Niklasson *et al.* 2005, B523). The acidity and high solubility in water (reactions 9 and 10) of gaseous acetic acid are responsible for its corrosivity on lead. The formation of a film of water on the surface in 95% RH acts as an electrolyte. The acidification results in dissolution of the passive oxide layer (reaction 11). Acetic acid forms three acetate complexes with lead in aqueous solution (reactions 12, 13, 14). One lead acetate complex, $Pb(CH_3COO)_2(aq)$, is very water soluble and deliquesces. When lead oxide and lead hydroxy acetate are present the pH will be neutral or slightly alkaline. The pH condition of slightly above neutral is expected in which acetate (reaction 8) and hydroxy complexes compete in the water film on the lead

surface. "…the dissolution of the PbO passive film by acetic acid (reaction 11) and the presence of a surface electrolyte (cf. The appreciable solubility of lead acetate and lead hydroxy acetate) together result in the formation of an electrochemical corrosion cell (reactions 2 and 3)." (Niklasson *et al*. 2005, B524). If exposure to acetic acid is discontinued, the reaction with PbO will cause an increase in pH. "…once neutralization is complete the PbO passive film is stable in contact with the resulting lead hydroxy acetate solution." (Niklasson *et al*. 2005, B524). Lead hydroxy acetates have limited water solubility. Lead hydroxy carbonate (reaction 6) reacts more readily with acetic acid than lead oxide and may transform to hydroxy acetate.

3.4.4.1.1 Corrosion Tests on Lead exposed to Acetic Acid

Results of published corrosion tests on lead exposed to acetic acid are listed in Table 3.7 (Appendix 1.4). The corrosion of lead was tested by immersion in solutions (0.1, 0.01, 0.001, 0.0001 N) of acetic acid for 40 weeks at 45° C (Coles *et al*. 1958). Rate and extent of corrosion was determined by weight loss. As acid concentration increased, corrosion rate increased. Neutralization of the acid was not reached so that corrosion continued throughout the tests. The corrosion products identified by XRD were basic lead carbonates with a ratio of carbonate ($PbCO_3$) to hydroxide ($Pb(OH)_2$ less than 2:1 (Coles *et al*. 1958, 344). A transition occurred from lead carbonate towards $2PbCO_3.Pb(OH)_2$ during the tests. Corrosion was characterized by intercrystalline attack causing patches of pitting in the surface.

Table 3.7 Corrosion Products on Lead from Exposure to Acetic Acid

ppm	ppm yr	°C	RH %	Days	Compound description	ICDD	Formula	Analy Tech	Ref
no acid		25	95	28	plumbonacrite, litharge	19-0680 05-0561	$Pb_5O(OH)_2(CO_3)_3$, α-PbO	XRD IC Gravi-metric ESEM -EDX	Niklasson *et al.* 2005
0.0001 - 0.1 N solution		45		40 weeks	lead carbonate hydroxide		$2PbCO_3.Pb(OH)_2$	XRD	Coles *et al.* 1958
0.024 -0.14	0.024 -0.14	rt	54	12 months	plumbonacrite (major), hydrocerussite (minor)	19-0680	$Pb_5O(OH)_2(CO_3)_3$ $Pb_3(CO_3)_2(OH)_2$	XRD	Tetreault *et al.* 1998
0.04-43	0.01-21	rt	34-75	6 months	plumbonacrite (major), hydrocerussite (minor), lead acetate oxide hydrate	19-0680	$Pb_5O(OH)_2(CO_3)_3$ $Pb_3(CO_3)_2(OH)_2$ $Pb(CH_3CO_2)_2.2PbO.H_2O$	XRD SEM	Tetreault *et al.* 1998
0.17	0.01	25	95	28	lead acetate oxide hydrate, plumbonacrite, massicot	18-1740 19-0680	$Pb(CH_3CO_2)_2.2PbO.H_2O$, $Pb_5O(OH)_2(CO_3)_3$, β-PbO	XRD IC Gravi metric ESEM -EDX	Niklasson *et al.* 2005
0.5	0.1	19	50	120	plumbonacrite, hydrocerussite, lead oxide acetate, litharge		$Pb_5O(OH)_2(CO_3)_3$, $Pb_3(CO_3)_2(OH)_2$, $Pb(CH_3CO_2)_2.2PbO.H_2O$, α-PbO	XRD	Thickett 1997
0.5	0.1	19	100	120					
0.5	0.04	60	100	30	white, red			NA	
1.1	0.08	25	95	28	lead acetate oxide hydrate, plumbonacrite, litharge, massicot,	18-1740 19-0680 05-0561	$Pb(CH_3CO_2)_2.2PbO.H_2O$, $Pb_5O(OH)_2(CO_3)_3$, α-PbO, β-PbO,	XRD IC Gravi-metric ESEM -EDX	Niklasson *et al.* 2005
1.4	0.4	rt	54	120	plumbonacrite, lead acetate oxide hydrate		$Pb_5O(OH)_2(CO_3)_3$, $Pb(CH_3CO_2)_2.2PbO.H_2O$,	XRD	Tetreault *et al.* 1998
1.4	1.4	rt	54	12 months	plumbonacrite (major), hydrocerussite (minor)	19-0680	$Pb_5O(OH)_2(CO_3)_3$, $Pb_3(CO_3)_2(OH)_2$	XRD	Tetreault *et al.* 1998
5	1.6	19	50	120	plumbonacrite, hydrocerussite, lead oxide acetate, litharge		$Pb_5O(OH)_2(CO_3)_3$, $Pb_3(CO_3)_2(OH)_2$, $Pb(CH_3CO_2)_2.2PbO.H_2O$, α-PbO	XRD	Thickett 1997
5	1.6	19	100	120					

5	0.4	60	100	30	white, red			NA	
7.2	2.3	rt	54	120	Hydrocerussite lead acetate oxide hydrate, lead oxides	18-1740	$Pb_3(CO_3)_2(OH)_2$, $Pb(CH_3CO_2)_2$. $2PbO.H_2O$	XRD	Tetreault *et al.* 1998
<8	<3.9	rt	75	6 months	plumbonacrite (major), hydrocerussite (minor), lead acetate oxide hydrate	19-0680	$Pb_5O(OH)_2(CO_3)_3$, $Pb_3(CO_3)_2(OH)_2$ $Pb(CH_3CO_2)_2$. $2PbO.H_2O$,	XRD	Tetreault *et al.* 1998
14.4	4.7	rt	54	120	hydrocerussite lead acetate oxide hydrate, lead oxides		$Pb_3(CO_3)_2(OH)_2$, $Pb(CH_3CO_2)_2$. $2PbO.H_2O$	XRD	Tetreault *et al.* 1998
24	7.8	rt	54	120	lead acetate oxide hydrate, lead acetate trihydrate	18-1740	$Pb(CH_3CO_2)_2$. $2PbO.H_2O$, $Pb(CH_3CO_2)_2$. $3H_2O$	XRD	Tetreault *et al.* 1998
26	12.8	rt	34	6 months	plumbonacrite (major), hydrocerussite (minor), lead acetate oxide hydrate	19-0680	$Pb_5O(OH)_2(CO_3)_3$, $Pb_3(CO_3)_2(OH)_2$, $Pb(CH_3CO_2)_2$. $2PbO.H_2O$,	XRD	Tetreault *et al.* 1998
43	21.2	rt	34	6 months	lead chloride hydroxide			XRD	Tetreault *et al.* 1998

rt = room temperature; NA = not analysed

Lead was exposed to 0.5 ppm, 5 ppm, and 50 ppm (0.02, 0.2, 2.8 ppm yr) acetic acid at 100% RH and 30° C for 3 weeks. The amount of corrosion was determined by stripping and weighing the samples after testing: ranged from 1.06 g/dm^2 to 3.10 g/dm^2 respectively (Donovan and Stringer 1971, 135). This represents a greater loss than that on tin (<0.001 to 0.02 g/dm^2) and copper (0.02 to 0.60 g/dm^2) (Donovan and Stringer 1971, 135).

In another study lead was exposed to 0.5 ppm and 5 ppm acetic acid at 50% RH and 100% RH for 120 days at 19° C (0.16 and 1.6 ppm yr) and 30 days at 60° C (0.04 and 0.4 ppm yr) (Thickett 1997). The results showed little difference between the two vapour concentrations although considerably more corrosion was produced at 100% RH. The corrosion products identified were hydrocerussite (white crystals) ($Pb_3(CO_3)_2(OH)_2$), plumbonacrite (transparent crystals) ($6PbCO_3.3Pb(OH)_2.PbO$), litharge (red crystals) (PbO), and possibly lead oxide acetate (Thickett 1997). It was found that increasing the temperature or the relative humidity increased the emission rate of acetic acid from wood and the corrosion rate of lead (Thickett *et al*. 1998, 263).

Three tests were run exposing lead to differing variables of RH and duration (Tetreault *et al*.1998). In the first test lead was exposed to 1.4, 7.2, 14.4, and 24 ppm acetic acid concentration at 54% RH for 4 months (0.4, 2.3, 4.7, 7.8 ppm yr respectively). 1.4 ppm acetic acid produced plumbonacrite and lead acetate oxide hydrate; 7.2 ppm and 14.4 ppm acetic acid produced various lead oxides, lead acetate oxide hydrate, hydrocerussite; 24 ppm produced lead acetate oxide hydrate and lead acetate trihydrate; and lead acetate oxide hydrate was produced across the range. Lead acetate formed in all tests after one month. Hydrocerussite was found at 1.4, 7.2, 14.4 ppm. Preferred orientation of some of the compounds altered the intensity values of some d-spacings (Angströms) and made their identification by XRD difficult (Tetreault *et al*. 1998). Three compounds could not be identified by XRD, the problematic peaks were at d-spacings 3.42, 3.04, and 2.89 Angströms respectively.

In a second experiment lead was exposed to a range of acetic acid concentration from 0.024 to 14 ppm at 54% RH for 12 months (0.02 ppm yr to 14 ppm yr) (Tetreault *et al*. 1998). Results showed that plumbonacrite (major) and hydrocerussite (minor) were produced at 1.4 ppm yr. Weight gain decreased with increasing acid concentration from 1.4 ppm yr to 7.2 ppm yr. Above 7.2 ppm yr weight gain started to increase again. The lead corrosion that formed was porous and voluminous. Adsorbed acetic acid and water contributed to the weight gain. Below 7.2 ppm yr there was a delay in weight gain, above 7.2 ppm yr weight gain was immediate.

In a third experiment tarnished and untarnished lead was exposed to the range 0.04 to 43 ppm acetic acid concentration at 34 - 75 % RH for 6 months (0.01 ppm yr – 21 ppm yr) (Tetreault *et al.* 1998). Below 8 ppm at 75% RH more plumbonacrite than hydrocerussite occurred on tarnished and untarnished samples. More hydrocerussite than plumbonacrite occurred on untarnished sample in 26 ppm at 34% RH. The surfaces on which plumbonacrite formed the major basic lead carbonate were characterized by uniform corrosion for the most part (with some pitting). The surfaces on which hydrocerussite formed the major basic lead carbonate were characterized by clustered growths of corrosion and the presence of lead acetate oxide hydrate. Lead chloride hydroxide was found at 43 ppm at 34% RH. The chloride derived from the magnesium chloride used to regulate the RH in the acid-water-salt mixture. Sodium chloride did not react with the lead (Tetreault *et al*. 1998). At acetic acid levels below 6 ppm

plumbonacrite forms initially as a porous layer allowing further corrosion to proceed. Upon further carbonation it may form hydrocerussite. At 1.4 ppm a water-insoluble form of lead acetate oxide hydrate formed before or during the formation of black plumbonacrite (Appendix 7.1). At acetic acid levels above 6 ppm water-soluble lead acetate oxide hydrate formed that may contribute to faster corrosion on account of its solubility. Lead corrosion is more complex at these higher concentrations of acetic acid (Tetreault *et al*. 1998, 25). As a result of higher RH, especially over 67%, the number and mobility of the acetate ions increase due to increased water content, allowing faster corrosion of the lead. The maximum corrosion rate was reached at 1.4 ppm (plumbonacrite predominated) (Tetreault *et al*. 1998, 28). Lead acetate oxide hydrate played an intermediary role in the formation of basic lead carbonates. Several studies have shown that the formation of lead acetate precedes that of the lead carbonates in acetic acid vapours.

To summarize the study by Tetreault *et al*. (1998), the acetate compounds that formed were lead acetate hydroxide hydrate, lead acetate oxide hydrate and lead acetate trihydrate. Lead corrosion was found to be more complex at higher concentrations (> 6 ppm) of acetic acid. The maximum corrosion rate was reached at 1.4 ppm and a higher corrosion rate occurred at a RH greater than 67%. A soluble and insoluble form of lead acetate oxide hydrate was found.

As part of the European Commission COLLAPSE (Corrosion of Lead and Lead-Tin Alloys of Organ Pipes in Europe) project, the corrosiveness of acetic acid was tested. Lead was exposed to 0.17 and 1.1 ppm acetic acid at 25˚ C and 95% RH from 1 to 4 weeks (0.003 ppm yr - 0.01 ppm yr and 0.02 ppm yr – 0.08 ppm yr respectively) (Niklasson *et al*. 2005). The lead had an oxidized surface at the start of the tests (mainly litharge). The amount of adsorbed water on the surface at 95% RH at 22˚ C corresponds to 10 - 15 molecular layers. The corrosion process was monitored by weighing the test pieces on a regular basis. XRD was used to identify corrosion products, Ion Chromatography (IC) determined the amount of water-soluble anions in the corrosion, and ESEM-EDX was used to examine the morphology of the surface and analyse the corrosion layer (Niklasson *et al*. 2005, B520). At 0.17 ppm the lead test pieces became light blue-white and at 1.1 ppm they turned yellow with white at the edges. By the end of the 1.1 ppm tests the yellow had turned to reddish brown. The corrosion products formed in the presence of acetic acid vapour were litharge, massicot, plumbonacrite (lead

hydroxy carbonate), and lead acetate oxide hydrate (Niklasson *et al*. 2005, B525). Similar amounts of lead hydroxy carbonate formed at 0.17 and 1.1 ppm but the amount of lead acetate oxide hydrate increased ten times at 1.1 ppm. ESEM indicates that the lead acetate oxide hydrate was in the form of cauliflower-like clusters. The corrosion rate was found to be proportional to the acetic acid vapour concentration (Niklasson *et al*. 2005, B522).

Critical Review of Section 3.4.4.1.1 Corrosion Tests on Lead exposed to Acetic Acid

The studies that have been conducted on lead exposed to acetic acid vapor have been limited to pure lead (Tetreault *et al.* 1998; Niklasson *et al.* 2005). In order to overcome the gap in our knowledge regarding the influence of lead in the corrosion of leaded bronze by volatile acetic acid, this ternary alloy (Cu,Sn,Pb) was purposefully selected for testing in Chapter 4.

In the three studies in this section XRD was the predominant analytical method used for the identification of corrosion on lead from accelerated testing in volatile acetic acid (Thickett 1997, Tetreault *et al.* 1998, Niklasson *et al.* 2005). Lead oxides (litharge, massicot), plumbonacrite, hydrocerrusite, and lead acetate oxide were found in all three studies. Some difficulties were encountered with XRD: preferred orientation of some compounds occurred making identification very difficult and other compounds could not be identified (Tetreault *et al.* 1998). The addition of Ion Chromatography (IC) and ESEM-EDX to the repetoire of analytical techniques by Niklasson compensated for the difficulties encountered with XRD. IC provided quantitative analysis of water-soluble anions and ESEM-EDX provided elemental analysis of the corrosion. The experimental variables in Chapter 4 were designed to coincide with the acid concentration doses and RH levels in these studies. For this reason the XRD results from the leaded bronze test pieces in Chapter 4 may be compared to the XRD results in these studies.

A consistent trend in the corrosion rate over certain ranges of acid concentration was determined. Niklasson found the corrosion rate to be proportional to acid concentration from 0.01 ppm yr to 0.08 ppm yr at 95% RH and Tetreault found this to be the case from 14.4 ppm yr to 24 ppm yr at 54% RH. The corrosion rate followed the reverse trend, however, from 1.4 ppm yr to 7.2 ppm yr: weight gain was reported to decrease from 1.4 ppm yr to 7.2 ppm yr by Tetreault. Tetreault determined a pattern in

weight gain based on acid concentration that can be compared to the results from the leaded bronze test pieces in Chapter 4.

0.4 ppm yr acetic acid was determined to represent a crucial concentration: the level at which the first acetate compound formed, lead acetate oxide hydrate, and the maximum corrosion rate occurred in 54% RH (Tetreault *et al.* 1998). Based on these results acetic acid concentrations below and above 0.4 ppm yr were purposely selected for the experimental work in Chapter 4. Experimentation was carried out in Chapter 4 to determine the influence of various acid concentration levels on the corrosion of the lead component in leaded bronze.

RH levels were found to play a crucial role in corrosion by Thickett and Tetreault who determined that lead was very responsive to increasing RH. 67% was the critical RH level above which corrosion was found to increase (Tetreault *et al.* 1998). For this reason a RH level above 67% was selected as one of three RH levels for the experimental work in Chapter 4 to promote corrosion results within the time frame of the tests.

Lead acetate oxide was identified in all three studies and found to represent an intermediate compound that is transformed into lead acetate and/or lead carbonate. One of the goals in the experimental work of the thesis was to determine the influence of lead on the corrosion of a leaded copper alloy. The questions to be investigated in Chapter 4 included the role of lead in the prevention of the corrosive attack of acetic acid on copper in leaded bronze and the formation of lead corrosion products according to acid concentration and RH level.

3.4.4.2 Processes of Lead Corrosion by Formic Acid and Formaldehyde

Formic acid in the presence of oxygen rapidly corrodes lead (Hiers 1948, 213; Niklasson *et al.* 2007). Lead reacts with formic acid to form lead formate. A stable corrosion layer can form that protects the lead from further corrosion.

3.4.4.2.1 Corrosion Tests on Lead exposed to Formic Acid and Formaldehyde

Numerous tests have been carried out on lead exposed to formic acid and formaldehyde. Results are presented in Table 3.8 (Appendix 1.5). Lead was exposed to

0.6 ppm, 6 ppm, and 60 ppm formic acid at 100% RH and 30° C for 3 weeks. The amount of corrosion was determined by stripping and weighing the samples after testing: ranged from 0.14 g/dm^2 to 0.65 g/dm^2 respectively (Donovan and Stringer 1971, 135). This represents a greater loss than that on tin (<0.001 g/dm^2) and similar to that of copper (0.15 to 0.71 g/dm^2) (Donovan and Stringer 1971, 135).

Table 3.8 Corrosion Products on Lead from Formic Acid and Formaldehyde

ppm	ppm yr	°C	RH %	Days	Compound description	ICDD	Formula	Anal Tech	Ref
FORMIC ACID									
0.35	0.1	21	75	135	lead formate hydroxide	14-0831	$Pb(CHO_2)(OH)$	XRD	Tetreault *et al.* 2003
0.5	0.1	19	50	120	lead		Pb	XRD	Thickett 1997
0.5	0.1	19	100	120	plumbonacrite, hydrocerussite, litharge		$Pb_5O(OH)_2(CO_3)_3$, $Pb_3(CO_3)_2(OH)_2$, α-PbO		
0.5	0.04	60	100	30	white, colorless			NA	
1.5	0.5	21	54	135	lead formate, lead formate hydroxide	14-0825 14-0831	$Pb(CHO_2)_2$ $Pb(CHO_2)(OH)$	XRD	Tetreault *et al.* 2003
5	1.6	19	50	120	plumbonacrite, hydrocerussite, litharge		$Pb_5O(OH)_2(CO_3)_3$, $Pb_3(CO_3)_2(OH)_2$, α-PbO	XRD	Thickett 1997
5	1.6	19	100	120					
5	0.4	60	100	30	white			NA	
8.8	3.2	21	54	135	lead formate, lead formate hydroxide	14-0825 14-0831	$Pb(CHO_2)_2$, $Pb(CHO_2)(OH)$	XRD	Tetreault *et al.* 2003
FA* + HP		20	NS	17/ 56	hydrocerussite, plumbonacrite, lead formate, lead formate hydroxide		$Pb_3(CO_3)_2(OH)_2$, $Pb_5O(OH)_2(CO_3)_3$, $Pb(CHO_2)_2$, $Pb(CHO_2)(OH)$	XRD 17 days wt. loss 56 days	Raychaud-huri 2000
FA*			high		hydrocerussite, plumbonacrite, lead formate, lead formate hydroxide		$Pb_3(CO_3)_2(OH)_2$, $Pb_5O(OH)_2(CO_3)_3$, $Pb(CHO_2)_2$, $Pb(CHO_2)(OH)$		
FORMALDEHYDE									
0.5	0.1	19	50	120	no change		Pb	XRD	Thickett

0.5	0.1	19	100	120	hydrocerussite, plumbonacrite, litharge, lead		$Pb_3(CO_3)_2(OH)_2$, $Pb_5O(OH)_2(CO_3)_3$, α-PbO, Pb		1997
0.5	0.04	60	100	30	white, colorless			NA	
5	1.6	19	50	120	no change		Pb	XRD	Thickett 1997
5	1.6	19	100	120	hydrocerussite, plumbonacrite, litharge, lead		$Pb_3(CO_3)_2(OH)_2$, $Pb_5O(OH)_2(CO_3)_3$, α-PbO Pb		
5	0.4	60	100	30	white			NA	
F*		20	high	17/56	hydrocerussite, plumbonacrite, lead oxide		$Pb_3(CO_3)_2(OH)_2$, $Pb_5O(OH)_2(CO_3)_3$, α-PbO	XRD	Raychaud -huri 2000
F*			high (no light)		lead oxide		α-PbO		
F* + HP			NS		lead oxide hydrocerussite, plumbonacrite, lead formate		α-PbO, $Pb_3(CO_3)_2(OH)$, $Pb_5O(OH)_2(CO_3)_3$, $Pb(CHO_2)_2$		

FA = formic acid; F = formaldehyde, HP = hydrogen peroxide, NS = not specified ,
* = concentrations not specified; NA = not analysed

Lead was exposed to 0.5 and 5 ppm formic acid at 50% RH and 100% RH for 120 days at 19˚ C (0.16 ppm yr – 1.6 ppm yr) and 30 days at 60° C (0.04 ppm yr – 0.4 ppm yr) (Thickett 1997). The results showed some difference between the two vapour concentrations although considerably more corrosion was produced at 100% RH. The corrosion products identified were hydrocerussite (white crystals) ($Pb_3(CO_3)_2(OH)_2$), plumbonacrite (transparent crystals) ($6PbCO_3.3Pb(OH)_2.PbO$), and litharge (red crystals) (PbO) (Thickett 1997). Plumbonacrite was the first corrosion product to form thus mirroring the results of Tetreault *et al.* (1998). Formaldehyde was found to cause much less corrosion than acetic or formic acid (Thicket *et al.* 1998, 263).

Corrosion experiments were carried out exposing lead to 0.04 to 20 ppm formic acid at 54% (0.01 – 7.3 ppm yr) and from 0.04 to 40 ppm formic acid at 75% RH (0.01 – 14.7 ppm yr) for 135 days (Tetreault *et al*. 2003). At 54% RH the corrosion rate slowed down after 27 days on account of compounds that formed on the surface. A change of color occurred at the lowest concentration (0.035 ppm/0.01 ppm yr). Significant weight gain occurred above 0.1 ppm (0.03 ppm yr). Lead formate and lead hydroxide formate were identified at 1.5 (0.5 pm yr) and 8.8 ppm (3.2 ppm yr). A maximum weight gain

occurred in 1.5 ppm (0.5 pm yr). One might expect the highest concentration to produce the most weight gain but this was not the case.

At 75% RH significant weight gain occurred above 0.35 ppm (0.12 ppm yr). Exposure to formic acid ranging in concentration from 0.1 (0.03 ppm yr) to 8.8 ppm (3.2 ppm yr) at 54% and 75% RH caused significant weight gain in all tests and produced lead formate and lead formate hydroxide. The latter was identified at 0.35 ppm (0.12 ppm yr). Maximum weight gain due to corrosion occurred at 1.5 ppm (0.5 pm yr) formic acid. Most color change occurred in the first 27 days above 0.35 ppm (0.12 ppm yr) (grey and blue colors, matt) (Tetreault *et al*. 2003, 240).

Critical Review of Section 3.4.4.2.1 Corrosion Tests on Lead exposed to Formic Acid

In the three studies that tested lead in volatile formic acid the acid concentrations ranged from 0.04 ppm yr to 14.7 ppm yr and the RH from 50% to 100% (Donovan and Stringer 1971, Thickett 1997, Tetreault *et al*. 2003). XRD was used in two studies to identify the corrosion products, the third study did not identify corrosion. The detection of lead hydroxide formate from 0.12 ppm yr formic acid and lead formate from 0.5 ppm yr formic acid concentration by Tetreault was not repeated in the study by Thickett. Although Thickett tested formic acid concentrations well above these levels (1.6 ppm yr) the only compounds identified were hydrocerussite, plumbonacrite, and litharge. This discrepancy cannot be readily explained considering all test variables (including RH levels) and analytical technique were similar.

High levels of RH can counteract low acid concentrations and high acid concentrations can counteract low RH levels in the formation of corrosion. This is exemplified by lead hyroxide formate that formed at a lower acid concentration in a higher RH (0.12 ppm yr in 75% RH) and at a higher acid concentration in a lower RH (0.5 ppm yr in 54% RH). The maximum weight gain occurred at 0.5 ppm yr formic acid that parallels the maximum corrosion rate of lead in acetic acid (1.4 ppm yr) (Tetreault *et al.* 2003).

3.4.4.3 Corrosion Tests on Lead exposed to Mixtures of Acetic Acid, Formic Acid, and Formaldehyde

Various mixtures of formic acid, acetic acid and formaldehyde were tested with lead for 135 days at 75% RH (Tetreault *et al*. 2003). Results showed that formaldehyde alone or mixed with formic acid and acetic acid did not contribute significantly to corrosion of lead. Acetic acid alone caused more corrosion than formic acid alone. In 0.2 ppm (0.07 ppm yr) acetic acid corrosion was well established and was identified as plumbonacrite. The presence of formic acid inhibited the corrosion capacity of acetic acid. In a mixture of formic and acetic acids the formation of lead formate compounds retarded the formation of lead acetate compounds. This is "attributed to a modification of the chemical nature of the corrosion layer." (Tetreault *et al*. 2003, 241). XPS analysis can also contribute to the modification of the surface by incurring a positive charge effect that decreases the electronic conductivity of the surface layer (Tetreault *et al*. 2003, 243). “No significant oxidation of formaldehyde into formic acid occurred in the vapour phase in the presence of weak oxidants such as acetic or formic acids or in the presence of the copper or lead metal surfaces." (Tetreault *et al*. 2003, 243). The concentration of acetic acid was found to increase in the presence of formic acid for which no explanation was offered (Tetreault *et al*. 2003, 247).

In another experiment tarnished and untarnished lead was exposed to a carbonyl mixture (formic acid 0.2 ppm/0.01 ppm yr, acetic acid 0.3 ppm/0.02 ppm yr , formaldehyde 0.6 ppm/0.05 ppm yr) and particle board (formic acid 0.2 ppm/0.01 ppm yr, acetic acid < 0.07 ppm/0.006 ppm yr, formaldehyde 0.9 ppm/0.08 ppm yr) for 33 days at 54, 75 and 100% RH (Tetreault *et al*. 2003) The untarnished lead corroded more than pre-tarnished (natural patina) lead. No corrosion occurred on pre-tarnished lead at 54% RH. Higher weight gain occurred in the test with particleboard than with mixed carbonyls. The author believes more tests should be run for reliable results (Tetreault *et al*. 2003, 243).

Since the typical oxidizing agent for formaldehyde in the atmosphere is the hydroperoxy radical, corrosion tests were run using formaldehyde with hydrogen peroxide as oxidizing agent, formaldehyde and moisture, formic acid with hydrogen peroxide, and formic acid with moisture (Raychaudhuri and Brimblecombe 2000, 229). Some tests were run in the dark to determine the role of photooxidation (Raychaudhuri

and Brimblecombe 2000). The tests with formaldehyde and formic acid produced the basic lead carbonates, plumbonacrite, hydrocerussite, lead oxide and lead formate in some cases. Most of the tests with formic acid produced lead hydroxide formate as well (Raychaudhuri and Brimblecombe 2000, 228). It was determined that carbonates are more stable than formates when the formic acid concentration is below 0.7 ppb, therefore formates would not be expected at these low levels (Raychaudhuri and Brimblecombe 2000, 228). Specifically, the partial pressure of formic acid over a saturated lead formate solution in equilibrium with cerussite was calculated to be 0.48 ppb and with hydrocerussite 0.68 ppb. These carbonates form when the pressure of formic acid falls below these levels (Raychaudhuri and Brimblecombe 2000, 229). Formate did not form in the tests with formaldehyde without an oxidizing agent. It was found that light increased the rate of attack by formaldehyde.

Equilibrium between lead formate and lead carbonates can be expressed as follows (Raychaudhuri and Brimblecombe 2000, 229):

$$Pb^{2+}_{(aq)} + 2Fo^{-}_{(aq)} + CO_{2(g)} + H_2O_{(l)} \Leftrightarrow$$

$$PbCO_{3(s)} + 2HFo_{(g)} \qquad (1)$$

$$3Pb^{2+}_{(aq)} + 6Fo^{-}_{(aq)} + 2CO_{2(g)} + 4H_2O_{(l)} \Leftrightarrow$$

$$Pb_3(CO_3)_2(OH)_{2(s)} + 6HFo_{(g)} \qquad (2)$$

Fo^{-} represents formate ($HCOO^-$)
(Raychaudhuri and Brimblecombe 2000, 229).

Critical Review

Conflicting results are presented by Tetreault regarding the influence of carbonyl compound mixtures added to acetic acid on lead corrosion. In an earlier study it was found that the addition of low molecular weight carboxylic acids or aldehydes increased the corrosion rate and decreased the corrosion resistance of lead (Tetreault *et al.* 1998, 26). In a later study it was determined that formic acid inhibited the corrosive effect of acetic acid on lead (Tetreault *et al*. 2003, 241). This discrepancy could be due to

differing ratios of formic to acetic acid. Formaldehye was not found to be very corrosive to lead by itself or mixed with formic and acetic acid (Tetreault *et al.* 2003; Raychaudhuri and Brimblecombe 2000). This was also found to be true in tests run by Tetreault of copper in formaldehyde, formic and acetic acid mixtures (Section 3.2.5.2.3). The addition of hydrogen peroxide to formaldehyde was found necessary to catalyze its oxidation to formic acid and to produce formates on lead (Raychaudhuri and Brimblecombe 2000).

3.4.4.4 Critical Review of Lead Corrosion by Acetic and Formic Acid

The corrosive effects of acetic acid on lead have been studied much more thoroughly than the corrosive effects of formic acid. Detailed study of acetic acid has produced some conflicting theories regarding the order the corrosion processes follow on lead. This discrepancy deals mainly with the order of formation of lead carbonate, lead hydroxy acetate and lead acetate oxide hydrate. The researchers do agree, however, that a cyclical process is set up that can lead to the total destruction of the metal. Acetic acid is much more corrosive to lead than formic acid. Formic acid may produce a passivating layer that can protect the lead from further corrosion. This is an area that requires further research. Acetic acid was the only acid variable tested in the experimental work in Chapter 4 in order to contain the thesis to a manageable length. The studies combining acetic and formic acid, with and without formaldehyde, show the complexities involved in the reaction of these two species on lead. These complexities must be kept in mind when considering the formation of the acetate/formate compound identified in the Case Studies in Chapter 5.

Chapter 4 Experimental Methods for Corrosion Testing

4.1 Principal Aims of the Project

The principal aim of the project was to acquire the knowledge necessary for the prevention of corrosive attack by acetic acid and the subsequent formation of acetate and other corrosion compounds on bronze. The objective was to determine the conditions required for the safe storage and stabilization of objects corroded by acetic acid. Preserving the patina on metal artifacts complicates the evaluation of testing data. Two sets of tests were carried out.

In order to achieve these goals it was necessary to assess the conditions in which acetic acid attacks copper alloys and forms acetate compounds (Test Series I). The different variables that played a contributing role are composition and structure of the metal used in testing, contaminants such as sodium, state of metal surface before exposure to acetic acid vapour, concentration of acetic acid vapour, and level of relative humidity (RH).

A second series of tests (Test Series II) exposed corrosion products commonly found on archaeological bronze, malachite and chalconatronite, to high levels of acetic acid vapour and RH. The influence of a conservation material, sodium sesquicarbonate, on bronze corrosion was tested by exposing sodium sesquicarbonate on its own and mixed with malachite in equal portions to acetic acid vapour. The purpose of mixing it with malachite was to simulate a copper alloy with malachite patina that has been treated with sodium sesquicarbonate. Obviously, the texture and structure of corrosion layers are quite different. Powdered mineral samples were used as an initial test on reactivity; the high surface area on the mineral samples is much more reactive to volatile organic acids.

In addition to controlling the variables of conservation chemicals in treatments, and acetic acid vapour concentrations and relative humidity levels in storage, another means of protecting metals from corrosion involves the application of corrosion inhibitors and protective coatings. Protective coatings are examined in Chapter 6.

4.2 Test Series I

Test Series I consisted of two parts.

Part One: New, non-corroded copper alloys and ancient, corroded archaeological copper alloys were included in the tests to evaluate the influence of surface condition on corrosion when exposed to acetic acid vapour.

Part Two: The same new, non-corroded copper alloys in part one were re-evaluated to determine the reproducibility of the results.

4.2.1 Test Series I: Part One

4.2.1.1 Selection and Evaluation of Metals used in Testing

4.2.1.1.1 New Metals

The acetate corrosion products in the Agora Excavation collection were found to represent a serious problem on bronze objects of various compositions. Since the goals of this project include the characterization, mitigation and prevention of acetate corrosion on bronze (copper-tin alloy) antiquities and works of art, brass (copper-zinc alloy) was not included as this alloy post-dates the Classical and Hellenistic Greek period for the most part (Craddock 1978, 1). It was also thought prudent to narrow the focus of the research by avoiding the corrosion phenomenon of dezincification in this examination of the corrosive effects of acetic acid. For these reasons bronze with a negligible zinc content was selected from the commercially available standards. Tin bronze consisted of an average tin content of 5% in the Middle Bronze Age and 7-9% from the Geometric Period through the Archaic Greek and Classical Periods, into the Hellenistic Period (Craddock 1976, 99-104; Craddock 1977, 103-110). The maximum tin content found during these periods was approximately 15%. Although the tin content (16%) of ASTM B584 slightly exceeds the maximum, this alloy was chosen for its low lead (0.25% max) and zinc (0.25%) content (Table 4.1). Intentionally leaded bronze, i.e. bronze containing significantly more than 1% lead, occurred in the Archaic Period and was characterized by increasingly higher lead content in the Hellenistic period, with some examples reaching 20 to 30% lead. Lead content varied widely in each period from

the Late Bronze Age through the Hellenistic and averages are difficult to determine (Craddock 1976, 99-104; Craddock 1977, 103-110). In this project a leaded tin bronze was chosen to represent an alloy common to the Hellenistic period. ASTM B505 contains 8% tin and 8% lead, an alloy composition more common to the Hellenistic period (Craddock 1977, 107). The influence of lead on corrosion was an important factor to be examined in this project.

The two new copper alloy standards chosen were tin bronze ASTM B584 (C91100) and leaded tin bronze ASTM B505 (C93400) (Table 4.1). Tin bronze B584 (C91100) consisted of 84% (wt.) copper, 16% (wt.) tin. Metallographic examination showed a cast structure with extensive α and δ eutectoid phase around Cu α phase dendrites (Appendix 2.1). In tin bronze the α phase consists up to 9.1% tin and the δ phase from 20 to 21% tin (ASM 1990, 1481). The leaded tin bronze ASTM B505 (C93400) consisted of 84% (wt.) copper, 8% (wt.) tin, and 8% (wt.) lead (Table 4.1). Metallographic examination showed essentially a cast structure, large lead globules, α and δ eutectoid phase in places, and some coring (Appendix 2.2). Coring is segregation of alloying elements during solidification at the microlevel of castings (ASM 2004, 58). Another name for it is dendritic segregation. Two phases, alpha phase and eutectoid phase, promote different reactions. Lead does not modify the α or δ phase during corrosion (Robbiola *et al*. 1998, 2100). Galvanic corrosion could occur between dissimilar metals in contact with one other, for example Pb and the alpha phase.

Table 4.1 Elemental Composition (% weight) of New Metal

Tin bronze ASTM B584 (C91100)		(Appendix 2.1)
Element	Major elements	Maximum impurities
aluminum		.005
antimony		.20
copper	84	
iron		.25
lead		.25
nickel		.50
phosphorus		1
silicon		.005
sulfur		.05
tin	16	
zinc		.25

Leaded tin bronze ASTM B505 (C93400)		(Appendix 2.2)
Element	Major elements	Maximum impurities
aluminum		.005
antimony		.50
copper	84	
iron		.15
lead	8	
nickel		1
phosphorus		.50
silicon		.005
sulfur		.08
tin	8	
zinc		.8

4.2.1.1.2 Ancient Coins

Natural corrosion on archaeological bronze, consisting of oxides, carbonates and chlorides, will react with acetic acid and form multiple-component compounds. One such compound is a sodium copper carbonate acetate that has been identified on bronzes in two collections in Europe, the Agora Excavations and Museum, Athens, and the British Museum, London. Likewise, non-archaeological bronze objects exposed to the atmosphere will form a patina based on oxides, carbonates, and sulphates that will react with acetic acid.

Copper alloy coins from the Greek and Roman periods were used in accelerated corrosion testing since a large part of the Agora bronze collection dates to these periods (Appendices 3.1 – 3.6). Coins that were commercially available in the numismatic market were used to represent a range of composition and corrosion. These may be considered sacrificial test objects as they do not derive from catalogued antiquities

collections and lack archaeological provenance. Six coins were donated by a private collector for the tests. This approach allows destructive technical evaluations on comparable materials; such destructive testing would be inappropriate for provenanced archaeological artifacts (Maxwell-Hyslop and Williams 1976).

The rationalization for using archaeological objects covered with oxide, carbonate and chloride corrosion in addition to new metal coupons is twofold. It is difficult to replicate the microstructure of corrosion formed naturally during burial over centuries using accelerated, artificial conditions. Authentic archaeological objects, both uncleaned and chemically stripped, would provide the most favorable base on which to replicate the development of acetate corrosion found in collections of archaeological copper alloys (Robbiola *et al.* 1998, 2100). One of the goals of the project was to determine the influence of oxides and carbonates on the attack by acetic acid and on the formation of acetate corrosion.

Cross sections of the copper alloy coins were analysed by XRF (Kevex) at the Getty Conservation Institute (GCI) by David Scott and the author and by Electron Probe Microanalysis (EPMA) at the GCI by Eric Doehne. A Kevex 0705A XRF Spectrometer operating at 50-55 kV, 40-50 mA, with a barium-strontium secondary target was used. The detection limit of the elements analysed was 0.5%. Accuracy was ±10% for major elements and ±20% for minor elements. The microprobe analysed 5 spots on each coin that were averaged. The EPMA results were far removed from the XRF data and were discounted as unrepresentative of the composition on account of the small beam size and the inadequate number of spot tests carried out per coin. XRF analysis was applied to the core of the coins in cross section thereby eliminating altered composition on or near the corroded surface. XRF provides compositional analysis (Table 4.2). For a visual assessment and metallographic description see Table 4.3. A range of alloy composition was selected for testing. Of the six coins used four were copper tin bronze (coin 1, 3, 4, 6), one was heavily leaded copper tin bronze (coin 2) (Appendix 2.3), and one was almost pure copper (coin 5) (Appendix 2.4) (Appendices 3.1-3.6).

Table 4.2 XRF Analysis of Coins Elemental Composition (% wt)

	Cu	Pb	Sn	Fe	Ni	Zn
Coin 1	81	2	17	0.4	nd	nd
Coin 2	69	23	8	0.14	0.18	nd
Coin 3	87.5	3	9.4	369 ppm	0.18	nd
Coin 4	84	2	14	nd	nd	nd
Coin 5	98.5	1	nd	626 ppm	0.34	nd
Coin 6	95	4	1.3	429 ppm	nd	nd

(nd = not detected, below the detection limit)

4.2.1.2 Preparation of Metals for Testing

The new test coupons were cut from a bar of ASTM metal with an electric saw for metal and then wet-sanded with different grades of abrasive paper from grit size 240 down to 600. They varied in length and width and measured approximately 3 mm in thickness. The coins were cut with a slow-speed metallurgical saw with diamond-impregnated rim into wedges so that the same coin could be subjected to all levels of acetic acid exposure for comparative purposes. The coin wedges contained two corroded surfaces and two freshly cut, uncorroded surfaces with smooth edges.

Sodium Contamination

After working for many years with the collection of bronze objects in the Agora Excavations and Museum, Athens, it was noted that chemicals used by conservators for cleaning and stabilization, such as sodium sesquicarbonate and sodium hydroxide, and the degree to which these treatments are carried out, can affect the stability of bronze in subsequent storage and display (Paterakis 1998, 254).

Table 4.3 Description, Visual Assessment and Metallographic Examination of Copper Alloy Coins (carried out in consultation with David Scott 2004)

Coin 1
Description: possibly Greek, 4th to 1st c. BC.
Visual and microscopic examination: Covered with light blue corrosion.
Metallographic exam: Worked and annealed. Extensive intergranular corrosion. Annealing was the final stage (straight twins). Sulphide inclusions and Pb globules. A bit of the α and δ phase.
Coin 2
Description: Greek 3rd c. BC, Head of Zeus
Visual and microscopic examination: Malachite on surface.
Metallographic exam: Hot working caused twinned crystals at the edge, i.e. recrystallization at the edge. Traces of Cu in corrosion crust.
Coin 3
Description: Carthage 3rd c. BC. Obv. Head of Persephone, Rev. horse and palm
Visual and microscopic examination: Small black spots on head, rust-colored area.
Metallographic exam: Shows a cast morphology, dendrites. Scatter of inclusions (Cu sulphides), may be more than one kind of inclusion. α and δ eutectoid appears dark. Corrosion crust confirms authenticity. Redeposited Cu in areas of surface near edge. Corrosion is evident along slip planes. It was cast, then cold worked at the edge to shape it.
Coin 4
Description: Greek, South Italy, about 3rd c. BC
Visual and microscopic examination: Contains cuprite and malachite.
Metallographic exam: Was made as a sheet, then worked very heavily. The grains are oriented lengthwise. Homogeneous tin bronze. Striking caused strain. Dissolution of grain boundaries. Heavily worked. Small recrystallized grains. Twinned grains.
Coin 5
Description: Divus Augustus AD 14-41
Visual and microscopic examination: Areas of dark grey, yellow and green.
Metallographic exam: Variable grain size. Corrosion cracks. Worked and annealed grains. Straight twin lines show it was annealed last. Lead globules. Lengthwise channels are due to porosity, not to cutting.
Coin 6
Description: Trajan/Arabia AD 98-117
Visual and microscopic examination: Thin green corrosion crust.
Metallographic exam: Cold worked, annealed, and cold worked again. Deformed twins show it was heavily worked after annealing. Cold worked in the final stage. Heavily strained. Lead globules visible. Non-metallic inclusions (i.e. Cu sulphides) are present. Not much cuprite is present but there is a thin layer in places.

Incomplete stripping of objects leaves corrosion products, such as copper carbonates, on the surface that may combine with acetic acid vapour to form multiple-component compounds containing carbonate and acetate. Inadequate rinsing and neutralization of chemicals can leave residues that interact with the metal. Residual sodium from sodium hydroxide (NaOH) and sodium sesquicarbonate ($Na_2CO_3.NaHCO_3.2H_2O$), two products used extensively in 20th century conservation treatments, has been found to contribute to multi-component acetate compounds containing sodium. Treatment with sodium sesquicarbonate by soaking in solutions ranging from 5% to 25% was used for many years in an attempt to clean and stabilize bronze (Lucas 1932, 89; Oddy and Hughes 1970, 185; Plenderleith 1934, 52;). Complex acetate compounds containing sodium have also been discovered on bronzes that have not been treated with chemicals. Another source of sodium, in the case of archaeological objects, is the burial environment. In the British Museum the source of sodium in sodium copper carbonate acetate [$NaCu(CO_3)(CH_3CO_2$] and sodium acetate trihydrate compounds found on Egyptian bronzes was sodium hydroxide from cleaning and the saline soil of Egypt (Thickett and Oldyha 2000, 63). The predominant salt in Middle Eastern soil is sodium chloride (Thickett 1998, 10). Conservators must be made more aware of the role sodium and other chemical residues and contaminants play in the formation of acetate corrosion. This is vital to ensure the conscientious application of these chemicals in the future and to encourage conservators to assign appropriate storage criteria for the adequate protection of chemically treated or contaminated objects.

Treatment of Metal Test Coupons and Coins with Sodium Compound

Half of the new metal coupons and ancient coin wedges were treated with sodium sesquicarbonate in order to introduce sodium to replicate residual salt from burial or from standard conservation treatments for stabilization and cleaning of archaeological copper alloys commonly adopted over the past sixty years (Table 4.4). They were soaked in a 5 % solution (50g/liter) sodium sesquicarbonate in deionized water for 6 days. Upon removal they were rinsed in deionized water and allowed to air dry. Effective drying and constant weight was ensured by subsequently placing the test pieces in the oven at 105˚ C overnight followed by equilibration in a desiccated vacuum jar.

Characterization of Patina on Test Coupons and Coins Prior to Corrosion Testing

Digital photographic images were taken of the test coupons and coins before testing. Constant weight was obtained of all coupons and coins prior to testing by placing the test pieces in the oven at 105˚ C overnight followed by equilibration in a desiccated vacuum jar. The process of achieving a constant weight that involved heating prior to testing afforded ample opportunity for corrosion to occur in the form of copper/tin/lead oxides. It is known that soaking archaeological bronzes in sodium sesquicarbonate can cause the formation of more cuprite, copper carbonate, as well as new chalconatronite on copper alloys (Scott 2002, 363,364). XRD analysis was run on one example of the new leaded and unleaded bronze coupons, with and without pretreatment with sodium sesquicarbonate, before corrosion testing (Table 4.5). Cuprite, the only corrosion compound identified by XRD on the new bronze, was found on those coupons that had been treated with sodium sesquicarbonate (Table 4.5) (Appendices 4.1-4.2). The absence of XRD identifications of corrosion products on the other new bronze test coupons would suggest an amorphous corrosion state as confirmed by other researchers, or that too little corrosion product was present (López-Delgado *et al*. 2001, 5209). There are early stages in the development of cuprite, for example, that cannot be detected by XRD and require other analytical means such as XPS (X-ray Photon Spectroscopy) (López-Delgado *et al*. 2001, 5207). A tarnishing of the surface, however, would indicate the formation of cuprite. XRD analysis was run on the coins before corrosion testing without pretreatment with sodium sesquicarbonate. Coin 2 was analysed before and after pretreatment (Table 4.5).

Corrosion products typical to archaeological bronze were identified on the untreated coins: copper oxides, copper hydroxy carbonates, copper hydroxy chlorides as well as calcium silicate (Table 4.5). Treatment with sodium sesquicarbonate is known to cause the formation of additional cuprite, copper carbonate and chalconatronite on archaeological bronzes. One coin (coin 2) was analysed by XRD after treatment with sodium sesquicarbonate and calcite was identified as a new product (Table 4.5). On the other coins used in this study, however, it is not confirmed that pre-treatment with sodium sesquicarbonate caused the formation of chalconatronite or other corrosion products.

4.2.1.3 Experimental Method

The variables involved in the experimental method included the selection and evaluation of metals examined in Section 4.2.1.1. These included composition and structure of the metal used in testing, contaminants such as sodium, and state of metal surface before exposure to acetic acid vapour. In Section 4.2.1.3 the other variables in the experimental method, acetic acid vapour concentration and level of relative humidity (RH), are presented.

4.2.1.3.1 Generation of Controlled Humidity and Acidic Atmospheres

In the corrosion tests modern and ancient bronze compositions are exposed to various levels of acetic acid vapour concentration and relative humidity replicating common storage conditions. In particular three levels of each are examined (high, medium and low). Ancient Greek and Roman bronze coins with naturally formed corrosion from burial are included in the study. One of the goals of this project is to be able to recommend safe storage and display practices for bronze works of art and antiquities. Controlling the level of acetic acid vapour or relative humidity is a means to achieve this goal. Numerous cost-effective means are available for mitigating acetic acid emissions and relative humidity in addition to the more costly central heating and cooling systems. Data exist from the testing of pure copper exposed to varying levels of relative humidity and acetic acid vapour (see Chapter 3).

Table 4.4 Test Series 1: Part One 12 Test Chambers

Acetic acid vapour concentration	32 % RH ($CaCl_2.6H_2O$) April 8 - May 21, 2004 (6 weeks/42days)	52% RH $(MgNO_3)_2.6H_2O$ May 3 - June 17, 2004 (6 weeks + 3 days/45 days)	86% RH $(Na_2SO_4).10H_2O$ May 21 - July20, 2004 (8 weeks +2 days/58 days)
40ppm	Test 1	Test 5	Test 9
	Group 1 L + U + coin 6	Group 9 L + U + coin 3	Group 17 L + U + coin 5
	Group 2* L + U + coin 4	Group 10* L + U + coin 1	Group 18* L + U + coin 2
4 ppm	Test 2	Test 6	Test 10
	Group 3 L + U + coin 6	Group 11 L + U + coin 3	Group 19 L + U + coin 5
	Group 4* L + U + coin 4	Group 12* L + U + coin 1	Group 20* L + U + coin 2
0.4 ppm	Test 3	Test 7	Test 11
	Group 5 L + U + coin 6	Group 13 L + U + coin 3	Group 21 L + U + coin 5
	Group 6* L + U + coin 4	Group 14* L + U + coin 1	Group 22* L + U + coin 2
Control (no acid)	Test 4	Test 8	Test 12
	Group 7 L + U + coin 6	Group 15 L + U + coin 3	Group 23 L + U + coin 5
	Group 8* L + U + coin 4	Group 16* L + U + coin 1	Group 24* L + U + coin 2

L = leaded tin bronze B505; U = unleaded tin bronze B584; * = treated with sodium sesquicarbonate
Each test contained 2 ASTM metal coupons and 1 coin wedge not treated with sodium sesquicarbonate and 2 ASTM metal coupons and 1 coin wedge treated with sodium sesquicarbonate. Each test contained a total of 4 ASTM coupons and 2 coins wedges. Table 4.2 lists coin compositions. Table 4.5 lists XRD results.

Table 4.5 Test Series 1: Part One XRD Results of Metals Prior to Corrosion Testing

Test piece	Test piece #	ICPDS	Compound	Formula
Unleaded tin bronze	17U	02-1436	Copper tin	CuSn
Leaded tin bronze	17L	02-1436	Copper tin	CuSn
Unleaded tin bronze *	18U	01-1142 17-0865	Cuprite Copper tin	Cu_2O $Cu_5.6Sn$
Leaded tin bronze *	18L	05-0667	Cuprite	Cu_2O
Coin 1		03-0892 01-0959 03-0884	Cuprite Copper hydroxy carbonate (malachite) Copper oxide (tenorite)	Cu_2O $CuCO_3.Cu(OH)_2$ CuO
Coin 2		18-0306	Calcium silicate	$CaSiO_3$
Coin 2 *		47-1743	Calcite	$CaCO_3$
Coin 3		05-0667 23-0950	Cuprite Copper chloride hydroxide hydrate	Cu_2O $Cu_46Cl_{24}(OH)_68.(H_2O)_4$
Coin 4		18-0306 05-0667	Calcium silicate Cuprite	$CaSiO_3$ Cu_2O
Coin 5		03-0884 05-0667	Copper oxide (tenorite) Cuprite	CuO Cu_2O
Coin 6		04-0836 02-1067	Copper cuprite	Cu Cu_2O

* = XRD run after treating with sodium sesquicarbonate; U = unleaded tin bronze B584
L = leaded tin bronze B505

4.2.1.3.2 Selection of Acetic Acid Vapour Levels

Most corrosion tests reviewed in Chapter 3 incorporate a range of acid vapour concentrations from less than 1 ppm to 100 ppm or higher. The lowest concentration chosen as the starting level was 0.4 ppm since it represents the smallest concentration found in the Agora Museum and British Museum cases (range from 1039 μgm^{-3} [400 ppb/0.4 ppm] to 2880 μgm^{-3} [1152 ppb/1.15 ppm] was measured in these institutions) (Paterakis 2003, 321). The next two levels of increasing concentration, 4 and 40 ppm, were chosen according to methodologies of other studies. Typically the acid concentration is increased in multiples of 10, for example 0.4, 4, and 40 ppm or 0.5, 5, and 50 ppm were commonly used in the corrosion tests reported in Chapter 3. These levels were chosen to facilitate comparison of results with the other studies. 40 ppm acetic acid was the maximum concentration used in the current testing as studies have

shown that this concentration is adequate for producing acetate compounds on copper and lead within a relatively short time. This level ensured corrosion results within the time allotted for the tests.

It might be presumed that the low concentration of 0.4 ppm would require a lengthy period of time that could exceed the test duration in order to promote corrosion. At the acetic acid level of 0.4 ppm acetate corrosion could take many years to develop. Since the duration of the tests was a maximum of 58 days it was anticipated that this level might not produce acetate. To confirm this the three acetic acid concentrations used in the experimental work in Chapter 4 were converted into dose concentration (ppm x days x (1yr/365days) in Table 4.6 to facilitate comparison with the published LOAED figures for acetic acid (Table 4.7). The lowest observed adverse effect level [LOAEL] is used to determine the lowest observed adverse effect dose [LOAED]. "LOAED is the cumulative dose concentration [LOAEL x time] at which the first signs of adverse effects are observed." (Tetreault 2003a, 23). Tetreault and Thickett agree on the LOAED of acetic acid on pure copper in 50%/60% RH: 0.4/0.44 ppm yr (Tetreault 2003a, 26; Thickett 1997). Tetreault and Thickett found LOAED values of 0.024 to 0.032 ppm yr for acetic acid on lead in 50% to 75% RH. The LOAED of acetic acid reported by all the researchers ranged from 0.004 to 0.44 ppm yr on pure copper and from 0.0016 to 0.12 ppm yr on lead. The ranges result from different RH levels and methods of assessment. The greater sensitivity of lead to acetic acid is apparent from these LOAED figures. Tarnished lead protected the metal from corrosion producing higher LOAED levels (0.28 ppm yr and 1.2 ppm yr) (Tetreault 2003a, 26).

The concentrations of 0.4 ppm and 4 ppm in the tests in 52% RH correspond to the dose concentration of 0.049 ppm yr and 0.493 ppm yr respectively (Table 4.6). 0.493 ppm yr matches the LOAED for copper and 0.049 ppm yr exceeds the LOAED for lead in this RH (Table 4.7). Copper would be expected to corrode in 0.493 ppm yr but not in 0.049 ppm yr whereas lead could corrode in 0.049 ppm yr. A LOAED for the formation of acetate on copper is 0.5 ppm yr at 40% RH (Cano and Bastidas 2002) and on lead is 0.4 ppm yr at 54% RH (Tetreault *et al.* 1998). These minimum doses for the formation of acetate were used as a guide in the selection of the acetic acid doses in the tests in Chapter 4. The lowest doses (0.046 - 0.063 ppm yr) would not produce acetate whereas the median doses of 0.460 – 0.635 ppm yr could produce acetate on lead and on copper

(Table 4.6). The highest doses (4.602 – 6.356 ppm yr) would be expected to produce acetate on both metals (Table 4.6).

Table 4.6 Conversion of test acetic acid concentrations into LOAED

RH %	Days	ppm	Dose Concentration (ppm yr)
86	58	0.4	0.063
		4.0	0.635
		40	6.356
52	45	0.4	0.049
		4.0	0.493
		40	4.931
32	42	0.4	0.046
		4.0	0.460
		40	4.602

Table 4.7 Published LOAED figures for acetic acid on copper and lead*

Assessment	RH %	Days	LOAED μg m^{-3} yr	LOAED ppm yr	Reference
Copper					
na	50-60	na	1000	0.4	Tetreault 2003a, 26
vo	50	120	1100	0.44	Thickett 1997
vo	100	120	90	0.036	Thickett 1997
wl	100	21	10	0.004	Clarke and Longhurst 1961
wl	100	21	10	0.004	Donovan and Stringer 1972
vo,ea	100	21	70	0.028	López-Delgado *et al.* 1998
Lead					
wg	23-44	76	10	0.004	Eremin and Wilthew 1998
vo	50	120	300	0.12	Miles 1986; Tetreault and Stamatopoulou 1997
vo	50	120	60	0.024	Thickett 1997
wg	75	180	80	0.032	Tetreault *et al.* 1998
wl	100	21	4	0.0016	Donovan and Stringer 1972
wg[1]	54	180	3000	1.2	Tetreault *et al.* 1998
wg[2]	75	180	700	0.28	Tetreault *et al.* 1998

* From Tetreault 2003a, Appendix 2, 107. na=not available; vo=visual observation; wl=weight loss; ea=electrochemical analysis; wg=weight gain; [1,2] tarnished lead

4.2.1.3.3 Selection of Relative Humidity levels

Collections of art and antiquities are often subjected to a wide range of relative humidity (RH) and fluctuations in RH in storage or on display. The influence of moisture

in corrosion processes has been studied extensively and much research regarding corrosion prevention and stabilization by controlling the relative humidity has been carried out (Faltermeier 1999; Golfomitsou and Merkel 2004; Graedel 1987, 2160; Hatchfield 2002, 59; Organ 1970, 81; Scott 1990, 202; Thickett 2007; Thickett 2008). Many of the corrosion studies reviewed in Chapter 3 included a range of relative humidity levels in testing for comparative purposes. Typically they included a level below 50%, one around 50% and a third above 50% RH. In this project three levels of RH were chosen for testing:

1) There is no consensus on the appropriate RH level to prevent bronze disease. A level below 35% has been reported to be required in the prevention of bronze disease (Organ 1970, 73-84) whereas others claim less than 46% RH can be adequate protection (Scott 1990, 203). The range 35% RH to a maximum of 45% RH is commonly used by many conservators as a guide for the prevention of bronze disease in storage and display (Cronyn 1990, 227; Tsatsouli 2004). 32% RH was chosen in these tests as it falls below all recommended levels for the prevention of bronze disease. It is important to determine if a low level that protects against bronze disease would also protect metals from corrosion by acetic acid;

2) 52% RH is too high to prevent bronze disease but is lower than the equilibrium relative humidities (eqRH) of a sodium copper carbonate acetate (approximately 65% eqRH) and sodium acetate trihydrate (75% eqRH) (Thickett 1998, 9). 52% RH would stabilize these acetate compounds in the crystalline state and represent a safe level for objects afflicted by acetate compounds in storage. Not until the eqRH is surpassed will they deliquesce. It should be noted that mixed salts behavior differently from single salts by responding to a range in RH (Price and Brimblecombe 1994; Price 2000);

3) A RH above 67% was preferred since the corrosion of lead was found to increase above this RH (Tetreault *et al.* 1998). 86% RH was selected as it exceeds the equilibrium RH levels of sodium copper carbonate acetate and sodium acetate trihydrate. It provides abundant moisture to ensure the development of corrosion within the time allotted for the exposure tests.

The technique of using saturated salt solutions to maintain a stable relative humidity in test chambers has been used by many researchers. Saturated solutions of salts were used to maintain these specific levels of relative humidity in the test chambers: $CaCl_2.6H_2O$ for 32% at 20° C, $(MgNO_3)_2.6H_2O$ for 52% at 24.5° C, and $Na_2SO_4.10H_2O$ for 86% at 20° C (Gibson *et al*. 1997a, 5; Gibson *et al*. 1997b, 15; Greenspan 1977, 94).

The target RH of a saturated solution of $Na_2SO_4.10H_2O$ of 93% was not reached. These saturated salt solutions maintained a stable RH during the course of testing. Contamination from saturated salt solutions can sometimes pose a problem (Piechota 1992). Based on the XRD results of my test samples (Tables 4.16 – 4.19) there was no indication of contamination of the metal corrosion by the salt compounds chloride, nitrate and sulphate.

4.2.1.3.4 Determining Acidic Concentration of Atmosphere

Specific levels of acetic acid vapour concentration and relative humidity were reached by mixing specific amounts of acetic acid with saturated solutions of the salts (Table 4.9). This method of forming known vapour concentrations of acids in a stable relative humidity within an enclosed environment has been used by numerous researchers such as Gibson *et al*. (1997a, 3) and Tetreault *et al*. (2003, 246). Two different units are used to quantify concentration of acid vapour: ppm = parts per million = 1 pollutant molecule for every group of 1 million air molecules, and ppb = parts per billion = 1 pollutant for every group of 1 billion air molecules. They represent the volume fraction of pollutants in the ambient air. The other unit of measurement is mg m^{-3} = milligrams per cubic meter or μg m^{-3} = micrograms per cubic meter, representing the quantity of a pollutant per unit volume.

For acetic acid the two units of measurement are related as follows (at 21° C and atmospheric pressure 101.3 Kpa): ppm/ppb = mg m^{-3}/μg m^{-3} is multiplied by 24.04 dm^3 (molar volume of a perfect gas), then divided by 60.05 g/mol (molecular weight of acetic acid) (Tetreault *et al*. 2003). Table 4.8 may be used for a simpler conversion between mg m-3/μg m-3 and ppm/ppb (Grzywacz 2006, 26). Ppm and ppb are used throughout this thesis since most authors reported acid levels in these units of measurement.

Table 4.8 Conversion Factors Acid Concentrations (from Grzywacz 2006, 26)

	from	to	multiply x
Acetic acid	mg m^{-3}/μg m^{-3}	ppm/ppb	0.40
Formic acid	mg m^{-3}/μg m^{-3}	ppm/ppb	0.50
Acetic acid	ppm/ppb	mg m^{-3}/μg m^{-3}	2.49
Formic acid	ppm/ppb	mg m^{-3}/μg m^{-3}	1.91

In the preparation of the acid/salt solution mixtures the recommendations offered by Gibson *et al*. (1997b) and Tetreault *et al*. (2003) were followed initially but it was found that adjustments were required in the amounts of acetic acid used (Gibson *et al*. 1997b, 15). Tetreault recommends this formula to arrive at vapour phase concentration: ppm (vol) acetic acid = 23 x content of salt solution in v/v % (Tetreault *et al.* 2003, 246). Using the following figures provided by Gibson *et al*. (1997b) and Tetreault's formula recalculating the result did not confirm observations.

Table 4.9 Amounts of Acetic Acid and Saturated Salt Solutions used for Tests

32% RH			
µl acetic acid start of test April 8	g saturated calcium chloride solution	Target ppm acetic acid	µl acetic acid added to bag & date
45 + 10 g solid salt	15	40	3 µl April 9, 12, 21, 26 May 4; 4 µl April 20, May 3, 5; 6 µl May 6, 8
7 + 10 g solid salt	15	4	Replaced acid/salt mixture April 15 (readings too high). Added 2 µl April 22, May 6, 14; 1 µl May 3, 5, 8, 17, 18
1 + 10 g solid salt	15	0.4	Replaced acid/salt mixture April 15 (readings too high)

52% RH			
µl acetic acid start of test May 3	g saturated magnesium nitrate solution	Target ppm acetic acid	µl acetic acid added to bag & date
30	15	40	10 µl May 8; 3 µl May 21, June 9 Replaced acid/salt mixture May 25(readings too low). Replaced acid/salt mixture May 27 (readings too high).
1.25	15	4	1 µl May 3, 17, 21, 22, June 9; 2 µl May 7 Replaced acid/salt mixture May 25(readings too low). Replaced acid/salt mixture May 27 with 2 µl acid instead of 1.25 µl (readings too low).
0.1	15	0.4	

86% RH			
µl acetic acid start of test May 21	g saturated sodium sulphate solution	Target ppm acetic acid	µl acetic acid added to bag & date
60	15	40	300 µl June 21; 100 µl June 25; 60 µl June 17, 19; 10 µl May 22; 3 µl May 28; Replaced acid/salt mixture June 9 (salt drying out, RH too low). Replaced acid/salt mixture June 24 (acid level too low) - used 120 µl acid. Replaced acid/salt mixture July 6 (salt drying out, RH too low) - 120 µl acid.
1.25	15	4	1 µl May 22; 0.5 µl May24; 2 µl June 17; 3 µl June 19, 10 µl June 21; Replaced acid/salt mixture June 24 (acid level too low) - used 2.5 µl

			acid. Replaced acid/salt mixture July 6 (salt drying out, RH too low) - 2.5 μl acid.
0.1	15	0.4	Replaced acid/salt mixture June 24 (acid level too low) - used 0.1 μl acid. Replaced acid/salt mixture July 6 (salt drying out, RH too low) - 0.1 μl acid.

Based on the recommendations of Gibson *et al*. (1997b, 15) 0.5% weight of acetic acid was added to 99.5% weight of saturated calcium chloride solution for a target acid concentration of 70 ppm (175 mg m^{-3}). This amount (175 mg m^{-3}) was estimated from 386 mg m^{-3} reported for 1.0 % weight of acetic acid (Gibson *et al*. 1997b, 15). Initially the author made dilutions from this first mixture with the aim of arriving at 40, 4 and 0.4 ppm acetic acid (Table 4.9). Although atmospheric concentrations change linearly with concentration of acid in the salt solution (L. Gibson pers comm. 2003) it was found that with dilution it was not possible to obtain these target concentrations.

A considerable amount of experimentation was required to adjust the proportion of acid to saturated salt solution. For the other two salt compounds the recommended ratio of acid to saturated salt solution above did not apply since different salts create different acidic vapour concentrations (L. Gibson pers comm. 2003). Each saturated salt solution has a different rate of pushing the acid out of solution in a process referred to as the "salting out effect". This is attributed to an empirical relationship that states the log of the activity coefficient of non-electrolytes [acid] is proportional against the concentration of salt solutions (Gibson *et al*. 1997a, 5). Prior to beginning the corrosion tests, glass jars with a septum in the screw lid were used as airtight receptacles for the determination of the acid to salt ratio by measuring the acid vapour concentration in the jar. Air samples were removed from the jar with a gas chromatograph syringe and adjustments made to the quantity of acetic acid mixed into saturated salt solution until the target concentrations were reached. Accurate vapour phase concentrations of acetic acid vapour were determined with a Hewlett Packard 5890A Gas Chromatograph with Flame Ionizing Detector (GC-FID). A Hewlett Packard GC Chem Station (1996 rev. A.04.01) was used to record chromatograms and to calculate peak areas. Since 0.4 ppm acetic acid was smaller than the detection limit of the GC-FID, this level was determined by extrapolating back to zero acid concentration using a linear least squares regression program.

4.2.1.3.5 Test Chambers

Once the correct proportions of acetic acid to saturated salt solution were determined for each of the vapour concentrations the acid/salt mixture was poured into a petrie dish (Table 4.9). Each metal test piece was placed flat in a separate, small petrie dish thereby contributing a total of 4 new metal coupons and 2 corroded coin wedges in 6 petrie dishes in each corrosion test. A total of 12 test chambers were set up (Table 4.4). Each test chamber included two groups of test pieces: each group consisted of one unleaded tin bronze, one leaded tin bronze, and one corroded coin wedge. One group was treated with sodium sesquicarbonate (group number 2, 4, 6, 8, 10, 12, 14, 16, 18, 20, 22, and 24) (Table 4.4). 72 new metal coupons and coin wedges were used in total. The 6 metal test coupons and coin wedges and the separate acid/salt mixture were enclosed in transparent Tedlar® bags equipped with a stainless steel valve fitting for filling the bag with air and a stainless steel septum fitting for removing air samples (Figure 4.1). Tedlar® is 98% polyvinyl fluoride polymer and 2 % epoxy resin, gas impermeable, chemically inert, flexible, and 2 ml thick. They were purchased from SKC Incorporated (Appendix 19). Since the Tedlar® bags are closed on all sides they were cut open along one end allowing the placement of the acid/salt solution and metal test coupons and coin wedges, then sealed by folding the edges a few times and closing with a Mitsubishi plastic sealing clip provided for sealing bags made from barrier films such as Escal™. It was necessary to fold the Tedlar® a few times since it is considerably thinner than Escal™. These plastic sealing clips are available as part of the RP System™, the atmospheric modification preservation system, manufactured by Mitsubishi Gas Chemical America, Inc. After sealing the bags were inflated with purified laboratory air to slightly less than maximum capacity. Laboratory air was passed through 4 layers of filtration to produce ultra pure air for the tests. The layers are Puracarb Media, Purakol Media, CP Blend Media, and angel hair wool. Puracarb, Purakol and CP Blend are activated charcoal that target different contaminants: Puracarb removes acid from corrosive pulp and paper environments, Purakol Media removes toxic and corrosive gases, and CP Blend Media removes indoor pollutants. All are manufactured by Purafil (Appendix 19). The angel hair wool removes particulate matter. The volume of the Tedlar® bags after cutting and sealing was 1700 ml. The targeted exposure levels were 0.4, 4, and 40 ppm acetic acid vapour concentration at 32%, 52%, and 86% relative humidity. Three control tests (4, 8, 12) were run without acetic acid vapour, at 32%, 52% and 86% RH (Table 4.4). All tests were carried out at room temperature of 20° C (± 2°

fluctuation) in an air conditioned laboratory at the Getty Conservation Institute in Los Angeles.

Figure 4.1 Test Chambers using Tedlar® bags

4.2.1.3.6 Monitoring Acidic Concentration during Testing

Concentrations in these test chambers were monitored by sampling the air with a gas-tight syringe and analyzing acetic acid concentration with gas chromatograph with flame ionizing detector (GC-FID), Hewlett Packard 5890A. Software used was HP GC Chem Station 1996, Rev. A.04.01. The technique is described in Section 4.2.1.3.4, Determining Acidic Concentration of Atmosphere. The RH in the Tedlar® bags was monitored with hair thermohygrometers with an accuracy of ±5%.

The gas chromatograph was calibrated using a known amount of acetic acid in a known volume of air in a standard dilution bottle. This standard dilution bottle with a volume of 2210.43 ml was purged with nitrogen and injected with 3 µl acetic acid, then placed in an oven at 105° C. The acidic acid vapour concentration in the bottle equated to 575 ppm. Once equilibration was reached 6 samples of increasing size were removed from the bottle with a gas chromatographic syringe and injected into the GC-FID to form a calibration curve. The calibration curve ranged from 1.43 ppm to 57.5 ppm. The software plots area on the y axis verus concentration in ppm on the x axis. Area = ng/volume injected. The ppm is read from the calibration curve made up of 6 points.

Observations

Acetic acid vapour concentration level was found to drop during the tests on account of a combination of factors; the "salting out effect" (see Section 4.2.1.3.4), slow leakage from the bag, and adsorption of acid by the metal and glass in the bag (Gibson *et al*. 1997a, 5). Adsorption capacity of the materials exposed to acid has a direct effect on acidic vapour concentration in an enclosed space (L. Gibson pers comm. 2003). Acetic acid was injected with a syringe through the valve in the bag into the acid/salt solution in the chambers as needed during the tests when the vapour concentration decreased. Injecting through the valve fitting alleviated the need to open the bags in order to replenish the acid. The advantage to using the Tedlar® bags was the ease of removing air samples for analysis and injecting acid as needed to boost acid vapour concentration without having to open the test chambers. The Tedlar® bags were kept in a positive pressure, inflated state, to compensate for the lack of a completely airtight seal.

Dosimeters

Tube samplers, badges and dosimeters can be used to measure the levels of pollutants in the air (Gibson *et al*. 1997a, 2; Grzywacz 2006, 29). Tube samplers are exposed for a certain length of time, then the reactive sorbent is analysed. Badges can indicate when certain concentrations have been reached and can be analysed for cumulative levels. Dosimeters are glass tubes containing a reagent that measure concentration of the pollutant by color change. The advantages of dosimeters are ease of use and relative low cost. It is known that inaccuracies in dosimeter readings due to interference by other acidic gases can occur (Gibson *et al*. 1997a, 2). Two types of dosimeters for detection of acetic acid vapour, made by Gastec and Draeger, were measured for accuracy in this project (Appendix 19) (See Chapter 7, Figure 7.1). The Gastec dosimeter detection range was 5 to 100 ppm acetic acid and the Draeger dosimeter detection range was 10 to 200 ppm. These dosimeters were monitored independently in the corrosion tests in Tedlar® bags containing each of the acid plus saturated salt solution mixtures. The acetic acid vapour concentration was measured with the GC-FID to determine the accuracy of the dosimeter readings.

Observations

The Gastec tubes were found to read consistently lower than the Draeger tubes. Tests with a target acetic acid vapour concentration of 20 ppm reached an equilibrium in concentration after 3 hours and were accurately read by the Gastec dosimeters in the chambers with calcium chloride and sodium sulphate. A stabilized reading of acetic acid concentration in the sodium sulphate test chamber was reached after 4 hours with both dosimeters.

Paper Indicator Strips

A-D Strips for acetic acid were tested in conjunction with the Gastec dosimeter tubes in 32% RH chambers with 40, 4 and 0.4 ppm acetic acid vapour concentration (Appendix 19). A-D Strips are manufactured by the Image Permanence Institute and are acid-base indicator papers that turn from blue to shades of green to yellow (maximum concentration acetic acid). Their detection range is 1 to 20 ppm acetic acid. It was found that at lower concentrations (4 ppm) the A-D Strips required more than 5 hours to give an accurate reading. At higher concentrations (40 ppm) they required 4 hours to reach an accurate reading. Due to difficulty in distinguishing color changes and matching color the A-D Strips were considered to be less accurate than the dosimeter tubes.

4.2.1.4 Analytical Results after Corrosion Testing

Following the corrosion tests all coupons and coins were weighed directly from the test chamber, without heating or drying, to prevent alteration of the corrosion formed during the tests. The procedure was that all coupons and coins after weighing were kept in the same relative humidity in which they were tested, without acetic acid, for stabilization of the corrosion morphology to permit subsequent examination and analysis.

4.2.1.4.1 Gravimetric Analysis

Weight was recorded for the test coupons and coins before corrosion testing after heating in oven overnight at 105° C followed by equilibration in a desiccated vacuum jar until a constant value was obtained. Following the corrosion tests all coupons and coins

were weighed directly from the test chamber (Appendix 5.1 - 5.3). The analytical balance measured to three decimal places with a weighing error of ±0.001 g. Heating or drying to achieve a constant weight was not carried out as it may have altered some hydrated corrosion products and interfered with XRD analysis after testing.

Results of Gravimetric Analysis

Taking into account the weighing error most of the significant weight changes were recorded for the test coupons and coins in 40 ppm acetic acid at 86% RH (Tables 4.10, 4.11). The weight change was plotted against Pb content for the test coupons in 40 ppm at all RH levels with a range in standard error from ±0.06% to ±0.14% in Figure 4.2. The weight change was plotted against Pb content for the coins in all acid concentrations and RH levels to examine the influence of Pb content overall (standard error ±0.06% to ±0.64%) (Figure 4.3).

Table 4.10 Average weight % changes of test coupons with standard error

32 % RH			
ppm	Dose concentration ppm yr	Leaded ASTM B505 (8% Pb)	Unleaded ASTM B584 (0.25% Pb)
0.4	0.046	0.02 ±0.0001	0.04 ±0.01
4	0.460	0.05 ±0.001	0.07 ±0.04
40	4.602	0.09 ±0.02	0.1 ±0.07
52% RH			
0.4	0.049	- 0.22 ±0.13	0.008 ±0.06
4	0.493	- 0.06 ±0.06	- 0.06 ±0.10
40	4.931	- 0.01 ±0.01	0
86% RH			
0.4	0.063	0.01 ±0.01	- 0.03 ±0.17
4	0.635	0.11 ±0.01	0.12 ±0.05
40	6.356	0.49 ±0.06	0.26 ±0.14

ASTM compositions are listed in Table 4.1; Negative values indicate possible loss of minute particles on transfer; Based on gravimetric results in Appendices 5.1- 5.3.

Table 4.11 Weight change % of coins with standard error after exposure to 40 ppm acetic acid

Coin	Pb %	% RH	% weight change
Coin 2	23	86	1.13 ±0.28
Coin 5	1	86	- 0.28 ±0.16
Coin 3	3	52	0.71 ±0.29
Coin 1	2	52	0.11 ±0.12
Coin 6	4	32	0.08 ±0.06
Coin 4	2	32	- 1.53 ±0.64

Coin compositions are listed in Table 4.2; Negative values indicate possible loss of minute particles on transfer; Based on gravimetric results in Appendices 5.1- 5.3

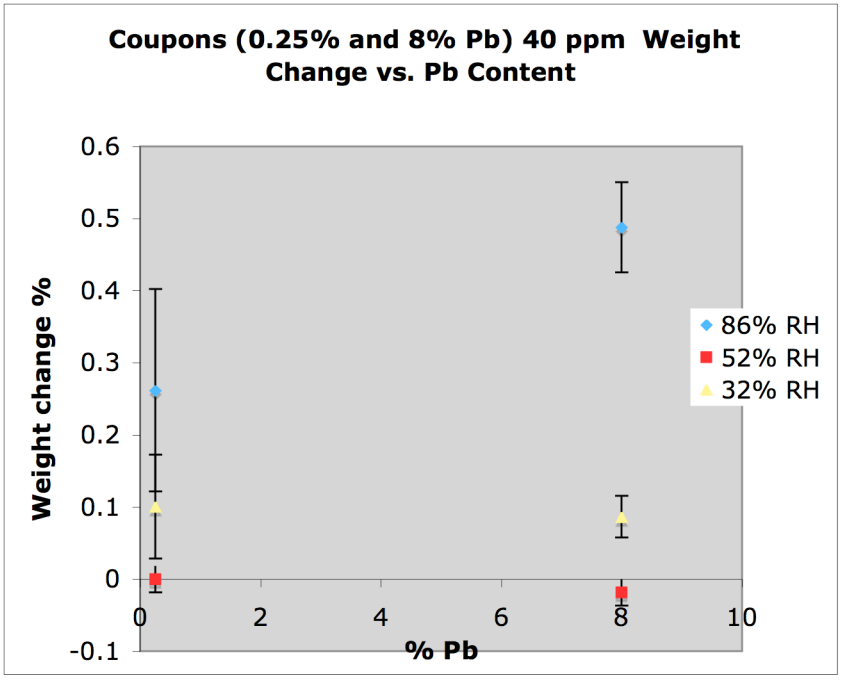

Figure 4.2 Graphic representation of Table 4.10 showing weight change of test coupons according to RH level in 40 ppm acetic acid

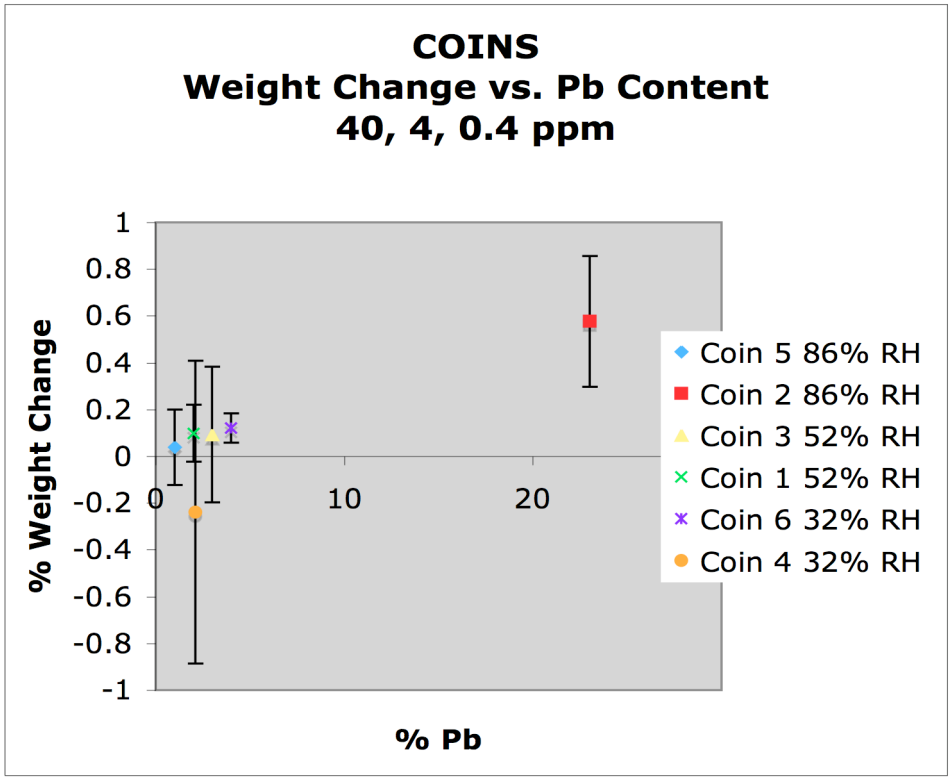

Figure 4.3 Graphic representation of Table 4.11 portraying weight change of coins in all acetic acid concentrations; Negative values indicate possible loss of minute particles on transfer.

86% RH

The coupons gained maximum weight at 86% RH: the leaded coupons gained 0.49% and the unleaded coupons gained 0.26% on average (Table 4.10). At 86% RH the weight gain of the leaded coupons surpassed that of the unleaded coupons. Increased corrosion above 67% RH is attributed to an increase in the number and mobility of acetate ions (Tetreault *et al.* 1998, 25). The weight changes of the coins did not follow the clear cut trend of the coupons based on Pb content that is explained in a subsequent section. Coin 5 (predominantly copper and low in alloy content) and Coin 4 (heavily worked) lost weight in 40 ppm at 86% RH that may have resulted from the dissolution of the pre-existing corrosion patina or loss of corrosion powder prior to weighing (Table 4.11; Appendix 5.3).

52% RH

Comparing overall the weight changes of the test coupons according to RH, the smallest weight gain occurred in 52% RH (Figure 4.2). The leaded coupons demonstrated weight loss in 52% RH in all acid concentrations (Table 4.10). Significant weight loss was observed in the leaded coupons in the dose concentration of 0.049 ppm yr acetic acid (0.4 ppm tests) in 52% RH which exceeds the LOAED for lead (0.024-0.032 ppm yr, 50-75% RH) (Table 4.7, Table 4.10). A similar trend, namely decreasing weight gain, was found on lead coupons in 1.4 ppm yr to 7.2 ppm yr acetic acid in 54% RH by Tetreault (Tetreault *et al.* 1998). This was attributed to the formation of a water-insoluble lead acetate oxide that inhibited corrosion. The extent to which the lead component in the leaded test coupons contributed to this decrease in corrosion in 52% RH is a subject for further research. In 52% RH Coin 3 gained more weight on average than Coin 1 in 40 ppm (Table 4.11). Since both coins have similar lead content this difference in weight gain may be attributed to differences in manufacture. Coin 3 was cold worked in the final stage of manufacture (whereas Coin 1 was annealed) that could have contributed to its susceptibility to corrosion (Table 4.3).

Comparison of the influence of Pb content and RH

A comparison of the coins in all acid concentrations shows that lead content in the range from 1 to 4% Pb had little influence whereas 23% Pb had substantial influence on weight change (Figure 4.3, Table 4.11). It also shows that RH had little influence on weight change for the coins containing 1 to 4% Pb. This trend is matched by the leaded (23% Pb) test coupons: greater Pb content and higher RH promoted increased weight gain (Figure 4.2). The difference between the behavior of the coins and the test coupons may be explained by two factors. The test coupons are of consistent alloy composition and manufacture whereas the coins vary in % Pb content, alloy composition, manufacture (annealed versus cold-worked), and possible contaminants (Table 4.3).

Comparison of LOAED with weight change

Most of the significant weight gain occurred in the dose concentration of 6.356 ppm yr acetic acid (40 ppm tests) in 86% RH that exceeds the LOAED for copper (0.4 ppm yr, 50-60% RH) by one order of magnitude and the LOAED for lead (0.024-0.032

ppm yr, 50-75% RH) by two orders of magnitude (Tables 4.7, 4.10, 4.11). Lead was found to corrode more than copper by one order of magnitude in the dose concentration of 0.28 ppm yr (100% RH) that exceeds the LOAED for lead (Donovan and Stringer 1971).

A gradual increase in corrosion was found for lead over a12-month period in different concentrations of acetic acid at 54% RH (Tetreault *et al.* 1998, 23). The minimum and maxmum dose concentrations tested for the first two months were 0.03 ppm yr and 5.5 ppm yr that may be compared to the tests from 0.049 ppm yr and 4.931 ppm yr dose concentrations at 52% RH (0.4, 4, 40 ppm tests) in this chapter (Table 4.6). The slope was found to increase proportionally with increasing acetic acid concentration (Tetreault *et al.* 1998, 23). This parallels the overall trend in the Chapter 4 tests at 52% RH which shows a gradual decrease in weight loss from 0.4 to 4 ppm (Table 4.10). An increase in corrosion was also found for copper in the dose concentration of 0.5 ppm yr acetic acid at 100% RH (Lopez-Delgado *et al.* 1998). A substantial weight gain was determined on both coupons in a similar dose concentration, 0.6 ppm yr, from 0.06 ppm yr in the tests at 86% RH (Table 4.10).

An increase in weight with increasing acid concentration in high RH has been found on pure copper (Donovan and Stringer 1971; Lopez-Delgado *et al.* 2001) and pure lead (Coles *et al.* 1958; Donovan and Stringer 1971; Niklasson *et al.* 2005; Tetreault *et al.* 1998). The results of the test coupons at 86% RH in the current study parallel this trend (Table 4.10).

4.2.1.4.2 SEM and SEM-EDS of Coupons and Coins Corroded by 40 ppm Acetic Acid at 86% RH (the coupons and coins were removed from the Tedlar® test chambers for examination and analysis)

SEM imaging and SEM-EDS were used to follow the development and growth of corrosion during the tests exposing two copper alloys and ancient coins to 40 ppm acetic acid at 86% RH. Intermittent examination and analysis during the corrosion tests illustrates the sequence and extent to which the copper and alloy elements of lead and tin responded to the test conditions. Imaging coupled with EDS elemental analysis aids in the identification of active species and provides a plethora of information that would otherwise be lost if examination was restricted to after corrosion testing.

SEM and SEM-EDS of Unleaded Bronze

Unleaded Bronze Test Piece 18U (treated with Na sesquicarbonate) (Group 18, Test 9 in Table 4.4):

The metallographic examination of the unleaded tin bronze (ASTM B584) revealed a cast structure with an extensive α + δ eutectoid phase around copper rich α phase dendrites (Figure 4.4). After one week of exposure to 40 ppm acetic acid at 86% RH most of the surface was covered with a growth of irregular and somewhat feathery crystals (Figure 4.5). In 18U the high tin content of corrosion on the alpha + delta eutectoid (Spectrum 1) and the high copper content of corrosion in the alpha phase dendrites (Spectrum 2) were indicated by SEM-EDS (Table 4.12) (Figure 4.6) (Appendix 6.2). Since this bronze consists of 85% (wt.) copper and 17% (wt.) Sn (see Table 4.1) one would expect the extensive areas of crystallization to represent the α phase (since this is the copper rich solid solution of Sn in Cu that usually contains up to 9.1% Sn). The δ phase is an intermetallic compound of fixed composition $Cu_{31}Sn_8$ (Scott 2004, 27,28). The overall reading of the photo at 50x magnification reveals extensive corrosion that has masked the dendritic pattern of the metal (Figure 4.7). Photos taken at 400x and 500x magnification show long white parallel lines that are an artifact of the detector BSE (back scattered electrons). The GSE (gaseous secondary electron) detector revealed these areas to be striations in the metal surface in gaps between the crystalline corrosion that are the result of sanding and polishing (Figure 4.5). At 2000x magnification the eutectoid shows smooth, flat corrosion maintaining the parallel striations from sanding. After 2 to 3 weeks there is a proliferation of the copper compound crystal growth bordering on the eutectoid that is visible at 400x magnification. After 8 weeks of corrosion testing the gaps have been filled for the most part by these copper compounds creating a mostly uniform covering. Examination under greater magnification reveals crystal fibers or needles that have grown up from the surface that appear to be "capped" by cubic or prysmatic crystals forming a "head" (Figure 4.8). Perhaps these are copper acetate, copper hydroxide or copper hydroxide acetate crystals that grew from the cuprite on the surface and are "capped" most likely with copper acetate crystals. Three corrosion layers or phases may be present: (1) the first layer is cuprite on the metal surface; (2) the second layer consists of needles that may be copper hydroxide acetate or copper acetate grown up from the surface; (3) the third layer consists of cubic or prismatic crystals most likely of copper acetate on top of the needle-like crystals in layer 2. Although 18U was

treated with sodium sesquicarbonate prior to corrosion testing, sodium was not detected by EDS. The detection limit of the EDS was 1% for sodium.

Table 4.12 Results of SEM-EDS Analysis and Selected XRD Results (elements listed in order of prominence from greater to lesser)

Test piece	Week of test	Appendix	Spect-rum	Major elements	Minor elements	Observations	Identification Hypothetical *Confirmed by XRD
18U	1	6.1	1	Cu, O, Sn	C	Tin-rich from α + δ eutectoid	Tin oxide
			2	Cu, O	Sn, C	Copper-rich from α phase	Copper oxide (cuprite)
17L	1	6.9	1	Cu	O, C, Pb	Copper-rich	Copper oxide (cuprite)
			3	Cu, Pb	O, C, Sn	Copper and lead-rich	Lead oxide, Lead hydroxy carbonate, lead acetate
			4	Cu	O, C, Pb, Sn	Copper-rich	Copper hydroxy acetate
	8	6.13	1	Pb	O, C	Lead-rich	Lead hydroxy carbonate(hydrocerussite)
			2	Cu, O	C, Pb	Copper- rich	Copper oxide (cuprite)*
			3	Cu,O	Pb, C, Sn	Copper-rich	Copper acetate hydrate*
18L	2	6.16	1	Cu, O	C, Pb	Copper-rich	Copper oxide (cuprite)
			2	Pb	Cu, O, C	Lead-rich	Lead hydroxy carbonate(hydrocerussite)
			3	Cu	O, Pb	Copper-rich	Copper acetate hydrate*
	8	6.18	1	Pb	O, C	Lead-rich	Lead hydroxy carbonate(hydrocerussite)*
			2	Cu, O	C, Pb	Copper-rich	Copper oxide (cuprite)*
Coin 2	2	6.20	1	Pb	O, Sn, C, Cl, Ca, Cu, Si, P	Lead-rich	lead hydroxy carbonate (hydrocerussite)* lead carbonate (cerussite)* calcium carbonate
			2	Pb	O, Sn, C, Cl, Ca, Cu, Si	Lead-rich	lead hydroxy carbonate (hydrocerussite) lead carbonate (cerussite) calcium carbonate
			3	Pb	O, Sn, C, Cl, Ca, Cu, Si, P	Lead-rich	lead hydroxy carbonate lead carbonate (cerussite) calcium carbonate
			4	Pb, O, Sn	C, Ca, Cu, Si, P	Lead and tin-rich	

U = unleaded bronze ASTM B584; L = leaded bronze ASTM B505

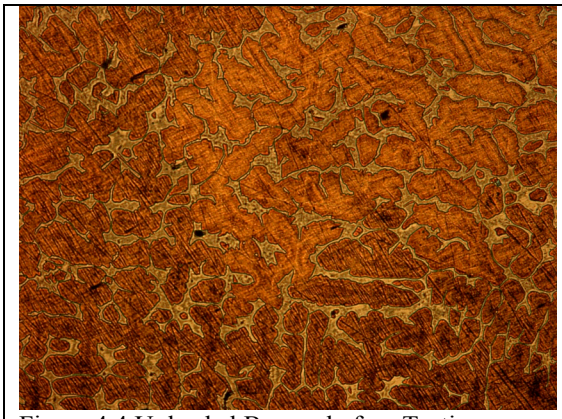

Figure 4.4 Unleaded Bronze before Testing ASTM B584 (Table 4.1 for composition) (Appendix 2.1)

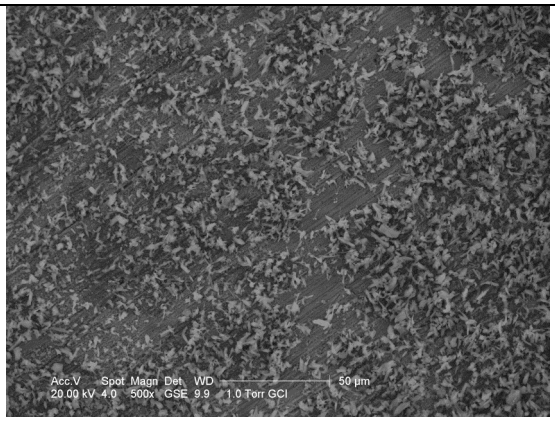

Figure 4.5 18U after 1 week 500x (Appendix 6.1)

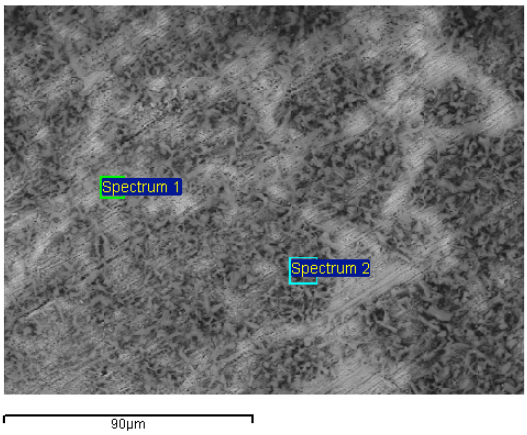

Figure 4.6 18U after one week (Appendix 6.2)

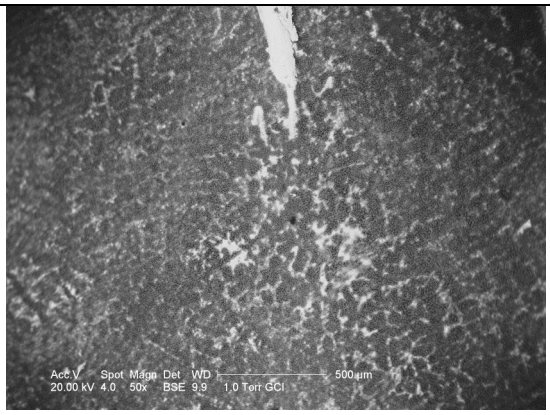

Figure 4.7 18U after one week 50x (Appendix 6.3)

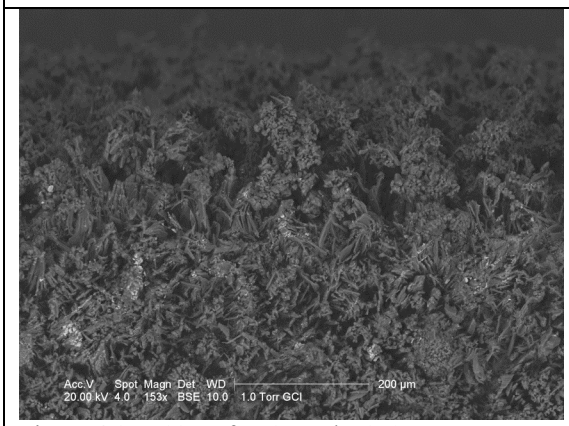

Figure 4.8 18U after 8 weeks 153x (Appendix 6.4)

Unleaded Bronze Test Piece 17U (not treated with sodium sesquicarbonate) (Group 17, Test 9 in Table 4.4):

17U differs from 18U in that it was not treated with sodium sesquicarbonate prior to testing. After one week of corrosion testing in 40 ppm acetic acid vapour at 86% RH the dendritic structure of the metal is clearly visible in the corrosion pattern (Figure

4.10). Based on the SEM-EDS results of 18U and the fact that 17U and 18U are the same tin bronze, we can assume that the darker areas are the copper rich α phase dendrites and the surrounding light colored areas are the α + δ eutectoid phase. Greater magnification reveals darker copper corrosion surrounded by lighter corrosion. Round features are visible with the GSE detector at 400x magnification on 17U 3 weeks into testing (Figure 4.11). These round features may result from poorly formed α phase dendrites. These are not to be confused with the round features representing initial corrosion noted by several researchers with the AFM at much higher magnification on bronze and pure copper (Kleber and Schreiner 2003, 294, 298). After 8 weeks of corrosion testing long bands of whisker-like crystals had apparently developed along the dendritic borders (Figure 4.12). Four corrosion layers or phases may be distinguished on 17U: the first three are those described under 18U and the fourth layer consists of thin, whisker-like crystals that have grown sideways from the "capping" crystals (layer 3) over the needle-like crystals (layer 2) (Figure 4.13). The crystalline habit of copper acetate formation has been corroborated in another study in which copper acetate crystals grew perpendicular from vertical crystals of copper hydroxide acetate, eventually covering the surface (López-Delgado *et al*. 1998).

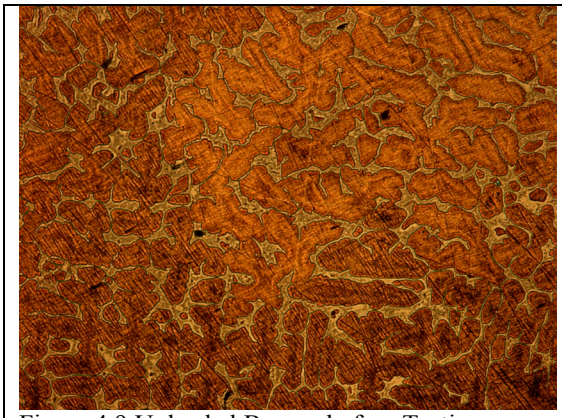

Figure 4.9 Unleaded Bronze before Testing ASTM B584 (Table 4.1 for composition) (Appendix 2.1)

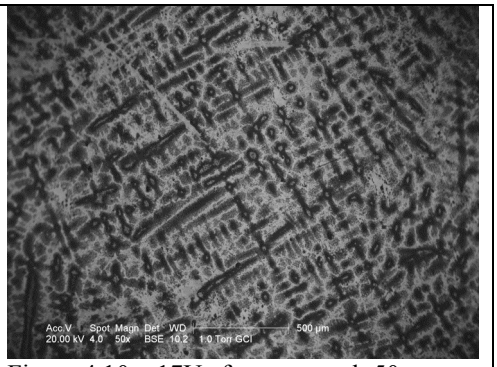

Figure 4.10 17U after one week 50x (Appendix 6.5)

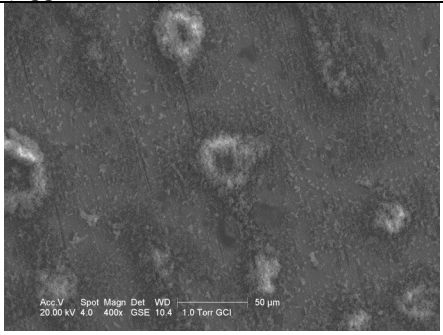

Figure 4.11 17U after 3 weeks 400x (Appendix 6.6)

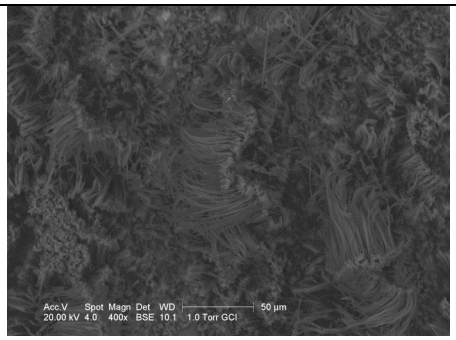

Figure 4.12 17U after 8 weeks 400x (Appendix 6.7)

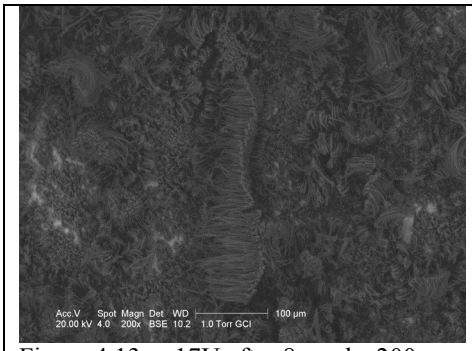

Figure 4.13 17U after 8 weeks 200x (Appendix 6.8)

The cuprite layer serves for the growth of subsequent layers 2, 3 and 4. In Figure 4.13 the thicker needles in layer 2 that connect the surface of the metal with the copper acetate "capping" crystals are visible to the right of the long band of whisker-like crystals. They serve as the conduit of ions between the metal and the upper crystal formations. SEM examination of the long bands of whisker-like crystals revealed "trees" of darker and lighter corrosion growing from the surface. These lengths of whisker-like crystals seem to be oriented as are the dendrites, in a largely parallel and perpendicular pattern. Perhaps they formed as the result of increased copper content at the border with the eutectoid where the migration of copper into the dendrite is known to occur (Scott 2004, 27,28). Galvanic corrosion can occur at the junction of the eutectoid and the dendrite since they are made up of dissimilar compositions that would enhance corrosion at this juncture. After 8 weeks many areas of the surface are exposed with a raw metal appearance. The dendritic structure of the metal is still visible after corrosion testing.

Comparison of the Dendritic Structure in the Corrosion Pattern of Test Pieces 17U and 18U (18U treated with sodium sesquicarbonate)

The dendritic structure of the metal that is reproduced in the corrosion pattern of 17U is hardly detectable in 18U. The copper acetate crystals in 17U (Figure 4.13) form long bands of whisker-like crystals that apparently follow the orientation of the dendrites. The copper acetate crystals in 18U do not form long bands as seen in 17U but instead are more uniformly distributed (Figure 4.8). Since test coupons 18U and 17U were prepared from the same piece of metal, explanations for this difference must be sought. One explanation may be variation in dendritic structure that can occur within a metal body depending on fluctuations in temperature during cooling of the pour. Perhaps the metal cut for test piece18U, or more precisely, the area examined and photographed

with the SEM, is characterized by a less defined dendritic structure. Another explanation may be sought in the sodium sesquicarbonate treatment on test coupon18U (ASTM B584). Treatment with sodium sesquicarbonate most likely initiated corrosion prior to the start of testing since soaking bronze in sodium sesquicarbonate is known to produce cuprite and malachite (Oddy and Hughes 1970, 186). The surface of the samples may have been covered with amorphous cuprite at the start of corrosion testing that could not be identified by XRD. Sodium was not detected, perhaps due to the limited number of EDS spot analyses performed or due to the detection limit.

The high tin content of corrosion on the alpha + delta eutectoid in 18U will be shared by 17U since they are from the same metal (Table 4.12, Figure 4.6). Sodium may have reacted with the tin in the alpha + delta eutectoid equalizing the extent of corrosion across the alpha phase and the eutectoid. It is not known what influence tin corrosion may have had on the formation of copper acetate hydrate.

Comparison of Crystal Morphology in the Corrosion of Test Pieces 17U and 18U (18U treated with sodium sesquicarbonate)

The crystals on 17U and 18U have been determined to be copper-rich (SEM-EDS) (Table 4.12) and represent copper acetate hydrate and cuprite according to XRD analysis (Table 4.16). Their morphologies do not match the irregular, plate-like crystals of copper acetate or the rectangular, prismatic crystals of copper hydroxide acetate found in other studies, however (López-Delgado *et al*. 1998, 4146, fig. 12; López-Delgado *et al*. 2001, 5210, fig. 19, 20). One could attempt to attribute the differences in crystal morphology to variations in acetic acid vapour concentration (100 to 300 ppm at 100% RH in the López-Delgado tests and 40 ppm at 86% RH in the current study). Dissimilarities are likewise found, however, with crystals from lower acid vapour concentrations and relative humidities (10 to 100 ppm acetic acid vapour in 40% and 80% RH) (Cano and Bastidas 2002, 329). Perhaps the differences in crystal morphology may be attributed to the presence of alloys (Table 4.1). The López-Delgado *et al*. (1998) and the Cano and Bastidas studies (2002) were carried out on pure copper. Darker colored crystals that are attributed to cuprite are seen interspersed among the lighter colored crystals attributed to copper acetate hydrate in 17U and 18U. Thin whisker-like crystals have grown sideways from the copper acetate "capping" crystals over the surface in 17U (Figure 4.13). The absence of the whisker-like crystal morphology in 18U (Figure

4.8) may be associated with the pre-treatment of this test piece with sodium sesquicarbonate. .

SEM and SEM-EDS of Leaded Bronze

The metallographic examination of the leaded tin bronze (ASTM B505) showed mostly α phase with some α + δ eutectoid in places (Figure 4.14). There is some coring but a dendritic structure is not apparent. Large lead globules are seen throughout. It is very likely that the surface could have been lead enriched by the sanding and polishing procedures and that lead oxide, lead hydroxide, and/or copper and tin oxides were present on the surface before corrosion testing (see Wadsak *et al.* 2002, 799 for similar findings on copper alloy). These may have been amorphous and therefore could not be identified by XRD. The introduction of acid destroys the protective lead oxide/hydroxide layer (sulfuric acid in the case of Wadsak *et al*. 2002, 799).

Leaded Bronze Test Piece 18L (treated with sodium sesquicarbonate) (Group 18, Test 9 in Table 4.4):

Test piece 18L was pre-treated with sodium sesquicarbonate. After one week of testing at 86% RH and 40 ppm acetic acid vapour the appearance of 18L (Figure 4.15) is similar to that of 17L (Figure 4.21). Droplets, visible as opaque areas, are delineated by a light crystalline border. Apparently water condensed on the surface at this high relative humidity. After two weeks of testing (Figure 4.16) appearance is still similar to that of 17L (Figure 4.22). Higher magnification (1500x) of 18L (Figure 4.16) reveals three distinct corrosion morphologies: large prismatic crystals, low lying fine crystalline covering, and long light crystals. EDS (Spectrum 1) of the dark green crystals shows mostly copper with some lead (Figure 4.17) (Appendix 6.16) (Table 4.12). They contain more oxygen and carbon than do the other two crystal types. The long, light crystals are predominantly lead (Spectrum 2) and the fine crystalline covering is predominantly copper (Spectrum 3) (Figure 4.17) (Appendix 6.16). The elemental analysis of the dark crystals closely matches Spectrum 1 (Figure 4.20) (Appendix 6.9) of the dark crystal in 17L. This crystal group appears to have completed its formation by the time the first EDS scans were run one week into testing. The low lying crystals and light, lead-rich crystals are more developed by the second week of testing on 18L compared to their counterparts on 17L one week into testing. By week two more dark crystals had formed on 18L and long light crystals had begun to cover them. At the time of the first EDS

scans, the surface of 18L was drier and the corrosion more crystalline whereas 17L was wetter and the corrosion was still forming. By the fourth week of testing the lead-rich corrosion on 18L covered the large copper-rich crystals (Figure 4.18). The lead-rich corrosion is characterized by a tabular morphology and a smooth, cracked surface in places (Figure 4.18). After 8 weeks of corrosion testing the light crystals (Spectrum 1) showed less copper and the elemental ratio of the dark crystals (Spectrum 2) remained unchanged (Figure 4.19) (Appendix 6.18) (Table 4.12). Spectrum 1 probably corresponds to hydrocerussite and Spectrum 2 to cuprite. The third crystal morphology is most likely copper acetate as identified by XRD (Table 4.12).

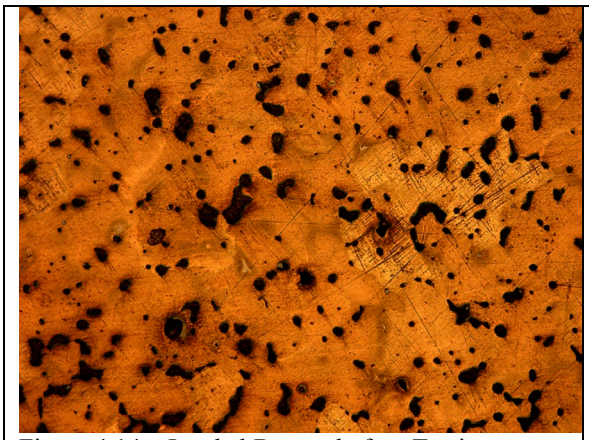

Figure 4.14 Leaded Bronze before Testing ASTM B505 (Table 4.1 for composition) (Appendix 2.2)

Figure 4.15 18L after one week 50x (Appendix 6.14)

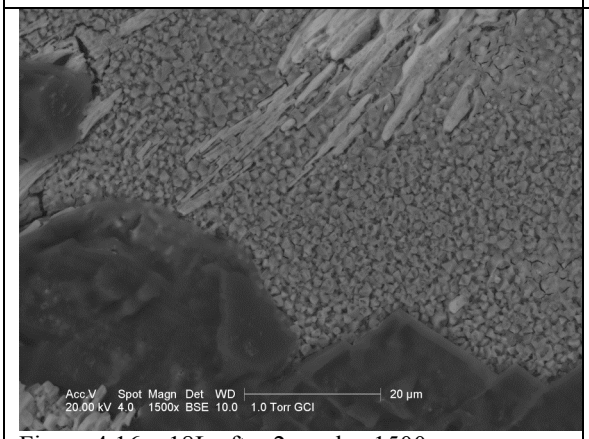

Figure 4.16 18L after 2 weeks 1500x (Appendix 6.15)

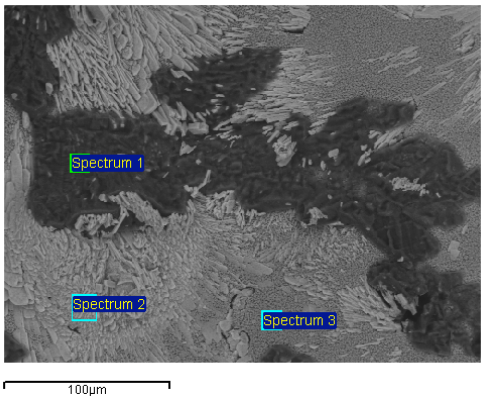

Figure 4.17 18L after 2 weeks (Appendix 6.16)

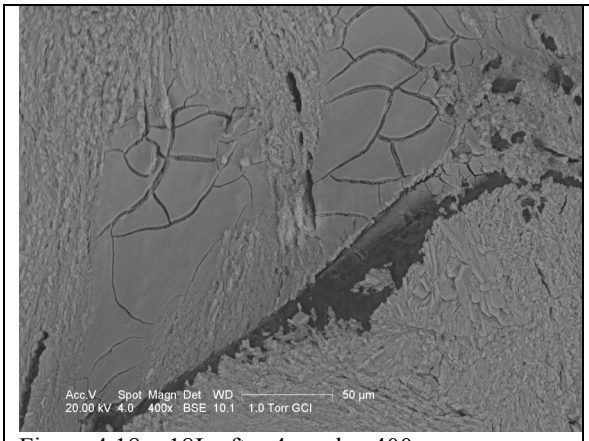

Figure 4.18 18L after 4 weeks 400x (Appendix 6.17)

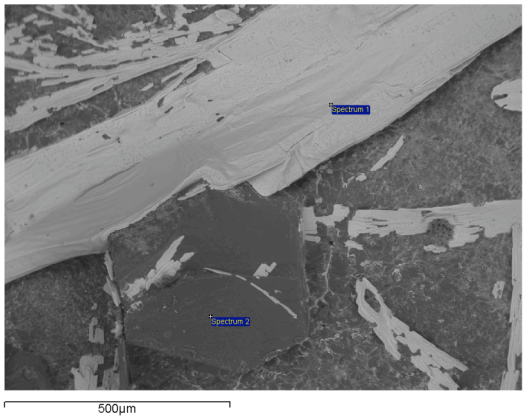

Figure 4.19 18L after 8 weeks (Appendix 6.18)

Leaded Bronze Test Piece 17L (not treated with sodium sesquicarbonate) (Group 17, Test 9 in Table 4.4):

After one week of corrosion testing SEM/EDS analysis of a dark crystal (Spectrum 1) showed mostly copper and oxygen with some carbon, tin and lead (Figure 4.20) (Appendix 6.9) (Table 4.12). The crystal showed sensitivity to the electron beam from the spot analysis indicating that it is a hydrated crystal. EDS on two spots (Spectrum 3 and 4) of the surface surrounding these dark crystals detected mostly copper and lead with some oxygen, carbon and tin. The spot lighter in color (Spectrum 3) contained a higher amount of lead. These areas were coated with what may have been lead oxide hydrate, in which copper was beginning to penetrate due to dissolution of the lead oxide by attack of acetic acid vapours. Lead oxide hydrate is soluble in dilute acid (Appendix 7.1). It could also have been lead acetate since lead acetate and lead acetate trihydrate are very soluble in water. The pH of the viscous liquid was found to be 5-6 that matches the pH of a 5% lead acetate solution (5.5 - 6.5) (Merck 1996).

RH in the SEM chamber is 5 to 10% that rapidly dehydrated the wet corrosion products. The photo in Figure 4.21 was taken at 50x magnifcation one week after start of corrosion testing. By the time the next image was taken only minutes later dehydration was evident, small light crystals were beginning to form in the viscous liquid. Two weeks after the start of corrosion testing there is a progression of crystallization of the viscous liquid. In Figure 4.22 the lighter crystals appear to be thin with sharp edges that can be seen forming within the gaps free of darker copper corrosion as well as around and interspersed with the darker copper-rich crystals. By the 3rd week dark copper corrosion crystals have increased in relation to the lighter lead-rich crystals. At higher

magnification the dark copper-rich crystals are predominating the lighter lead-rich crystals. The darker crystals appeared a blue-green color in the optical microscope and were observed to occur randomly on the surface. Dehydration was observed during the course of SEM imaging causing a light crust to form (D. Carson pers comm. 2004). 4 weeks after start of corrosion testing examination with the optical microscope revealed long, transparent crystals lying on the surface. These clear crystals became dehydrated during the evacuation of the SEM chamber, causing them to turn a lighter shade. After 8 weeks EDS indicates that these light crystals are lead rich. They are much more prolific than in earlier photos. They have a smooth surface and appear to have precipitated from a liquid state (Figure 4.23). They are surrounded by dense, dark, copper corrosion crystals. A large dark crystal, the flat light smooth crystals, and the surrounding dense smaller dark crystals were analysed by SEM/EDS 8 weeks after the start of corrosion testing (Figure 4.24) (Appendix 6.13). The large dark crystal showed predominantly copper and oxygen with some lead (Spectrum 2). The light crystals showed mainly lead (Spectrum 1), and the dense dark crystals (Spectrum 3) showed mostly copper with oxygen, lead, carbon and tin (in decreasing quantity) (Table 4.12). This pattern of relative intensities and wavelength resembles that of Spectrum 4 on 17L from one week into corrosion testing (Figure 4.20) (Appendix 6.9). The copper, detected with the lead-rich compound in Spectrum 3 one week into corrosion testing (Figure 4.20) (Appendix 6.9)., is absent after 8 weeks of corrosion testing (Figure 4.24) (Appendix 6.13, Spectrum 1). By the end of the tests the bulk of the copper was found distributed between cuprite and copper acetate hydrate. The lead-rich compound was identified by XRD as hydrocerussite at the end of the corrosion tests (Table 4.12). Since it differs radically in appearance from the earlier lead-rich crystals, it may be deduced that the lead-rich crystals after 2 weeks of testing in Figure 4.22 are another lead compound, perhaps lead oxide, lead carbonate, lead hydroxy acetate or lead acetate. Spectrum 1 probably corresponds to lead carbonate or lead acetate, Spectrum 2 to cuprite and Spectrum 3 to copper acetate hydrate (Table 4.12) after 8 weeks of testing 17L in Appendix 6.13.

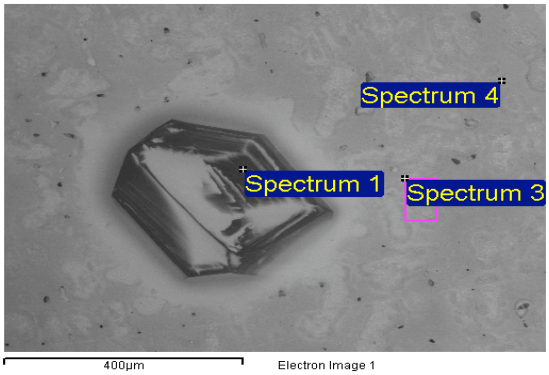

Figure 4.20 17L after one week (Appendix 6.9)

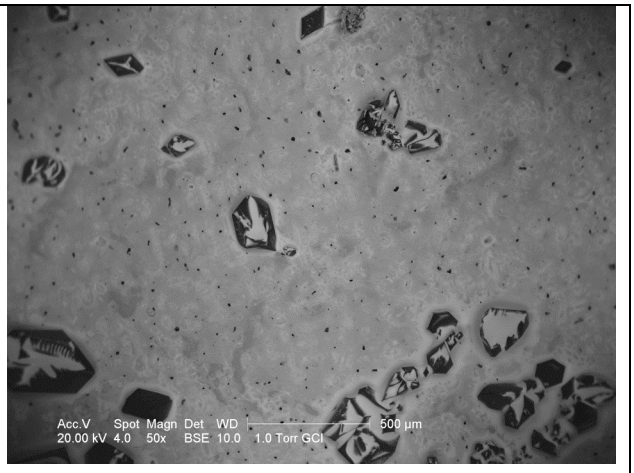

Figure 4.21 17L after one week 50x (Appendix 6.10)

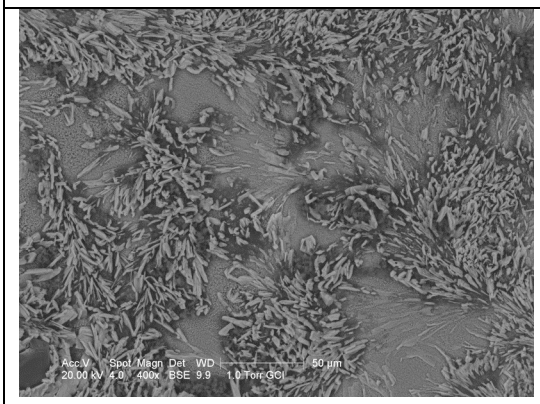

Figure 4.22 17L after 2 weeks 400x (Appendix 6.11)

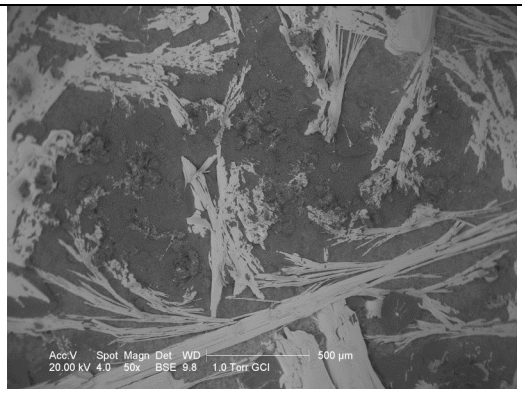

Figure 4.23 17L after 8 weeks 50x (Appendix 6.12)

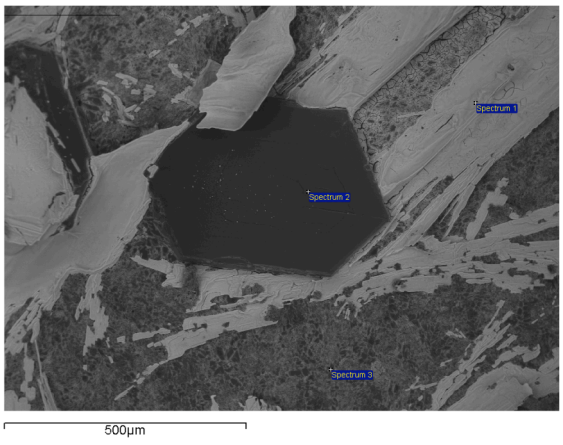

Figure 4.24 17L after 8 weeks (Appendix 6.13)

Comparison of Leaded Bronze Test Pieces 18L and 17L (18L treated with sodium sesquicarbonate)

The lead-rich crystals on 18L and 17L showed a loss of copper by the end of testing. 8 weeks after the start of corrosion testing examination with the optical microscope revealed more blue/green crystals on the surface of 18L than on 17L and long, clear lead-rich crystals on both. Perhaps the sodium sesquicarbonate on 18L activated the copper ions that accounts for a greater number of blue/green crystals. A wet surface was visible in the SEM photos of leaded tin bronze 17L and 18L after 1 week of corrosion testing at 86% RH and 40 ppm acetic acid. The test coupons were covered with a thick, viscous liquid. Dark crystals were interspersed on the surface coated with this liquid. The lead-rich crystals precipitated from solution or became dehydrated during examination in the SEM. After 8 weeks of testing the crystal morphology and placement of the corrosion compounds on 17L (Figure 4.24) and 18L (Figure 4.19) were remarkably similar. After 8 weeks of corrosion testing the two metals continued to appear very similar. Lead appeared to have dissolved from the scattered lead globules in the alloy and to have spread over the surface. Acetic acid reacts with lead metal and dissolves lead oxide hydrate and lead carbonate (Appendix 7.1). This neutralizes the acid and releases acetate ions that then contribute to electrochemical corrosion. The acetate ions and lead ions in solution diffuse to areas of high carbonate concentration and higher pH where they are precipitated as hydrocerussite. The acetate ion is released during this reaction and goes back into the water layer constituting a corrosion cycle. This explains the migration of lead over the surface of the metal. This would also explain the reason hydrocerussite was identified rather than lead acetate on 17L and 18L, i.e. it has a greater tendency to form and is a more stable compound.

SEM and SEM-EDS of Ancient Coins

Two coins were examined in the SEM, Coin 2 and Coin 5. Coin 2 was treated with sodium sesquicarbonate before corrosion testing. The corrosion on Coin 2 was analysed by SEM-EDS. The ancient corroded surfaces (not the new cut surfaces) of the coins after corrosion testing in 40 ppm acetic acid vapour at 86% RH were examined and analysed.

Coin 2, Treated with Sodium Sesquicarbonate before Corrosion Testing by 40 ppm Acetic Acid at 86% RH (Group 18 in Test 9, Table 4.4)

After the first week of corrosion testing dried solution droplets on the surface appear opaque to the SEM (Figure 4.25). A crystal could be seen on top of a patch of corrosion (Figure 4.25). This is an euhedral crystal with sharp edges. It appears to be growing from the saturated solution on evaporation in the SEM. Copper ions are being fed from the corrosion patch through the liquid to create the crystal. The pH of the colorless liquid before desiccation in the SEM chamber was measured with pH paper and was found to be pH 5 – pH 6. Although this matches the pH of a 5% aqueous solution of lead acetate, identification cannot be based on pH alone (Merck 1996). After 2 weeks of testing EDS revealed lead to be the predominant element (Table 4.12) (Figure 4.26) (Appendix 6.20, Spectra 1,2,3,4). Spectrum 4 revealed three predominant elements, Pb, O and Sn. Spectrum 1 and 4 revealed calcium, carbon and silica, elements included in the compounds identified by XRD prior to corrosion testing (Table 4.5). Spectra 2 and 3 have the highest concentration of lead. Phosphorus was detected in Spectra 1, 3 and 4 (Table 4.12). By the second week the crystals seen after the 1st week have disappeared and it will be noted that Cu is now but a trace element in all four spectra (Table 4.12). After 4 weeks of corrosion testing long light crystals are seen on the surface of the coin drastically changing the appearance (Figure 4.27). After 8 weeks of corrosion testing the coin is covered with lead-rich crystals (Figure 4.28). The clear liquid has dried and these crystals have taken its place. The crystals are brittle and delicate, forming thin sheets with a laminar structure. A few small crystals, perhaps what remains of the dark crystals from the early weeks of the test, can be seen interspersed among the tabular flakes of lead crystals (Figure 4.28). The calcium and phosphorus identified by EDS after 2 weeks of testing could derive from burial (Figure 4.26) (Appendix 6.20) (Table 4.12). The appearance of the coin has changed radically from the 1st week of testing (Figure 4.25).

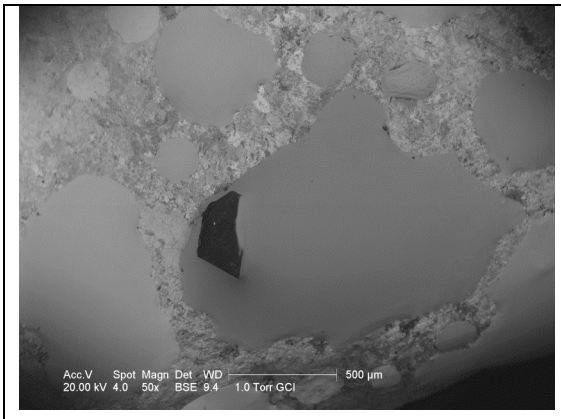

Figure 4.25 Coin 2 after one week 50x (Appendix 6.19)

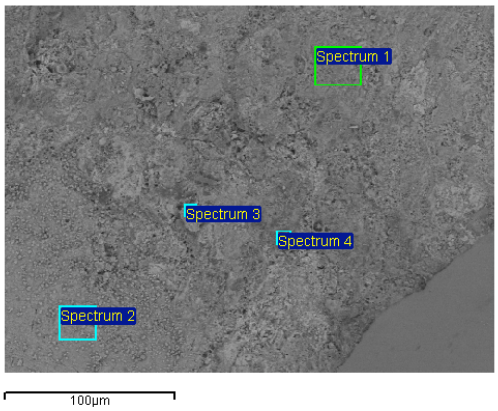

Figure 4.26 Coin 2 after 2 weeks (Appendix 6.20)

Figure 4.27 Coin 2 after 4 weeks 50x (Appendix 6.21)

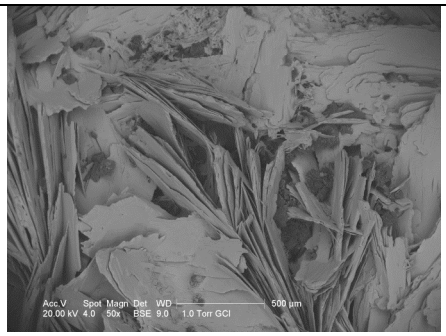

Figure 4.28 Coin 2 after 8 weeks 50x (Appendix 6.22)

Coin 5, Not Treated with Sodium Sesquicarbonate, Corroded by 40 ppm Acetic Acid at 86% RH (Group 17 in Test 9, Table 4.4)

After corrosion testing XRD identified copper acetate hydrate and cuprite (Table 4.19) on this predominantly copper coin (1% Pb, < detection limit Sn) (Table 4.2). Copper oxide and cuprite were identified prior to testing by XRD (Table 4.5). After 1st week whisker-like crystals were found growing out from the surface (Figure 4.29). After 2nd week of testing the surface of the coin appears similar to that of Coin 2. There is a development of the long crystals from the 1st week to the 3rd week of testing. After the 1st week the crystals are even in width along their length and grow in a parallel fashion, some curving as they grow. After the 2nd week another crystal morphology is seen, thinner and more whisker-like crystals that are more similar to those found on 17U and 18U. The long crystals are growing in cracks and gaps in the corrosion surface of the coin (Figure 4.30). After 8 weeks of testing at 400x magnification we can distinguish at least two crystal morphologies (Figure 4.31): long, thin needle-like crystals and shorter, thicker crystals. Perhaps the two crystal morphologies represent two different species of

copper acetate, only one of which was identified by XRD (copper acetate hydrate) (Table 4.19).

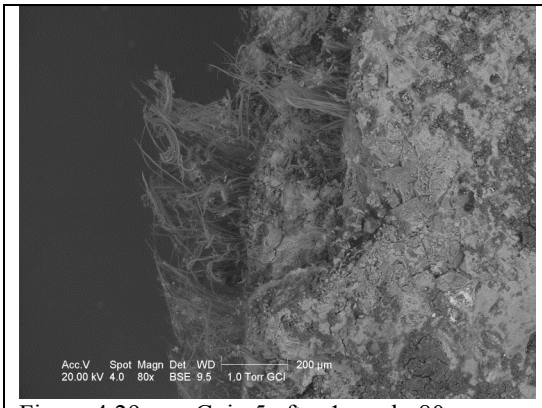

Figure 4.29 Coin 5 after 1 week 80x (Appendix 6.23)

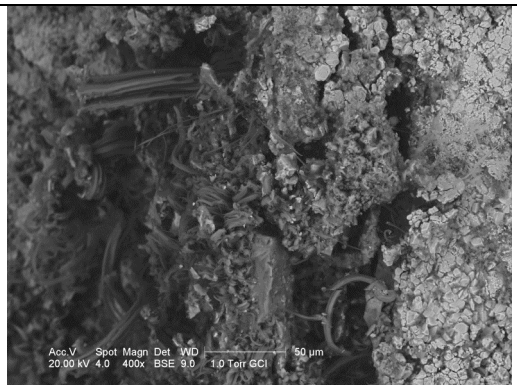

Figure 4.30 Coin 5 after 1 week 400x (Appendix 6.24)

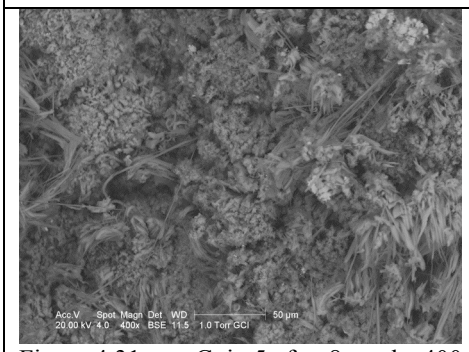

Figure 4.31 Coin 5 after 8 weeks 400x (Appendix 6.25)

4.2.1.4.3 FTIR Analysis of Coins and Coupons corroded by 40 ppm Acetic Acid at 86% RH

A PerkinElmer Spectrum One FTIR Spectrometer with Attenuated Total Reflectance (ATR) with diamond crystal was used at UCLA. Overall data collection ranged from 4000 cm^{-1} to 450 cm^{-1} with best resolution of 0.5 cm^{-1}. Optical module contains a Class II/2 Helium Neon (HeNe) laser emitting visible, continuous wave radiation at 633 nm with maximum output power of 1 mW. PerkinElmer's IR Spectrosocpy software was used to identify compounds. FTIR can characterize anions or chemical groups in poorly crystalline compounds that cannot be identified by XRD (Scott 2002, 9). FTIR compliments XRD by identifying amorphous compounds. The use of a beam condenser and diamond cell allows analysis of small samples. FTIR and XRD do not detect compounds that contribute less than 5 to 10% of a mixed sample. FTIR can distinguish between neutral and basic copper acetate (Scott 2001, 89). FTIR cannot differentiate with complete success between the basic copper acetate compounds (Scott

2001, 78). Infrared studies in the low wavenumber range, 50 to 600 cm^{-1}, would be very helpful in characterizing the differences but 650 cm^{-1} is the lowest range available with most FTIR instrumentation (Scott 2001, 78).

The copper acetates consist of two groups: the basic copper (II) acetates and the neutral copper (II) or copper (I) acetates (Scott 2002, 271) (Table 4.13). The International Centre for Diffraction Data (ICDD) file number is included for those compounds that have been registered (Table 4.13). Five varieties of basic copper (II) acetate have been characterized by FTIR and are labeled A, B, C, D, and H (Table 4.14) (Gauthier 1958, 17-19, 27-43; Rahn-Koltermann *et al*. 1991, 1020-1024; Scott 2002, 271). The basic copper acetates are the most difficult to characterize. The basic copper (II) acetates can be presented as:

$$[Cu(CH_3COO)_2]_x[Cu(OH)_2]_y \bullet nH_2O$$

where values x, y, and n are variable (Scott 2002, 272). They are all variations on this formula. Compounds A, B, C, D, and H have been characterized with FTIR, Raman Spectroscopy, and XRD (Appendices 8.1, 9, 10.1). Three varieties of the neutral copper (II) or copper (I) acetates have been characterized and are labeled E, F, and G (Table 4.13) Of this group the compound that has been most thoroughly characterized is neutral copper (II) acetate monohydrate, compound F. Compound D can be difficult to characterize since the acetate ions are located between the positively charged copper hydroxide layers and can be exchanged with other anions such as chloride, sulphate or nitrate (Scott 2002, 275). This can occur in all the basic copper acetates. Substitution of some of the copper hydroxide layers may explain the variation in XRD data for these compounds and the many unidentified d-spacings (Angströms) for complex mixtures of variable compounds (Appendix 10.1).

Table 4.13 Characterization of Copper Acetates

Chemical name	formula	ICDD* number	color
Basic copper (II) acetate (A)	$[Cu(CH_3COO)_2]_2 \cdot Cu(OH)_2 \cdot 5H_2O$	NA	Blue
Basic copper (II) acetate (B)	$[Cu(CH_3COO)_2]Cu(OH)_2 \cdot 5H_2O$	NA	Pale blue
Basic copper (II) acetate (C)	$Cu(CH_3COO)_2[Cu(OH)_2]_2$	NA	Blue
Basic copper (II) acetate (D)	$Cu(CH_3COO)_{2[}Cu(OH)_2]_3 \cdot 2H_2O$	NA	Green
Basic copper (II) acetate (H)	$Cu(CH_3COO)_2[Cu(OH)_2]_4 \cdot 3H_2O$	NA	Blue- green
Copper (II) acetate (E)	$Cu(CH_3COO)_2$	ICDD 27-1126	Pale blue
Copper (II) acetate hydrate (F)	$Cu(CH_3COO)_2 \cdot H_2O$	ICDD 27-0145	Blue green
Copper (I) acetate (G)	$Cu(CH_3COO)$	ICDD 28-0392	Not stated

From Scott 2001, 76 and Scott 2002, 271, 272
NA = not available; * International Centre for Diffraction Data

Results of FTIR Analysis of Coupons and Coins Corroded by 40 ppm Acetic Acid at 86% RH

Two analytical campaigns were carried out with FTIR (Appendix 11). During preparation of the corrosion samples for analysis a distinction between green, blue, and white crystals was apparent through the binocular microscope so an attempt was made to segregate the samples by color. The first campaign was carried out upon completion of the corrosion tests in 2004 and the second campaign was carried out 7 months later in 2005. Neutral and basic copper acetates were distinguished by FTIR. Analysis in 2004 by FTIR identified neutral copper acetate $Cu(CH_3COO)_2 \cdot H_2O$ (Compound F) on leaded 17L and coin 5 and found similarities with this compound on unleaded 17U indicating a neutral copper acetate (Table 4.13; Appendix 11) . Analyses of the other samples indicated one or a mixture of the basic copper acetates (A, B, C, D, or H) (Appendix 11, Table 4.14). (Copper (II) acetate hydrate B was indicated in the blue corrosion on leaded 17L (Appendix 11, Appendix 12.2) and copper (II) acetate hydrate D was indicated in the green corrosion on leaded 18L in the initial campaign (Appendix 11, Appendix 12.3) (Scott 2002, 271). FTIR supported the XRD identification of the white corrosion on coin 2 as hydrocerussite. A shift can be seen over a seven month period from the initial analysis in 2004 to the subsequent analysis in 2005: 1) analyses in 2004 revealed a split between neutral and basic copper acetates where analyses in 2005 indicated basic copper

acetates only; 2) neutral copper acetate transformed to basic copper acetate in the green corrosion of unleaded 17U and leaded 17L, and in the corrosion of coin 5 (Appendix 11).

Table 4.14 FTIR Basic Copper Acetate Database

Compound Abbreviation	Compound no. FTIR database*	Name
A	CU0075	Copper acetate 6_1 compound A
B	CU0001	Verdigris Yoko compound B 1-2
B	CU0073	Copper acetate 1_2 compound B
C	CU0016	Compound C EK2 upper
D	CU0002	Verdigris compound D (D-YT) 1999
D	CU0085	Copper acetate 2_2 compound D
D	CU0076	Copper acetate D-YT
H or A	CU0020	Copper acetate hydrate beaker 5-1: H or A
H or A	CU0019	Copper acetate hydrate beaker 4-1: H or A
H or A	CU0022	Copper acetate hydrate beaker 6-2: H or A

*David Scott's database at UCLA

The FTIR spectra have bands in the ranges 1400 to1500 cm^{-1}, 900 to1000 cm^{-1}, and 600 to 700 cm^{-1} (Appendix 8.2) that correspond to the FTIR spectra of Scott's copper acetate compounds (Appendix 8.1) and to the Raman spectra for the copper acetates (Appendix 9) (Chaplin *et al*. 2006, 227; D. Scott pers comm. 2005). Bands in the 3200 to 3500 cm^{-1} range correspond to the stretching vibrational mode of water originating from the OH groups (Lopez *et al*. 1998, 4144; Wadsak *et al*. 2002, 797). Bands at 2955 cm^{-1} (only 1 occurrence in these samples) and 3010 cm^{-1} (no occurrences in these samples) result from the CH stretching modes of acetate. Carbonates are not indicated in these samples by the absence of bands at 1600 and 1603 cm^{-1}. The symmetric CH deformation mode of acetate that occurs at 1350 cm^{-1} can be seen in four samples. The C-C symmetric stretching fundamental in the copper acetate dimer occurs near 950 cm^{-1} (Trentelman *et al*. 2002, 219). Metal-water vibrations occur at 480 to 650 cm^{-1} as indicated in most of the samples analysed (Trentelman *et al*. 2002, 220).

Two strong bands in the range 1400 to 1700 cm^{-1} correspond to asymmetrical and symmetrical vibrational modes of the carboxylate (COO^{-}) group (most of my samples demonstrate this) (Appendix 8.2, Appendix 12.2). They correspond to free acetate groups and may be attributed to adsorbed acetic acid on the amorphous cuprite phase surface (Lopez *et al*.1998, 4144). The asymmetrical (V_{as}) and symmetrical (V_s) vibrational modes of the COO^{-} group are separated (Table 4.15). V_{as} and V_s groups are

"experimental evidence of acetate groups coordinated with copper, probably through an (sic) unidentate link, due to high separation between both asymmetric and symmetric bands." (Lopez *et al*. 1998, 4144). This is otherwise explained as the acetate ligand forming bidentate links between copper atoms creating a dimeric species (Trentelman *et al*. 2002, 220). The V_{as} and V_s bands are often split into two forming a total of four bands as seen in the 50, 100 and 200 ppm acetic acid tests on copper (Lopez *et al*. 1998, 4144). Copper acetate dihydrate, $Cu(CH_3COO)_2.2H_2O$, represents such a dimeric structure "in which two copper atoms are held together by four acetate bridges." (Lopez *et al*. 1998, 4144). The length of the separation between the two bands varies with concentration of acetic acid vapour. A decrease in the separation between the V_{as} and V_s vibrational modes indicates a buildup of acetate compound that bridges the two copper atoms from 50 to 300 ppm. This implies that the higher the acetic acid concentration, the more acetate will form between copper atoms and the closer together will be the two vibrational modes (Lopez *et al*. 1998, 4144).

Table 4.15 Vibrational Modes of the Carboxylate Group (expressed as wavelength cm^{-1})

	Vibrational mode	10 ppm	50 ppm	100 ppm	200 ppm
water		3409	3466		3392, 3284, 2489
COO^-group	V_{as}	1570s	1618	1609vs	1605
			1570	1564sh	1560
	V_s	1415s	1420	1427s	1448
			1415	1398sh	1422

From Lopez *et al*. 1998, 4144.
s = strong; vs = very strong; sh = shoulder

4.2.1.4.4 XRD of Coupons and Coins Corroded from 40, 4, and 0.4 ppm Acetic Acid at 86%, 52%, and 32% RH (Tables 4.16-4.19)

XRD was carried out on all coupons and coins corroded in 0.4, 4, and 40 ppm acetic acid at 86% RH (Table 4.16, Table 4.19) and 52% RH (Table 4.17. Table 4.19) and on those coupons and coins from 40 ppm acetic acid at 32% RH (on account of minimal corrosion on the coupons from 4 and 0.4 ppm acetic acid at 32% RH analysis was not carried out) (Table 4.18, Table 4.19).

Prior to and following the corrosion tests the test coupons and coins were rotated during surface analysis by the Getty Siemens diffractometer in order to obtain a representative assessment of the surface corrosion. One exception was Coin 2 in which a

single spot was analysed due to the small size of the coin. At the Getty Museum Research Laboratory a Siemens D5005 X-ray Diffractometer was used. The spectra were collected from 3° to 80° 2Θ. Radiation was from a copper source, generator settings 40 mA, 45kV. The software program used to identify compounds was Bruker Advanced X-rays Solutions. Inc. DiffracPlus, Release 2004, EVA Version 10.0, revision 1. The samples analysed at UCLA in 2005 consisted of corrosion that was removed from the test coupons and ground in a mortar and pestle. In these cases an attempt was made to sample the white and blue corrosion separately as indicated in Tables 4.16 and 4.19. The volume of powdered sample approximated 200 mg. At UCLA Powder x-ray diffraction patterns were obtained using a PANalytical XPert Pro powder diffractometer with theta-theta geometry. The spectra were collected from 5° to 80° 2Θ. Radiation was from a copper source, generator settings 40 mA, 45kV. The software program used to identify compounds was PANalytical XPert Data Collector. The UCLA XRD data is based upon work supported by the Natural Science Foundation under equipment grant no. DMR-0315828.

Limitations of XRD

The dependence on crystalline compounds is a limiting factor of XRD analysis. Some copper acetates have d-spacings (Angströms) over 17 that many XRD machines cannot reach. Debye-Scherrer cameras and the General Area X-ray Diffraction System (GADDS) can detect these d-spacings (Angströms) (Scott 2001, 78). The Siemens X-ray Diffractometer at the Getty could not reach d-spacings (Angströms) over 17.

Table 4.16 XRD Results ASTM Test Pieces after Corrosion Testing, 86% RH, 58 days

Acid conc.	Test piece	Compound	Formula	ICPDS	Year	Appendix
40 ppm (6.3 ppm yr)	17L	copper acetate hydrate	$C_4H_6CuO_4.xH_20$	14-0811	2004	4.3
		cuprite	Cu_2O	05-0667	2004	4.3
		[1](blue powder)	no match		2005	
		copper acetate hydroxide hydrate (and unidentified compound)	$Cu_2(OH)_3(CH_3COO).H_2O$	50-0407	2006	4.10
	17U	copper acetate hydrate	$C_4H_6CuO_4.H_20/(CH_3COO)_2Cu.H_20$	27-0145	2004	4.5
		copper tin	$Cu_5.6Sn$	17-0865	2004	4.5
		[1] (blue powder)	no match		2005	
		copper acetate hydroxide hydrate	$Cu_2(OH)_3(CH_3COO).H_2O$	50-0407	2006	4.7
		copper tin	$Cu_5.6Sn$	71-0122	2006	4.7
	18L *	copper acetate hydrate	$C_4H_6CuO_4.xH_20$	14-0811	2004	4.4
		cuprite	Cu_2O	05-0667	2004	4.4
		[1] (blue powder) hydrocerussite and unidentified compound	$Pb_3(CO_3)_2(OH)_2$	13-0131	2005	4.9
		copper acetate hydroxide hydrate	$Cu_2(OH)_3(CH_3COO).H_2O$	50-0407	2006	4.11
		hydrocerussite	$Pb_3(CO_3)_2(OH)_2$	13-0131	2006	4.11
	18U *	copper acetate hydrate	$C_4H_6CuO_4.H_20/(CH_3COO)_2Cu.H_20$	27-0145	2004	4.6
		copper tin	$Cu_5.6Sn$	17-0865	2004	4.6
		[1] (blue powder)	no match		2005	
		copper tin (and unidentified compound)	$Cu_5.6Sn$	71-0122	2006	4.8
4 ppm (0.6 ppm yr)	19L	hydrocerrussite	$Pb_3(CO_3)_2(OH)_2$	13-0131		
	19U	copper tin	$Cu_5.6Sn$	17-0865		
	20L *	hydrocerrussite cuprite	$Pb_3(CO_3)_2(OH)_2$ Cu_2O	13-0131 05-0667		
	20U *	copper tin	$Cu_5.6Sn$	17-0865		
0.4 ppm (0.06 ppm yr)	21L	similar to 22L, less developed peaks				
	21U	copper tin	$Cu_5.6Sn$	17-0865		
	22L *	similar to 21L, more developed peaks unidentified compound				
	22U *	copper tin similar to 21U unidentified compound	$Cu_5.6Sn$	17-0865		

* = treated with sodium sesquicarbonate; [1] = UCLA; L = leaded bronze ASTM B505; U = unleaded bronze ASTM B584

Table 4.17 XRD Results ASTM test pieces after Corrosion Testing, 52% RH, 45 days

Acid conc.	Test	Compound	Formula	ICPDS
40 ppm (4.9 ppm yr)	9L	1) at least one unidentified compound 2)perhaps undeveloped copper acetate		
	9U	1) copper tin 2) perhaps undeveloped copper acetate	$Cu_5.6S$	31-0487
	10L *	1) perhaps cuprite 2) perhaps undeveloped copper acetate		
	10U *	1) copper tin 2) perhaps cuprite 3) unidentified peak 4) similar to 9U scan 5) perhaps undeveloped copper acetate	$Cu_5.6Sn$	31-0487
4 ppm (0.4 ppm yr)	11L	1) indication of lead oxide 2) at least one unidentified compound, not a copper acetate 3) similar to 9L scan	Pb_2O	02-0790
	11U	1) copper tin 2) similar to 9U scan but without any indication of copper acetate 3) scan stops at 65 Θ	$Cu_5.6Sn$	31-0487
	12L *	1) maybe cuprite 2) acetate peaks in 10L are missing		
	12U *	1) copper tin 2) similar to 10U scan 3) perhaps cuprite	$Cu_5.6Sn$	31-0487
0.4 ppm (0.04 ppm yr)	13L	1) lead oxide	Pb_2O	02-0790
	13U	1) copper tin 2) similar to 9U scan without any indication of copper acetate	$Cu_5.6Sn$	31-0487
	14L *	1.) perhaps cuprite 2.) similar to 12L scan		
	14U *	1) copper tin 2) similar to 12U scan 3) perhaps cuprite	$Cu_5.6Sn$	31-0487

*treated with sodium sesquicarbonate; L = leaded bronze ASTM B505; U = unleaded bronze ASTM B584

Table 4.18 XRD Results ASTM Test Pieces after Corrosion Testing, 32% RH, 42 days

Acid concentration	Test piece	Compound	Formula	ICPDS
40 (4.6 ppm yr)	1L	at least one unidentified compound		
	1U	copper tin unidentified compound	$Cu_5.6Sn$	17-0865
	2L *	at least one unidentified compound		
	2U *	copper tin	$Cu_5.6Sn$	31-0487
4 (0.4 ppm yr)	3L 3U 4L 4U	NA		
0.4 (0.04 ppm yr)	5L 5U 6L 6U	NA		

NA=not analysed; * = treated with sodium sesquicarbonate; L = leaded bronze ASTM B505; U = unleaded bronze ASTM B584

XRD of Leaded and Unleaded Test Coupons Corroded at 32% RH and 52% RH

Results of the testing at 32% RH revealed only copper tin by XRD on all test coupons (1U, 1L, 2U, 2L) at 40 ppm (4.6 ppm yr) acetic acid concentration (Table 4.18). No corrosion products were detected by XRD. The desiccated environment of 32% RH seems to have inhibited corrosion, even at this acetic acid dose of 4.6 ppm yr that exceeds the LOAED for copper (0.4 ppm yr) and lead (0.02-0.03 ppm yr).

The results of corrosion testing at 52% RH are presented in Table 4.17. The d-spacings (Angströms) and intensities of the test coupons from the 40 ppm acid concentration (4.9 ppm yr) are presented in Appendix 10.6. Copper tin of the bronze was detected on all unleaded test coupons (9U – 14U) in all acetic acid concentrations (Table 4.17). Cuprite was indicated on all test coupons (10L, 10U, 12L, 12U, 14L, 14U) pre-treated with sodium sesquicarbonate. The leaded bronze test coupons that were not pre-treated produced an unidentified corrosion compound in the 40 ppm (4.9 ppm yr) and 4 ppm (0.4 ppm yr) acetic acid atmospheres. Lead oxide was found on the leaded bronze test piece 13L in the 0.4 ppm (0.04 ppm yr) acetic acid atmosphere and is indicated in the 4 ppm (0.4 ppm yr) acetic acid atmosphere (11L) (Table 4.17). Pre-treatment with sodium sesquicarbonate appears to have promoted the oxidation of copper before and/or during the tests. Treatment of bronze with sodium sesquicarbonate is known to promote the growth and copper oxides and carbonates (Oddy and Hughes 1970, 186). Perhaps the cuprite served as a protective layer inhibiting the corrosion of the lead component during exposure to acetic acid vapour. Lead corrosion is not found to coexist with cuprite on the test coupons except for 18L (86% RH) (Table 4.16).

In the current study the corrosion products identified by XRD from the tests run at 52% RH were cuprite and lead oxide (Table 4.17). No corrosion compounds were identified from the tests run at 32% RH (Table 4.18). Corrosion compounds formed in both relative humidty levels that could not be identified by XRD. We may assume the surfaces were covered with amorphous copper and lead oxides prior to testing, based on the results of similar tests by other researchers (López-Delgado *et al*. 2001, 5209). The difficulty encountered with the identification of corrosion products by XRD is shared by other researchers. Thickett could not identify corrosion from 4 months exposure to 0.5 and 5 ppm acetic acid at 50% and 100% RH (Thickett 1997, 7). It has been confirmed

that the first corrosion to develop on copper in acetic acid vapour is amorphous cuprite that could not be identified by XRD (López-Delgado *et al*. 2001, 5209). After exposure to moisture the cuprite layer may be non-stoichiometric on account of the defects in the cuprite caused by the interaction of physisorbed water (Aastrup *et al*. 2000, 965). The lattice diffraction pattern of a non-stoichiometric compound would be shifted and therefore difficult to identify by XRD (D. Scott pers comm. 2007). In the tests run at 32% RH, the atmosphere may have been too dry for electrochemical corrosion or galvanic corrosion to occur. The controls displayed even less corrosion than those tests with acetic acid vapour.

XRD of Leaded and Unleaded Test Coupons Corroded at 86% RH

Two sets of XRD analyses were run on the test coupons corroded at 86% RH. The intial set was carried out at the Getty Conservation Institute (GCI) in 2004 and the subsequent set at UCLA in 2005 and the GCI in 2006.

Initial XRD Tests (2004) on Leaded and Unleaded Coupons corroded in 40 ppm Acetic Acid at 86% RH

The d-spacings (Angströms) and intensities of the test coupons exposed to 40 ppm (6.3 ppm yr) acetic acid concentration are presented in Appendix 10.2. In 2004, after the corrosion tests, analysis was carried out with the Siemens X-ray Diffractometer at the Getty Conservation Institute. Copper acetate hydrate (14-0811) and cuprite (05-0667) were identified in the tests with 40 ppm (6.3 ppm yr) acetic acid concentration on the leaded bronze (17L, 18L) (Table 4.16, Appendices 4.3, 4.4, 10.3). Neutral copper acetate was confirmed on leaded 17L by FTIR analysis. Copper acetate hydrate (27-0145) and copper tin (17-0865) were identified on the unleaded bronze (17U, 18U) (Table 4.16, Appendices 4.5, 4.6, 10.4). Neutral copper acetate was confirmed on unleaded 17U by FTIR analysis. The formation of acetate compounds was expected as the dose 6.3 ppm yr acetic acid far exceeds the LOAED of acetic acid for corrosion of copper (0.4 ppm yr) and lead (0.02-0.03 ppm yr) and the LOAED for the formation of acetate on copper (0.5 ppm yr) and lead (0.4 ppm yr). Copper acetate hydrate and cuprite were found on pure copper exposed to moisture and acetic acid vapour by other researchers (López-Delgado *et al*. 1998, 4143). Cuprite is believed to serve as an ionic membrane permitting acetic acid to penetrate to the metal surface where it reacts with copper and allows the release the dissolution products to the overlying corrosion surface

(López-Delgado *et al*. 1998, 4143). Once the copper is attacked by acid and is mobilized, copper hydroxide hydrate can form prior to copper acetate. In the study by López-Delgado and colleagues, hydroxides were found inside water droplets with the SEM (López-Delgado *et al*. 1998, 4145; López-Delgado *et al*. 2001, 5209). The intermediary corrosion products, copper hydroxide hydrate and copper oxide hydrate, were not identified by XRD in the current study. Since analysis was carried out only at the end of corrosion testing the formation of these intermediary products cannot be confirmed.

An aqueous layer adsorbed on the metal surface is required for the formation of carboxylate compounds (Gil and Leygraf 2007a, C277). The solubility of copper in water is determined by the potential-pH equilibrium, Figure 4.32 shows the role pH plays in the dissolution of copper (Pourbaix 1974; Pourbaix 1976, 29C).

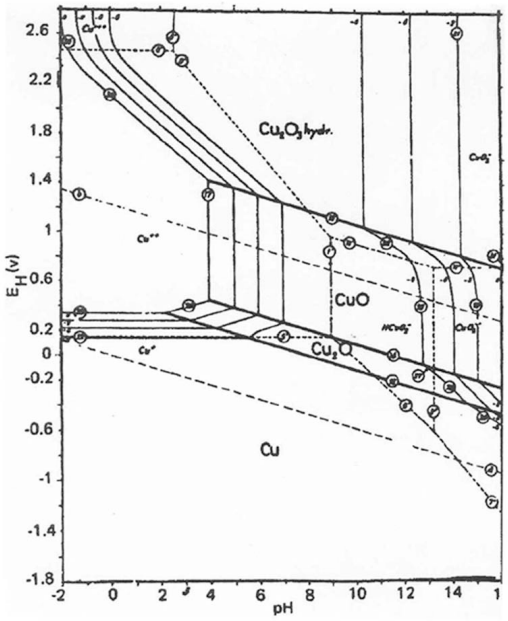

Figure 4.32 Potential-pH equilibrium diagram for the copper-water system at 25°C. (Pourbaix 1974; Pourbaix 1976, Fig. 15, 29C)

Surface hydroxyl bonds form in the water layer over the cuprite surface according to the following electrochemical reactions:

$Cu \rightarrow Cu^{+} + e^{-}$ (anodic reaction) and $\frac{1}{2} O_2 + H^{+} + 2e^{-} \rightarrow OH^{-}$ (cathodic reaction)

(Gil and Leygraf 2007a, C277).

Acetic acid dissolves in the water layer producing protons (H^+) and acetate ions ($CH3COO^-$) that replace the hydroxyl bonds.

$$CH_3COOH \rightarrow H^+ + CH_3COO^-$$

"The result is a ligand-induced dissolution triggered by the weakness of the surface metal atoms that participate in the ion exchange." (Gil and Leygraf 2007a, C277). Copper first forms cuprous ions that may form one of two reactions in aqueous solution: (1) cuprous ions react with hydroxyl ions (OH^-) forming cuprous oxide, (2) cuprous ions oxidize to cupric ions, react with acetate ions forming copper acetate (Figure 4.33) (Gil and Leygraf 2007a, C278). It was found that copper acetate forms in a parallel process with cuprite formation (Gil and Leygraf 2007a, C276). See Appendix 7.2 for the solubilities of copper compounds.

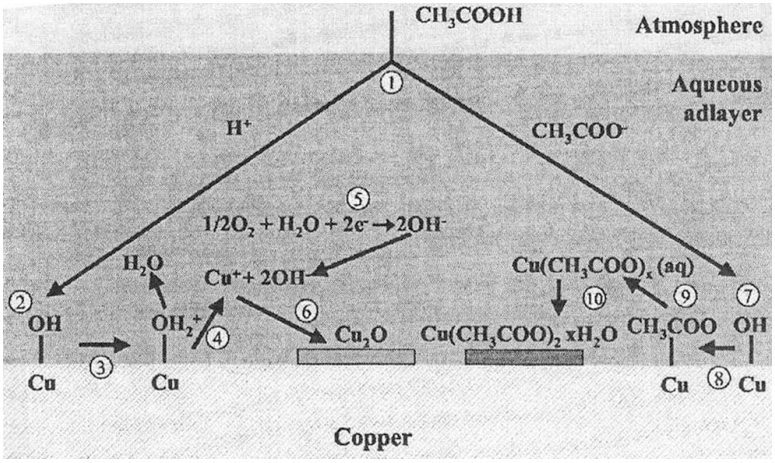

Figure 4.33 Schematic description of two possible reactions for atmospheric corrosion of copper by acetic acid. Taken from Gil and Leygraf 2007b, Fig. 10, C616.

Subsequent XRD Tests (2005, 2006) on Unleaded and Leaded Coupons corroded in 40 ppm Acetic Acid at 86% RH

ASTM B584 contains only a trace of lead (0.25%) distinguishing it from the leaded bronze ASTM B505 (9% lead). In 2005 the corrosion on 17U and 18U was sampled in two places and the powder run on the X-ray Diffractometer at UCLA. The copper acetate hydrate compound found in 2004 had been replaced by unidentified, dissimilar compounds on 17U and 18U (Table 4.16). The same test coupons were again analysed at the Getty in 2006 on the Siemens diffractometer. Copper acetate hydroxide hydrate (50-0407) and copper tin (71-

0122) were found on 17U whereas copper tin only was identified on 18U (Table 4.16, Appendices 4.7, 4.8, 10.5)

In 2005 the analysis of the leaded coupons revealed hydrocerussite (13-0131) and an unidentified compound that had replaced the copper acetate hydrate and cuprite on 18L from 2004 (Table 4.16) (Appendix 4.9). The corrosion on 17L could not be identified. In 2006 17L and 18L were analysed while rotating in the Siemens Diffractometer at the Getty (Appendix 10.5). Copper acetate hydroxide hydrate (50-0407) and an unidentified compound were found on 17L (Table 4.16, Appendix 4.10). Copper acetate hydroxide hydrate (50-0407) and hydrocerussite (13-0131) were found on 18L (Table 4.16, Appendix 4.11). Copper acetate hydroxide was found as an intermediary corrosion product prior to the formation of copper acetate in tests by Lopez (López-Delgado *et al*. 1998, 4143).

Influence of the Lead Component on Corrosion of Test Coupons based on XRD Analysis

The corroded surface of the leaded bronze coupons prior to corrosion testing could have been enriched with lead oxide/hydroxide and may have contained copper oxide and tin oxide as well, resulting from their preparation for testing. These presumptions are based on the findings of Wadsak *et al*. from tests on a single phase quartenary bronze (consisting of 76.5% Cu, 9% Pb, 7% Sn, and 6% zinc) with lead precipitations that was subjected to 80% RH with and without 200 ppb SO_2 (Wadsak *et al*. 2002, 791). In the Wadsak study cuprous oxide, some tin oxide and zinc oxide, and lead oxide/hydroxide enrichment of the surface were detected by XPS and were attributed to corrosion during preparation of the metal prior to corrosion testing. It is important to note that these corrosion products were amorphous and couldn't be identified by XRD. The lead oxide/hydroxide prevented further corrosion, especially the development of cuprous oxide, during exposure to 80% RH (Wadsak *et al*. 2002, 799). This protective coating was destroyed by the introduction of 250 ppb acid vapour (SO_2 in this case) (Wadsak *et al*. 2002, 799).

No lead corrosion was identified on the test coupons exposed to 32% RH in this study. Lead oxide was found at 0.4 (0.04 ppm yr) and 4 ppm (0.4 ppm yr) (52% RH) on the test coupons not treated with sodium sesquicarbonate (11L, 13L) that may have served to protect the copper from attack by acetic acid (Table 4.17). Treatment of the

comparable test coupons (12L, 14L) with sodium sesquicarbonate may have encouraged acid attack on the copper as indicated by an absence of lead oxide and the presence of cuprite (Table 4.17). Corrosion of the lead component was expected as both of these acetic acid doses at 52% RH exceed the LOAED for lead (0.02-0.03 ppm yr) (50-75% RH).

Copper acetate hydrate was identified on both the leaded bronze test coupons exposed to 40 ppm (6.3 ppm yr) acetic acid concentration at 86% RH (17L, 18L) (Table 4.16). The dose was sufficiently high to react with the copper to form copper acetate.

In the study by Wadsak *et al*. more adsorbed water formed on the surface of quartenary bronze (containing 9% lead) during corrosion testing at 80% RH than on pure copper (Wadsak *et al*. 2002, 799). In the current study more water was adsorbed onto the surface of the leaded bronze than on the unleaded bronze at 86% RH. This was also noted on pure lead compared to pure copper by other researchers (Clarke and Longhurst 1961, 442). The current study confirms that leaded bronze has a greater affinity for adsorbing moisture than does copper tin bronze.

The potential-pH diagram for Pb-H_2O system (Figure 4.34) shows a very small region of stability for the surface oxide. The surface oxide is prone to dissolution in acidic environments. In these conditions the corrosion of lead will continue unless an overlying layer of a more stable corrosion product forms (Graedel 1994, 923).

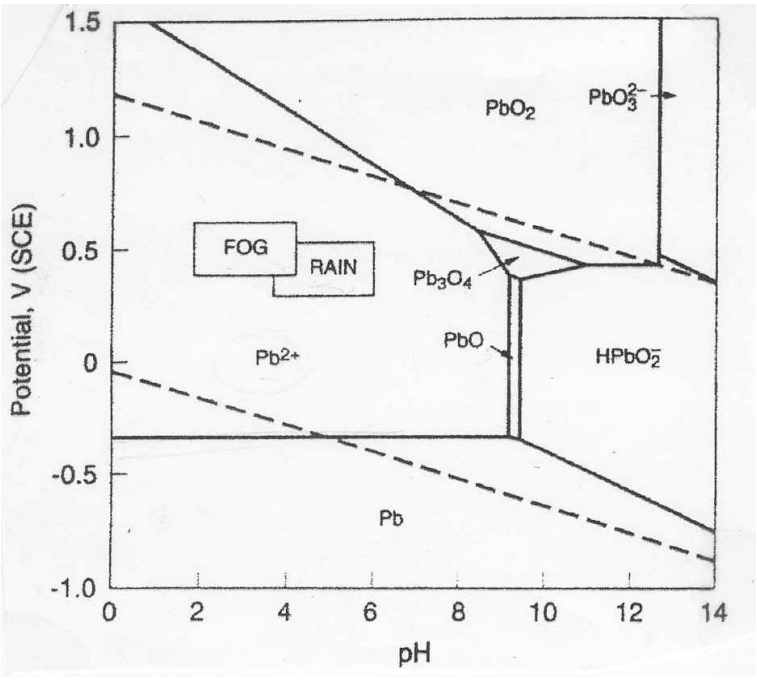

Figure 4.34 Potential-pH equilibrium diagram for the lead-water system at 25°C. Fog and rain can be very acidic and promote Pb corrosion (Pourbaix 1974; Graedel 1994, Fig. 1, 925)

As seen in the formula below, the reaction of the acetic acid with the lead alloy through the electrolyte of the adsorbed water on the surface of the metal causes the formation of water-soluble lead acetate hydrate or lead acetate oxide hydrate. “The acetic acid vapour can be dissolved in the water layer … The acetate ions produced can interact with lead oxide to form lead acetate oxide hydrate."(Tetreault *et al*.1998, 24). Hydrocerussite (lead carbonate hydroxide) was found on both leaded bronze test coupons in 86% RH at 4 ppm acetic acid (19L, 20L) (Table 4.16). Apparently this level of acid concentration was adequate to react with the lead producing lead carbonate hydroxide but not high enough to produce copper acetate that formed in 40 ppm acid concentration. Hydrocerussite resulted from the reaction of Pb oxide by the acetic acid. This dissolution neutralizes the acid and releases acetate ions that then contribute to electrochemical corrosion. The acetate ions carry the lead ions away to areas of high carbonate concentration and higher pH where they are precipitated as hydrocerussite (Tetreault *et al*. 1998, 24). The acetate ion is released during this reaction and goes back into the water layer constituting a corrosion cycle (Tetreault *et al*. 1998, 25). This would explain the presence of hydrocerussite rather than lead acetate on 18L, 19L and 20L, i.e. hydrocerussite has a greater tendency to form and is a more stable compound.

Reaction of lead with acetic acid vapour (Donovan 1986, 78):

" $2Pb + 4CH_3.CO_2H \rightarrow 2Pb(CH_3CO_2)_2$ (lead acetate) + $2H_2O$

$2Pb(CH_3CO_2)_2 + CO_2 + 3H_2O \rightarrow Pb(OH)_2.PbCO_3$(insoluble) + $4CH_3CO_2H$

anodic reaction: $Pb \rightarrow Pb^{2+} + 2e$

cathodic reaction: $O_2 + 2H_2O + 4e \rightarrow 4OH^-$

The lead ions from the acidic area of the anode diffuse toward the alkaline area of the cathode and CO_2 is absorbed from the atmosphere:

$2Pb^{2+} + 4OH^- + CO_2 \rightarrow Pb(OH)_2.PbCO_3$ (hydrocerussite) + H_2O

the hydrocerussite precipitates and the acetic acid is regenerated causing further attack" (Donovan 1986, 78).

The reaction of lead to organic acids is illustrated using formic acid as the reactant (Figure 4.35) (Graedel 1994, 925). Acetic acid should react similarly to formic acid in the diagram. Deposited hygroscopic particles or condensed water on the surface can produce conditions on the surface allowing these reactions to proceed. Pb^{2+} ions diffuse from the metal into the water. The rectangular boxes represent species present as solution constituents (in this case formic acid), the ovals represent precipitated species (in this case lead formate, lead carbonate, lead hydroxy carbonate). Many of the reactions depend on the acidity of the solution (Graedel 1994, 925).

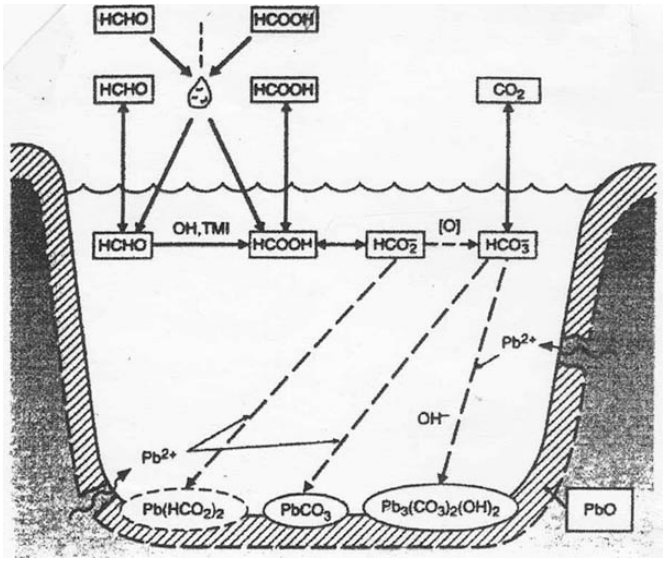

Figure 4.35 Illustration showing pitting corrosion in an aqueous film on lead. Atmospheric corrosion of lead by organic acid (formic acid and formaldehyde are represented here). Dashed ovals indicate constituents that have not been confirmed by laboratory or field studies. Dashed arrows indicate solvation or reaction processes that have not been confirmed by laboratory or field studies. TMI refers to transition metal ions. Taken from Graedel 1994, Fig. 5, 92.

XRD of Ancient Coins corroded from 40, 4, and 0.4 ppm Acetic Acid at 86%, 52%, and 32% RH (Table 4.19)

Coins from all corrosion tests were analysed by XRD with the exception of Coin 6 corroded in 0.4 ppm acetic acid at 32% RH and coin 4 corroded in 0.4 and 4 ppm acetic acid at 32% RH (Table 4.19). This was on account of negligible corrosion formation. From XRD, patina on the majority of ancient coins prior to corrosion testing detected copper oxides (Table 4.5). Coin 2 and Coin 5 from 40 ppm acetic acid at 86% RH are discussed in more detail.

Coin 2, a heavily leaded Greek coin (23%Pb, 69% copper, 8 % tin) dating to the 3rd c. BC, is an exception (Table 4.2). Metallographic examination revealed twinned crystals at edge from hot working and bits of copper in the corrosion crust (Table 4.3, Appendix 2.3). XRD prior to corrosion testing revealed calcium silicate and calcite on the surface, but no oxides of copper or lead (Table 4.5). After treatment with sodium sesquicarbonate, exposure to 40 ppm acetic acid (6.3 ppm yr) at 86% RH produced lead carbonate, hydrocerussite and cerussite (Table 4.19). Hydrocerussite was confirmed by FTIR analysis. This is not surprising given the high lead content of the coin. Lead carbonate $PbCO_3$ was found after corrosion testing in 2004. In subsequent powder

analysis in 2005 at UCLA the white corrosion was identified as hydrocerussite and the blue corrosion as cerussite. This coin serves as an example of the lead protecting copper from acid attack (based on the absence of copper compounds) by acting as a sacrificial sink. It is possible that copper acetate may have been present on Coin 2 upon completion of the corrosion tests that was not detected in the one spot analysis. This coin wedge was too small for rotation during analysis in the Siemens diffractometer.

Coin 5 is a Roman coin attributed to Divus Augustus from AD 14-41. Metallographic examination shows variable grain size, corrosion cracks, worked and annealed grains (Table 4.3) (Appendix 2.4). Straight twin lines indicate annealing was the last stage. Lead globules are evident. Lengthwise channels are due to porosity. Cuprite is evident on the surface. XRF revealed a composition of 98.5 % copper, 1.2 % lead (Table 4.2). XRD indicated tenorite and cuprite on surface prior to corrosion testing (Table 4.5) and copper acetate hydrate after exposure to 40 ppm (6.3 ppm yr) acid concentration (Table 4.19, Appendix 4.12). The neutral copper acetate was confirmed by FTIR analysis. Melaconite (CuO) was found in the 2005 powder analysis. Tenorite and cuprite formed from exposure to the lower acetic acid concentrations (Table 4.19).

Table 4.19 XRD Results of Ancient Coins after Corrosion Tests

Coin	Test-Group (Table 4.4)	RH %	ppm	Compound	Formula	ICPDS
Coin 5	9-17	86%	40 (6.3 ppm yr)	Copper acetate hydrate	$C_4H_6CuO_4.H_20$/ $(CH_3COO)_2Cu.H_20$	27-0145
				[1]Melaconite	CuO	41-0254
	10-19		4 (0.6 ppm yr)	Tenorite	CuO	05-0661
				cuprite	Cu_2O	05-0667
	11-21		0.4 (0.06 ppm yr)	Tenorite cuprite	CuO Cu_2O	05-0661 05-0667
Coin 2 *	9-18		40 (6.3 ppm yr)	Lead carbonate	$PbCO_3$	03-0352
				[1](white) hydrocerussite	$Pb_3(CO_3)_2(OH)_2$	13-0131
				[1](blue) Cerussite	$PbCO_3$	76-2056
	10-20		4 (0.6 ppm yr)	NA		
	11-22		0.4 (0.06 ppm yr)	NA		
Coin 3	5-9	52%	40 (4.9 ppm yr)	cuprite	Cu_2O	05-0667
	6-11		4 (0.4 ppm yr)	cuprite	Cu_2O	05-0667
	7-13		0.4 (0.04 ppm yr)	cuprite	Cu_2O	05-0667
Coin 1 *	5-10		40 (4.9 ppm yr)	Cuprite malachite tenorite	Cu_2O $CuCO_3.Cu(OH)_2$ CuO	03-0892 01-0959 03-0884
	6-12		4 (0.4 ppm yr)	Cuprite	Cu_2O	03-0892
	7-14		0.4 (0.04 ppm yr)	Cuprite	Cu_2O	03-0892
Coin 6	1-1	32%	40 (4.6 ppm yr)	Copper cuprite	Cu Cu_2O	04-0836 02-1067
	2-3		4 (0.4 ppm yr)	Copper cuprite	Cu Cu_2O	04-0836 02-1067
Coin 4 *	1-2		0.4 (0.04 ppm yr)	Not determined		

NA = not analysed; * = treated with sodium sesquicarbonate; [1]UCLA 2005

4.2.2 Test Series I: Part Two (Tables 4.20-4.22; Appendices 4.13-4.16)

The purpose was to assess the reproducibility of the corrosion tests in Part One of Test Series I. One test was chosen from Part One, Test no. 10, to reproduce (Table 4.4). The same two copper alloys and the same environmental conditions were used in Part Two. The Getty Conservation Institute was unwilling to allow acetic acid testing in their environmental chamber and lab for the continuation of my project thereby necessitating the procurement of another laboratory. Further corrosion testing for this project was carried out in Madrid by Dr. Emilio Cano of the Centro Nacional de Investigaciones Metalúrgicas (CENIM), CSIC, Avda. Gregorio del Amo 8, E-28040
Madrid, Spain, following my experimental design. My experimental design was developed from my own experiments and was provided to Dr. Emilio Cano (Table 4.20). At the same time, I carried out control tests (without acid) at the Getty Center in Los Angeles. The data in Figures 4.36 to 4.40 and in Tables 4.20 to 4.22 were provided by Dr. Emilio Cano.

4.2.2.1. Selection and Preparation of Metals used in Testing

The same unleaded and leaded copper tin alloys (ASTM B584 and ASTM B505 respectively) tested in Test Series I: Part One were exposed to the same conditions as in test 10 of Test Series I: Part One (Table 4.4): 4 ppm acetic acid vapour at 86% RH for 8 weeks and 2 days. The same protocol for the preparation of metals in Test Series I: Part One was followed. 3 leaded and 3 unleaded bronze coupons plus 3 leaded and 3 unleaded bronze coupons treated with sodium sesquicarbonate, totaling 12 coupons, were tested (Table 4.20). The same number and distribution of test coupons were exposed to 86% RH without acid forming the control tests (Table 4.20).

Table 4.20 Test Series I: Part Two

Test Series I: Part Two	
Test coupons exposed to 4 ppm acetic acid vapour concentration at 86% RH for 8 weeks	
Unleaded	Leaded
U I	L II
U III	L III
U VI	L V
Unleaded with sodium sesquicarbonate	Leaded with sodium sesquicarbonate
US II	LS I
US IV	LS II
US VI	LS III
Test coupons exposed to 86% RH for 8 weeks (Controls)	
Unleaded	Leaded
U II	L I
U IV	L IV
U V	L VI
Unleaded with sodium sesquicarbonate	Leaded with sodium sesquicarbonate
US I	LS IV
US III	LS V
US V	LS VI

U=unleaded; US=unleaded w/sesquicarbonate; L=leaded; LS=leaded w/sesquicarbonate

4.2.2.2 Generation of Acidic and Humidity Atmosphere

The controlled relative humidity of 86% and acetic acid atmosphere of 4 ppm were generated in a test chamber (Figure 4.36).

4.2.2.2.1 Test Chamber

The decision to reproduce Test 10 (Table 4.4) was in part based on the capacity of the test chamber in Madrid that could reach a maximum concentration of 4 ppm acetic acid vapour. The highest level of RH (86% RH) was selected from Test Series I to enhance the corrosive effects of the acid during the 8-week test period. The test coupons were positioned horizontally on watch glasses in the test chamber during the testing following the protocol in Test Series I: Part One.

Figure 4.36 Test chamber volume (≅ 1m^3) with test coupons for acidic environments (field of view is approximately 45 cm across, photo by Emilio Cano, Diana LaFuente)

"The test chamber was constructed in-house. Compressed air (generated by an oil-free compressor) is passed through several particle filters, activated carbon filter and an air dryer/purifier (Peak Scientific AD70L-40). The flow is controlled using a mass flow controller (Aalborg GFC17). The air flow is then divided into three channels, 'humid', 'polluted', and 'dry', and each one is equipped with a flow meter and a valve. The 'humid' flow passes through a heated bubbler filled with distilled water; the 'polluted' flow goes to the emission chamber where an emission tube (glass tube filled with acetic acid) releases acetic acid vapour; and the 'dry' flow goes directly to the mixing chamber where it is mixed again with the other two channels. Then air combined from the three channels passes into the exposure chamber and then out through a psychrometer that measures and controls the relative humidity" (E. Cano pers comm. 2009). A diagram of the test chamber is provided in Figure 4.37.

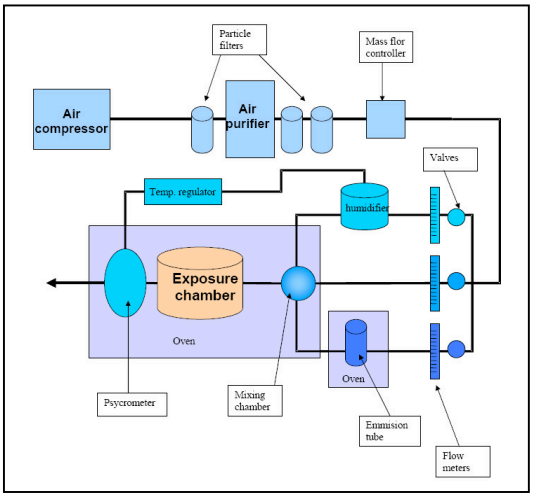

Figure 4.37 Operational diagram of test chamber (provided by E. Cano 2009)

4.2.2.2.2 Controlling and Monitoring Acidic Concentration and Relative Humidity during Testing

"The emission rate of acetic acid was controlled by regulating the opening of the emission tube and the temperature of the emission chamber. The tube was weighed weekly, and the concentration was calculated using the weight loss and total air flow. The psychrometer was a Pt100 temperature probe covered with a cotton wick. The RH was measured comparing the temperature of this wet-bulb temperature with the dry-bulb temperature (i.e. the temperature of the exposure chamber). When the RH falls below the desired RH, the wet-bulb temperature decreases and a temperature controller is used to heat the bubbler, increasing the total amount of water added to the system, and in turn increasing the RH of the chamber. This system allows for a real time sensible control of the RH, with standard RH variation of ±2%. The exposure conditions were adjusted to obtain an acetic acid concentration of 4 ppm at 30° C and RH 86%" (Figure 4.37) (E. Cano pers comm. 2009). The controls were run in a glass bell jar at room temperature using a saturated solution of sodium sulphate to maintain a RH of 86% without acetic acid. The bell jar remained unopened for the duration of the test.

4.2.2.3 Analytical Results after Corrosion Testing - Test Series I: Part Two

4.2.2.3.1 Gravimetric Results

Test Series I Part Two differs from Part One in that the test coupons were removed from the test chamber weekly for weighing. Sources of error include fluctuations in RH, temperature, and acetic acid concentration during exposure and weighing error (Table 4.21). The reported maximum fluctuations in the experimental parameters of RH, temperature and acetic acid concentration are sufficiently low to avoid significant changes in weight. Weighing error is restricted to the balance resolution of 0.1 mg as the coupons were weighed in the watch glasses to prevent the accidental dislodgment and loss of powdery corrosion products during weighing. The coupons were weighed immediately upon removal from the test chamber to avoid skewed results from desorbtion of water from the watch glass and the mass gain was displayed on a graph (Figure 4.38). In the mass gain determinations the maximum standard error was ±0.0006 g for the L coupons, ±0.0003 g for the LS and US coupons, and ±0.0002 g for the U the coupons (Figure 4.38). The most extensive mass gain occurred with the leaded coupons

followed by the leaded/sesquicarbonate, unleaded/sesquicarbonate coupons, and finally the unleaded coupons (Figure 4.38).

Table 4.21 Sources of Experimental Error

RH %	± 2
Temp. °C	± 1
Acetic acid ppm	± 0.5
Balance accuracy	± 0.1 mg

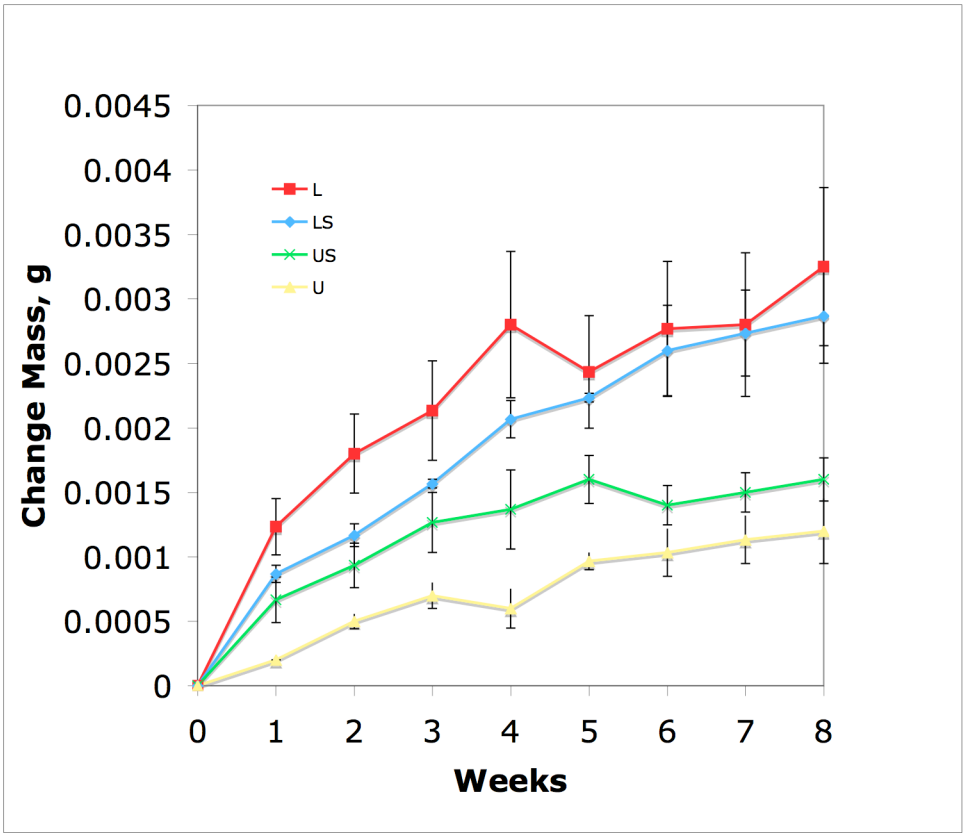

Figure 4.38 Mass gain during corrosion testing
L=leaded; LS=leaded/sesquicarbonate; US=unleaded/sesquicarbonate; U=unleaded

Upon completion of corrosion testing total mass loss was determined by stripping two test coupons from each group (i.e. two leaded, two unleaded, two leaded and two unleaded treated with sodium sesquicarbonate). The chemical stripping process was followed according to G1-03 ASTM, specifically designation C.2.3 for removing the copper corrosion products: 100 mL sulphuric acid in reagent water to make 1000 mL for 1-3 minutes; and designation C.4.1 was used to remove lead corrosion products from the

leaded bronze coupons: 10 mL acetic acid boiling solution in reagent water to make 1000 mL for 5 minutes. Mass loss information was registered after repeated cleaning cycles according to section 7 of G1-03 ASTM (ASTM 2003a) and was graphed for four test coupons in Figure 4.39.

Regarding the sources of experimental error in Table 4.21, weighing error is the only relevant source in the mass loss determinations and is restricted to the balance resolution of 0.1 mg. Since each point on the graph represents one weight (not a mean) a standard error does not apply to the individual points in Figure 4.39. Instead, the mean for each coupon was determined from all plotted points and the standard error derived from this (Table 4.22). The overall standard error was ±0.0004 g for the leaded coupons and ±0.0001 g for the unleaded coupons.

The leaded coupons were first stripped of copper corrosion followed by lead corrosion. In the leaded coupons mass loss due to the removal of copper corrosion occurs around 200 to 300 seconds and around 450 to 550 seconds due to the removal of lead corrosion (Figure 4.39). Total mass loss due to corrosion removal was reached after approximately 450 to 550 seconds for the leaded test coupons but was reached much more quickly, in less than 100 seconds, for most of the unleaded test coupons. The graphs indicate more extensive corrosion of the leaded coupons and an increase in corrosion with sodium sesquicarbonate (Figure 4.39). Weight loss is reflected accordingly: leaded/sesquicarbonate > leaded > unleaded/sesquicarbonate > unleaded (Table 4.22).

The discrepancy between the maximum mass gain displayed by the L coupons and the maximum mass loss displayed by the the LS coupons may be explained by the fact that the mass gain was determined from the mean of three coupons whereas the mass loss was determined from one coupon only. For this reason mass gain may be considered more representative of the overall performance.

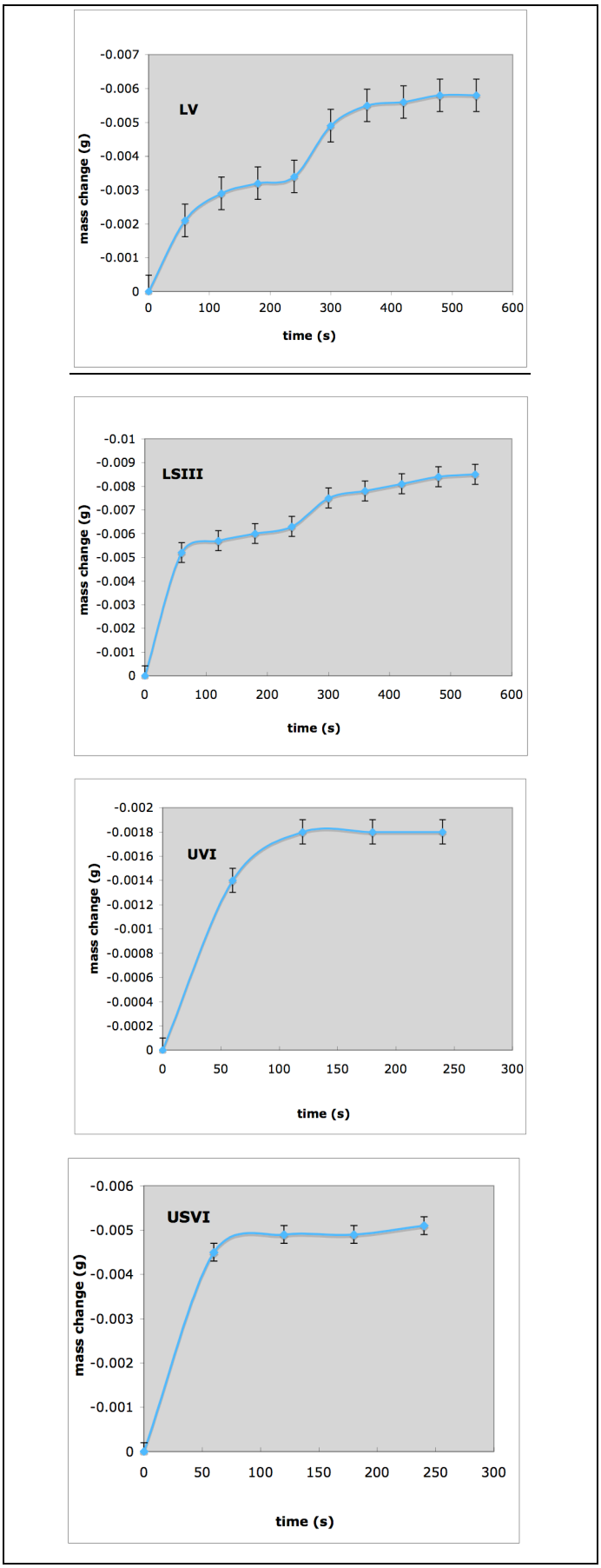

Figure 4.39 Mass loss during removal of corrosion in multiple cleaning cycles after corrosion testing: test coupons LV, LSIII, UVI , USVI (Table 4.22)
L=leaded; LS=leaded/sesquicarbonate; U=unleaded; US=unleaded/sesquicarbonate

Table 4.22 Weight Loss of Test Coupons after Corrosion Testing

Test coupon	Maximum Weight Loss g	Standard Error g
L V	0.0058	±0.0004
LS III	0.0085	±0.0004
U VI	0.0018	±0.0001
US VI	0.0051	±0.0001

L=leaded; LS=leaded/sesquicarbonate; U=unleaded; US=unleaded/sesquicarbonate

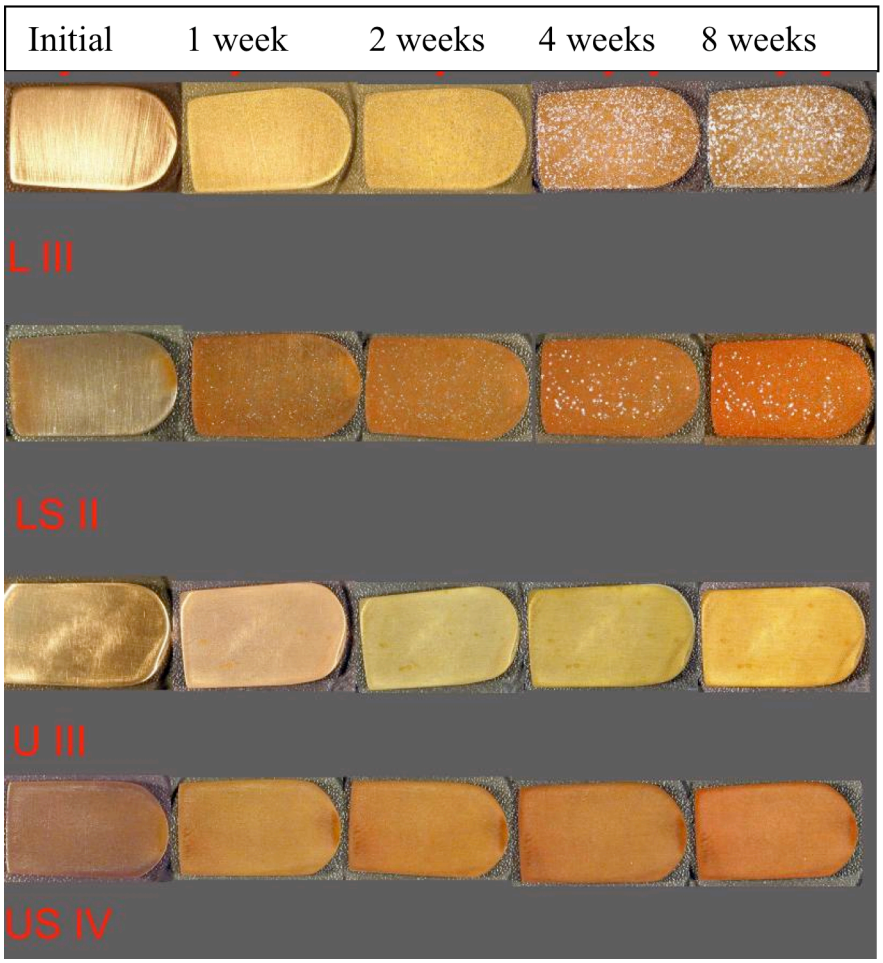

Figure 4.40 Photographic record during corrosion testing (field of view is 12.5 cm across) L=leaded; LS=leaded/sesquicarbonate; U=unleaded; US=unleaded/sesquicarbonate; Prepared by Dr. Emilio Cano and Diana LaFuente

The test coupons were examined weekly when they were removed from the test chamber for weighing (Figure 4.40). White corrosion pustules formed on the leaded coupons treated with sesquicarbonate after one week and on the leaded coupons without sesquicarbonate after 4 weeks. Tarnishing was visible on all the unleaded coupons treated with sesquicarbonate from the start of the test. The leaded coupons corroded more than the unleaded coupons as evidenced by their greater mass gain (Figure 4.38)

during testing and greater weight loss after removal of the corrosion (Figure 4.39, Table 4.22).

Comparison with the results from Part One Test and other researchers

The Madrid tests may be compared to the Los Angeles tests in Part One since the same dose concentration was tested: 0.635 ppm yr at 86% RH (Table 4.6). This dose concentration exceeds the LOAED levels reported for copper and lead in Table 4.7. Weight loss for the leaded coupons was found to exceed weight loss for the unleaded coupons (Table 4.22). Other researchers have studied weight changes of lead and copper in various concentrations of acetic acid vapour and have determined greater weight change for lead over copper. The difference in weight gain between pure lead and pure copper exposed to the dose concentration 0.28 ppm yr acetic acid vapor in 100% RH exceeded that found for the leaded and unleaded coupons in this study and reflects the contribution of lead to corrosion (Table 4.23) (Donovan and Stringer 1971). The difference in % weight change between the Part One and Part Two tests may be explained by coupons of greater mass but equivalent exposed surface areas used in Part Two compared to those in Part One.

Table 4.23 Corrosion of Metals by Acetic Acid at 30° C and 100% RH for 3 weeks expressed as g/dm^2

	Acetic acid vapour		
Metal	0.028 ppm yr	0.28 ppm yr	2.87 ppm yr
Cu 99.99%	0.02	0.18	0.60
Pb 99.90%	1.06	1.57	3.10

* from Donovan and Stringer 1971, Table II, p. 135

Table 4.24 % Weight change - Comparison of Part One and Part Two of Test Series I, 0.635 ppm yr 86% RH

Test Series I:	Unleaded bronze ASTM B584 (0.25% Pb)	Leaded bronze ASTM B505 (8% Pb)
Part One (Los Angeles)	0.12±0.05	0.11±0.01
Part Two (Madrid)	0.0095±0.002	0.0195±0.0007

4.2.2.3.2. XRD of Coupons after Corrosion Testing from Test Series I: Part Two

XRD analysis was run on one leaded coupon and one unleaded coupon, with and without sodium sesquicarbonate, at the completion of corrosion test (Table 4.25; Appendices 4.13-4.16). The diffractometer used in the Madrid laboratory was a Bruker AXS, Model D8 with open ring. The diffractograms were obtained using a cobalt tube, and grazing angle incidence (1º). The spectra were collected from 10° to 80° 2Θ.

According to Cano, an unidentified source of chloride contamination in the Test Chamber caused the formation of chlorides on all test coupons (Table 4.25) (E. Cano pers comm. 2009). In spite of this, the white corrosion on the leaded test coupons (LS II with sesquicarbonate and L III without sesquicarbonate) was identified as hydrocerussite (Table 4.25). Cuprite and copper tin were the non-chloride compounds identified on the unleaded test coupons (U III, US IV) (Table 4.25).

Table 4.25 XRD Results of ASTM Test Coupons from Test Series I: Part Two revealing Chloride Contamination in the Environmental Chamber

Acid Conc.	Test piece	Compound	Formula	ICPDS	Appendix
4 ppm (0.6 ppm yr)	L III	Hydrocerussite; Malachite; Lead chloride hydroxide; Paratacamite	$Pb_3(CO_3)_2(OH)_2$; $CuCO_3.Cu(OH)_2$; PbClOH; (Cu,Zn)2(OH)3Cl	13-0131; 41-1390; 52-0289; 70-0821	4.13
	LS II	Hydrocerussite; Cuprite; Lead chloride hydroxide; Paratacamite; Atacamite	$Pb_3(CO_3)_2(OH)_2$; Cu_2O; PbClOH; (Cu,Zn)2(OH)3Cl; $Cu_2Cl(OH)_3$	13-0131; 05-0667; 52-0289; 70-0821; 25-0269	4.14
	U III	Cuprite; Copper tin; Paratacamite; Atacamite; Nantokite	Cu_2O; CuSn; (Cu,Zn)2(OH)3Cl; $Cu_2Cl(OH)_3$; CuCl	05-0667; 04-0836; 70-0821; 25-0269; 06-0344	4.15
	US IV	Cuprite; Paratacamite; Atacamite; Nantokite	Cu_2O; (Cu,Zn)2(OH)3Cl; $Cu_2Cl(OH)_3$; CuCl	05-0667; 70-0821; 25-0269; 06-0344	4.16

L=leaded; LS=leaded w/sesquicarbonate; U=unleaded; US=unleaded w/sesquicarbonate
Prepared by Dr. Emilio Cano

4.2.3 Comparison of Results from Test Series I: Part Two with Test 10 (Table 4.4) of Test Series I: Part One

XRD corroborates the results of Test 10 (Table 4.16) in the formation of hydrocerrusite and cuprite on the leaded test coupons, copper tin on the unleaded test coupons, and the absence of acetates (Table 4.25). This finding is identical to that in Part One despite the unexpected presence (and possible influence) of chloride in Part Two. Part Two provides independent confirmation of Part One test results. It represents an unpublished confirmation of the data from the Tedlar® bags with standard testing under rigorous conditions in a certified laboratory facilty in Madrid. The Part Two tests confirmed that the Tedlar® bags served as an appropriate substitute for standard (ASTM) testing procedures in environmental chambers.

4.3 Test Series II (Appendices 4.17-4.21, Appendices 10.7-10.10;)

Results presented in this thesis have shown that the development of corrosion on artifacts proceeds through stages. The purpose of Test Series II was to determine the influence of acetic acid vapour and conservation materials on the transformation or conversion of pre-existing bronze corrosion products. One goal of these tests was designed to recreate the carbonyl compounds identified on bronzes in this study thereby simulating the corrosion processes that occur on the objects in wooden storage cabinets.

In Test Series II corrosion products commonly found on archaeological bronze, malachite and chalconatronite, were exposed to high levels of acetic acid vapour and RH. The influence of a conservation material, sodium sesquicarbonate, on bronze corrosion was tested by exposing sodium sesquicarbonate, on its own and mixed with malachite in equal portions, to acetic acid vapour. The purpose of mixing it with malachite was to simulate a copper alloy with malachite patina that has been treated with sodium sesquicarbonate. Obviously, the texture and structure of corrosion layers are quite different. Powdered mineral samples were used in these tests; the high surface area on the mineral samples is much more reactive to volatile organic acids.

4.3.1 Selection of Corrosion Compounds and Conservation Materials used in Testing

Tests were run on the following compounds: 1) chalconatronite, 2) sodium sesquicarbonate with malachite (1:1), 3) malachite, and 4) sodium sesquicarbonate. The

chalconatronite was obtained from Petrie sample #6 that was identified by XRD in Chapter 5 (Appendix 16). The malachite for testing was provided by Dr. David Scott. Malachite, a very common copper carbonate that forms during burial, can be transformed into chalconatronite (sodium copper carbonate hydrate) when exposed to sodium during burial (Frondel and Gettens 1955). Chalconatronite can also result on bronze containing a patina of malachite from treatment with sodium sesquicarbonate (Horie and Vint 1982, 185). Based on these published cases sodium sesquicarbonate was chosen as the sodium-based compound for testing the effects of sodium contaminant (simulating either from burial or conservation treatment) in Test Series II.

4.3.2 Experimental Method

A very high level of acetic acid vapour (500 ppm) and a high RH (85%) were chosen to encourage chemical reactions to occur within the short duration of the tests. The corrosion products, corrosion products mixed with sodium sesquicarbonate, and sodium sesquicarbonate on its own were exposed in Petrie dishes in an airtight bell jar for 16 or 21 days to these levels of acid vapour and RH. The acetic acid dose concentrations based on these test durations equate to 22 ppm yr to 29 ppm yr. After removal from the test chamber the compounds were ground and analysed with the GADDS (General Area X-ray Diffraction System) at the Getty Conservation Institute by the author.

The level of acetic acid vapour (500 ppm) was determined with a Gastec passive dosimeter and the RH (85%) was measured with a thermohygrograph. These atmospheric conditions were created by placing glacial acetic acid (as supplied) in an open beaker and deionized water in another open beaker inside the bell jar.

4.3.3 Results of XRD Analysis of Powdered Corrosion exposed to 500 ppm Acetic Acid at 85% RH in Test Series II

The first test (1) involved chalconatronite. The conversion of chalconatronite into a sodium copper carbonate acetate was successfully carried out under the test conditions described above (Appendix 4.17, Appendix 10.7):

(1) Chalconatronite + acetic acid$^{(vapour)}$ + RH (21 days)→ a sodium copper carbonate acetate.

The design of the second test (2) involved the simulation of the corrosion on a bronze object with a malachite patina that was treated with sodium sesquicarbonate and then subjected to off-gassing in wooden storage. This simulation was achieved by mixing equal parts of malachite with sodium sesquicarbonate and exposing this mixture to 500 ppm acetic acid at 85% RH. After removal from the test chamber, the mixture formed blue/green crystals surrounded by blue crystals while drying. These were analysed separately by XRD. The reaction of malachite and sodium sesquicarbonate is known to form chalconatronite in the presence of moisture (Horie and Vint 1982). By adding acetic acid vapour, while the reaction may have first formed chalconatronite in the test chamber, it resulted in the formation of a sodium copper carbonate acetate in the green crystals (Appendix 4.18, Appendix 10.8):

(2) Sodium sesquicarbonate + malachite + acetic acid$^{(vapour)}$ + RH (16 days)→ a sodium copper carbonate acetate.

The blue crystals could not be identified (Appendix 4.19, Appendix 10.8).

The third test (3) determined the influence of acetic acid on malachite without the influence of sodium. Malachite (copper carbonate) exposed to these conditions was partially transformed into copper acetate (both malachite and copper acetate were identified by XRD) (Appendix 4.20, Appendix 10.9):

(3) Malachite + acetic acid$^{(vapour)}$ + RH (21 days) → copper acetate + malachite.

The fourth test (4) proved the hypothesis that residues of sodium from sodium sesquicarbonate or other sources can react with volatile acetic acid forming a compound containing sodium and acetate, such as sodium acetate trihydrate (Tennent *et al*. 1992, 878). Sodium sesquicarbonate was exposed on its own to 500 ppm acetic acid at 85% RH (Appendix 4.21, Appendix 10.10):

(4) Sodium sesquicarbonate + acetic acid$^{(vapour)}$ + RH (16 days) → sodium acetate trihydrate.

4.4 Conclusions of Experiments from Test Series I (Part One and Part Two) and Test Series II

Among the novelties of this research is the formation of acetate corrosion on copper tin bronze and on leaded copper tin bronze (without artificial patination) for the first time. Another novelty is the successful formation of acetate on authentic, naturally corroded archaeological bronzes under test conditions for the first time. Yet another novelty is the successful the transformation of corrosion typical to archaeological bronzes (i.e. carbonates) to acetate (after removing the corrosion from the object, under controlled conditions of elevated levels of acetic acid concentration and relative humidity). The accelerated corrosion tests of leaded and unleaded copper alloys exposed to acetic acid successfully provoked the formation of acetate corrosion compounds.

In Test Series I the study of the corrosion mechanisms involved in this acetate formation on new and archaeological bronze contributes significantly to our understanding of the dangers of storing collections in unsuitable environments. The results from Test Series II contribute to our knowledge of the chemical reactions that take place between bronze corrosion, commonly resulting from burial conditions and conservation chemicals, and acetic acid vapour. With this knowledge, means of mitigation and prevention may be developed.

The influence of alloy composition is crucial in the corrosion behavior of copper alloys: environmental conditions such as relative humidity and volatile acidic levels must be controlled accordingly. This study shows that the relative humidity 52%, that is suitable for many materials in museum collections, does not provide adequate protection against the corrosion of bronze exposed to certain levels of acetic acid. In high concentrations of acetic acid vapour, the higher the lead content of bronze the higher the risk to the object and the greater the precautions and protective measures required. In lower acetic acid vapour levels, lead may protect the copper from corrosion by acting as a sacrificial sink but only to a point.

The present study indicates that the patina plays a major role in subsequent corrosion of bronze by acetic acid. Copper carbonate patina on leaded bronze would provide some degree of protection for the lead alloy. This factor, taken into account with the concentration of acetic acid vapour, determines the processes of corrosion, the protective qualities of lead and the extent of vulnerability of the copper, and the

formation of acetate compounds. The extent of damage inflicted on the object depends on composition and micromorphology of the metal as well as composition and morphology of corrosion. There are no simple answers but there are clear conditions to be avoided.

SEM/EDS, FTIR, and XRD were complimentary techniques in so far as they provided apparently consistent results regarding the corrosion on the test coupons and coins exposed to 86% RH. The bulk of analysis concentrated on the tests run at 86% RH since this high moisture level produced the most corrosion. XRD was run on samples from the 52% and 32% RH tests as well. The tests run at 40 ppm acetic acid vapour concentration may be considered accelerated corrosion tests since 40 ppm greatly exceeds the levels reported in museum cases. The levels that have been measured in museum storage cases more recently range from 0.14 to 1.2 ppm. It should be kept in mind that acetic acid concentration can greatly exceed these levels in wooden cases of new construction or those that have been freshly painted or on direct contact. Although acetic acid vapour concentration of 4 ppm did not produce acetates within the duration of the tests, this does not preclude their formation over a longer exposure time. The present tests were constrained to less than 100 days. Bronze artifacts are commonly stored in wooden cases for decades.

The examination of the surface of the metal coupons and coins with the SEM and elemental analysis by EDS on specific spots on the surface were very useful for distinguishing the phases of the binary and ternary alloys and for extrapolating the identification of corrosion sequences based on dominant elements. The same spot was targeted in repeated analysis whenever possible. In some cases, however, the same spot could not be located on account of corrosion growth. SEM proved to be an appropriate means to monitor the development of crystal morphology over the course of corrosion testing (specifically 17U, 18U, 17L, 18L, coin 2 and coin 5). EDS was a suitable tool for monitoring the changes in elemental composition of crystal formation over time (specifically 17L and 18L), crystal growth, and the changes of lead and other species.

Copper hydroxide as a precursor to copper acetate hydroxide and copper acetate hydrate was not identified since XRD analysis was not carried out during the corrosion testing. A shift from neutral to basic copper acetate occurred from completion of the corrosion tests (40 ppm acetic acid at 86% RH) in 2004 to 2006, as evidenced by

subsequent XRD analysis in 2006 (Table 4.16). The transformation from neutral to basic copper acetate is as follows:

$$Cu(CH_3COO)_2 \quad + \quad CO_2 \quad \rightarrow [Cu(CH_3COO)_2]_x\,[Cu(OH)_2]_y \bullet {}_zH_2O$$

neutral basic

where x, y, and z are variable (Scott 2002, 272).

Copper acetate hydroxide hydrate $Cu_2(OH)_3(CH_3COO) \bullet H_2O$ (50-0407) and hydrocerussite were found on the leaded bronze from the 40 ppm/86% RH exposure two years after the corrosion tests. The initial analysis two years prior indicated copper acetate hydrate and cuprite. The test coupons and coins were removed from acetic acid vapour and stored in average room temperature and RH during this two-year period. Copper acetate hydroxide formed in tests on pure copper from100 ppm acetic acid where it was the major component but was found from 50 and 200 ppm acetic acid as well (López-Delgado *et al*. 1998, 4143).

The inability of XRD to characterize some of the corrosion compounds on the test coupons and coins was a major obstacle in the understanding and interpretation of corrosion behavior. This may be attributed to mixtures of compounds, an amorphous state of some compounds, and a shift in the lattice diffraction pattern forming non-stoichiometric compounds as a result of hydration and possible electrochemical corrosion. Considerable data analysis is necessary in order to identify non-stoichiometric compounds with XRD. A few trends have been pointed out in the diffraction pattern characterization of copper acetate compounds. Many have strong d-spacings at 7, 9.3, 11.5, and 12 Angströms or 7, 9, and 11 Angströms or a combination of these (Scott 2001, 80). Some of the copper acetate compounds have the most intense d-spacings at 15, 16, or 17 Angströms (Scott 2001, 78). Other compounds have strong d-spacings around 2.5, 3.6 and 6.5 Angströms.

Corrosion on bronze and leaded bronze is much more complex than corrosion on unalloyed copper in high humidity (Wadsak *et al*. 2002, 795). The two studies that have exposed leaded copper tin bronze to acetic acid succeeded in forming acetate on leaded copper tin bronze test coupons that had been artificially patinated with copper sulphide (Bastidas *et al*. 1995; López-Delgado *et al*. 1997). No other studies testing the influence

of acetic acid on tin bronze and unpatinated leaded tin bronze have been found to date. Especially helpful are the reports of analytical success and failure regarding the identification of corrosion compounds. The current study serves to confirm the limitations of XRD and the advantages of including other analytical means, such as XPS (X-ray Photoelectron Spectroscopy), AFM (Atomic Force Microscopy), and SIMS (Secondary Ion Mass Spectrometry), for the characterization of corrosion compounds.

The Influence of Sodium Sesquicarbonate in Corrosion Tests

It has been observed in the Ancient Athenian Agora collection that 40 % of bronzes from the North Slope of the Acropolis were treated with sodium compounds and subsequently displayed acetate corrosion. Although half of the test coupons and coins were treated with sodium sesquicarbonate no compounds containing sodium were identified by XRD or FTIR nor was sodium identified by SEM-EDS because of low values below the detection limit (1%). Sodium sesquicarbonate possibly served as a catalyst between the acetic acid and the copper without contributing the sodium ion to the formation of corrosion compounds.

In Test Series I: Part One sodium sesquicarbonate appeared to activate copper corrosion in 86% RH and 40 ppm acid concentration on the leaded bronze as evidenced by SEM-EDS of coin 2. Copper corrosion was active in the early stages of testing. This appeared to diminish over the course of testing, ending with a predominance of lead corrosion. Sodium sesquicarbonate was found to encourage acid attack on copper in leaded bronze at 52% RH as well. On pure copper, corrosion was found to proceed over the entire metal surface in a uniform manner when acetic acid vapour from 10 and 50 ppm tests was adsorbed by the water layer coating the surface (from 100% RH) (López-Delgado *et al*. 1998, 4147). In the bronzes tested in this study, the irregularities in the cast structure, e.g. the dendritic structure, and the binary and ternary phase system may account for the comparatively non-homogeneous development of corrosion in the tests. This may have been accentuated by sodium sesquicarbonate, as it caused the formation of crystal morphology different from that found on comparable test coupons not treated with the carbonate. In Test Series I: Part Two (4 ppm acetic acid vapour and 86% RH) sodium sesquicarbonate was found to encourage corrosion of the leaded alloy. Corrosion developed sooner on those leaded coupons treated with sodium sesquicarbonate. The

unleaded coupons treated with sodium sesquicarbonate developed tarnishing immediately.

Test Series II serves to illustrate the contribution of sodium to the formation of carbonyl corrosion. Sodium in sodium sesquicarbonate reacted with malachite, under the influence of acetic acid vapour, forming a sodium copper carbonate acetate. Chalconatronite exposed to acetic acid vapour produced a sodium copper carbonate acetate. Sodium sesquicarbonate on its own exposed to acetic acid vapour formed sodium acetate trihydrate. These are the first known tests to determine the reaction of bronze corrosion products with volatile acetic acid, with and without the addition of conservation chemicals, by exposure of the compounds alone (without the bronze objects).

Influence of Tin in the Corrosion Tests

The role tin may play in the corrosion of the copper tin alloys should be considered. Although XRD did not detect tin oxide in these tests there are instances of tin oxide production by electrochemical corrosion tests on binary and ternary bronze (Beljoudi *et al*. 2001b, 234). Tin was not found to play a protective role in the corrosion study on quartenary bronze (Wadsak *et al*. 2002, 801). On archaeological bronzes tin oxide can combine with moisture forming viscous corrosion products in the so-called Type I corrosion mechanism (Robbiola *et al*. 1998, 2105). The solubilities of tin compounds are listed in Appendix 7.3. This gel-like tin oxide is amorphous and serves as a passivating layer that can retard attack on the copper. The highest tin content was detected by EDS in the areas of green corrosion characterized by a low lead content. Although tin and lead were present in equal amounts (9% wt) in the leaded bronze it would appear that less tin corrosion was activated than lead and that the influence of tin was minimal.

The Influence of Lead in the Corrosion Tests

In Part One of Test Series I it was found that in low concentrations of acetic acid (0.4 ppm) lead alloy in tin bronze may protect the copper from corrosion when exposed to high humidity. In these tests lead oxide, that may have formed from polishing the test coupons, may have withstood the lower acetic acid concentrations (0.4 ppm) providing

protection for the copper from acetic acid. The high concentration of 40 ppm would have been adequate to dissolve any lead compounds present, exposing the copper to attack. Within a certain range of acidic concentration (0.4 to 4 ppm) the cyclical formation of lead carbonate hydroxide is promoted. If this range is exceeded (40 ppm) the copper is attacked and copper acetates form. In one case the two were found to coexist (18L 2006). Heavily leaded coin 2 formed lead carbonate hydroxide in 40 ppm acetic acid concentration with an absence of copper acetate. This coin demonstrated maximum weight gain in relation to greatest Pb content in 86% RH (Figure 4.3). In Part Two of Test Series I (4 ppm acetic acid vapour in 86% RH) the leaded bronze coupons corroded to a greater extent than the unleaded coupons as evidenced by superior weight gains during corrosion testing (Figure 4.38) and superior weight losses after corrosion removal (Table 4.22).

Leaded bronze may be prone to greater damage in the long run by acetic acid attack on account of the cyclical corrosion process between lead and acetate ions in the presence of moisture. Lead acetate hydrate is a transitional, unstable compound that forms fleetingly during the production of the stable lead carbonate hydroxide. Lead acetate hydrate might have been detected on the leaded bronze coupons and coin if analysis had been carried out during the course of the corrosion testing. Depending on the percent lead content and structure of the metal, this cyclical corrosion process could lead to the severe disintegration of a leaded bronze object in storage.

Chapter 5 Case Studies

5.1 Introduction

With this chapter I have extended the analytical investigation of carbonyl corrosion on bronze beyond the Ancient Athenian Agora in Greece to selected museums in the United Kingdom (Paterakis 2003). The carbonyl compounds are defined as simple organic carboxylic acids that contain the carbonyl group [C=O] (Hawley 2001, 213). The carbonyl compounds of interest in this study, acetate and formate, derive from acetic (ethanoic) acid and formic (methanoic) acid. Carboxylic acids are often found in materials used for the construction of storage and display cases in museums, in particular wood and wood products (Evans 1951; Lane 1987; Lang 1995; Thickett 1998; Werner 1967).

The history of the discovery of carbonyl corrosion on metal was presented in Chapter 2. However, another corrosion product of similar color and appearance that derives from different sources is found on bronze, chalconatronite [$Na_2Cu(CO_3)_2.3H_2O$] (Gettens and Frondel 1955). As it can be easily confused visually with carbonyl corrosion, scientific analysis is required to differentiate it from the carbonyl compounds. Chalconatronite can co-exist with carbonyl corrosion compounds on the same artifact.

In the present study, archaeological bronzes from the following collections have been selected for corrosion analysis: Petrie Museum, Ashmolean Museum, Fitzwilliam Museum, Liverpool Museum, British Museum, and the Athenian Agora. These museums were selected because a proliferation of blue corrosion was present in the bronze collections. Corrosion suspected of containing carbonyl components was sampled and analysed by X-ray Diffraction (XRD) at the Getty Conservation Institute and University of California Los Angeles (UCLA), Los Angeles. The history of the objects is researched in terms of provenance, alloy composition, conservation treatments, patina (pre-existing corrosion), and storage factors. The results from the experimental work in Chapter 4 are here applied to the interpretation of the corrosion products found in these Case Studies. This represents a wider survey than undertaken before.

5.1.1 History of the Discovery of Chalconatronite

Chalconatronite, $Na_2Cu(CO_3)_2.3H_2O$, was first found on archaeological Egyptian bronzes and was characterized and named by Gettens and Frondel in 1955 (Gettens and Frondel 1955, 64; Gettens 1963). It was identified in the hollow interior of a figurine of the deity Sekhmet (or Buto) in the Fogg Museum, on the hollow interior of the base of the "Cat and Kittens" statue of the Saite-Ptolemaic period in the Gulbenkian Collection, and on the underside of a Coptic censer dating no later than the 8th c. AD in the Freer Gallery. In these cases the chalconatronite "appears to have resulted from …contact with the very special conditions that prevail in the soils of the more extremely arid parts of Egypt which contain alkali carbonates…" (Gettens and Frondel 1955, 72). Natron ($Na_2CO_3.10H_2O$) or trona ($Na_2CO_3.H_2O$) are present as efflorescence on the soil or in deposits of salt lakes in the Lower Nile Valley (Gettens and Frondel 1955, 72). Dissolved natron ($Na_2CO_3.10H_2O$) or trona ($Na_2CO_3.H_2O$) in the soil react with malachite of the bronze producing chalconatronite. In the case of the hollow statuettes it was found on the interior and was compared to mineral formation in a vug (Gettens and Frondel 1955, 72). A vug is "a small unfilled cavity in a lode or in the rock, usually lined with a crystalline layer of different composition from the surrounding rock." (Webster 1949). Atacamite and paratacamite seem to be the common copper corrosion products on the exterior of archaeological bronzes from arid regions including Egypt and Mesopotamia (Gettens and Frondel 1955, 72). Although no mention was made of cleaning or conservation of these Egyptian artifacts (Gettens and Frondel 1955, 64) we cannot rule out the possibility of the removal of chalconatronite from the exterior during a cleaning treatment.

Gettens and Frondel (1955, 68) noted that chalconatronite is one of six natural carbonates containing copper as an essential component and one of three that has been found as an alteration product on metal objects (the other two are malachite and azurite). "Although these corrosion products are formed on artifacts they are in every sense true minerals. The chemical substances formed in the earth on man-made objects are formed by truly natural processes" (Gettens and Frondel 1955, 68). Chalconatronite is not considered an intermediate copper product but is a carbonate like malachite and azurite that is an ultimate product of copper mineralization and is stable to CO_2 (Gettens and Frondel 1955, 69). "The occurrence of chalconatronite on these bronzes certainly confines their origin to the few exceedingly arid places of the world and supports the

stylistic and historic evidence of their Egyptian provenance." (Gettens and Frondel 1955, 74).

Since the publication of its diagnostic characteristics in 1955, the identification of this compound has not been limited to archaeological objects of Egyptian provenance, however. Chalconatronite can result from the reaction of sodium sesquicarbonate (Horie and Vint 1982, 185) and sodium carbonate with malachite during stabilization treatment (Pollard *et al*. 1990, 150). The effects of conservation treatments on the formation of chalconatronite will be discussed in this chapter.

5.1.2 Extent of Corrosion and Activity of Acetates and Formates

The artifacts damaged by carboxylic acids from various selected museums around the world were described and presented in chronological order in Chapter 2. The formation of acetates and formates on copper alloy objects in collections can be attributed primarily to their storage or display in wood or other materials containing wood products (Hatchfield 2002, 67). The sources of these contaminants will be discussed in more depth (section 5.4.1 and 5.5.2) based on the case studies presented in the current chapter.

Carbonyl corrosion occurring on the surface of copper tin bronze (see Figure 5.1 for acetic acid on copper) is less disruptive on this alloy than bronze disease (which results from the reaction of copper chloride embedded under the cuprite layer with moisture) (Figure 5.2). Nantokite (CuCl) provides the source of paratacamite ($Cu_2Cl(OH)_3$) that erupts on the surface of the metal.

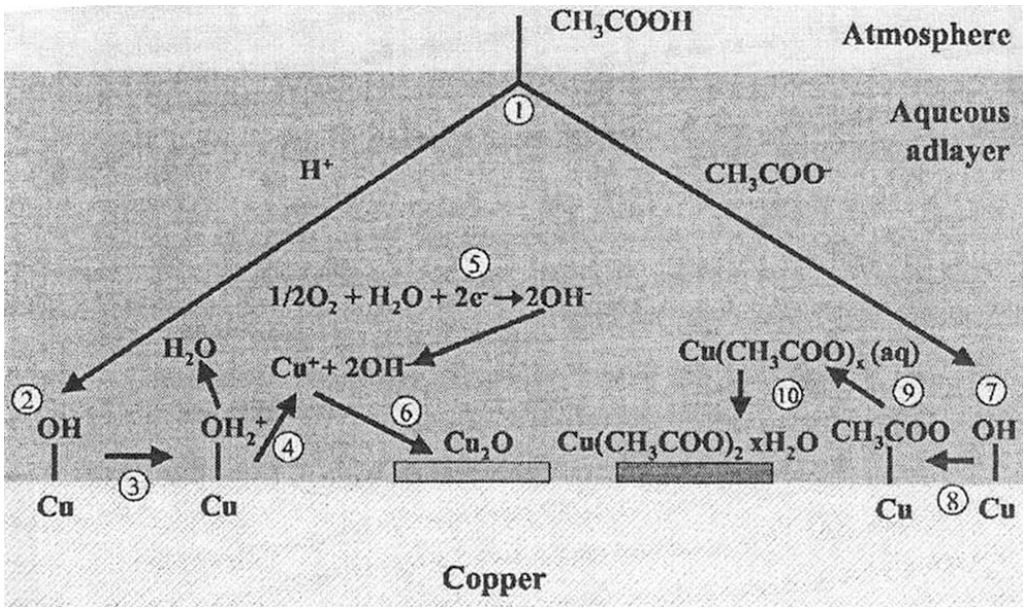

Figure 5.1 Schematic description of two possible reactions for atmospheric corrosion of copper by acetic acid (Gil and Leygraf 2007b, Fig. 10, C616)

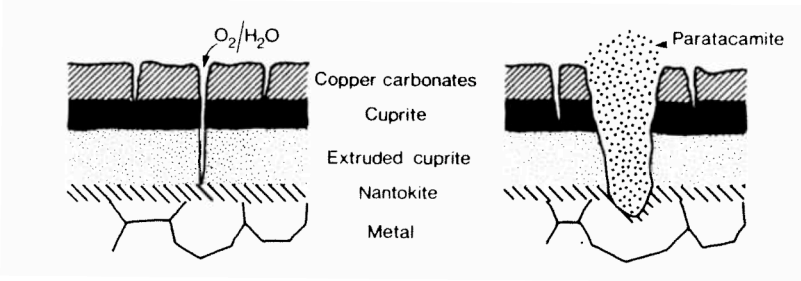

Figure 5.2 Development of bronze disease (Cronyn 1990, 227)

On copper and copper tin the carbonyl corrosion reaction occurs on the surface. However, in the case of binary phase leaded bronze, reaction of acidic vapour with the separate lead phase in the alloy (Figure 5.3) follows the configuration of the lead globules that are immiscible in the alloy causing damage below the surface (Figure 5.4).

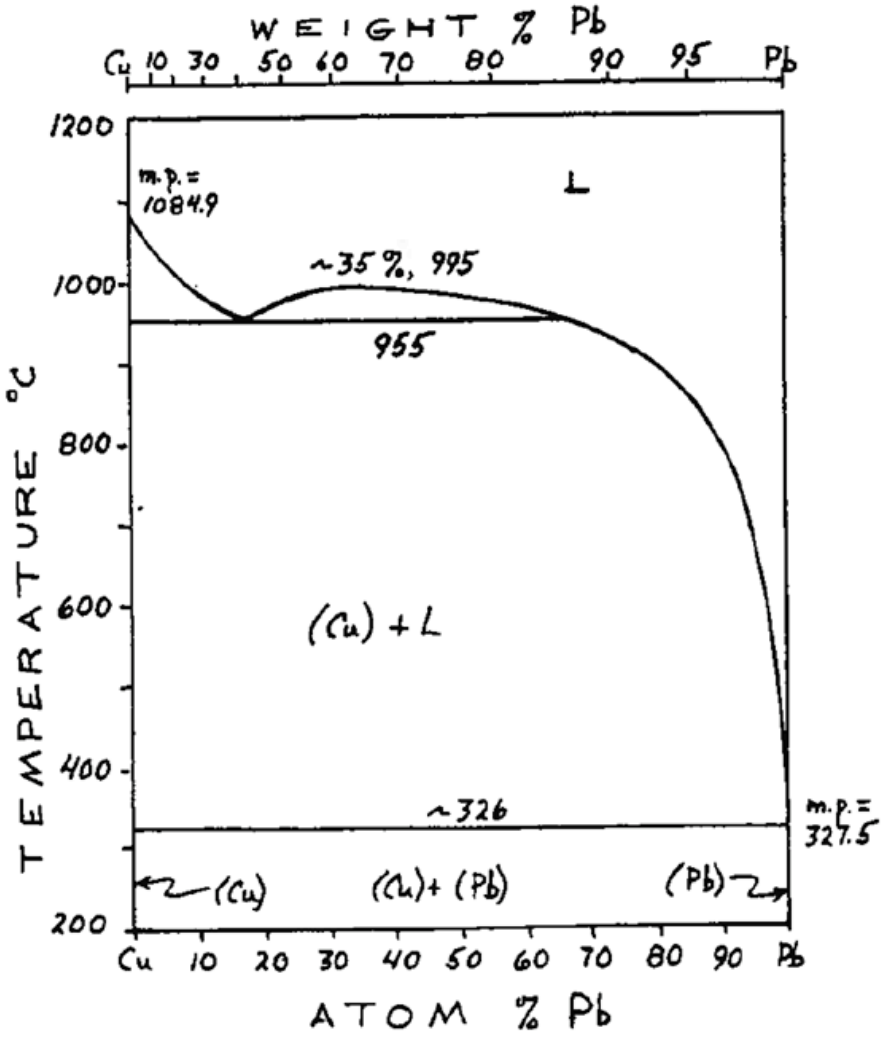

Figure 5.3 Cu-Pb phase diagram (Moffatt 1984)

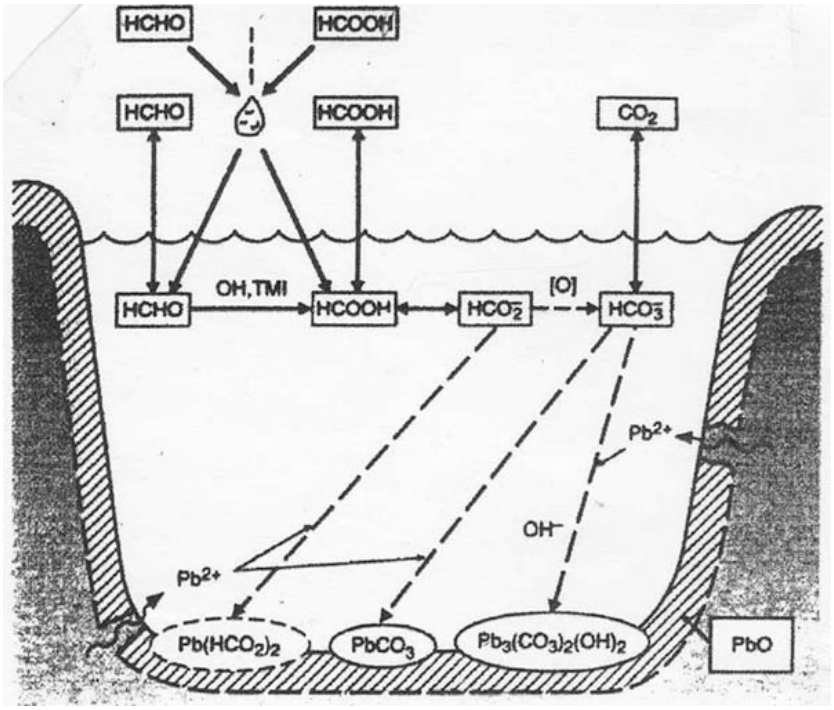

Figure 5.4 Illustration showing pitting corrosion in an aqueous film on lead. Atmospheric corrosion of lead by organic acid (formic acid and formaldehyde are represented here). Dashed ovals indicate constituents that have not been confirmed by laboratory or field studies. Dashed arrows indicate solvation or reaction processes that have not been confirmed by laboratory or field studies. TMI refers to transition metal ions (Graedel 1994, Fig. 5, 92)

Regarding the susceptibility of copper and lead to corrosion by acetic and formic acid (expressed in g of corrosion/dm^2 of metal surface), pure copper corroded slightly more in formic acid vapour than in acetic acid vapour whereas lead corroded much more in acetic acid than in formic acid (results for tin were similar) (Donovan and Stringer 1971, 135) (Table 5.1).

Table 5.1 Corrosion of Metals by Acetic and Formic Acid at 30° C and 100% RH for 3 weeks expressed as g/dm^2

Corrosion of metals by acetic and formic acid at 30° C and 100% RH for 3 weeks expressed as g/dm^2						
	Acetic acid vapour			Formic acid vapour		
	0.5 ppm	5 ppm	50 ppm	0.5 ppm	5 ppm	50 ppm
Cu 99.99%	0.02	0.18	0.60	0.15	0.19	0.71
Pb 99.90%	1.06	1.57	3.10	0.14	0.65	0.35
Sn 99.90%	< 0.001	< 0.001	0.02	< 0.001	< 0.001	< 0.001

* from Donovan and Stringer 1971, Table II, p. 135

Carbonyl compounds such as formic acid, when added to acetic acid, were found to increase the corrosion rate and decrease the corrosion resistance of lead (Tetreault *et al.* 1998, 26).

Hygroscopic salt residues can modify the local moisture content facilitating attack by acetic acid. Objects have been found to be more vulnerable to attack by acetic acid as a result of treatment with sodium compounds (Tennent *et al.* 1992, 875). High RH exacerbates the problem by promoting cycles of deliquescence and efflorescence (e.g. on mollusca) (Tennent *et al.* 1992, 875).

In combating the corrosive attack by acetic and formic acid, "desiccation … is frequently used successfully, although it should be remembered that the corrosive acids may be absorbed on susceptible surfaces and may cause rapid corrosion on subsequent exposure at high humidities – even after items are removed from the spaces where the vapours were generated." (Donovan and Stringer 1971, 138).

5.1.3 Saqqara Bronzes

In 2006 I examined the bronze collection of the Petrie Museum of Egyptian Archaeology, UCL, London. The online catalogue (http://www.petrie.ucl.ac.uk/index2.html) and Petrie Conservation Manager Susi Pancaldo's observations (S. Pancaldo pers comm. 2007) were used to select corroded bronzes in the collection for analysis. After analysis of several blue and blue/green corrosion samples I found that most of the objects analysed were from Saqqara (Figure 5.5). Copper sodium formate acetate was found on five objects, sodium formate was found on one object, and chalconatronite was found on two objects (one in association with copper sodium formate acetate) (Appendix 16). Since the majority of the objects were identified with carbonyl corrosion I focused further on the Saqqara bronzes in the subsequent museum collections I visited to collect corrosion samples for analysis: Fitzwilliam Museum, Ashmolean Museum, Liverpool Museum, British Museum. All of the Saqqara bronzes I sampled had been excavated between 1964 and 1976 (Appendix 15, Figure 5.6, Figure 5.7). As an approach this project was the first to use objects from a single Egyptian site collected from various museums. Bronzes from the same context had been sent to different museums in the UK.

The Sacred Animal Necropolis in North Saqqara was excavated by the Egypt Exploration Society between 1964 and 1976. The site dates from c. 2680 BC (early 3rd dynasty) to shortly before the Persian conquest in 525 BC. The objects recovered included wooden shrines, bronze statues in wooden shrines, metal standing altars, offering stands, incense stands, ritual objects, metal vessels, votive objects and sculpture. The objects of interest in the current work are published in *The Temple Furniture from the Sacred Animal Necropolis at North Saqqara 1964-1976*, C.I. Green, 1987, and *The Sculpture from the Sacred Animal Necropolis at North Saqqara 1964-1976,* E. A. Hastings, 1997. Many pieces, previously thought to belong to the Late Period (715 – 332 BC), are now thought to be much older, i.e. from the New Kingdom period (1539-1075 BC) or the late New Kingdom/Libyan Period (1196 – 1075/1075 – 715 BC (3rd Intermediate Period) (Hastings 1997, xxxiv). A few wooden shrines were found in Saqqara with wooden and bronze statues inside (H5-602, H6-412, and H5-1022) (Green 1987, 5-7). These storage conditions represented centuries of exposure of the bronze to acetic acid emissions from the wooden shrines. The type of wood used in the construction of the shrines is not specified. There are a number of small bronze figurines from Saqqara that preserve their original wood base. The peak period for small votive bronzes at Saqqara was the Late Period, 715 BC to 332 BC. The small votive objects on wooden bases were probably not enclosed in wooden shrines (H.Whitehouse pers comm. 2007).

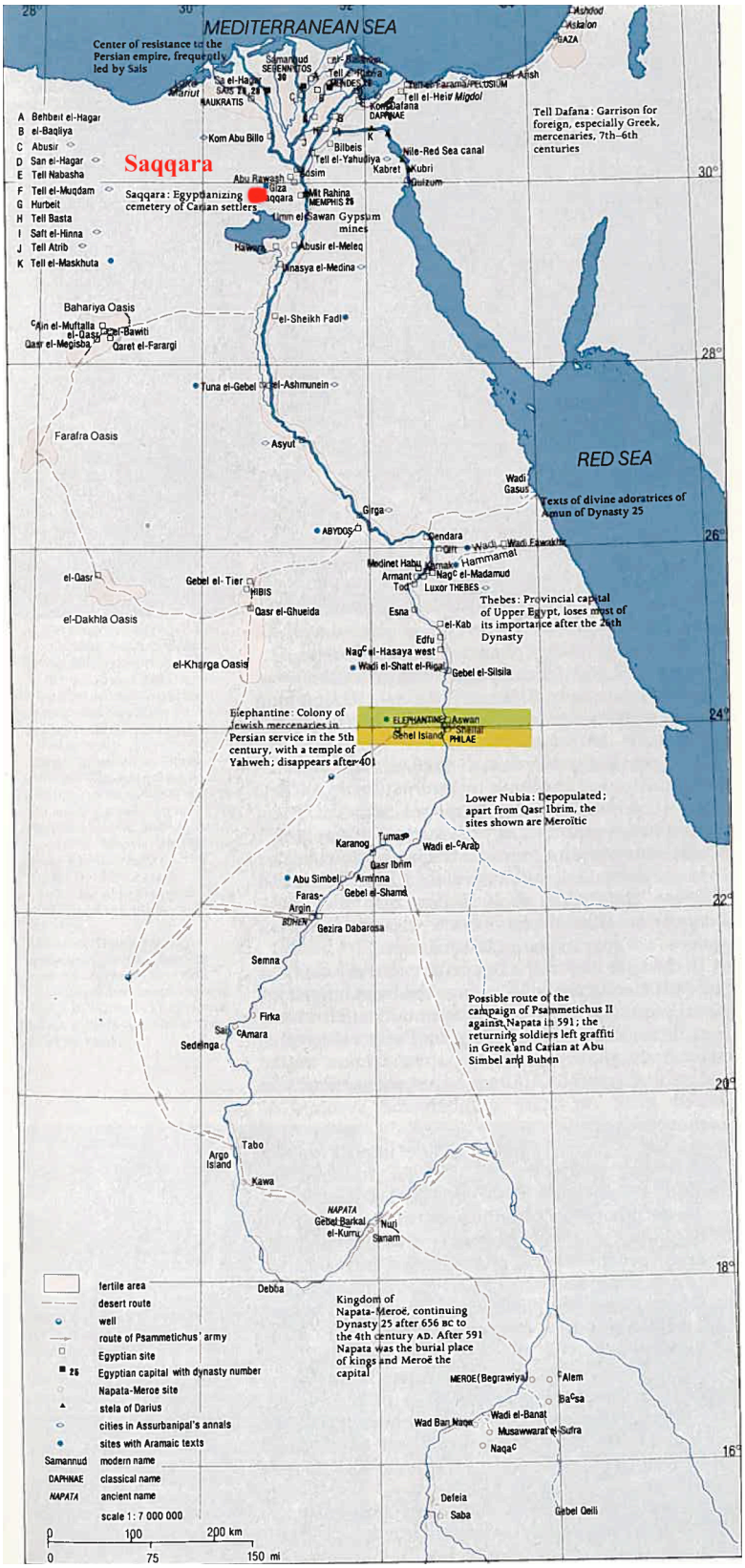

Figure 5.5 Egypt in the Late Period (712 BC – 4th c AD) (Baines and Málek 1989, 49)

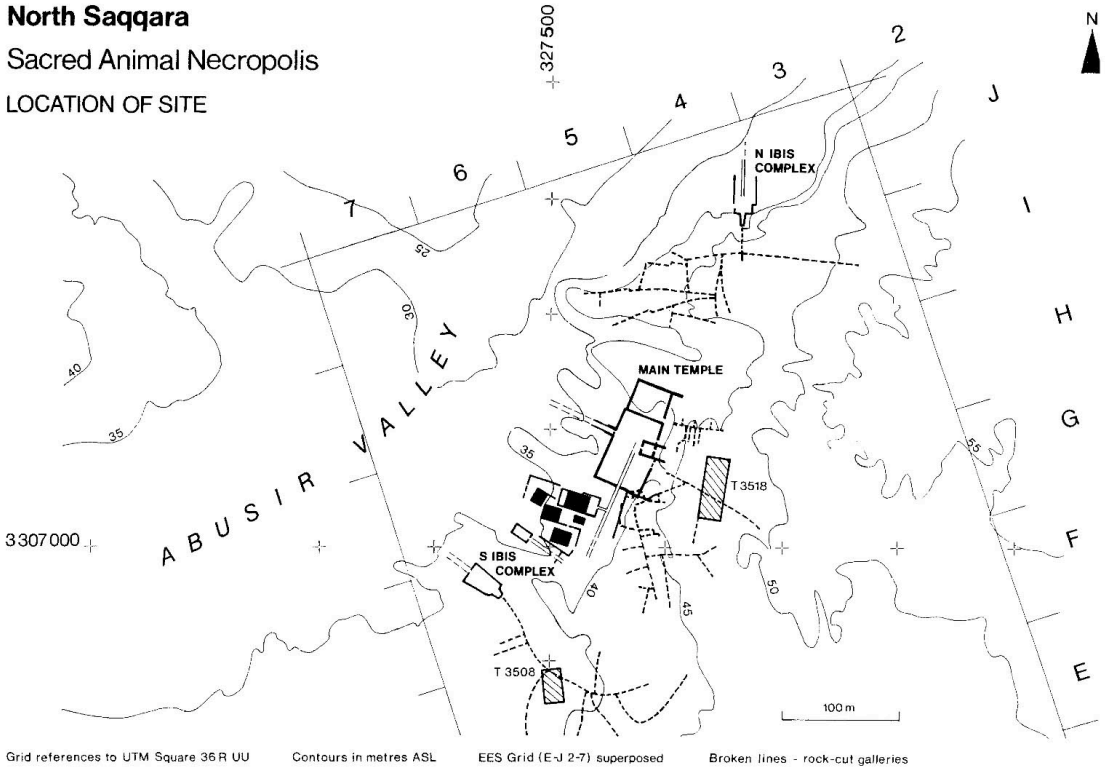

Figure 5.6 The main temple in North Saqqara in quadrant H5 (C.I. Green 1987, iv, courtesy of the Egypt Exploration Society)

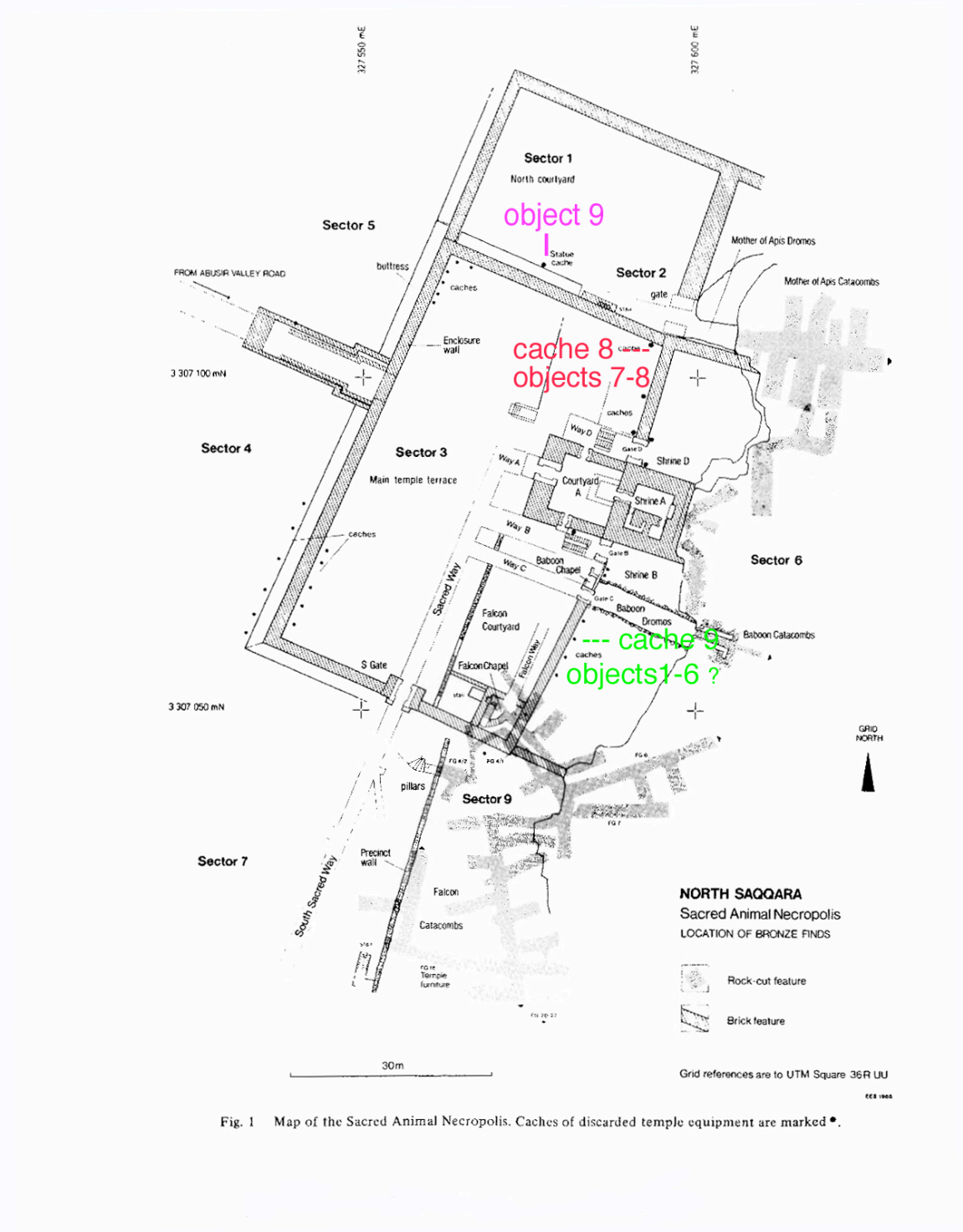

Fig. 1 Map of the Sacred Animal Necropolis. Caches of discarded temple equipment are marked •.

Figure 5.7 Main Temple in North Saqqara showing location of finds (C.I. Green 1987, xiv, courtesy of the Egypt Exploration Society) (color coding refers to Appendix 15)

An unidentified blue corrosion was found on many of these bronzes. Chalconatronite is a strong candidate since it is partially soluble in water and is found on objects buried in Egypt (Frondel and Gettens 1955), followed by acetate or formate compounds on those objects initially enclosed in wooden shrines. Carbonyl compounds that are at least partially soluble in water include copper (I) acetate, copper (II) acetate

monohydrate, copper (II) basic acetate, and probably the hygroscopic copper (II) acetate (Appendix 7.2). Objects not exposed to the volatile organic vapours of wood or other sources of acetic and formic acid before or during burial would not have formed acetate or formate corrosion. Unfortunately, the blue corrosion found on bronzes during the 1995 Saqqara excavation was not identified (Nicholson and Smith 1996). The determination of acetates or formates on the freshly excavated bronzes would indicate exposure before or during burial to wood or other sources of acetic and formic acid and the recovery of water-soluble compounds would indicate a desiccated burial environment. There is no evidence, however, that the bronzes from either excavation campaign were originally encased in wooden shrines. To date no identifications of acetate or formate on recently excavated bronze (that has not undergone conservation treatment or storage in wood) are known.

5.2 History of Conservation Treatments producing New Corrosion Products

The objects that underwent corrosion analysis in this study were excavated from Saqqara between 1964 and 1976 and other locations dating back to the 19th century. The excavation dates in the Main Temple at Saqqara range from 1964 to 1976 and site locations consist of 4 areas and a fifth category of unlisted (Figure 5.7) (Appendix 15): 1) Sector 3 Falcon Gallery 16, Cache 9 (Objects 1-6); 2) Sector 3 Northeast Corner, Cache 8 (Objects 7-8); 3) Sector 1 North Courtyard, pit, south wall (Object 9); 4) H5 Quadrant redim (Objects 10-11); and 5) unlisted (Objects 12-22). It should be noted that these locations within sectors are based on the excavation report (Green 1987). Objects in categories 4 and 5 are without archaeological context from the Main Temple area in quadrant H5 (Figure 5.6, Figure 5.7).

A review of the conservation treatments carried out during this time span at the various museums that acquired the bronzes may assist in the interpretation of their current condition and distinguish between acetate/formates and chalconatronite formed during use and burial and the growth of these minerals following excavation as secondary corrosion. The conservators who worked at Saqqara are Panagiota Manti, Jennifer Gosling, Siobhan Stevenson, Walter Gneisinger, and Abd el-Aziz Sayed Abd el-Rasheed Soltan. Conservators in the UK who worked on the Saqqara bronzes include Celestine Enderly, Paul Crabtree, Orma Cohen, and Fleur Shearman at the British

Museum. The treatment records for the Petrie Museum bronzes in this study are anonymous.

5.2.1 Saqqara

Conservation treatments on the objects from two excavation campaigns at Saqqara are reported, the 1964-1976 and the 1995 campaigns.

5.2.1.1 1964-1976 Excavation Campaign - Conservation Treatment

Objects from the 1964-1976 campaign are those under investigation in this study. One of the archaeologists involved with Saqqara, Jeffrey Spencer, Keeper of Egyptian Antiquities, British Museum, reported in an email: "On the excavation at Saqqara in the 1960s it was routine to try to strip the corrosion products from bronzes- at least, the more solid ones - by the use of alkaline Rochelle salt. This may have generated a fair selection of additional chemicals!" (J. Spencer pers comm. 29th October, 2007).

Alkaline Rochelle salt for stripping archaeological bronzes is made by dissolving "1 oz. (28.4 grams) of commercial flake caustic soda in a pint (0.568 litre) of cold water, and dissolve 3 oz. (85.2 g) of Rochelle salt (sodium potassium tartrate) is this solution." (Plenderleith 1956, 239; Stambolov 1985, 103). Rochelle salt is potassium sodium tartrate ($KNaC_4H_4O_6 .4H_2O$), a white powder used in medicine as a mild laxative, as a food preservative, and in electronics. Tartrate is a salt or ester of tartaric acid ($(CHOH)_2(COOH)_2$). Tartaric acid is a white crystalline organic acid obtained from tartar in wine vats and used in the food industry. This alkaline solution of Rochelle salt transforms the cupric salts (malachite) and the resulting cuprous salts (cuprite) can be removed with a 10% solution of sulphuric acid (Plenderleith 1956, 239, 240). It is probable that many of the Saqqara bronzes that appear to have been chemically cleaned underwent the alkaline Rochelle salt treatment. It is not known if sulphuric acid was used on the Saqqara bronzes. Completely stripped bronze has a copper colored metallic surface unless repatinated. Alkaline Rochelle salt was first recommended for the cleaning of archaeological bronze in the 1930s (Lucas 1932). Zinc and sodium hyrdroxide electrochemical treatment has also been used for stripping bronzes (Plenderleith 1956). Very few conservation treatment records exist for these Saqqara bronzes, all extant records are included in Appendices 13.1-13.5.

5.2.1.2 1 1995 Excavation Campaign - Conservation treatment 1996 – 2007

Although these Saqqara objects post-date those analysed in this study (from the 1964-1976 campaign), their conservation treatments are based on a few standard treatments that have been used for decades and most likely mirror treatments adopted for the Saqqara bronzes of 1964 to 1976 in the museums in the UK.

A second point of consideration is the fact that the conservation treatment reports include observations offering clues to the identification of the blue corrosion found on freshly excavated material in 1995. Articles regarding a cache of bronze situlae found in Saqqara in 1995 describe the presence of corrosion as blue to blue/green, powdery turquoise-blue, powdery light blue, and highly hygroscopic (Nicholson and Smith 1996; Nicholson 2006). The solubility of this corrosion in water during conservation treatments aids in narrowing down the possible candidates in the identification of the compound(s) (Appendix 7.2).

Major bronze discoveries at Saqqara will be presented from the 1995 excavation campaign. These objects are relevant to this study because they derive from the same excavation as the 1964 to 1976 bronzes and present the advantage of freshly-excavated corrosion prior to alteration by conservation treatment. During the 1995 season a cache of bronzes, mostly situlae (metal vessels shaped like a bucket or vase), were found concreted together by bronze corrosion products of a blue/green color (Nicholson and Smith 1996). There are approximately 560 objects in this cache found at the Sacred Animal Necropolis dating to the 4th to 3rd century BC (Nicholson and Smith 1996). They were found at the top of the entrance steps to the Hawk Catacomb in North Saqqara. There were also figures of Osiris, Isis, Horus, Anubis and the Apis bull along with miniature offering tables. Conservation work began in 1996. Most of the objects were heavily leaded cast bronze situlae and some heavily leaded cast bronze small statues (Gosling *et al.* 2004, 5). “Details of the surface decoration on the copper alloy objects was obscured by thick compact layers of powdery light blue corrosion and totally disfigured by dense, voluminous pustules of hard green corrosion product, most like copper carbonates (malachite and azurite).”(Gosling *et al.* 2004, 5) (Figure 5.8, Figure 5.10). Surface detail was preserved at the interface of red cuprite and the voluminous

carbonate corrosion or at the interface of a thin black copper oxide layer and light-blue corrosion product (Figure 5.9) (Gosling *et al.* 2004, 5). In the cache of 1995 were found wood fragments, small wooden carvings, and a larger woodcarving containing a metal (?) inlay that may have been from shrines (Gosling *et al.* 2004, 7).

The cache of objects was separated, cleaned and treated with corrosion inhibitor BTA and lacquered with Incralac®. All pieces were packed in acid-free tissue paper and placed inside perforated self-seal bags within airtight plastic boxes with silica gel (Nicholson 2006, 20).

Conservation on this cache did not recommence until 2003, after the construction of a new storage magazine in Saqqara in 2003. They were stored in the antiquities magazine of the Supreme Council for Antiquities (SCA) in Saqqara. Separation and cleaning were carried out in 1996. At the time the blue corrosion product was thought to be azurite and was removed by soaking the object overnight (not specified in what) and then removed (not specified how) (Nicholson 2004, 8).

Figure 5.8 Saqqara situla acc. No. 132, with voluminous hard green corrosion. The field of view is approximately 5 cm across (Manti and Gosling 2007, courtesy of the Egypt Exploration Society)

Figure 5.9 Detail of another Saqqara situla (acc. no. not available) with red/purple corrosion layer. The field of view is approximately 3 cm across (Manti and Gosling 2007, courtesy of the Egypt Exploration Society)

Figure 5.10 Detail of a third Saqqara situla (acc. no. not available) with powdery light blue corrosion, field of view is approximately 3 cm across (Manti and Gosling 2007, courtesy of the Egypt Exploration Society)

The description of the blue corrosion as azurite is most likely incorrect as azurite is insoluble in water (Appendix 7.2). The most likely candidate for the blue corrosion is chalconatronite, sodium copper carbonate hydrate, a compound that is partially soluble in water and is found on objects buried in Egypt (Appendix 7.2). The green corrosion was hard and did not soften by soaking. Most of the objects belong to the 4th c. BC. The bronzes (at least the figures) may have been buried in a wooden shrine that has not survived (Nicholson 2004, 9). If this is the case, if indeed the bronzes were enclosed in

(unspecified) wood for many years, acetic acid and formic acid volatiles from the wooden shrines could have reacted with the bronze producing any number of compounds containing acetate and formate. Some of these compounds that are soluble in water to varying degrees are copper (I) acetate, copper (II) acetate monohydrate, copper (II) basic acetate, and probably the hygroscopic copper (II) acetate. In the consideration of the possibility of copper acetates and formates resulting from encasement in wood shrines, the following variables may account for their displacement from the wooden shrines: 1) disintegration of the wood subject to burial conditions, 2) earthquake or other natural disasters, 3) man's intervention (looting, relocation). The preservation of the acetate and formate compounds and their resistance to conversion during burial depends on their solubility, acidity and alkalinity of the soil, and other burial conditions.

Work on the bronzes continued in 2004 (Nicholson 2005). The registered objects were given a Plastazote™ (polyethylene) packing. Conservation work comprised cleaning, stabilization and lacquering (Nicholson 2005, 13). A wrought copper alloy object with active corrosion was treated with benzotriazole (Nicholson 2005, 14). Identification of the corrosion products was not carried out. The objects were packed in acid free tissue and placed in polyethylene boxes with silica gel. Some of the more important objects may be put on display in the new Saqqara museum. Most of the collection consisted of heavily leaded, cast copper alloy situlae. The cache discovered also included some cast copper alloy figures, fragments of rope and wooden objects, faience amulets and small stone and plaster artifacts. Surface dirt and "powdery turquoise-blue corrosion product" were softened by immersion of the objects in tap water for a minimum of one hour (Nicholson 2005, 14). After immersion these layers were removed by brushing using soft and firm toothbrushes. Malachite was removed with various mechanical means such as glass bristle brushes, scalpel, and vibrotool. The objects were dried by immersion in acetone baths and then placed in a 3% w/v solution of benzotriazole in ethanol (duration not specified). Detached fragments were adhered with Araldite 5-minute epoxy resin. All treated objects were lacquered with 5% Incralac® (acrylic copolymer in toluene with 0.5% w/v benzotriazole) with the addition of Santocel™ matting agent. Registered objects were packed in carved polyethylene Plastazote™ foam while the other objects were packed in acid free tissue paper inside polyethylene Stewart™ boxes including silica gel (self-indicating and non-self-indicating) (Nicholson 2005, 14).

Joins of fragmentary objects were sought. Some of the copper alloys objects were offering tables made from hammered sheets (Nicholson 2006, 20). Voluminous corrosion and pustules obscured decorative details on the cast objects, including a heavily leaded, cast copper alloy offering table (Nicholson 2006, 20). On the basis of Nicholson's report, conservation treatment appears to mirror that of 2004 regarding removal of the blue corrosion, adhering detached fragments, and the application of a corrosion inhibitor. Temporary reassembly of some sheet (i.e. wrought) copper-alloy offering tables and situlae was carried out with Loctite™ (cyanoacrylate adhesive).

Blue corrosion was described as "…powdery light blue corrosion product, with cracks. Note the corrosion follows the decoration pattern. This product is highly hygroscopic." (Manti and Gosling 2007). The determination of hygroscopicity is presumably based on the water solubility of this corrosion product. Some of the decoration (relief) was cast and some was incised (hieroglyphs). Detail was preserved at the interface of a very thin black corrosion layer and the light blue corrosion product. The blue corrosion is described as a thick layer (Manti and Gosling 2007). In some cases dilute formic acid and 2Na-Ethylene Diamine Tetraacetic Acid (EDTA) were applied to soften the hard green corrosion to facilitate its mechanical removal. The presence of lead in the corrosion product was determined with Plumbtesmo spot test papers (Manti and Gosling 2007).

Further identification of the blue corrosion on the situlae and figures cannot be made without technical analysis including XRD. Unfortunately none of the blue corrosion from the 1995 cache was analysed nor was it sampled for analysis prior to conservation treatment (Gosling *et al.* 2004, 5; P. Manti pers comm. 2007).

5.2.2 Petrie Museum

My attention was drawn to blue corrosion on several Egyptian bronzes at the Petrie Museum by Susi Pancaldo of the Petrie Museum in 2005 (Petrie Museum 2009). My survey, conducted with the aid of the museum's online catalogue and in person, determined that the majority of bronzes with blue corrosion derived from the Saqqara excavations in Egypt, (i.e. 6 objects of 7, Appendix 13.1). From museum records, three sources of acetate (PVA, acetic acid, and EDTA) and one source of formate (formic

acid) have been mentioned in the conservation materials used in the Petrie Museum over the years.

Jaeschke and Jaeschke state that objects were stabilized at the Petrie Museum by immersion in sodium sesquicarbonate in the 1950s and 1960s (Jaeschke and Jaeschke 1988, 18). This often produced deposits of pale green corrosion products and sometimes redeposited metal. The pale green deposits were removed mechanically or after softening with a dilute solution of formic acid. Benzotriazole (BTA) in Industrial Methylated Spirits (IMS) or distilled water was used, sometimes it was brushed on and the object not coated subsequently. Usually the objects were coated with Ercalene™ (nitrocellulose lacquer), however, after treatment with BTA, starting in the late 1960s.

In the early 1960s copper alloy objects were soaked in Calgon™ solution (sodium hexametaphosphate), then boiled in alkaline Rochelle salt, then boiled in dilute sulphuric acid and finally returned to the Calgon™ solution. Immersion in Calgon™ and boiling in 10% sulphuric acid were often used as pretreatments to electrolysis. There are no detailed notes on the electrolysis process at the Petrie Museum although we know that both and acidic and alkaline electrolytes were used. After stripping electrolytically the object was washed in several changes of hot water and dried in an oven or under an infrared lamp. Sometimes after immersion in alkaline Rochelle salt it was determined that it was not safe to proceed with the acid treatment so the object was "stabilized" with sodium sesquicarbonate. Sometimes the object from the alkaline Rochelle salt bath was immersed sequentially into a 15% solution of sulphuric acid and then a 15% solution sodium carbonate (Jaeschke and Jaeschke 1988, 19).

In the 1950s bronzes were treated by immersion in Fehling's solution (copper sulphate with alkaline Rochelle salt) followed by sulphuric acid and electrolysis (Jaeschke and Jaeschke 1988, 19). Redeposited copper was removed mechanically after treatment with sulphuric acid or electrolysis. Sometimes a 20% citric acid solution was used to soften the corrosion prior to immersion in the Fehling's solution (Jaeschke and Jaeschke 1988, 19). Metaquest A (an ethylene diamine tetra-acetic acid (EDTA)-based chelating agent) was used on an object with a lead core to remove corrosion. EDTA can be a source producing acetate reactions. Cathodic reduction of the lead was carried out to reduce the corrosion products that had caused the statue to split, probably with an

alkaline electrolyte since the statue was subsequently washed in sulphuric acid, then washed in water. No date is given for this treatment.

Ercalene™ (cellulose lacquer) was frequently used as a protective coating. PVA (polyvinyl acetate) was as used as a coating and consolidant. PVA is another possible source of acetate. Wax (unspecified) was also used as a consolidant. Incralac® replaced Ercalene in the 1970s for those objects treated with BTA. Adhesives used included epoxy resins, waxes, HMG (cellulose nitrate), Paraloid B48 in acetone (in chronological order from oldest to most recent) (Jaeschke and Jaeschke 1988, 19).

5.2.3 Ashmolean Museum

Of the conservation materials mentioned by Norman that may have been used at the Ashmolean Museum, vinegar stands out as a probable source of acetate (Norman 1988, 13). Chemical stripping was common practice in the early years using all methods available, electrolysis, electrochemical, chelating and sequestering agents, and acid stripping using mineral and organic agents. Chemical stripping was carried out for decades before the 1950s. Inlays and intentional surface treatment were sometimes lost during chemical stripping (Norman 1988, 13). Petrie recommended that bronzes be stripped by immersion in vinegar, a source of acetate (Petrie 1904). Fink and Eldridge's (1925) electrolytic method and Scott's (1926) electrochemical method (zinc and caustic soda) were used (Fink and Eldridge 1925; Scott 1926). It is known that one object in the Ashmolean was polished after stripping. These objects were never lacquered and one leaded bronze object today has a grey/white deposit covering much of the surface that is presumed to be the reaction of lead in the alloy with the display materials (Norman 1988, 14).

Although conservation treatment reports were first kept in 1957 in the Ashmolean Museum, predating the Saqqara bronzes from the Sacred Animal Necropolis (excavated from 1964 to 1976), many of the Saqqara bronzes in the Ashmolean do not have treatment reports. Perhaps this can be explained in part by the fact that many of the Saqqara bronzes were chemically treated with alkaline Rochelle salt in the field shortly after their excavation (J. Spencer pers comm. 2007) and required no further treatment for legibility after their arrival at the museum.

Radio-isotope (gamma-ray) fluorescence analysis using a solid state X-ray detector and multichannel analyser (XRF) of alloy composition was carried out by Dr. H. McKerrell in the Ashmolean Museum in 1971 on bronzes from this and other collections. The results must be regarded as qualitative and are not available for many objects in the current project (H. Whitehouse pers comm. 2007).

5.2.4 British Museum

The conservation materials and methods used over the years at the British Museum parallel those in the Petrie Museum and Ashmolean Museum. Five unregistered bronzes from Saqqara that were sampled for analysis are stored in the same wooden drawer to this day. Referring to these objects, Jeffrey Spencer states that "The group of objects in the wooden tray, however, I think were left untreated as being too fragmentary or ordinary to merit any cleaning, so they are as they came out of the ground plus any corrosion they have acquired in storage." (J. Spencer pers comm. 2007).

According to metals conservator Fleur Shearman at the British Museum, most Egyptian bronzes used to be stored in mahogany (F. Shearman pers comm. 2007). They were moved from wood to metals storeroom M4 in ca. 1997 that also housed large organics, e.g. mummies. Storeroom M4 is climate controlled but the climate control is said to have malfunctioned in the past. The RH level in M4 is reported to have been set at a suitable level for desiccated wood (F. Shearman pers comm. 2007). All the metals were subsequently moved into metal storage cabinets in the current metals storeroom in 2004 or 2005 that is not climate controlled.

Acetic acid concentration in the wooden cases housing the Egyptian bronzes was measured in the late 1990s and found to range from 439 ppb to 1181 ppb (0.4 ppm – 1.12 ppm) (Thickett 1998) (Chapter 2, Table 2.2).

5.2.5 Fitzwilliam Museum

Unfortunately no conservation treatment records exist for the objects analysed from the Fitzwilliam Museum. The sources of acetates in the Fitzwilliam Museum over the years include acetic acid if it was used for cleaning as promoted by Rathgen and wood shavings in which to store the objects during World War II. According to J.

Dawson, the book entitled *The Preservation of Antiquities* by Rathgen has been consulted by conservators at the Fitzwilliam Museum since its publication in 1905 (J. Dawson pers comm. 2006). One chemical method using a sodium compound promoted by Rathgen was Krefting's method for copper alloys, an electrochemical reduction using a 5 % solution sodium hydroxide and sheet zinc (Rathgen 1905, 139). Some hydrochloric acid (chlorine comes from the bronze corrosion) produced in the process of reduction acts on the sodium hydroxide to form sodium chloride (Rathgen 1905, 139). Rathgen also mentioned the cleaning of corroded bronze by immersion in concentrated acetic acid that is neutralized after washing with a dilute solution of soda or ammonia (Rathgen 1905, 121). In the 1920s and 1930s sodium sesquicarbonate was used to treat bronzes in the museum, until World War II (J. Dawson pers comm. 2006). Some objects were sent to the Ashmolean Museum where they were stripped (probably with zinc granules and sodium hydroxide) and lacquered (Dawson 1988, 72).

Over 500 bronze objects from Cyprus, Greece and Egypt in the Fitzwilliam Museum, Cambridge, reportedly developed corrosion caused by storage in wood shavings during the Second World War. U.R. Evans attributed this corrosion to acetic acid from the wood shavings, although he referred to the corrosion as "bronze disease", copper chloride hydroxide (Evans 1951, 706, 711; Evans 1961, 492, 493) The cases were upacked in 1946 at the end of WWII and a number of actively corroding bronzes were listed in 1948. Evans suspected the acidic content of the wood shavings and high humidity had triggered the corrosion epidemic and as a result recommended including soda lime to absorb acid from the atmosphere and silica gel to reduce relative humidity in the museum display cases (Dawson 1988, 75). Conservation treatment was carried out on the objects in question by Mr.Rayner using an electrolytic technique based on a combination of techniques developed by Colin Fink and Harold Plenderleith. This technique involved attaching the positive terminal of a milliammeter to bare metal on the object, a nib of sheet zinc was attached to the negative terminal, the zinc was dipped in dilute hydrochloric acid and touched to the diseased spot while running an electrical circuit. The hydrochloric acid dissolved the corrosion followed by blotting off the excess acid and corrosion. The procedure was repeated with phosphoric acid to create an insoluble, stable compound. Finally, the area was neutralized with sodium carbonate leaving a grey spot. This procedure met with a good deal of success, only a few objects are reported to have required re-treatment. While a few of these objects can be identified today by the telltale signs of the electrolytic stabilization spot treatment, unfortunately a

comprehensive list of those attacked by wood shavings and subsequently treated with this method does not exist. One object was singled out in the 1951 publication as being particularly resistant to treatment, a Roman 1st c. AD "Genius". There are scant conservation treatment records for specific objects, the Roman Genius is an exception. The other objects were reported to have remained stable 6 years later (J. Dawson pers comm. 1988).

Upon my visit to the Fitzwilliam Museum in October 2006 and after inspection of the artifacts I did not find any clear correlation between objects with the telltale signs (grey spots) of the localized electrochemical treatment from the 1950s and blue or blue-green corrosion typical of acetates and formates. Since this time no further investigation or research of these artifacts or of this phenomenon has been carried out at the Fitzwilliam.

All bronzes were stored in wooden cupboards until 1990 when a new storage area was constructed with steel Dexion racking and a controlled low relative humidity of approximately 35%. In 2003 metal storage cupboards were installed.

5.2.6 Liverpool Museum

On Sept. 28, 2007 I visited the bronze collection in the Liverpool Museum storehouse. I examined and photographed all objects mentioned by Lang in her MA dissertation entitled *The Corrosion of Metal Antiquities by Pollutants from Wooden Storage Materials: A Case Study* at N.M.G.M, except for Inv. No. 49.8.23 (figure with raised arms) that was not accessible (locked in a vault) (Lang 1995). The date of acquisition by the museum is indicated by the first set of digits in the inventory number, e.g. 1956 for object 56.22.215 and 1973 for object 1973.2.548.

Most of these objects had been stored in card trays in plywood and hardboard boxes from the time of their acquisition by the Liverpool museum (Lang 1995). They were still stored in these materials at the time of Rebecca Lang's examination of the collection in 1994. Since then they have been removed from the wooden boxes and stored on open metal shelves in a "dry" metals storeroom. The relative humidity of the "dry" metals store was reported to be 48% on Sept. 28, 2007.

Acetic acid concentration in the wooden cases housing the Egyptian bronzes was measured in the 1990s and found to range from 600 to 700 ppb (0.6 ppm – 0.7 ppm) (Lang 1995) (Chapter 2, Table 2.2). Formic acid was found to range from 150 to 220 ppb (0.1 to 0.2 ppm) (Lang 1995) (Chapter 2, Table 2.3).

5.2.7 Ancient Athenian Agora

Conservation treatment records were not kept prior to 1979 in the Agora. Several chemical cleaning and stabilization compounds containing sodium are known to have been used over the years: the cleaning agents Calgon (sodium hexametaphosphate/sodium polyphosphate), zinc and sodium hydroxide, alkaline Rochelle salt (5% sodium hydroxide and 15% sodium potassium tartrate), alkaline glycerol (15% sodium hydroxide and 40% glycerin in water); and the stabilization compounds sodium sesquicarbonate and sodium carbonate (Paterakis 2003). There are no conservation treatment records for any of the objects analysed in this study.

Acetic acid concentration in the wooden cases housing the bronzes was measured in the 1990s and found to range from 426 ppb to 519 ppb (0.4 ppm to 0.5 ppm) (Paterakis 2003) (Chapter 2, Table 2.2).

5.3 Identification of Corrosion

Corrosion was examined and analysed with SEM-EDS and XRD. SEM-EDS provided elemental analysis whereas XRD provided the identification of compounds.

5.3.1 Sampling and Analytical Techniques

The analytical technique of SEM-EDS was applied to two samples from the Athenian Agora whereas XRD was applied to all samples.

5.3.1.1 SEM-EDS

A Scanning Electron Microscope with Energy Dispersive Spectroscopy was used for examination and elemental analysis of two corrosion samples (samples Agora 1 and Agora 3a) from Agora bronze ring ΣT (Appendix 13.6). The samples had been prepared

for XRD analysis by grinding in a mortar with pestle. Examination and analysis was carried out under the following conditions: 0.8-1 Torr, 20°-22°, RH <20%, KV 3.0-10.00, by operator David Carson at the Getty Conservation Institute in 2004.

5.3.1.2 XRD

The corrosion samples were removed with a scalpel, ground in a mortar with pestle, then analysed by XRD. The samples were run on a Bruker D8 Discover GADDS (General Area X-ray Diffraction System) instrument using a Kristalloflex 760 X-ray generator K760-A21 at the Getty Conservation Institute (Bruker 1998, Bhuvanesh undated). The spectra were collected from 3° to 80° 2Θ. Radiation was from a copper source, generator settings 40 mA, 45kV. The software program used to identify compounds was Bruker Advanced X-rays Solutions. Inc. DiffracPlus, Release 2004, EVA Version 10.0, revision 1. "The GADDS instrument allows investigation of small specimen quantities ... . Applications for this instrument include rapid phase analysis, small angle scattering, degree of crystallinity determinations, and characterization of preferred orientation and texture." (http://www.dac.neu.edu/cammp/x-ray.htm, 2009).

The volume of powdered sample for the Getty GADDS was approximately 50 mg. After grinding the corrosion in a mortar with pestle the powdered sample was placed into a fine glass capillary tube of 0.5 mm diameter and inserted in the goniometer head with a brass hull and plasticine into the GADDS (Kugler 2003, 5). The use of ground samples in a capillary tube that is rotated during analysis provides a more homogeneous intensity distribution (Kugler 2003, 6). Smaller powdered samples were required for the Rigaku diffractometer that were adhered to the exterior of a glass spindle with mineral oil.

A few of the samples were analysed at the Cotsen Institute of Archaeology, UCLA, Los Angeles, on a Rigaku Corp. Rapid X-ray Diffractometer that uses Weissenberg geometry (Rigaku 2008). All angles of the diffracted beam are collected simultaneously on a curved imaging plate. The spectra were collected from 3° to 80° 2Θ. Radiation was from a copper source, generator settings 40-50 mA, 50kV. A collimated beam of 0.3 mm was used for small samples up to 0.8 mm for larger samples. R-Axis Rapid Auto Software and JADE, powder diffraction analytical software from Materials

Data, Inc., were used for identification. Much smaller samples were required for the Rigaku, a few particles were adhered to a spindle with mineral oil.

Limitations of XRD

The dependence on crystalline compounds for detection is not the only limiting factor of XRD analysis. Some copper acetates have d-spacings over 17 Angströms that many XRD machines cannot reach. The General Area X-ray Diffraction System (GADDS) and the Rigaku diffractometer used in this study can detect d-spacings over 17 Angströms, however (Scott 2001, 78).

5.3.2 Sampling in Museums

Saqqara Bronzes

The Saqqara bronzes sampled for XRD analysis are listed in Appendix 15.

Petrie Museum

Six of the sampled objects were from Saqqara and one was from another site in Egypt (UC 30449) (Appendix 14.1). Samples were removed from 7 objects of which only 3 had conservation treatment records (UC30808, UC30552, UC30669).

Ashmolean Museum

Of the 7 objects sampled, 4 were analysed (1971.138, 1969.482, 1969.483, 1969.484) (Appendix 13.2) (Appendix 14.2). All objects are from the Saqqara excavations.

British Museum

All 9 objects sampled for analysis of corrosion are from the Saqqara Excavations, BM 1-4 from inventoried bronzes and BM 5-9 from unregistered objects in a wooden drawer mentioned by Spencer (J. Spencer pers comm. 2007) (Appendix 13.3) (Appendix 14.3). The drawer holding the unregistered Saqqara bronzes is made completely of wood (no hardboard or particleboard). The wood species is unidentified. Some objects in this

drawer have Saqqara numbers but the objects I sampled did not have numbers or labels attached. Loose, unattached labels in drawer near the objects contained the following information: H6-102, H5-159, H6-28, 3508-8, H5-55.

Fitzwilliam Museum

In October 2006 the bronze collection was examined and 7 objects with blue or blue/green corrosion were sampled for analysis (Appendix 13.4) (Appendix 14.4). Only one object is from Saqqara, Egypt (E.38.1971).

Liverpool Museum

On Sept. 28, 2007 only those objects with corrosion that was likely to be a carbonyl compound and abundant enough for analysis were sampled (Appendix 13.5) (Appendix 14.5). Out of a total of 10 objects mentioned in Lang's dissertation, 4 were sampled (Lang 1995). In addition, 3 Saqqara bronzes were sampled.

Athenian Agora

Three campaigns of sampling and analysis have been carried out on the blue and blue/green corrosion on bronzes in the Athenian Agora: 1999, 2003, and 2006 (Paterakis 2003) (Appendix 13.6) (Appendix 14.6). The blue corrosion from 5 unregistered and undated bronzes, excavated between the years 1936 and 1981 from known areas of the excavation, were sampled and analysed in 1999. The blue and blue/green corrosion products on an undated bronze ring and seal from the 1932 excavation were analysed in 2003. Blue and white crystals on an axe head, excavated in 1938, and on a bronze rod, excavated in 1937, were analysed in 2006.

5.3.3 Corrosion Compounds

The identification of corrosion based on XRD for all objects in all museums is presented in Appendix 16. The corrosion identified in this study may be grouped into two categories: corrosion without carbonyl compounds and corrosion with carbonyl compounds.

5.3.3.1 Corrosion without Carbonyl Compounds

Some corrosion products are not the result of carboxylic acid contaminants (most commonly deriving from storage and display materials in museums). They form during burial and/or after excavation: chalconatronite and sodium lead carbonate hydroxide were identified in this study. Common corrosion products, such as cuprite, tenorite, malachite, and paratacamite, are included in Appendix 16 but are not included in this discussion since they are commonly found on archaeological bronzes.

5.3.3.1.1 Chalconatronite

Chalconatronite (sodium copper carbonate hydrate) has been discovered on Egyptian archaeological objects and is described as a corrosion product that forms naturally during burial (Frondel and Gettens 1955, 75) (Figure 5.11). Alkali carbonates dissolved in water on the surface of the ground or in the soil react with the copper alloy or the corrosion products, malachite or atacamite (Frondel and Gettens 1955, 75). Water of this nature is said to be typical of the arid regions of Egypt (Frondel and Gettens 1955, 75). Chalconatronite can also result from the reaction of sodium sesquicarbonate and sodium carbonate with malachite during conservation stabilization treatment on bronze (Horie and Vint 1982, 185; Pollard *et al*. 1990, 150).

Figure 5.11 Pale blue chalconatronite on Saqqara situla (1969.112.32 Liverpool Museum) (photo Ashley Cooke, reproduced with kind permission of National Museums Liverpool)

Petrie Museum (Appendix 13.1) (Appendix 10.12)

UC 30669 was found to contain chalconatronite on three fragments and chalconatronite with a sodium copper carbonate acetate on one fragment (Figure 5.12). UC 30668 was found to contain chalconatronite with copper sodium formate acetate. Neither object appears to have been chemically stripped. UC 30669 was stabilized with Benzotriazole and lacquered with Paraloid B72 in 1986. There are no treatment records for UC 30668.

Figure 5.12 Blue chalconatronite on Saqqara ewer fragments (UC30669 Petrie Museum) (field of view is approximately 18 cm across, photo Alice Boccia Paterakis, copyright of the Petrie Museum of Egyptian Archaeology)

British Museum (Appendix 10.14, Appendix 13.3)

Two of the unregistered Saqqara bronzes, BM5 and BM6, that apparently have not undergone conservation treatment (J. Spencer pers comm. 2007), were found to bear chalconatronite. They, therefore, are interpreted to represent examples of chalconatronite on bronze resulting from burial. The Osiris torso from which sample BM5 was removed appeared to be a leaded bronze by its high density (Appendix 13.3) (Figure 5.13). Compositional analysis carried out at the British Museum revealed 80% Cu, 3% Sn, and 16% Pb confirming a high lead content. A metallographic cross section of this figurine at the British Museum revealed an as-cast structure with α+ δ eutectoid and lead globules (Figure 5.14). The surface of the object was described with "pitting corrosion and big voids due to loss of lead globules" (Wang *et al*. 2009, 75). The lead globules have been replaced by cuprite and cerussite (Wang *et al*. 2009). XRD of the corrosion carried out at the British Museum confirmed the identification of chalconatronite (Wang *et al*. 2009).

Figure 5.13 Saqqara Osiris torso from which sample BM5 was removed (photo Alice Boccia Paterakis, field of view is approximately 4 cm across, © Trustees of the British Museum)

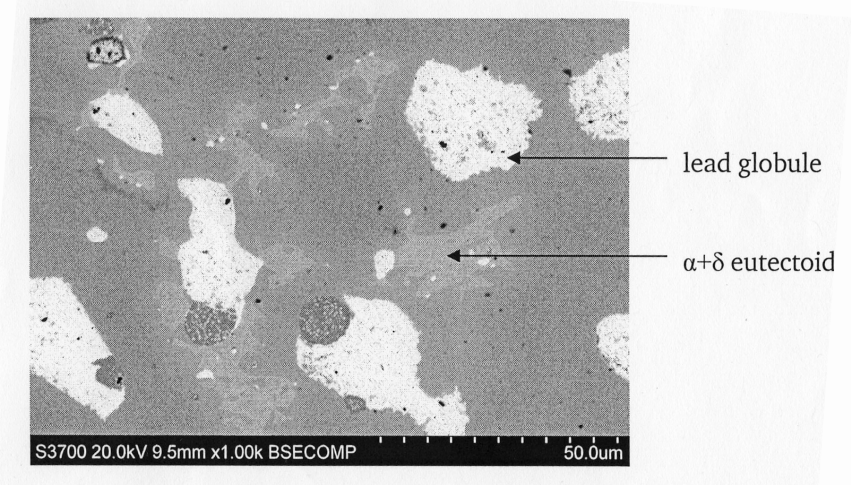

Figure 5.14 Backscatter image showing eutectoid and lead globules (some partially corroded) of the Osiris from which corrosion sample BM5 was removed (Wang *et al*. 2009, fig. 5, 76)

Liverpool Museum (Appendix 10.16, Appendix 13.5)

A pale green patina with white crystals on object 1969.112.32, from Saqqara, was identified as chalconatronite (Appendix 13.5, Sample 1) (Figure 5.11). The object had been treated with the corrosion inhibitor Benzotriazole ($C_6H_5N_3$) in 1987. White crystals on bronze sometimes result from excess Benzotriazole that was not rinsed off after treatment. This possibility may be confirmed by the identification of Benzotriazole with XRD (JCPDS 15-1163).

Agora (Appendices 6.26-6.27, 10.17, 13.6)

Bronze ring ΣT did not appear to have been chemically or mechanically cleaned. SEM-EDS with secondary imaging of palladium-coated sample Agora 1 identified copper, sodium, carbon and oxygen. XRD analysis confirmed these findings by the identification of chalconatronite (sodium copper carbonate hydrate). The corrosion was photographed at a magnification of 3930X (Appendix 6.26).

5.3.3.1.2 Sodium Lead Carbonate Hydroxide

Sodium lead carbonate hydroxide was found in one sample only, from the Egyptian statuette of Imhotep (E.55.1954) in the Fitzwilliam Museum (Appendix 13.4, Sample Fitz 2) (Appendix 10.15). The statuette appears to have been chemically cleaned with evidence of etching in places while preserving malachite in others. The blue powdery corrosion inside the base was identified as sodium lead carbonate hydroxide with quartz. Traces of copper may account for the blue coloration. Sodium could result from the soil, chemical cleaning or stabilization chemicals. Lead may be attributed to the alloy content of the bronze. Quartz, of course, derives from burial in the soil.

5.3.3.1.3 Thenardite and Connellite (sulphate-containing corrosion)

One spot analysis and two scanned areas with the SEM-EDS of sample Agora 3a from bronze ring ΣT detected chlorine, sulphur, and copper (Appendix 13.6). The sulfur to chlorine ratio was consistent in the scans indicating a sulfur-chlorine phase that was subsequently identified by XRD as connellite. The morphology of the corrosion under

40X magnification was geode-like with a smooth exterior and rough interior. SEM-EDS of both surfaces indicated the same elemental composition. An SEM photograph (1182X magnification) revealed the rough interior against the smooth surface (Appendix 6.27).

Thenardite [$Na_2(SO_4)$], sodium sulphate, was found with connellite [$Cu_{19}SO_4Cl_4(OH)_{32}$ - $3H_2O$], hydrated copper sulfate chloride hydroxide, by XRD in sample Agora 3a from bronze ring ΣT. Chalconatronite and paratacamite had also been identified by XRD in sample Agora 1 and sample Agora 2 from the same object (Appendix 10.17, Appendix 13.6, Appendix 16).

5.3.3.2 Corrosion with Carbonyl Compounds

The carbonyl compounds, acetate and formate, derive from the organic carboxylic acids, acetic and formic acid. Carboxylic acids are often found in materials used for the construction of storage and display cases in museums, in particular wood and wood products. The carbonyl compounds identified in this study are a sodium copper carbonate acetate, copper sodium formate acetate, sodium acetate hydrate, and sodium formate.

XRD analysis has verified the presence of acetate compounds in the Liverpool collection (Appendix 13.5, sample numbers 4, 5, 6, and 7; Appendix 10.16) that were indicated by Infrared Spectroscopy (IR) in 1995 (Lang 1995, 47) (Appendix 14.5). 17 samples from Lang's 10 case study objects all showed a similar IR pattern that is consistent with that of basic copper acetate found at the British Museum (Lang 1995, 47). These peaks correspond with the FTIR results of the ASTM coupons from the corrosion tests in Chapter 4 (Experimental Work) indicating neutral copper acetate, copper acetate hydrate and basic copper acetate (see Chap. 4, Results of FTIR Analysis). XRD identified specific carbonyl compounds (as follows).

5.3.3.2.1 A Sodium Copper Carbonate Acetate

Sodium copper carbonate acetate was first characterized at the British Museum and identified on many Egyptian bronze artifacts in that collection (Figure 5.15) (Thickett 1998; Thickett *et al.*1998; Thickett and Odlyha 2000). Thickett distinguished two sodium copper carbonate acetate compounds, Type A and Type B, that are single,

unique compounds and not mixtures (Paterakis 2003; Thicket 1998; D. Thickett pers comm. 2009). Two samples only were identified as Type B in the British Museum (Thickett 1998). Thicket based his characterization on a single phase compound in numerous samples from original corrosion products that was analysed by XRD, FTIR, Ion Chromatography (IC), Atomic Absorption Spectroscopy (AAS), Scanning Electron Microscopy with Energy Dispersive Analysis (SEM-EDS), Thermogravimetric Analysis (TGA) and microchemical tests (Thickett and Odlyha 2000, 65). Thickett believes Type A to have a similar stoichiometry to Type B but a different structure. The two compounds are distinguished by different XRD and FTIR spectra (Thickett 1998; D. Thickett pers comm. 2009). A sodium copper carbonate acetate was identified in all collections in these case studies of Chapter 5: Type A was found in all cases except for three instances in the Agora Excavation where Type B was identified. Type A is referred to as "a sodium copper carbonate acetate" throughout this study, Type B is referred to as "Type B". The diffraction pattern for Type A was published in 2000 (Thickett and Odlyha 2000) and for Type B in 2003 (Paterakis 2003). The sodium copper carbonate compounds (Type A and B) discovered at the British Museum require crystallographic characterization prior to their submission to the ICDD database (D. Thickett pers comm. 2009).

In the British Museum the blue corrosion was found in cracks in objects that had been chemically stripped and at breaks in a pale green corrosion layer high in sodium and chloride (Thickett *et al.*1998, 261). Chemical agents that had been used in cleaning were alkaline Rochelle salt or alkaline glycerol; sodium sesquicarbonate had been used for stabilization (Thickett *et al.*1998, 261). Most of the collection had been stored in wooden cabinets since the 1930s (Thickett *et al.*1998, 261).

Figure 5.15 A sodium copper carbonate acetate identified in sample BM7 from unregistered Saqqara situla (field of view is approximately 6 cm across, photo Alice Boccia Paterakis, © Trustees of the British Museum)

British Museum (Appendices 10.14, 13.3)

A sodium copper carbonate acetate was identified on 6 of the 9 objects sampled at the British Museum, often in combination with one or more other corrosion compounds. It was found on 68010, a hammered situla, and on 68048, a hammered base of a stand. 68010 was cleaned, lacquered with Incralac®, and mended with HMG cellulose nitrate adhesive, in 1977, then stabilized with BTA, gapfilled with polyester resin, and coated with Frigiline (cellulose nitrate lacquer) in 1985. 68048 was mechanically cleaned of a light blue deposit on the interior and lacquered with Incralac® in 1977. Bronze disease was noted in 1985. Four of the identifications were made on the unregistered hollow and solid cast Saqqara objects without conservation treatment records. Three of these (BM5, BM6, BM7) are most likely untreated (J. Spencer pers comm. 2007). The identification of a sodium copper carbonate acetate was confirmed by Raman spectroscopy at the British Museum on the object from which BM6 was removed (Figure 5.16; Figure 5.17) (Appendix 13.3) (Wang *et al*. 2009). The "Raman spectroscopy was carried out using a Jobin Yvon Infinity spectrometer with a green (532 nm) laser, using a maximum power of 2.4 mW at the sample. The corrosion products were measured using a power of 0.6 mW to avoid 'burning' the samples and to allow a comparison to be made with the reference spectrum in the British Museum in-house database for the 'pale blue' described as sodium copper carbonate acetate by Thickett and Odlyha (Thickett and Odlyha 2000)" (Wang *et al*. 2009, 81).

The Osiris figurine from which BM8 was sampled underwent compositional analysis at the British Museum. It was found to contain 88% Cu, 2% Sn, and 8% Pb (Wang *et al*. 2009). Metallographic cross section revealed an as-cast, equi-axed structure without eutectoids (Wang *et al*. 2009). The Osiris appears to have been partially stripped while preserving some malachite (Figure 5.26). The blue corrosion (BM8), removed from the underside of the object resting on cotton wool, was identified as a sodium copper carbonate acetate using XRD by the author at the Getty Conservation Institute (Appendix 13.3).

Figure 5.16 Unregistered Saqqara lamp spout (?) from which blue corrosion sample BM6 was removed, (photo Alice Boccia Paterakis, field of view is approximately 4 cm across, © Trustees of the British Museum)

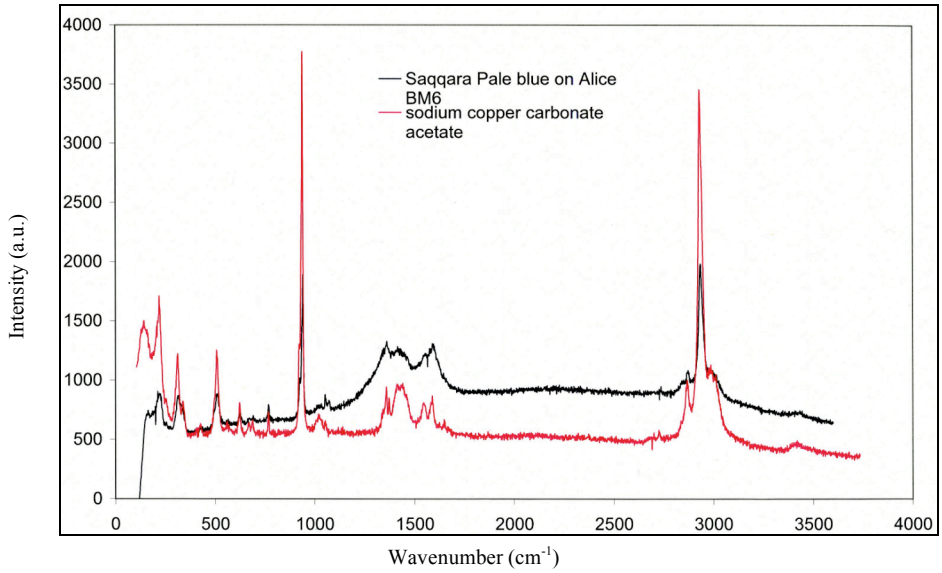

Figure 5.17 Raman spectrum of blue corrosion on unregistered Saqqara object (lamp spout?) from which BM6 was sampled compared to a sodium copper carbonate acetate (unpublished data from British Museum science records). Bands from 480 cm^{-1} to 650 cm^{-1} indicate metal-water vibrations; band at ± 950 cm^{-1} indicates C-C symmetric stretching of the acetate dimer; bands from 1400 cm^{-1} to 1700 cm^{-1} indicate assymetrical and symmetrical vibrational modes of the carboxylate group; 2955 cm^{-1} band indicates CH stretching mode of acetate.

Ashmolean Museum (Appendices 10.13, 13.2)

A sodium copper carbonate acetate was detected on the four objects analysed similar to that found in the British Museum (Appendix 10.14). Samples Ash 1 and Ash 4 (1971.138 and 1969.482) produced similar diffraction patterns as did Ash 5 (1969.483) and Ash 7. Quartz is indicated on samples Ash 1 and Ash 4 (1971.138 and 1969.482). At

least one unidentified compound is indicated on these four objects by d-spacings greater than 10.7 Angströms. Some of the objects hadn't been cleaned, some had been partially cleaned, and some were completely stripped chemically as determined by visual inspection in the absence of treatment records.

Fitzwilliam Museum (Appendices 10.15, 13.4)

A sodium copper carbonate acetate was detected on two of the seven objects investigated. Heavily leaded Egyptian bronze weight (E.GA.2797.1943) (Fitz 5) produced a soft powdery blue corrosion that was identified by XRD analysis as a sodium copper carbonate acetate. This object does not appear to have been chemically stripped.

The early Roman finial in the form of a panther (GR.1.1976) does not appear to have been chemically stripped. Two corrosion products were evident on the interior: dark corrosion (Fitz 7) on the inside near the curved end was surrounded by blue corrosion (Fitz 8). The dark corrosion is more granular than the blue. XRD analysis identified the dark corrosion as tenorite and a sodium copper carbonate acetate, the blue corrosion is a sodium copper carbonate acetate.

Liverpool Museum (Appendices 10.16, 13.5)

A sodium copper carbonate acetate was found on five of six objects analysed, combined with other compounds (except 1973.4.30). None of them have conservation treatment records. Object 1969.112.35, from Saqqara, is tentatively identified as bearing a sodium copper carbonate acetate with an unidentified compound. A brown corrosion layer, probably cuprite, was visible under the blue corrosion. This is similar to the morphology of corrosion found on the Agora bronzes that had been electrochemically cleaned with zinc and sodium hydroxide (Paterakis 2003).

Object 1973.4.30 is a hollow cast bronze censer handle in the shape of hawk's head. Its density would indicate a lead core and/or high lead content in the alloy (Lang 1995). In 1994 the side of the head lying in contact with the hardboard tray in the plywood and hardboard box displayed blue corrosion. The blue corrosion was identified as a sodium copper carbonate acetate (Sample 5). Other areas had a smooth cuprite layer. Desiccated wood from the handle is preserved in the hollow of the object. There are no signs of treatment.

Blue and white corrosion was sampled (Sample 6) from the completely mineralized center of one boss, specifically from the area with a detached fragment, on Object 56.22.215. The fragment was also sampled contributing to Sample 6. XRD analysis revealed a sodium copper carbonate acetate and an unidentified compound. No conservation treatment is apparent from examination. One other object identified with a sodium copper carbonate acetate is 1972.2.548.

Agora (Appendices 10.17, 13.6)

A sodium copper carbonate acetate was found on three objects AB 256, NSR-176, and N10763 and Type B (a sodium copper carbonate acetate) was found on ΠΘ 3844, AB 217, and ΣT seal. All appear to have undergone electrochemical or chemical cleaning (based on appearance) (Paterakis 2003, 318).

5.3.3.2.2 Sodium Acetate Hydrate

White crystalline sodium acetate hydrate has been found on bronzes in the Burrell Collection, Glasgow, Scotland, often in combination with a blue corrosion product containing acetate (Tennent and Baird 1992). White crystals of sodium acetate trihydrate were found in association with a sodium copper carbonate acetate, $NaCu(CO_3)(CH_3COO)$, identified by XRD and Fourier Transform Infrared Spectroscopy (FTIR), in the British Museum (Thickett and Odlyha 2000, 64, 65).

Sample BM5 provides an example from the current study of a sodium copper carbonate acetate coexisting with sodium acetate hydrate (and chalconatronite) (Appendix 13.3). XRD of BM 5 showed a sodium copper carbonate acetate (Appendix 10.14) whereas Raman spectroscopy of another corrosion sample from this object revealed sodium acetate trihydrate at the British Museum (Wang *et al*. 2009) (Figure 5.18).

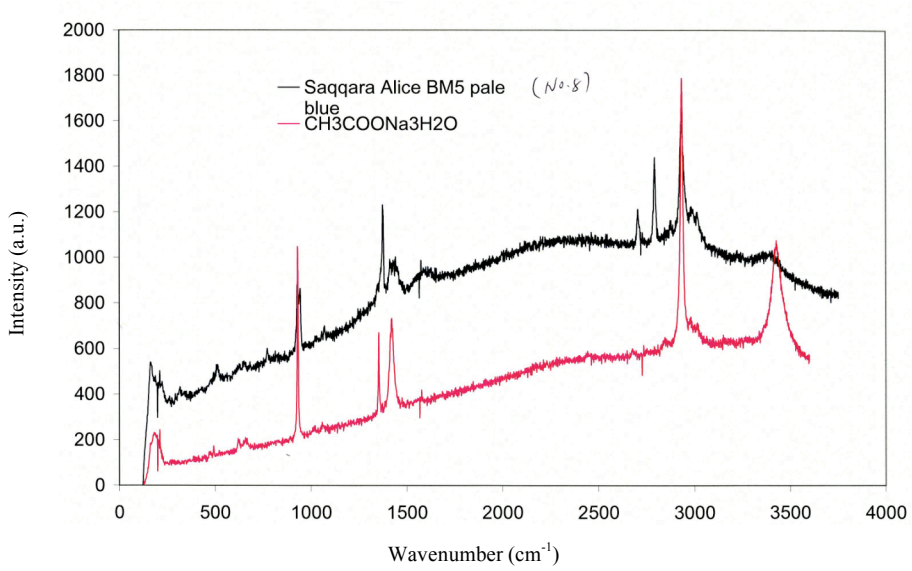

Figure 5.18 Raman spectrum of corrosion from unregistered Saqqara Osiris (from which sample BM5 was removed) compared to sodium acetate trihydrate (unpublished data from British Museum science records). Band at ± 950 cm^{-1} indicates C-C symmetric stretching of the acetate dimer; band at 1350 cm^{-1} indicates symmetric deformation of acetate; 2955 cm^{-1} band indicates CH stretching mode of acetate.

Another example of the coexistence of a sodium copper carbonate acetate with sodium acetate hydrate was found in the corrosion of the unregistered Saqqara situla (incomplete) from which sample BM7 was removed (Appendix 13.3) (Figure 5.19). The sample removed for analysis by the author consisted of white and blue crystals. XRD of this sample at the Getty Conservation Institute revealed a sodium copper carbonate acetate. The white crystalline component of the corrosion, sodium acetate trihydrate, was identified in another sample by Raman spectroscopy at the British Museum (Wang *et al.* 2009) (Figure 5.20). Raman spectroscopy at the British Museum confirmed a mixture of a sodium copper carbonate acetate and sodium acetate trihydrate (Wang *et al*. 2009) (Figure 5.20). XRD of another sample at the British Museum revealed chalconatronite, sodium acetate trihydrate, and quartz (Appendix 13.3). At the British Museum "X-ray Diffraction was carried out with a Philips PW 1120/90 diffractometer using Cu Kα radiation. The samples were run at 40 kV, 15 mA for about an hour. Diffraction lines were identified by matching them with ICDD standards." (Wang *et al*. 2009, 81). SEM-EDX compositional analysis of the corrosion on this situla was carried out at the British Museum to compliment XRD analysis and found copper, sodium, and oxygen with

silicon, calcium, sulphur and chlorine present in some samples (Wang *et al*. 2009). SEM-EDX analysis of a soil sample from the interior of the situla revealed sodium. "A Hitachi S-3700N Variable Pressure SEM with an Oxford INCA Energy System was used for elemental analysis and maps. The analyses were run at an accelerating voltage of 20 kV at a pressure of 50Pa and with a working distance of 10 mm. The detection limits for each element are variable but typically 0.1 – 0.3%." (Wang *et al*. 2009, 81).

Figure 5.19 Unregistered Saqqara situla from which sample BM7 was removed, (photo by Alice Boccia Paterakis, field of view is approximately 7 cm across, © Trustees of the British Museum)

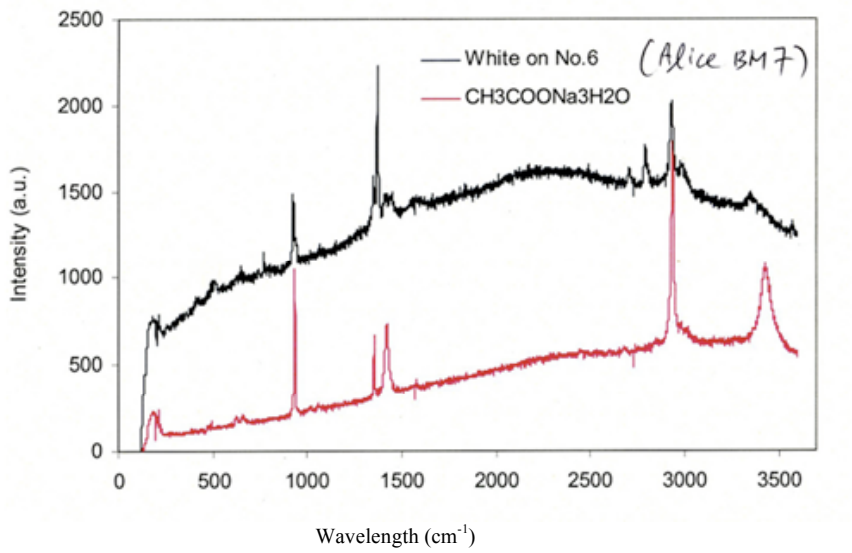

Figure 5.20 Raman spectrum of white corrosion from unregistered Saqqara situla (from which sample BM7 was removed) compared to sodium acetate trihydrate (Wang *et al*. 2009, fig. 8, 78). Band at ± 950 cm^{-1} indicates C-C symmetric stretching of the acetate dimer; band at 1350 cm^{-1} indicates symmetric deformation of acetate; 2955 cm^{-1} band indicates CH stretching mode of acetate.

Another example of sodium acetate hydrate coexisting with a sodium copper carbonate acetate was found on object 1978.291.123 in the Liverpool Museum. The object was mechanically cleaned, treated with BTA, and coated with microcrystalline

wax in 1985 (Appendix 13.5) (Appendix 10.16) (Figure 5.21). It was reported to have dark blue/green crystalline corrosion with white needle-like crystals on the lotus flower seat in 1994 (Lang 1995, 41). In 1994 the object was stored in a wooden chest of drawers in a card tray lined with acid-free tissue (Lang 1995, 41). In 2007 the corrosion was described as pale green with white crystals (Sample 7) concentrated in a few areas that, prior to analysis, were thought to be sodium acetate or BTA. The object is very dense, perhaps with a lead core, with an iron strip attached to the base. XRD analysis revealed sodium acetate hydrate (white crystals), a sodium copper carbonate acetate, and an unidentified compound (Appendix 13.5).

Figure 5.21 Sodium acetate hydrate and a sodium copper carbonate acetate on 1978.291.123 Liverpool (photo Ashley Cooke, reproduced with kind permission of National Museums Liverpool)

5.3.3.2.3 Copper Sodium Formate Acetate

Copper sodium formate acetate ($CuNaC_xH_yO_6$) in a ratio of 1:1:1:2 or 1:1:2:1 was first characterized on ancient Egyptian, Greek, Assyrian and Chinese copper alloys and published in 2002 (Trentelman *et al.* 2002, 217).

Petrie (Appendices 10.12, 13.1)

Copper sodium formate acetate was found on 5 of the 7 objects analysed from the Petrie (UC30808, UC30449, UC30660B, UC30668, UC30667). Three of the objects (UC30449, UC30668, UC30667) have no conservation treatment records. The record for UC 30808 states that the object was stripped prior to 1976, very possibly on site after its excavation in Saqqara between 1964 and 1976 (Appendix 15) (Figure 5.22).

Figure 5.22 Copper sodium formate acetate on Saqqara bull UC 30808 Petrie Museum (copyright of the Petrie Museum of Egyptian Archaeology)

British Museum (Appendices 10.14, 13.3)

Copper sodium formate acetate was found on 68010, hammered situla, in conjunction with a sodium copper carbonate acetate. This object underwent extensive

conservation treatment in 1977 and 1985 including the application of a corrosion inhibitor and lacquer.

Fitzwilliam Museum (Appendices 10.15, 13.4)

The blue corrosion on the metal components of Egyptian Coptic wooden casket (E.169.1891) (Appendix 13.4, sample Fitz 1) (acquired by the museum in 1891) was identified as copper sodium formate acetate. The metal components do not appear to have been removed or chemically treated in any way. A thick coating of wax covered the object, a material known to foster acidic attack on metal (Rocca and Mirambet 2007, 311). This corrosion was evident in 1985 photos. In spite of the fact that the object was relocated to suitable storage conditions in 1990 the corrosion was more pronounced when sampled in 2006 compared to the 1985 photos.

5.3.3.2.4 Sodium Formate

It is not unusual to find sodium formate on glass that has been stored in wood. Sodium formate was found on an enamel triptych stored in wood (Fitzhugh and Gettens 1971) and on glass lids of wooden storage boxes for textiles (Nockert and Wadsten 1978).

Petrie (Appendices 10.12, 13.1)

The degradation product(s) on the glass or faience inlay in the Uraeus of UC30552, a wooden head of a King or Osiris, was sampled for analysis by XRD. Unspecified areas of the head had been treated with sodium hexametaphosphate (Calgon™). The identification of sodium formate on the inlay material of the bronze uraeus is a result of the reaction of formic acid from the wooden storage on the glassy material of the inlay (Figure 5.23). The quartz could be a component of the glassy material or a contaminant from burial.

Figure 5.23 Sodium formate (green area) on glassy inlay in uraeus UC30552 Petrie Museum (copyright of the Petrie Museum of Egyptian Archaeology)

5.3.4 Unidentified Compounds (Appendices 4.22-4.26, Appendix 10.11)

Difficulties in the identification of corrosion by XRD may be attributed to several factors. Amorphous forms of corrosion cannot be identified by XRD (López-Delgado *et al*. 2001, 5209). Imperfect crystals and intermediate compounds will not provide diffraction scans found in the International Centre for Diffraction Data (ICDD) database. Non-stoichiometric compounds require extensive data analysis for their identification by XRD due to alteration in the peak spacing (D. Scott pers comm. 2007).

In total 42 objects were sampled for analysis. No identification could be made for five objects (9.5% of total) and several objects contained at least one compound that could not be identified in a mixture of otherwise identified compounds (Appendix 16). Mixtures were analysed rather than single crystals by XRD. These unidentified compounds represent original discoveries. Further work using other analytical techniques could be done to elucidate their identities, such as Fourier Transform Infrared Analysis (FTIR), Raman spectroscopy, and Thermogravimetric Analysis (TGA). Sampling procedures play an important role in the detection of carbonyl compounds. "…the greatest concentration of … acids is in the layers of corrosion product in intimate contact with the metal, examination of the powdery outer layers has frequently failed to show any traces of the contaminant which was evident in the lower layers." (Donovan and Stringer 1971, 138). The samples were scraped from the surface of the objects with a scalpel and then ground in a mortar with pestle. It cannot be ruled out that the sampling

procedures in some cases may have failed to remove corrosion next to the metal core, thereby excluding acid-containing corrosion.

The corrosion on three objects in the Fitzwilliam Museum could not be identified: E.38.1971 (Fitz 3), E.23.1940 (Fitz 4), and E.GA.3467.1943 (Fitz 6) (Appendix 16, Appendix 13.4). The x-ray diffraction patterns from the corrosion sampled on these three objects display similarities (Appendices 4.22-4.24, Appendix 10.11). The statuette of Horus from Saqqara (E.38.1971) (Fitz 3) appears to have been chemically cleaned. The diffraction pattern is similar to that of Fitz 6 (bronze spoon handle, E.GA.3467.1943) (Figure 5.24). The statuette of Sakhmet (E.23.1940) (Fitz 4) has not been chemically stripped. Egyptian bronze spoon handle (E.GA.3467.1943) (Fitz 6) does not appear to have been chemically stripped.

The corrosion on one object in the British Museum could not be identified, a blue chalky corrosion product on interior surface of unregistered Saqqara box (BM9) (Appendices 4.26, 10.11, 13.3, 16). This object is presumed to be a leaded bronze due to its high density. The corrosion on an axehead from the Agora (Agora A) also could not be identified (Appendices 4.25, 10.11, 13.6, 16). The diffraction patterns of the British Museum and Agora objects are diverse from one another and from the Fitzwilliam patterns. Further attempts to identify these compounds were beyond the scope of this project.

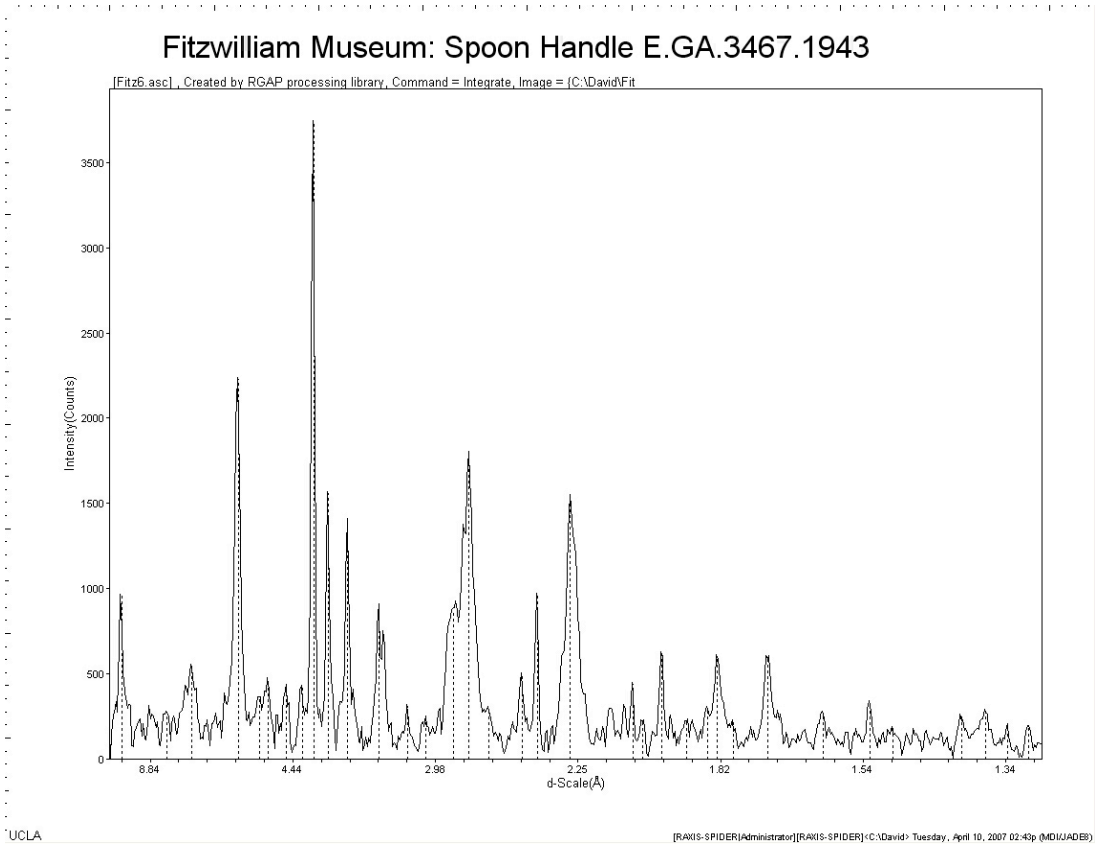

Figure 5.24 XRD scan of corrosion on E.GA.3467.1943, Fitzwilliam Museum

Inclusion of the copper sodium formate acetate and sodium copper carbonate acetate diffraction patterns in the International Centre for Diffraction Data database (ICDD) should facilitate their identification in many collections around the world. The sodium copper carbonate compounds (Type A and B) discovered at the British Museum and copper sodium formate acetate require crystallographic characterization prior to their inclusion in the ICDD database (D. Thickett pers comm. 2009).

5.4 Interpretation of Corrosion Process

In an attempt to comprehend the corrosion phenomena on the bronzes analysed in this study the following topics are examined: contaminants and their sources and the transformation of corrosion compounds.

5.4.1 Contaminants and Sources

The carbonyl compounds identified in this study all contain sodium and acetate, sodium and formate, or sodium, acetate and formate. The contaminants considered are sodium, acetic acid, and formic acid as contributants to the corrosion products identified in this study. Potential sources of possible effects of contaminants listed in order from most recent to consider are 1) storage environment and modern materials, 2) conservation treatments and materials, 3) handling during excavation, 4) burial, 5) treatment during use, and 6) vessel contents from antiquity.

5.4.1.1 Sodium

The potential sources of sodium in the copper sodium formate acetate, sodium acetate, sodium formate, and sodium copper carbonate acetate on bronze, taking into account the conservation literature, are "1) the burial environment, 2) chemical cleaning agents such as Calgon (sodium hexametaphosphate/sodium polyphosphate), zinc and sodium hydroxide, alkaline Rochelle salt (5% sodium hydroxide and 15% sodium potassium tartrate), alkaline glycerol (15% sodium hydroxide and 40% glycerin), 3) the stabilization compounds sodium sesquicarbonate and sodium carbonate and, 4) artificial patination agents such as sodium carbonate or bicarbonate (Tennent and Baird 1992), and sodium sulphite or sodium thiosulphate (Lucas 1932)." (Paterakis 2003, 324). The sources of sodium listed in order of importance from the most prevalent to the least prevalent based on conservation practices and subsequent work on archaeological bronzes is as follows: 1) chemical cleaning agents, 2) stabilization compounds, 3) burial environment, 4) patination agents.

Residual sodium from cleaning and stabilization compounds seems to contribute considerably to chemical reactions that occur on the surface of bronze when exposed to volatile carboxylic acids. An examination of the conservation application of sodium sesquicarbonate exemplifies the potency of sodium in this corrosion. Acetate was found by ion chromatography on a bronze object from the British Museum that had been stabilized with sodium sesquicarbonate (Tennent *et al.* 1992, 878). The object was soaked in water to extract the contaminants for analysis. The object showed the blue-green surface typical of the sesquicarbonate treatment but did not show any signs of deterioration in terms of crystallization or efflorescence. No acetates were found on other

bronzes of the same provenance that had not been treated with sodium sesquicarbonate (Tennent *et al.* 1992, 878). Sodium from conservation treatments was detected in crevices on bronzes whose corrosion was identified as a sodium copper carbonate acetate and sodium acetate trihydrate in the British Museum (Thickett and Oldyha 2000). This residual sodium contributed to the growth of the carbonyl compounds.

In Test Series II reported in Chapter 4 sodium sesquicarbonate was exposed to a high concentration of acetic acid vapour (±500 ppm) and high RH (±85%) that resulted in the formation of sodium acetate trihydrate. The result of this test proves the hypothesis that residues of sodium from sodium sesquicarbonate or other sources on the object can react with volatile acetic acid forming a compound containing sodium and acetate, such as sodium acetate trihydrate (Tennent *et al.* 1992, 878).

5.4.1.2 Acetic and Formic Acid

The potential sources of acetic acid and formic acid in carboxylate corrosion in order of most likely to least likely are 1) modern wooden storage cupboards, 2) the application of conservation materials containing acetic acid or acetate such as polyvinyl acetate and Na-EDTA (ethylenediamine tetracetic acid), 3) acid cleaning (Rathgen 1905, 121), 4) original wine or vinegar contents of vessels, and 5) volatile acid emissions from the ancient wooden shrines (for those objects that may have been enclosed in shrines).

All the bronzes examined in this study were initially stored in unsuitable organic materials such as card and wood upon their acquisition by the museums. Most were relocated into more suitable storage materials and conditions by the 1990's, those at the Petrie Museum and Ashmolean Museum are awaiting relocation.

Acetic acid concentration in the wooden cases housing the bronzes was measured in the British Museum, Liverpool Museum, and Athenian Agora collection in the 1990s and was found to range from 426 ppb to 1181 ppb (0.43 ppm – 1.19 ppm) (Table 2.2). Acetate was found in the corrosion products on objects from these collections indicating that this range of acetic acid concentration is adequate for the formation of acetate corrosion on bronze. Formic acid concentration was measured in the Liverpool Museum where two objects were confirmed to have copper sodium formate acetate. It ranged from 150 to 200 ppb (0.1 to 0.2 ppm) (Lang 1995) (Table 2.3). It should be kept in mind

that concentrations would have been higher when the cabinets were new. In the case of the Athenian Agora the storage cabinets were approximately 40 years old when sampled for acetic acid vapour.

There are documented cases of the formation of formate and acetate corrosion products on metal in a period of several months (Tennant and Baird 1992). The durability and longevity of the carbonyl compound corrosion products are not known, least of all in burial conditions, and will depend on the conditions of their surroundings. The transformation of corrosion compounds will be discussed in the next section.

5.4.2 Transformation of Corrosion Compounds

The development and changes of secondary corrosion on artifacts with pre-existing patina proceeds through stages. A very common copper carbonate such as malachite that forms during burial can be transformed into chalconatronite (sodium copper carbonate hydrate) when exposed to sodium during burial or after excavation (Frondel and Gettens 1955). Treatment of malachite-covered bronze with sodium sesquicarbonate can produce chalconatronite (Horie and Vint 1982, 185). Gettens and Frondel did not consider chalconatronite to be an intermediate corrosion product but rather an ultimate product of copper mineralization (Gettens and Frondel 1955, 69). It has been shown in the present research project that chalconatronite can behave as an intermediate product by transforming into a sodium copper carbonate acetate (reaction 2 below) or copper sodium formate acetate in the presence of formic and acetic acid volatiles.

Tests that exposed corrosion products to a high level of acetic acid vapour (500 ppm) at a high RH confirmed some of these conversions by XRD (Chapter 4, section 4.3). Malachite (copper carbonate) exposed to these conditions was partially transformed into copper acetate (both malachite and copper acetate were identified by XRD):

(1) Malachite + acetic acid + water vapour → copper acetate + (less) malachite

Blue, green and white corrosion on four Egyptian copper alloy objects in the British Museum were analysed by XRD, SEM-EDXA (energy dispersive x-ray analysis) and FTIR. A copper acetate with chalconatronite was found on three of the objects (Thickett

and Lee 1994, 2). Neutral copper acetate hydrate was found to transform to basic copper acetate (copper acetate hydroxide) over a 7-month period in normal atmospheric conditions (See Chapter 4, Test Series II, section 4.3). The carbon dioxide in the atmosphere reacted with the neutral copper acetate on the test coupons after the completion of corrosion testing, forming hydroxide. The transformation from neutral to basic copper acetate is as follows:

$$\underset{\text{neutral}}{Cu(CH_3COO)_2} + CO_2 \rightarrow \underset{\text{basic}}{[Cu(CH_3COO)_2]_x\,[Cu(OH)_2]_y \bullet {}_zH_2O}$$

where x, y, and z are variable (Scott 2002, 272).

Chalconatronite exposed to these test conditions produced a sodium copper carbonate acetate:

(2) Chalconatronite + acetic acid + water vapour → a sodium copper carbonate acetate

Sodium sesquicarbonate was mixed with malachite (1:1) (to mimic the conservation stabilization treatment for bronze commonly used in the past) and was exposed to these test conditions resulting in a sodium copper carbonate acetate:

(3) Sodium sesquicarbonate + malachite + acetic acid + water vapour → a sodium copper carbonate acetate

The identification of multiple compounds may indicate incomplete transformation processes. For example chalconatronite was found with a sodium copper carbonate acetate on British Museum objects BM5 and BM6 (Appendix 10.14). Another example consists of object UC30668 (Petrie Museum) on which were identified both chalconatronite and copper sodium formate acetate (Appendix 10.12). One may wonder why chalconatronite was not found on the other objects containing copper sodium formate acetate in the Petrie. The answer may be complete conversion of the chalconatronite. One may wonder why a carbonyl corrosion compound was not found on all four fragments of UC 30669 or why copper sodium formate acetate wasn't found on all of the copper alloy objects analysed at the Petrie (it was found on 5 of 7 objects). These anomalies may be accounted for by any number of variables that may include, but

are not limited to, copper alloy metallographic morphology, contaminants, wood species, humidity and temperature, concentrations of volatile acids, and conservation treatments.

Two carbonyl corrosion products were found together on one object in the Liverpool Museum, 1973.2.548: a sodium copper carbonate acetate and copper sodium formate acetate (Appendix 13.5) (Appendix 10.16). One explanation may be localized formation of corrosion. Another explanation for two carbonyl corrosion compounds on this object may be found in a conversion process from a sodium copper carbonate acetate to copper sodium formate acetate. In this case perhaps the carbonate component in a sodium copper carbonate acetate, under the influence of volatile formic acid, had partially converted into formate in the following hypothetical reaction:

(4) a sodium copper carbonate acetate + formic acid → copper sodium formate acetate

5.5 Conclusions

For the case studies bronze objects were selected on the basis of the tentative detection or suspicion of acetates from visual inspection that warranted further study and confirmation. Suspect corrosion was targeted on bronze objects mainly from Egypt in several museum collections in the UK.

Expressed as percentages based on the total of 42 objects analysed more than one compound (mixed compounds) was identified on 59% of the objects, a sodium copper carbonate acetate was identified on 59% of the objects, and compounds were present on 43% of the objects that could not be identified (Figure 5.25, Appendix 16, Table 5.2). The mixtures typically represented various combinations of two or more compounds including a sodium copper carbonate, sodium acetate, copper sodium formate acetate, chalconatronite, and unidentified compound(s).

5.5.1 Conservation Materials and Methods that May contribute to Carbonyl Corrosion

In this study the blue or blue/green and white crystalline carbonyl compounds were found on stripped surfaces as well as surfaces covered with copper oxide (cuprite and tenorite), copper carbonate (malachite), and chalconatronite.

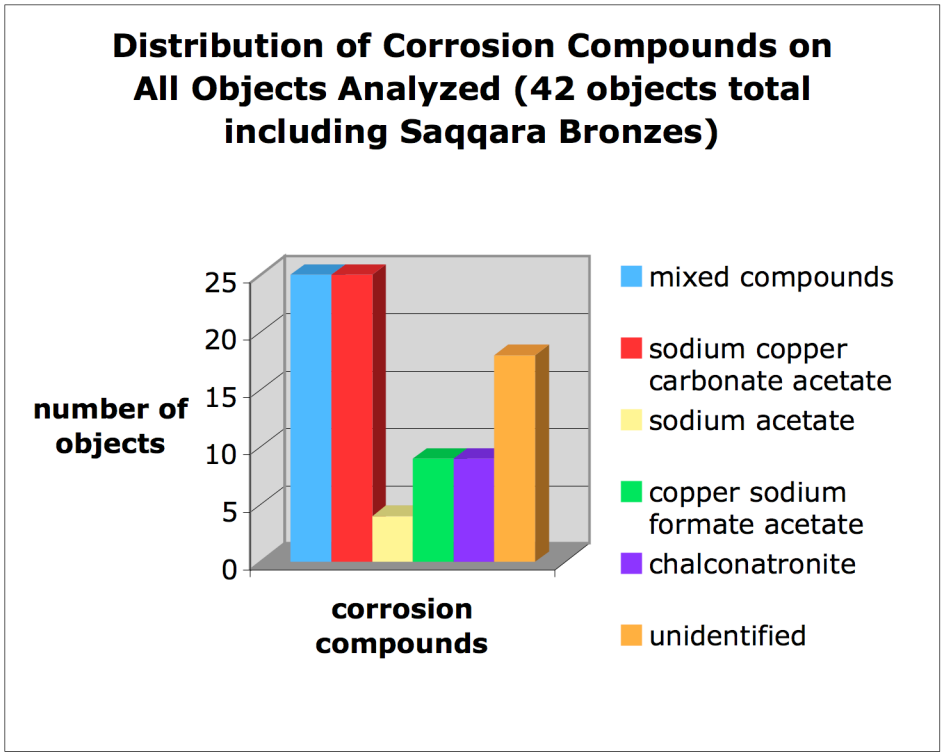

Figure 5.25 Distribution of corrosion compounds on all objects analysed including the Saqqara bronzes

The application of corrosion inhibitors and protective lacquers has not prevented attack by volatile carbonyl acids. The coatings may be too thin allowing permeation of acetic acid or they may have significant defects. Of course, there is the longevity factor of protection regarding corrosion inhibitors and coatings to consider.
Both films and inhibitors are known to lose their protective qualities after a certain length of time, usually a few years in the case of the corrosion inhibitor Benzotriazole ($C_6H_5N_3$) (Cronyn 1990, 229; Hatchfield 2002, 114). Many more than a few years had passed from the time these objects were treated to the time they were sampled for analysis. Also, the protective properties of cuprous and cupric benzotriazole compounds, resulting from treatment with the corrosion inhibitor BTA, against attack by acetic acid are not known.

It can be broadly stated that conservation materials and methods will certainly influence the form, rate, and degree of subsequent corrosion on bronze. Sodium in sodium sesquicarbonate was found to increase the rate of corrosion on the test coupons in Chapter 4. It was found to activate copper corrosion on leaded bronze in high levels of humidity (86% RH) and acetic acid concentration (40 ppm) in Chapter 4. Sodium

sesquicarbonate encouraged acidic attack on the copper and reduced the protective qualities of a lead oxide layer on leaded bronze. It may have contributed to the formation of different crystal morphology of the corrosion.

A few conservation products containing acetic acid or acetate, such as vinegar, PVA (polyvinyl acetate), and Na-EDTA (ethylene diamine tetraacetic acid) are known to have been used on bronzes but cannot be directly linked yet to the objects in this study. No cases of PVA or Na-EDTA causing carbonyl corrosion of bronze have been published to date.

5.5.2 Storage Factors

A confirmed source of acetic and formic acid contamination for the objects found to contain carbonyl compounds in this study is the wooden storage cupboards in the museums. The range in acetic and formic acid concentration measured in the wooden cases in the British Museum, Liverpool Museum, and Athenian Agora collection indicates a high level of contamination for the formation of acetate and formate corrosion on bronze (426 to 1181 ppb (0.43 to 1.2 ppm) acetic acid and 150 to 220 ppb (0.15 to 0.22 ppm formic acid).

The position of the objects in the wooden drawers also influences the location of the development of corrosion. The side facing down, against the wood, is more prone to the carbonyl corrosion as noted in several of the collections. One partially stripped Osiris votive figurine in the British Museum BM8 displayed blue corrosion on the underside resting on cotton wool in the wooden drawer (Appendix 14.3) (Figure 5.26). The bronzes in the Petrie Museum are still stored in their original wooden cabinets with tight fitting doors allowing minimal air circulation.

Figure 5.26 Saqqara Osiris from which blue corrosion sample BM8 was removed, (photo Alice Boccia Paterakis, field of view is approximately 12 cm across, © Trustees of the British Museum)

In the absence of evidence attesting to the placement of these bronzes in wooden shrines before burial and considering the lack of comprehensive treatment records, one may conclude that post-excavation modern storage in wood is the most likely cause for the formation of the acetates and formates documented in this study.

5.5.3 Detection of Acetates, Formates and Sodium

Analytical techniques such as X-ray Diffraction (XRD), Fourier Transform Infrared Spectroscopy (FTIR), Raman Spectroscopy, and Ion Chromatography (IC) are recommended for the identification of carbonyl corrosion. More than one technique is often required to realize identification or characterization. X-ray Diffraction was used for the analysis of corrosion in the case studies based on permission granted by the Getty Conservation Institute in Los Angeles. Confirmation of some of these identifications was achieved by the analysis of three Saqqara objects by Raman Spectroscopy by Dr. Wang in the British Museum. Her study emphasizes the usefulness of analytical techniques in addition to XRD in order to characterize carbonyl corrosion (Wang *et al*. 2009).

If these sophisticated and costly analytical techniques are beyond the reach of museums other, more modest, means are available for the detection of acetates, formates, and sodium in the form of spot tests, colorimetric tests, and precipitation tests (Feigl 1972; Halsbergh *et al.* 2005) (Appendix 17).

5.5.4 Cu-Sn-Pb Alloys

A lead-containing compound in a mixed corrosion sample first of all indicates a substantial lead component in the bronze. The importance of lead on the corrosion behavior of leaded bronze was examined in Chapters 3 and 4 and in section 5.3.3.1.2 in Chapter 5 regarding sodium lead carbonate hydroxide. Leaded bronze has a greater affinity for adsorbing water than does unleaded bronze. Therefore the presence of lead may promote the formation of an aqueous layer on the surface of the object that will facilitate the corrosion of lead.

It was found in the experimental work of this project that a layer of lead oxide on the surface of leaded bronze can or may help protect the copper from attack by acetic acid in low to moderate levels of acid concentration. There are indications that conservation treatments with sodium sesquicarbonate may reduce the protective qualities of the lead oxide layer. Lead may act also as a sacrificial sink by corroding preferentially thereby protecting the copper from attack. The minimum concentration level of acetic acid vapour that will destroy the lead oxide layer, allowing for the formation of carbonyl compounds to occur, has not been determined. Lead oxide was maintained during exposure of the leaded bronze to 0.4 ppm and perhaps to 4 ppm acetic acid vapour concentration at 52% RH whereas hydrocerrusite (a stable by-product of carbonyl corrosion of lead) was found at the higher RH of 86% in 4.0 ppm acetic acid vapour. This would indicate that a minimum ppm acetic acid level greater than 0.4 ppm is required to destroy the protective lead oxide layer at 52% RH. The absence of hydrocerrusite at 0.4 ppm and 4.0 ppm acetic acid vapour in 52% RH and the presence of hydrocerrustie at 4.0 ppm in 86% RH indicates that the carboxylic acid-induced corrosion cycles are promoted by high relative humidities.

Lead undergoes a corrosion cycle under the influence of acetic acid and high relative humidity that generates acetate ions (Niklasson 2005, Paterakis 2007, 98). During the exposure of lead to acetic acid vapour of concentration greater than 0.4 ppm, in this case in 4 ppm at 86% RH, lead acetate formed first as a transitional product resulting in the stable lead carbonate hydroxide (hydrocerussite) that is normally found on lead exposed to carboxylic acids. The combination of lead carbonate hydroxide with a

sodium contaminant resulted in sodium lead carbonate hydroxide on an Egyptian statuette of Imhotep (E.55.1954) in the Fitzwilliam Museum (Appendix 13.4).

This study has shown that method of manufacture, i.e. cast versus hammered, does not seem to be a determining factor in the final formation of carbonyl corrosion compounds on bronze. The lead content of cast bronze normally exceeds that of sheet bronze since lead is added to facilitate the casting process. Carbonyl compounds have been found on both. Nor does the presence of a core in a cast object seem to be a requirement for the development of carbonyl corrosion. The retention by the core material of residual contaminants or conservation chemicals may contribute to the formation of corrosion but is not a requirement. Today conservators avoid treating bronze objects preserving a core by immersion.

The Pb concentration and distribution of lead in the alloy will influence the form, rate, and extent of corrosion of all components of the alloy and will ultimately dictate the extent of degradation of the object by carboxylic acid. The higher the lead content the greater the potential for extensive corrosion damage.

5.5.5 Museums housing the Bronzes (Table 5.2)

Corrosion types were compared by museum to determine any patterns or trends in conservation treatment or storage conditions that consistently lead to acetate corrosion products, but numbers of analyses are too low to permit definite conclusions (Table 5.2). The Petrie and Ashmolean museums demonstrated some consistency in occurrence of corrosion species. Copper sodium formate acetate was found on most of the objects analysed in the Petrie (5 out of 7) and a sodium copper carbonate acetate was found on all four objects analysed in the Ashmolean. Some similarity could be based on conservation treatments particular to those museums but more likely would be similarity in storage conditions, i.e. wood species used in construction, volatile acidic concentration, and temperature and RH in the storage cabinets. The heartwood of chestnut, elm, and fir released 500 to 1600 ppm acetic acid of dried wood and 40 to 200 ppm formic acid of dried wood (after incubation for 6 months at 48° C and 100% RH) (Arni 1965, 463). The Petrie and Ashmolean museums both have records indicating storage problems in the recent past.

Table 5.2 Number of Objects identified with Corrosion by Museum

	Copper sodium formate acetate	A Sodium copper carbonate acetate	Chalconatronite	Sodium acetate	Total number objects with un-identified corrosion	Number of objects with mixed (more than one) compounds	Total number objects sampled
Petrie Museum	5	1	4	0	5	5	7
Fitzwilliam Museum	2	3	0	0	5	4	7
Liverpool Museums	1	5	1	1	4	5	6
Ashmolean Museum		4	1	0	0	2	4
British Museum	1	6	2	2	1	6	9
Agora Excavation * 1999 2003 2006		4-1999 1-2003 1-2006	1-2003	1-1999	1-2003 2-2006	2-2003 1-2006	5-1999 2 -2003 2-2006
TOTAL	9	25	9	4	18	25	42

* Analytical results of objects sampled in 1999 are published in Paterakis 2003, 313-339

Table 5.3 Museum Storage Conditions and Overall Dose Estimates Acetic Acid

Museum	Case materials	RH% (estimate)	Recorded ppm acetic acid	Time of storage (estimate)	Overall dose acetic acid (estimate) using 0.6 ppm average concentration
British Museum	mahogany cases until 1997	± 30% - 60%	nr	33 years	19.8 ppm yr
	mahogany cases 1997 -2004	low RH	0.4-1.12		
	metal cases since 2004	± 30% - 60%	nr		
Liverpool	card, plywood, hardboard boxes until 2000	± 30% - 60%	0.6-0.7	31 years	18.6 ppm yr
	open metal shelves since 2000	± 48%			
Petrie	wood	± 30% - 60%	nr	37 years	22.2 ppm yr
Ashmolean	wood	± 30% - 60%	nr	37 years	22.2 ppm yr
Fitzwilliam	wood until 1990	± 30% - 60%	nr	14 - 99 years	8.4 – 59.4 ppm yr (average 33.9 ppm yr)
	Dexion metal shelves 1990-2003	± 35%			
	metal cases since 2003	± 35%			
Athenian Agora	wood and plywood	± 40% - 80%	0.4-0.5	67 years	40.2 ppm yr

nr = not recorded

Using 0.6 ppm as an average based on recorded concentrations in museums, the dose was estimated for all the museums (Table 5.3). The dose estimates range from 18.6 ppm yr to 40.2 ppm yr. The average overall dose estimate for the 6 museums is 26.15 ppm yr, far exceeding the LOAED (the lowest observed adverse effect dose) of acetic acid for copper and lead (0.4 ppm yr for Cu and 0.024 ppm yr for Pb at 50% RH). This average dose is similar to the dose range of acetic acid (22 to 29 ppm yr) which caused the formation of acetate compounds on archaeological bronze patina in corrosion Test Series II (Section 4.3) in Chapter 4. The initial acid concentrations, when the cases were first built, may have been higher than the recorded levels after decades of offgasing. Temperature and relative humidity have been found to play a direct role in acidic emissions from wooden cases, increased levels promote offgasing and increased emission rates of acetic acid (Thickett *et al.* 1998).

5.5.6 Saqqara Bronzes

The Saqqara bronzes were listed according to site location and date of excavation to determine any meaningful trends with corrosion identification (Appendix 15). On limited available data there appears to be no consistency between site location or date of excavation of the Saqqara bronzes and species of corrosion. Knowledge of the excavation date, however, assists in narrowing down the range of possible conservation treatments and materials that may have been applied.

The corrosion on 22 bronzes from Saqqara was analysed in this study (Appendix 15). From the total number of objects analysed, more than one compound (mixed compounds) was found on 13 objects, a sodium copper carbonate acetate was found on 12, sodium acetate was found on 2, copper sodium formate acetate was found on 5, chalconatronite was found on 6, and unidentified compounds were found on 6 objects (Figure 5.27). Expressed as percentages based on the total of 22 objects analysed more than one compound (mixed compounds) was identified on 59% of the objects, a sodium copper carbonate acetate was identified on 54% of the objects, and compounds were present on 27% of the objects that could not be identified (Appendix 15, Figure 5.27).

A similar distribution of corrosion can be seen comparing the Saqqara bronzes (Figure 5.27) to all bronzes analysed (Figure 5.25), the Saqqara bronzes making up 52% of the total 42 objects. The only noticeable difference being fewer unidentified

compounds on the Saqqara objects (27% versus 43%). This could be interpreted to indicate fewer mixed compounds on the Saqqara bronzes. The mixtures typically represented various combinations of two or more compounds including a sodium copper carbonate, sodium acetate, copper sodium formate acetate, chalconatronite, and unidentified compound(s).

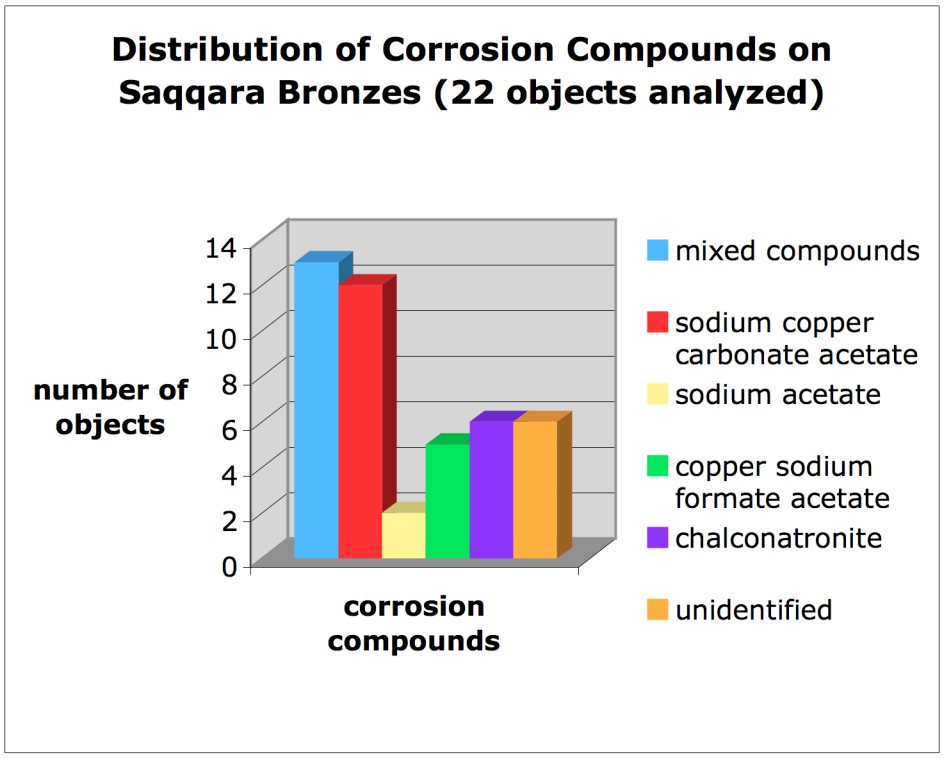

Figure 5.27 Distribution of corrosion on Saqqara bronzes

Very few conservation records exist for the Saqqara bronzes. Given the arid and alkaline nature of the burial conditions in Saqqara, adequate sodium may have been present in burial as sodium carbonate (Gettens and Frondel 1955) or sodium chloride (Thickett 1998) without the introduction of conservation chemicals for these reactions to occur. British Museum objects BM5 and BM6 carry chalconatronite that is the result of burial and not conservation treatment according to archaeologist Jeffrey Spencer (Appendix 13.3) (J. Spencer pers comm. 2007). However, too few conservation records exist; the absence of a conservation record does not confirm the lack of treatment. Of those objects found to carry chalconatronite in this study, with the exception of objects BM5 and BM6, we cannot know if the chalconatronite derives from burial in the saline soil or from treatment with sodium conservation compounds, or both. The possibility of their treatment in the field with alkaline Rochelle salt may have added to the sodium present from burial (J. Spencer pers comm. 2007). Reaction of acetic and formic acid

emissions (from the wooden cabinets in which these objects were stored) with the copper, cuprite, malachite, chalconatronite (from burial or conservation treatment), and sodium contaminant of the objects produced the carbonyl compounds found (Appendix 15). There are many significant independent variables such as specific burial conditions, and unfortunately many missing data on past conservation.

Chapter 6 Protective Coatings

6.1 Introduction

Coatings have been used to protect metal artifacts and works of art for centuries. In the early years before the development of polymer science natural organic materials, waxes in particular, were used. Synthetic waxes and polymers, in solution, emulsion, or dispersion, have replaced most natural organic coating materials. Improvements have been made to prolong the life of coatings thereby rendering them less prone to aging and, therefore, reversible for longer periods of time.

The provenance and condition of the object, its genre (decorative or archaeological), age, and location of display or storage are all factors that influence the choice of coating material. Outdoor conditions (weathering) are more extreme causing aging and breakdown of coatings at a faster rate than most indoor conditions. This factor must be taken into account in the coating maintenance of outdoor metals and in many cases requires more frequent removal and/or reapplication of coatings.

Coatings are normally applied after the artifacts have gone through the conservation process that includes stabilization of corrosion activity. Stabilization often involves the application of a corrosion inhibitor that may sometimes be included in the coating material as well. Coatings are viewed as a means of protecting the object from continued corrosion as a barrier, by sealing the surface from oxidation and moisture. Few coating materials are completely impervious to the permeation of oxygen and moisture, however. Coatings are also intended to protect the objects from other aggressive atmospheric elements such as Volatile Organic Compounds (VOCs) and ultraviolet light (UV) and from the secretions of skin during handling. Coating thicknesses for industrial purposes are measured in millimeters, 1 mm being a typical recommendation (Brown 1977, 226). Coating thickness for application on museum artifacts or works of art is usually minimal to limit discoloration. Horie brought the industrial use of polymers into the museums (Horie 2003).

In a review of coatings for archaeological bronzes two materials stand out as those most commonly used worldwide in the second half of the 20th century and early 21st century: Incralac® and Renaissance Wax®. Incralac® was developed in the 1960's

as a protective lacquer for outdoor copper and Renaissance Wax® was developed in the 1960s in the United Kingdom as a protective coating for many materials including metals. The formulation of Incralac® has changed throughout the decades of its use and is currently based on Paraloid B44, an ethyl methacrylate-butyl acrylate copolymer, with the corrosion inhibitor Benzotriazole (BTA) (Rocca *et al*. 2007, 310). Renaissance Wax is based on the formulation invented by Dr. Tony Werner in the British Museum and is a mixture of microcrystalline and polyethylene waxes (Plenderleith and Werner 1971). Much research has been carried out on the adoption of synthetic waxes as protective coatings on metal (Horie 2003; Otieno-Alego *et al*. 1998a; Otieno-Alego *et al*. 1998b; Rocca *et al*. 2007). One of the most desirable properties of coating materials has been used to promote the products to conservators: reversibility. Various grades of the Paraloid acrylates, in particular B72 and B44, have been commonly used in museums as 5 to 10% solutions for the past several decades and continue in use today to protect the objects from moisture and handling. The greatest challenge presented by the application of corrosion inhibitors and barrier coatings is achieving a homogeneous layer devoid of pits, holes, and discontinuities. Figure 6.7 depicts a SEM image of a cracked and irregular layer of a 15% solution of Paraloid B72 on a steel test coupon (Cano *et al*. 2010). The behavior and shortcomings of coating materials are examined in more detail in subsequent sections.

The characteristics, aging properties, and causes of failure of coatings are introduced followed by an examination of their permeation properties. The mechanisms of loss of adhesion are analysed and the causes are attributed to various diffusion processes and electrochemical reactions (Kinloch 1987). Polymers are characterized and two polymers were selected for experimental testing as protective coatings on bronze: one popular conservation lacquer of longstanding use (Incralac®) and one relatively new polymer (Poligen®), not as yet applied to original artifacts.

The experiment testing the protective qualities of the two coatings on bronze involved exposure to the aggressive elements of volatile acetic acid and high relative humidity for an 8-week period (Section 6.5). The tests were run by Dr. Emilio Cano in an environmental chamber in the certified laboratory of the Centro Nacional de Investigaciones Metalúrgicas (CENIM), CSIC, Madrid, Spain. Facilities at the Getty Conservation Institute were not available for these tests for reasons explained in Chapter 4 (Section 4.2.2). The experimental conditions of 4 ppm acetic acid and 86% RH were

chosen to match those in test # 10 of Test Series I: Part One carried out at the Getty Conservation Institute (Table 4.4) and Test Series I: Part Two carried out in the Madrid lab (Table 4.20) in Chapter 4. The same two copper alloys were used in the testing: tin bronze ASTM B584 and leaded tin bronze ASTM B505 (Table 4.1). Following application of the coatings to the surface of the test coupons the edges and reverse of the test coupons were masked with an epoxy resin to avoid edge effects. The coating on each test coupon was scribed following ASTM D1654-05, Standard Method of Evaluation of Painted or Coated Specimens Subjected to Corrosive Environments, before exposure to corrosive conditions (ASTM 2005). The coatings in the scribed areas and adjacent, unscribed areas were evaluated according to ASTM D1654-05. Optical microscopy was used to examine the condition of the films before and after corrosion testing. A comparison was established between the protective properties of intact coating next to damaged coating. Results are presented, damage mechanisms are discussed, and conclusions are drawn.

6.1.1 Characteristics

"An organic coating is principally effective in preventing corrosion of the substrate by acting as a barrier to corrosion processes." (Koehler 1981, 87). Loss of adhesion is attributed to water displacement that is intensified by pH values and to a greater affinity of the metal oxide for water than for the organic coating (Koehler 1981, 87). The rate determining step in the corrosion of an organic coated metal is related to the resistance of the organic coating to one (or more) these factors: 1) corrosion current flow, 2) diffusion of water, 3) diffusion of oxygen (Koehler 1981, 87). To facilitate and prolong the protective qualities of coatings on artifacts museums monitor and regulate the relative humidity and oxygen content in display and storage cases. Coatings also protect against handling.

6.1.2 Aging Properties

According to Holsworth (Holsworth 1982, 4), the following physical and chemical reactions can cause changes in polymers:

1) loss of plasticizers and solvents by volatilization or leaching;
2) oxidation catalyzed by catalyst residues of susceptible groups;
3) polymer chain breakage in the coating;

4) disassociation of side groups from the polymer chain;
5) reactions of residual double bonds (reactive groups);
6) decomposition of plasticizers and pigments by chemical reactions;
7) reactions in the new residues or groups formed;
8) deformation and stress of the coating caused by dimensional changes in the substrate from moisture or temperature changes. These can be triggered or accelerated by oxygen, ozone, humidity, and atmospheric contaminants (Holsworth 1982, 4).

Exposure to high levels of acetic acid and relative humidity may encourage many of the chemical and physical reactions in polymer coatings cited above. The endurance of two coatings to chemical and physical degradation that can occur during exposure to high levels of acetic acid and relative humidity were tested in Section 6.5.

6.1.3 Causes of Failure

There are four basic ways in which a coating can fail to be protective (Heitz 1992, 132). Intact coatings can fail if adhesion is reduced or lost by chemical or electrochemical reactions at the metal/coating interface. Defects or holes in the coating can allow pitting corrosion to occur in the metal substrate. Cathodic disbonding and blister formation can also cause failure (Heitz 1992, 132). These phenomena will be examined in more detail in the following sections. It is important to realize that good adhesion does not guarantee corrosion protection (Heitz 1992, 132). This emphasizes the short-lived protective qualities of protective coatings on art objects and artifacts and the need for their periodic removal and replacement. The goal of the conservator is to apply a homogeneous, uniform coating free of defects that is well-adhered to the substrate and that may be removed and reapplied when necessary.

6.2 Permeation Properties of Coatings

6.2.1 Introduction

To examine the protective qualities of polymer coatings on metal the permeation of coatings must be examined. Permeation may be defined as the passage of gases, vapours, liquids, and ions through the coating (Yaseen 1981, 24). Prolonged exposure to UV and moisture can disrupt this protection (Yaseen 1981, 24). Permeation of polymer

coatings is influenced by 1) moisture levels, 2) temperature, 3) degree of crosslinking, 4) intermolecular spacings, 5) total free energy levels in the molecular structures, 6) as well as thickness and application procedures (Yaseen 1981, 26). Water plays a major role in the permeation of polymer coatings. Generally, not enough of the background theory seems to have guided museum applications of protective coatings. The publication Materials for Conservation has assisted conservators in the adoption of protective coatings in museums (Horie 2003). For example, surface preparation before application of coatings may only consist of first degreasing the surface with acetone. However, even such simple removal of contaminants is often not used in museums. Lower concentrations are often used in museums to prevent a glossy surface forming thinner coatings and fumed silica is often added to reduce sheen forming a bulked, rough coating that is more susceptible to physical disruption.

6.2.2 Water – Liquid and Vapour

Water can be present in "a bound state or as a separate phase (cluster)" in polymers (Johnson *et al.* 1981, 10). Under normal conditions polymers contain water in the bound state. Coatings swell as water is absorbed either from the vapour or liquid state resulting in less resistance to the passage of contaminants. The high RH of 86% was chosen for my experimental work in Section 6.5 to enhance corrosivity of the acetic acid vapour during the 8-week test. Absolute humidity indicates the total amount of water available in the atmosphere and the relative humidity (RH) influences condensation on the coating surface (Holsworth 1982, 5). Water absorption by the coating depends on 1) length of exposure to water; 2) temperature; 3) coating thickness; 4) polarization conditions (Schwenk 1981, 103). Absorption of water has a plasticizing effect on polymers and can alter their glass transition temperature (Tg). The Tg of an amorphous polymer can be lowered by the influence of water (Johnson *et al.* 1981,10). Cluster formation occurs by water saturation of the polymer resulting in weakening of the polymer (Johnson *et al.* 1981, 10). Elevated temperatures are usually necessary for water saturation to occur, in the case of amorphous polymers temperatures must exceed the Tg (Johnson *et al.* 1981, 10). The Tgs of many polymers used as coating materials in conservation range from 30° to 80° C. Increases in temperature accelerate the permeation of water vapour, more so in pigmented polymer coatings than in clear polymer coatings (Yaseen 1981, 26). The physical state of the polymer determines the influence of water on Tg. Since polyethylene is a polycrystalline polymer the absorption of water will not

lower its Tg (Johnson *et al.* 1981,10). The more crosslinked the polymer the greater the impedence in degree and rate of permeation of water vapour (Yaseen 1981, 26).

6.2.3 Ions

The effects of external factors on the permeation of ions through coatings differ from those of water vapour. For example, increases in temperature do not accelerate the permeation of ions (Yaseen 1981, 27). The movement of ions through coatings requires more energy than for water vapour (Yaseen 1981, 27). The properties of ionic permeability and water vapour permeability are interrelated in coatings (Yaseen 1981, 27). Charges form on the surface of coatings when in contact with water or electrolytic solutions, sometimes functioning as "permselective membranes" (Yaseen 1981, 24). These charges can impede the permeation of ions (Yaseen 1981, 27).

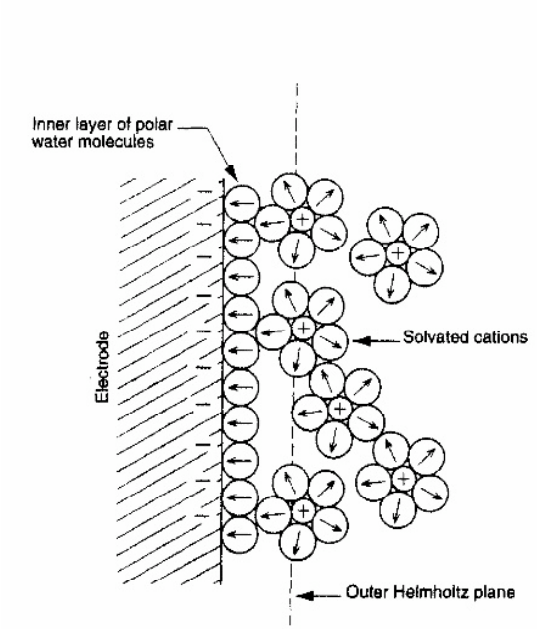

Figure 6.1 Formation of water on surface of metal (Jones 1996, fig. 2.1, 41)

Figure 6.1 illustrates the formation of a water coating on the uncoated metal surface that protects the surface from attack by ions. The H_2O molecules "are attracted to the conductive surface (of the metal) forming an oriented solvent layer, which prevents close approach of charged species (ions) from the bulk solution." (Jones 1996, 40). "The plane of closest approach of positively charged cations to the negatively charged metal surface is often referred to as the outer Helmholtz plane…" that limits electrochemical reactions at the surface (Figure 6.1).

The ionic permeability of a coating without defects or pores equals the DC conductivity (Schwenk 1981, 103). Prolonged exposure to UV and moisture, however, can disrupt this protection (Yaseen 1981, 24). Ionic permeability also pertains to gas (Koehler 1981, 95). Sulfur dioxide can penetrate a coating and react with water and oxygen forming sulfate ions (Koehler 1981, 95). One of the goals of my experimental work in Section 6.5 was to determine the ionic permeability of two coatings exposed to acetic acid vapour.

6.2.4 Crosslinking of Coatings

Polymer coatings have been found to be inhomogeneous and can differ in their protective behavior depending on thickness, degree of crosslinking, and conductivity (Mills 1981, 12). Some areas that are more crosslinked may be more protective. Less crosslinked areas are prone to high water uptake and are less protective of the metal substrate. These areas are more prone to corrosion. Conductivity of the coating will vary according to the degree of crosslinking (Mills 1981, 15). Exposure to corrosive conditions such as those used in my experimental section 6.5 can cause a reduction in the degree of crosslinking in the polymer coatings with subsequent increased risk of corrosion of the underlying metal. The physical and chemical reactions triggered by high acetic acid vapour concentration and relative humidity may allow greater water absorption and increased conductivity of the coating resulting in increased corrosion of the metal substrate.

Regarding the prevention of the formation of less crosslinked films, the method of application of the coating does not seem to affect the degree of crosslinking (Mills 1981, 13). The application of several coats as opposed to one coat was found to provide better protection and, in general, the thicker the film the more protective it will be (Mills 1981, 14).

6.3 Loss of Adhesion

6.3.1 Introduction

Five different mechanisms of adhesion loss of coatings on metal may be distinguished:
1) Osmosis
2) H_2O diffusion
3) cathodic electroosmosis
4) cathodic polarization
5) anodic polarization (Schwenk 1981, 104).

Osmosis will be examined first. Enhanced H_2O diffusion occurs in a temperature gradient of metals used in high temperatures (Schwenk 1981, 104) and does not pertain to archaeological and decorative arts bronzes in collections. The influence of moisture on coatings was examined in Section 6.2.2. The electrochemical reactions of cathodic electroosmosis, cathodic polarization, and anodic polarization affect the quality and soundness of the coatings. The consequences of adhesion loss will be examined according to the morphology of the coating detachment and its effects on the protective qualities of the coating.

6.3.2 Mechanisms of Adhesion Loss

6.3.2.1 Osmosis

Osmosis may be defined as the "movement of a solvent (as water) through a semipermeable membrane … into a solution of higher solute concentration that tends to equalize the concentrations of solute on the two sides of the membrane." (Merriam-Webster 2009). Osmosis does not involve the application of an electric field or an electric potential. Blistering of the coating is caused by water permeation through osmosis. Osmotic blisters can occur if the metal surface is contaminated with salt or other hydrophilic substances before the coating is applied, and then exposed to water or high humidity (Heitz 1992, 132). Migration of water to the salt particle occurs due to osmotic pressure between the salt solution and pure water. The greater the difference in salt concentration between the two solutions, the greater the osmotic pressure will be.

The pH of the salt solution in osmotic blisters depends on the type of salt (hydrolysis) (Heitz 1992, 133). Osmosis may be associated with electrochemical reactions.

6.3.2.2 Electrochemical Reactions

"…all aqueous corrosion reactions are considered to be electrochemical." (Jones 1996, 7). Most involve water or moisture but occasionally a metal may behave as a solid state electrolyte (Jones 1996, 7). The three mechanisms involved in the adhesion loss of coatings, cathodic electroosmosis, cathodic polarization, and anodic polarization, involve electrochemical reactions and are considered in the following review of electrochemistry.

Once the permeating substances, water or ions, reach the metal/coating interface electrochemical reactions are triggered. Electrochemical cells are established that consist of two metal electrodes, an anode and cathode, and an electrolytic solution that serves as an ionic conductor.

The electrolyte is the "… layer of water … between the organic coating and the metal oxide substrate" and is termed an "interfacial" water layer (Figure 6.1) (Koehler 1981, 93). The electrolyte serves as an ionic conductor in the electrochemical cell and influences the rate of detachment of the coating (Koehler 1981, 93). The thickness of the "interfacial" water layer will be influenced by the relative humidity (Koehler 1981, 93). "…the rate of … detachment is controlled by the interfacial conductance." (Koeher 1981, 93). The thicker the layer of water (electrolyte) the faster the detachment process (Koehler 1981, 93). The nature of the organic coating and the metal influence underfilm corrosion currents (Koeher 1981,93).

There are five categories of the "interfacial" water layer:
"1) That which always remains firmly adsorbed to a metal oxide surface.
2) Water adsorbed at the oxide-coating interface from the environment, below that level permitting mechanical detachment of the coating (i.e. detachment doesn't occur).
3) A layer of interfacial water of sufficient 'thickness' to permit mechanical detachment of the coating (i.e. doesn't involve corrosion).
4) A film of sensible water beneath the organic coating.
5) A liquid filled blister." (Koehler 1981, 94).

Oxidation occurs at the anode and reduction occurs at the cathode. On coated metals the anodic reactions result in pitting corrosion and anodic blisters; cathodic reactions consist of de-adhesion and cathodic blisters (Heitz 1992, 131). These forms of disbondment occur preferentially at coating defects and intentional scribes in coatings (where oxygen is more available) (Jones 1996, 491).

It is not uncommon for the interfacial water layer to vary from area to area in thickness and category according to Koehler's classifications (Koehler 1981, 94). Coatings most likely come in contact with water in category 1 and perhaps with the metal oxide film in places (Koehler 1981, 94). An increase in water in the category 1 areas would contribute to a loss in adhesive strength (Koehler 1981, 94). Category 2 is to be expected for an organic coating (Koehler 1981, 94). The conduction currents are reported to be "appreciable" for well-bonded coatings of category 2 (Koehler 1981, 95). Categories 4 and 5 represent corrosion that produces failure of the coating.

In the case of coatings with mechanical damage or pores thereby exposing the underlying metal, electrochemical reactions can form more easily in the presence of ions. Three electrolytic reactions occur at the metal/coating interface when ions permeate the coating. Cathodic disbondment occurs from the formation of alkaline OH^- by cathodic reduction of dissolved oxygen:

$$O_2 + 2H_2O + 4e^- \rightarrow 4OH^-$$

The examples that illustrate these reactions in the literature are based on iron. Examples illustrating copper could not be located. Therefore the following reaction, equations (1) – (3), and Figures 6.2, 6.3, and 6.6 are based on iron.

The anodic reaction (on iron) is:

$$Fe \rightarrow Fe^{2+} + 2e^-$$

that occurs at the coating defect (Jones 1996, 490).

The following is an example of the reactions when Na and Cl attack steel (Schwenk 1981, 104):

(1) $Fe - 2e^- + 2\ Cl^- + H_2O = (Fe(OH)^+ + Cl^-) + (H^+ + Cl^-)$

(2) $O_2 + 4e^- + 4Na^+ + 2\ H_2O = 4\ (Na^+ + OH^-)$

(3) $2H_2O + 2e^- + 2\ Na^+ = 2\ (Na^+ + OH^-) + H_2$

The left side of these equations represents the polarization current and the ionic migration; the right side contains the reaction products (that establish the pH) (Schwenk 1981, 104). Equation (1) represents anodic blisters and equations (2) and (3) represent cathodic blisters.

In coatings with a high permeability for ions, the coated areas form the cathode and the defects become the anode. O_2 and H_2O permeating the coating set up cathodic areas and cause minimum corrosion under the film (Figure 6.2).

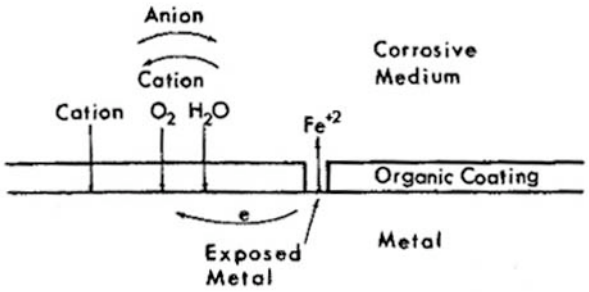

Figure 6.2 Coated metal acts as a cathode, defect in coating acts as the anode (Koehler 1981, Fig. 1, 88)

Figure 6.3 illustrates the same process introducing sodium into the reaction. Sodium hydroxide forms under the coating and the metal dissolves at the anode producing pitting. The cathodic reaction products cause loss of adhesion and blistering (Schwenk 1981, 103). To summarize the corrosion of metal with defective coatings, the coated metal serves as the cathode and the uncoated metal at a defect in the coating serves as the anode. This causes cathodic blistering under the intact coating and pitting in the metal at the defect (Schwenk 1981, 105).

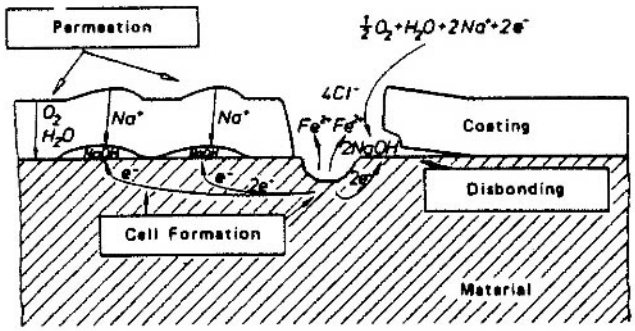

Figure 6.3 Coating acts as cathode, defect in coating acts as anode (Schwenk 1981, Fig. 1, p. 103)

Care in the handling, transport, and storage of coated metal artifacts and artworks is vital to maintain an intact, uncompromised coating for protection against corrosion. The morphology of the metal surface and smoothness of the coating applied will influence the preservation of the intact coating. As mentioned earlier, polymer coatings containing fumed silica (usually added as a matting agent) tend to provide a rougher surface increasing the risk of coating disruption during handling. Polyethylene foam materials are commonly used in the museum today providing a soft, protective support during packing of the artifact for transport or storage.

6.3.2.2.1 Cathodic Electroosmosis – Cathodic Blistering

Electroosmosis is defined as "the movement of a liquid through a capillary tubing or porous solid driven by an electrical potential difference." (http://electrochem 2009). In cathodic electroosmosis "hydroxyl ions are formed by the electrochemical reduction of oxygen or water" at the cathode (Heitz 1992, 132). For the reaction to continue cations (Na^+) must diffuse through the coating. The electrochemical reactions in equations (2) and (3) above generate OH^- at the cathode contributing to the alkalinity of the blisters. The "migration of alkali cations" (e.g. potassium and sodium) also contributes to this (Schwenk 1981, 104). Sodium acetate forms cathodic blisters on steel with a pH up to 12 (Schwenk 1981, 107). Cathodic electroosmosis is the driving force of cathodic blistering; an alkaline solution is "transferred to the metal/coating interface cathodically" (Schwenk 1981, 104). Cathodic blisters occur where the coating functions as a cathode. This can occur in the cathodic blisters resulting in disbonding. The water-soluble reaction products cause the transport of water by osmosis and osmosis causes the growth of blisters in coatings (Schwenk 1981, 104). Cathodic blisters are not corrosive.

6.3.2.2.2 Cathodic Polarization – Cathodic Disbonding

Polarization is defined as "the change of potential of an electrode from its equilibrium potential upon the application of a current." (http://electrochem 2009). In cathodic polarization the ions travel from one electrode to the other through the coating/metal water interface. Cathodic disbonding is caused by the development of high alkalinity by a cathodic reaction. Cathodic disbonding can occur at the rim of holidays (defects in the coating) resulting in the formation of liquid under the coating at the cathode, with subsequent peeling of the coating from the metal (Schwenk 1981, 108) (Figure 6.3). This peeling of the coating caused by the alkaline cathodic reaction can be retarded by neutralization in the presence of acid (Schwenk 1981, 109). This peeling of the coating is a manifestation of cathodic disbonding (Schwenk 1981, 103).

6.3.2.2.3 Anodic Polarization – Anodic Detachment and Blistering

Anions (e.g. chloride) cause anodic detachment, blistering and corrosion of the metal surface (Koehler 1981, 95; Schwenk 1981, 109). Anodic blisters occur in anodic areas of coatings. "Hydrogen ions are formed as the result of anodic dissolution of the metal and of hydrolysis of the corrosion products…" (Heitz 1992, 133). The contents of anodic blisters are weakly acidic. These electrochemical reactions depend on the simultaneous permeation of anions (e.g. Cl^-) through the coating (Heitz 1992, 133). The greater the electrical resistance of the coating, the smaller the tendency for the formation of anodic blisters (Heitz 1992, 133). An example of an anodic blister may be seen in Figure 6.4.

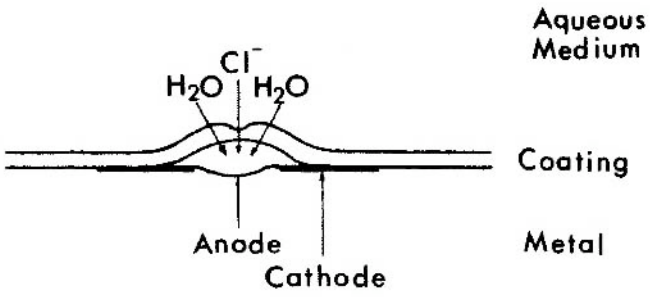

Figure 6.4 Anodic blister formation (Koehler 1981, Fig. 15, 93)

Chloride ions permeated the thinner areas of the coating, the iron oxidized forming ferrous chloride, followed by water permeation of the coating by osmosis forming a blister. The acidic ferrous chloride established the blister as anodic and the surrounding metal under the coating became the cathode. A pH of less than 4 is required for the ferrous iron to be sufficiently soluble in water to cause detachment of the coating (Koehler 1981, 94). Contaminants on the surface of the metal prior to coating could cause a similar corrosion mechanism (Koehler 1981, 94).

One type of anodic detachment involves the dissolution (i.e. corrosion) of a thin layer of metal, caused by the ingress of an aggressive anion (e.g. Cl^-), under the coating thereby forming a hollow in the surface of the metal (Figure 6.5).

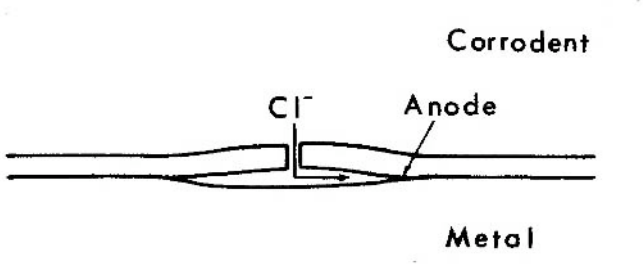

Figure 6.5 Anodic corrosion and dissolution of metal surface (Koehler 1981, Fig. 14, 93)

The corrosion that occurs on the exposed metal in coated metals that have been scribed, as in ASTM D1654-05, is presented as an example. An illustration of the corrosion of a scribed area on coated copper could not be located so an illustration showing iron is presented here (Figure 6.6). The build up of anodic corrosion products causes oxide lifting to occur, similar to filiform corrosion (Jones 1996, 490). “Both result in a build up of compact corrosion products in crevices or at the interface between coating and metal.” (Jones 1996, 491). A nantokite (copper chloride) layer in archaeological copper alloys would complicate this corrosion process (Figure 5.2).

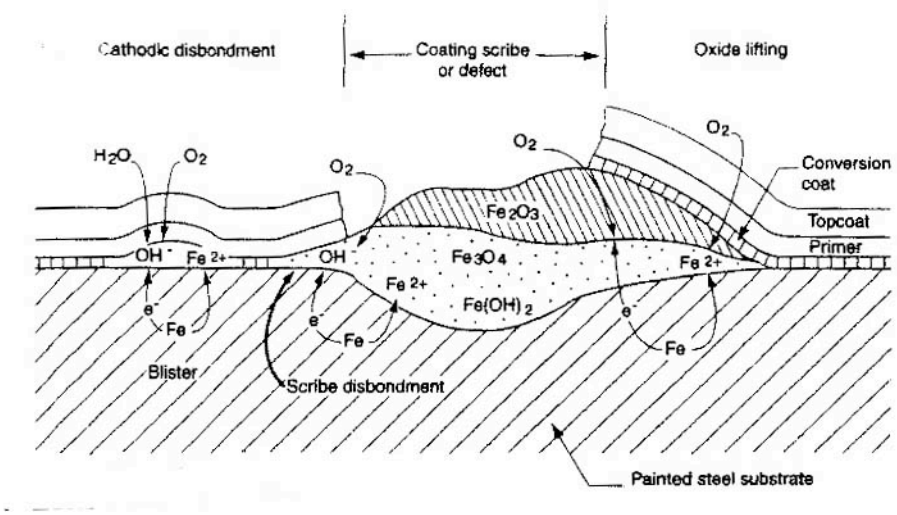

Figure 6.6 Corrosive attack mechanisms at the scribe in the coating (Jones 1996, Fig. 14.7, 491)

6.3.2.2.4 Comparison of Anodic and Cathodic Blistering

Anodic blistering is encouraged by anodic polarization and cathodic blistering is encouraged by cathodic polarization (Schwenk 1981, 108). Both anodic and cathodic blisters may coexist on the same metal (Schwenk 1981, 108). Anodic and cathodic blisters may be distinguished by their pH. Anodic and cathodic blistering are characterized by critical potential ranges that can overlap (Schwenk 1981, 108). Anodic blisters are typically smaller than cathodic blisters since cathodic blisters are caused by water enrichment during electroosmosis resulting in the depletion of water from the anodic blisters (Schwenk 1981, 107).

Atmospheric pollutants, such as SO_2, become hydrated, forming acids, such as sulphuric acid, that increase "the activity of the anodic reaction, the general atmospheric corrosion rate, and the breakdown of coatings at defects." (Jones 1996, 491). The influence of acetic acid on coated bronze was tested in Experimental Section 6.5.

6.3.2.2.5 Electrochemical Testing

Electrochemical methods have been devised to evaluate coatings on metals. Electrochemical impedance spectroscopy (EIS) can detect degradation of coatings that falls outside the scope of this project (Jones 1996, 494).

6.3.3 The Role of Detachment Morphology on the Protective Qualities of Coatings

It is important to distinguish between disbonding, blistering, and peeling since they have very different consequences on the protection of metal. Disbonding represents varying degrees of detachment, peeling is the physical loss of the coating from the surface, and blistering is the uplifting of the coating. There is no correlation between the disbonding, blistering, peeling caused by a cathodic reaction and corrosiveness since the cathode is alkaline and, therefore, not corrosive to metals (Schwenk 1981, 110).

A coating that is blistering or disbonding can still be protective as long as the associated solution is not corrosive (Schwenk 1981, 110). If the blisters are open or the coating is peeling off the surfance protection is lost (Schwenk 1981, 110). Some degree of adhesion of the organic coating to the substrate should be maintained, excellent adhesion does not guarantee protection (Koehler 1981, 87). It is important for conservators to realize that the degree of adhesion to the surface is not as crucial as maintaining an intact, uncompromised coating layer.

6.4 Polymers

6.4.1 Introduction

Various polymers have been used as protective coatings on metals since their first formulation. The characteristics and properties of polymer coatings most sought after by conservators for protecting metal artworks and antiquities are as follows:

- Ease of applicability
- Reversibllity
- Low toxicity
- Suitable aesthetic qualities
- Transparency
- Non-yellowing

Most polymers adopted by conservators have been designed for industrial use and therefore must be selected with caution after thorough investigation of their properties. These investigations often involve corrosion testing on new metal. However, coatings on

uncorroded surfaces are not always comparable to coatings applied to archaeological or museum objects. Archaeological metals are candidates for extensive corrosion based on their burial environment. Most objects in collections and museums are characterized by some degree of corrosion unless they have been chemically stripped and coated immediately. Chemical stripping of archaeological metals was a practice carried out in the first half of the 20th century but is no longer acceptable today. Applying a coating to the surface of a corroded object presents many challenges not encountered with a smooth, uncorroded metal surface. A raised and irregular surface morphology creates voids that can be difficult to penetrate with the coating thereby increasing the difficulty in achieving a homogeneous and intact layer. The roughness of the surface increases the risk for mechanical damage to the coating through handling.

6.4.2 Characteristics

A polymer is "a macromolecule formed by the chemical union of five or more identical combining units called monomers." (Hawley 1981, 834). Synthetic polymers can consist of less than 5 monomers: dimers (2), trimers (3), and tetramers (4).

The synthetic polymers, often referred to as plastics, can be classified into three categories: thermoplastic polymers (thermoplasts); thermosetting polymers (thermosets); and elastomers (rubbers) (Schweitzer 2004, 470). Thermoplasts are defined as "long-chain linear molecules that can be formed by heat and pressure" above their glass transition temperature (Tg) (Schweitzer 2004, 470). Polymers are not characterized by a specific corrosion rate and may be attacked solvation or chemical reaction (Schweitzer 2004, 470). Solvation is defined as "the penetration of the plastic by a corrodent, which causes softening, swelling, and ultimate failure." (Schweitzer 2004, 470). The various attack mechanisms of plastics are dehydration, radiation, oxidation, hydrolysis, physical disintegration, thermal degradation, or a combination of these (Schweitzer 2004, 471).

6.4.3 Polymers chosen as Coatings for Corrosion Testing

Two synthetic polymers chosen for this study are thermoplasts. One is a synthetic polymer in solution (Incralac®) and the other is a synthetic polymer wax in emulsion form (Poligen®). Incralac® was chosen since it has been used on copper and copper alloys to protect against corrosion since the 1960s and continues to be used today.

Poligen® was chosen for its hydrophobic properties and for the fact that it has been tested as a new polymer coating material on metals by the European consortium PROMET (Innovative Conservation Approaches for Monitoring and Protecting Ancient and Historic Metals Collections from the Mediterranean Basin) with promising results. Waxes have been applied on top of acrylic coatings such as Incralac® on metals for both indoor and outdoor bronzes for years. The application of Renaissance Wax® on top of Incralac® has been adopted for years in the conservation of bronze (Plenderleith and Werner 1971). The wax is easier to apply to a coating of acrylic, it helps consolidate any gaps and defects in the barrier coating, and it serves to waterproof the surface. The influence of RH on the corrosivity of acetic acid to metal and the solubility in water of some acetate corrosion compounds that form on metal justify the selection of a hydrophobic wax as a protective coating for bronze subjects subjected to acetic acid vapour.

6.4.3.1 Polymer Solutions

One advantage of polymer solutions is that the rate of drying can be controlled by the choice of solvent(s). Another advantage is that the polymer concentration may be altered in the solutions whereas it is fixed in emulsions (Table 6.2, Solids Content %).

6.4.3.1.1 Acrylics

Acrylic polymers have been used by conservators for decades for coating metals. “The high molecular weight of the acrylic-based polymers provides good resistance (to corrosion)” (Rocca and Mirambet 2007, 310). Acrylics (solvent base) demonstrate fair resistance to acidic conditions, good resistance to alkalis, solvents, and water, and very good resistance to weathering (Jones 1996, 480). Commonly used acrylics have been the Paraloids (Rohm & Haas), the most popular have been Paraloid B72, an ethyl/methacrylate, and Paraloid B44, an ethyl methacrylate/butylacrylate copolymer in the protective lacquer Incralac® (Appendix 19).

6.4.3.1.2 Incralac®

Description

Incralac® contains an acrylic-based polymer that has been used on copper and copper alloys to protect against corrosion from handling and bronze disease since the 1960s. It is still very popular among conservators today for the treatment of archaeological and decorative bronzes, both indoors and outdoors. Incralac® was originally developed by the International Copper Research Association as a protective coating for new copper outdoors. The formulation of Incralac® appears to have changed over time. In 1984 and 1985 it was reported to consist of Paraloid B-44, an ethyl acrylate-methyl methacrylate copolymer, with Paraplex G-60 as a leveling agent (an epoxidized soyabean oil) (Erhardt *et al*. 1984, 84.22.2; Stambolov 1985, 114). In 2007 it was reported to be an ethyl methacrylate-butyl acrylate copolymer (Paraloid B44) plus benzotriazole (BTA) as corrosion inhibitor and/or UV protector (Rocca and Mirambet 2007, 310).

The BTA in Incralac® is a chelating agent that functions both as a corrosion inhibitor and protects the Incralac® from deterioration caused by the diffusion of copper ions into the lacquer (Erhardt *et al*. 1984, 84.22.2). Concentration of BTA has been found to decrease markedly in aged Incralac® (Brown 1977). Outdoors volatilization of the BTA in the Incralac® takes place so that after 5 to 6 years the inhibitor was found to be mostly ineffective (Brown 1977).

Application as a Conservation Material on Copper and Copper Alloys

INCRA, the company that invented Incralac®, tested various finishes for metal and found the acrylic polymers to be the best for maintenance finishes outdoors since they were claimed to be insensitive to UV and reversible (Brown 1977, 226). When combined with BTA and solvents that do not contain oxygen (e.g. toluene, xylene), they were reported to last five to ten years with a minimum coating thickness of 1 mm required (Brown 1977, 226). This represents a very thick industrial coating, much thicker than is used on museum objects. Barrier coatings on museum objects are typically made with 5% polymer solutions such as Paraloid B72 or Paraloid B44 that produce much thinner films (see Section 7.3.2.1 in Chapter 7). These museum coatings are measured in terms of micrometers (μm), not millimeters (mm) (Table 6.1). Standardized tests for protective coatings on metals, such as ASTM D1654-05

(Standard Method of Evaluation of Painted or Coated Specimens Subjected to Corrosive Environments) do not specify a required coating thickness. It is stated that Incralac®, indoors, should last indefinitely (a claim not substantiated by data) (Brown 1977, 226).

Failure of Incralac® on Copper and Copper Alloys

UV absorption of Incralac® was found to increase on aging, either due to the reaction products of degradation or to absorption of UV absorbing pollutants (Erhardt *et al*. 1984, 84.22.2). Incralac® on outdoor bronzes by itself and as part of multiple coating system was tested by Ellingson *et al*. 2004 (Rocca and Mirambet 2007, 310). The acrylic polymer in Incralac® was found to be permeable to water (De Witte 1973/74, 144; Rocca and Mirambet 2007, 310). Weak adhesion between Incralac® and the bronze substrate was found to allow corrosion to take place at the interface (Rocca and Mirambet 2007, 310).

In another study Incralac® was found to fail as a coating on outdoor bronze after ten years becoming insoluble. It was removed by swelling with solvents followed by water-blasting (Erhardt *et al*. 1984, 84.22.2.). Insolubility is attributed to the cross-linking of polymer chains that is a result of exposure to UV (Erhardt *et al*. 1984, 84.22.3). Mechanical failure of the film was attributed to mechanical stress. The Tg of Paraloid B44 in Incralac® is 60° C. The coefficient of thermal expansion of acrylics is approximately five times that of copper alloys. "Changes in temperature cause differential contraction or expansion of Incralac® and the metal and puts stress in the Incralac®. Crosslinking increases brittleness thereby encouraging failure under conditions of temperature change." (Erhardt *et al*. 1984, 84.22.3). Thermal extremes plus crosslinking are the causes cited for the mechanical failure of the coating on outdoor sculpture (Erhardt *et al*. 1984, 84.22.3).

Aging Tests of Incralac® Coating without Metal Substrate

De Witte ran accelerated aging tests on Incralac®, Paraloid B72, polyvinyl acetates, and other coatings as test films (not on metal substrate) by exposing them to hydrogen sulphide and to the light of a xenon arc (De Witte 1973/74). Incralac® was found to be permeable to water, water vapour, and hydrogen sulphide (De Witte 1973/74, 144). Distensibility was lost after aging and the films were harder according to

pencil hardness and softer according to Clemen Hardness Tester (De Witte 1973/74, 146). New and aged Incralac® showed good abrasion resistance (De Witte 1973/74, 147). Incralac® lost some adhesion and elasticity upon aging (De Witte 1973/74, 148). Aged Incralac® was found to be soluble (swelled) only in dimethyl formamide.

Aging Tests of Incralac® on Other Metals

Lane tested Incralac®, Paraloid B72, and microcrystalline wax on lead objects under conditions of accelerated corrosion to mimic unsuitable storage conditions (Lane 1980). Lead objects were placed in a flask with a trace of acetic acid, moisture and carbon at 60 C for one week (Lane 1980, p.55). After testing all objects were covered with a uniform layer of corrosion. Incralac® was found to accelerate corrosion on lead objects compared to uncoated lead objects. Incralac® and Paraloid B72 preserved surface detail whereas microcrystalline wax did not. None of the coatings tested prevented corrosion (Lane 1980, 54). Overall the coatings were found to accelerate the corrosion (Lane 1980, 54).

Incralac® has also found application as a protective coating on silver. Silver coated with Incralac®, Frigilene (cellulose nitrate), and Monarch Shield silicone lacquer was tested for protection against tarnish, ease of application, and resistance to abrasion (Moncrieff 1966, 7). Incralac® was found to give the best results in each category (Moncrieff 1966, 7).

6.4.3.2 Synthetic Polymer Waxes

Synthetic polymer waxes are thermoplasts. Since waxed-based coatings are reversible and transparent they lend themselves to conservation (Rocca and Mirambet 2007, 311). Synthetic waxes are recommended over organic waxes since the latter can produce organic acids in the presence of moisture (Rocca and Mirambet 2007, 311). Microcrystalline and polyethylene waxes were developed for industrial purposes and not specifically for the conservation of artefacts. For this reason these waxes have been tested on uncorroded and corroded bronze (Price *et al*. 1995). It was found that the method of application plays a major role in film morphology that in turn determines the protective quality of the wax coating. Wax coatings were tested on artificially patinated

bronze and it was found that each type of patina requires its own type of wax for the best corrosion protection (Otieno-Alego *et al*. 1998b, 315-319).

6.4.3.2.1 Polyethylene

Polyethylene (PE) was first used in conservation in the 1950s as a moisture vapour barrier for panel paintings (Horie 2003, 88). Polyethylene $(H_2C{:}CH_2)_x$ is composed of the carbon-hydrogen bond and is made by polymerizing ethylene gas (Horie 2003, 85).

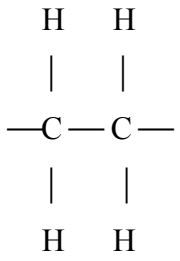

The characteristics of polyethylene depend on its "molecular structure and crystallinity, molecular weight, and molecular weight distribution." (Schweitzer 2004, 474). Density is related to the molecular structure and indicates the properties of the polymer. Increasing density follows increasing percentage crystallinity and increasing hardness in a close to linear fashion (Horie 2003, 87). High Density Polyethylene (HDPE) has greater percentage crystallinity, greater density, and greater hardness than Low Density Polyethylene (LDPE) (Horie 2003, 87). High molecular weight (HMW) and ultra high molecular weight (UHMW) are the two forms of polyethylene most often used for corrosion resistance. "Polyethylene is resistant to most mineral acids, including sulfuric up to 70% concentration; inorganic salts, including chlorides; alkalies; and many organic acids." (Schweitzer 2004, 474). UHMW PE is compatible with 10% and 50% acetic acid up to a temperature of 140 F (60 C), and with 80% acetic acid up to 80 F (27 C) (Schweitzer 2004, 468). However, it is subject to degradation by photo and light oxidation from UV. It does not support biological growth (Schweitzer 2004, 467). The specific gravity of low-density PE is 0.91-0.925, medium-density is 0.926-0.940, and high density is 0.941-0.959. The low molecular weight (LMW) grade has an average m.w. of 24,000 and a softening point of 108° C (Horie 2003, 86). The high molecular weight (HMW) grade has an average m.w. of 200,000-500,000 with a softening point of 130 C (Horie 2003, 86; Schweitzer 2004, 467), the ultra high molecular weight

(UHMW) grade has an average m.w. of 3.1 million (Schweitzer 2004, 467). PE has a low Tg, -20º C (Horie 2003, 87,182). PE is not soluble in solvents at room temperature and must be heated to melt the crystalline areas (Horie 2003, 87). Solvents for PE are trichloroethylene, methyl cyclohexane, and tetrachloromethane that cause PE to swell at room temperature (Horie 2003, 87).

Polyethylene Wax and Polyethylene Wax Emulsions

Wax is a low molecular version of PE (Horie 2003, 85). Paraffin wax and microcrystalline wax are PE waxes. PE wax is soluble up to 20% at room temperature (Horie 2003, 87). "PE and (PE) waxes are inert to aqueous chemicals and to many organic solvents." (Horie 2003, 87). Photo-oxidation of PE and PE waxes causes "crosslinking, embrittlement and discoloration." (Horie 2003, 87).

6.4.3.2.2 Poligen® ES 91009

Poligen® is a polyethylene wax in emulsion form. An emulsion is described as "a stable mixture of two or more immiscible liquids held in suspension by small percentages of substances called emulsifiers." (Hawley 1981, 409). "All emulsions are comprised of a continuous phase and a disperse phase…" (Hawley 1981, 409). Water serves as one of the phases. "An emulsion sets to a film, first by loss of the dispersant, usually water, and then by coalescence of the small polymer particles. In order for this to happen the particles must by soft enough to flow into one another." (Horie 2003, 5). Horie uses the term emulsion interchangeably with dispersion and claims that dispersion is the correct term to use (Horie 2003, 28). However, a description of dispersion states the opposite: the polymer particles are the dispersant in the bulk substance (water) that is the continuous phase (Hawley 1981, 385). Most dispersion polymers are made from a polymer or copolymer of high molecular weight or one that may be cross-linked (Horie 2003, 29). Dispersions consist of polymer(s), water, an emulsifying agent, and an initiator (Horie 2003, 29). The emulsifiers used in their formulation are described as neutral (poly(vinyl alcohol) or cellulose ethers) or ionic (sodium carboxymethyl cellulose or poly(acrylic acid) (Horie 2003, 29). A major distinction between dispersions and solutions is that up to 70% of polymer can be held in a stable dispersion at very low viscosities (Horie 2003, 29). To increase the viscosity of dispersions water-soluble polymers or solvents that swell the polymer particles may be added (Horie 2003, 29).

Dispersions may be considered more complex than solutions since their aging properties are harder to predict due to the emulsifier contaminants (Horie 2003, 29). In order for emulsions to solidify into a coherent film the temperature of application must exceed the Tg of the polymer. Additives may be added to the dispersion to lower the Tg of the polymer, such as solvents and plasticizers (Horie 2003, 29). The minimum film-formation temperature (MFFT) is defined as "the lowest temperature at which a coherent film is created…" (Horie 2003, 29. Two important properties of dispersions are the MFFT of the liquid dispersion and the Tg of the solidified film (Horie 2003, 29).

Description

Poligen® ES 91009 is manufactured by BASF as a coating for metal and paper and for use in wastewater treatment (BASF 2004). It is reported by the manufacturer to be an emulsion free of catalyst residues, transparent, self-emulsifying, micronized, and surfactant-free (BASF 2006). Neither the solubility data, the MFTT, nor the Tg are provided by the manufacturer (Table 6.2).

Experimental - Poligen® ES 91009

Poligen® ES 91009 was selected as a new polymer coating material for testing by a European consortium, PROMET (Innovative Conservation Approaches for Monitoring and Protecting Ancient and Historic Metals Collections from the Mediterranean Basin) was a research project funded by the 6th Framework Program of the European Union, with the participation of 21 partners from 11 different countries from the Mediterranean Basin (Egypt, France, Greece, Italy, Jordan, Malta, Morocco, Spain, Syrian Arab Republic and Turkey and also the Czech Republic), with the aim of developing new techniques and materials to improve the conservation of the metallic cultural heritage (PROMET 2009). This project resulted in the following three published case studies regarding Poligen® ES 91009 (Cano *et al*. 2007; Cano *et al*. 2010; Siatou *et al*. 2007, 115-120).

Case Study No. 1 – Comparison of Poligen® ES 91009 and Paraloid B72 by SEM

Corrosion tests were run by Siatou *et al*. of Poligen® ES 91009 and Paraloid B72 on pure, uncorroded copper and corroded brass (approx. 84% Cu, 6% Zn, 5.0% Pb, 5.0%

Sn) (Siatou *et al*. 2007, 115-120). The pure copper was degreased in acetone before exposure. The brass was prepared for the tests by artificially patinating the surface forming brochantite (copper sulfate hydroxide), antlerite (copper sulfate hydroxide), and $Cu_2(OH)_3NO_3$ (copper nitrate hydroxide). The loose corrosion products were removed from the corroded brass before coating with Poligen® since it was found that discoloration, cracking and exfoliation of the film occurred wherever there were loose green corrosion products. Brown corrosion products did not produce this effect.

Poligen® was applied by immersion and the coupons were dried flat in a fumehood for 24 hours (constitutes accelerated drying). Coated and uncoated coupons were tested in the climatic chamber with cycling RH. Coupons were placed on a Plexiglas rack at 20 to 30 degrees to the vertical during corrosion tests. Exposure consisted of 30 dry/wet cycles: 16 hr at 90% RH followed by 8 hr at 55% RH, 24 hour duration, totaling 30 days. There were longer periods of 55% RH on the weekends when the climatic chamber was not operating. Control coupons of each category were exposed to stable conditions of average room temperature and RH (not specified).

Siatou *et al*. (2007) after testing evaluated the coupons in the center, not within 1 cm of the edges, to avoid problems of edge effects (Siatou *et al*. 2007, 118). Examination by SEM revealed the Poligen® films to be "membrane-like, tightly adhered to the substrate and follow(ing) the underlying uneven surface of the coupon." Alloy spots appeared on the metal surface under the Paraloid B72 but not under the Poligen® during corrosion tests. This implies that Poligen® afforded better protection than Paraloid B72.

Case Study No. 2 – Comparison of Poligen®, Renaissance Wax, and Paraloid B72 using Electrochemical Techniques

Cano *et al*. (2007) evaluated Poligen® ES 91009 with and without corrosion inhibitors, Paraloid B72 (ethyl/methacrylate copolymer) solution with and without corrosion inhibitors, and Renaissance Wax (Cosmolloid 80 hard and BASF A microcrystalline waxes in paste form). These coatings were tested on polished, clean steel and on pre-corroded steel by the electrochemical techniques of polarization resistance (R_p) and electrochemical impedance spectroscopy (EIS) (Cano *et al*. 2007). They were applied by brushing.

Cano *et al*. (2007) determined that the polarization results and the EIS results were in agreement (Cano *et al*. 2007, 125). SEM examination showed that the Poligen® coating on both the polished and pre-corroded coupons was intact without any signs of defects after immersion in the electrolyte solutions (Cano *et al*. 2007, 124, 125). Poligen® was more protective when corrosion inhibitor M370 (ammonium salt of tricarboxylic acid by Cortec Co.) was added. The Paraloid B72 on pre-corroded steel showed cracking. Renaissance Wax gave the worst performance of all.

Case Study No. 3 – Comparison of Poligen®, Renaissance Wax, and Paraloid B72 using Electrochemical Techniques (continued with other experimental variables)

Cano *et al*. (2010) compared the effectiveness of different application methods and the addition of corrosion inhibitors to Poligen®, Renaissance Wax, and Paraloid B72 as protective coatings on steel (Cano *et al*. 2010). This represents a continuation of the research presented in Case Study No. 2. Different corrosion inhibitors and a different application method were introduced in the 2010 study. The corrosion inhibitors tested were a blend of triazoles (M435), an ammonium salt of tricarboxylic acid (M370), a calcium sulphonate (M109), and a bis-oxazoline (Alkaterge-TTM) (Cano *et al*. 2010, 453). Poligen® ES 91009 and Renaissance Wax were used as commercially supplied and Paraloid B72 was applied as a 15% solution (volume) in acetone. The application techniques of brushing and immersion, both commonly used by conservators, were tested. Application by brushing consisted of two layers. The thickness of the coatings was measured with an Elcometer 300 thickness gauge. The reported thickness is the average of 20 points per specimen. A high standard deviation in coating thickness measurements was determined.

The coatings were evaluated with the electrochemical techniques of polarization resistance (R_p), corrosion potential (E_{corr}), and electrochemical impedance spectroscopy (EIS). Application by immersion produced much thicker coatings of Poligen® and Renaissance Wax whereas little change in thickness occurred with Paraloid B72 (Table 6.1). Cano *et al*. (2010) report that immersion gave a more uniform coating than brushing. Comparing the application by brushing, Poligen® produced the most uniform surface, Paraloid B72 shows brush strokes, cracks and irregularities, and Renaissance Wax produced a rough surface (Figure 6.7).

Table 6.1 Thickness of Protective Coatings based on Cano *et al*. (2010)

Coating Material	Clean metal surface by brushing	Corroded metal surface by immersion	Clean metal surface by immersion
Renaissance Wax*	1 μm	4 μm and 16 μm	3 μm
Poligen® ES 91009*	1 μm	27 μm and 42 μm	23 μm
Paraloid B72[1]	7 μm	6 μm and 7 μm	7 μm

* as commercially supplied; [1] 15% solution (volume) in acetone; from Cano *et al*. 2010, Table 1, 455

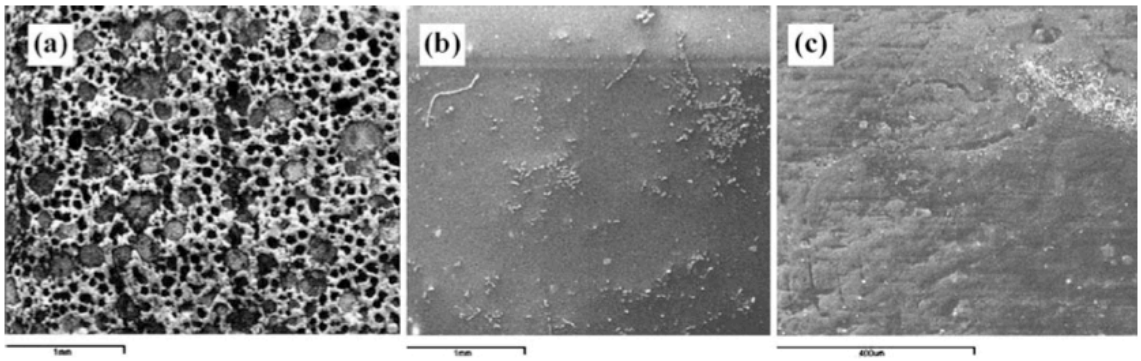

Figure 6.7 SEM photos of Renaissance Wax (a), Poligen® ES 91009 (b), Paraloid B72 (15% solution vol. in acetone) (c) each applied by brushing 2 coats on clean steel coupons (With kind permission from Springer Science+Business Media: *J. Solid State Electrochemistry,* Electrochemical characterization of organic coatings for protection of historic steel artifacts, vol. 14, 2010, p. 460, Cano, E., Bastidas, D.M., Argyropoulos, V., Fajardo, S., Siatou, A., Bastidas, J.M. and Degrigny, C., Fig. 8).

The electrochemical techniques for evaluation of the coatings showed the thickest layer of Poligen® without corrsion inhibitors to be the most protective, followed by Paraloid. Renaissance Wax offered the least protection (Cano *et al*. 2010, 462). The corrosion inhibitors were not found to enhance the protective qualities of the coatings and in some cases decreased their protective function.

These studies revealed several advantages of Poligen®. Poligen® coatings gave good protection with a thickness about one half the thickness of the Paraloid B72 coating (Cano *et al*. 2007, 125) and even better protection in thicker layers (Cano *et al*. 2010, 462). Also, Poligen® gave a more uniform coating than Paraloid B72 (Cano *et al*. 2007, 125) and provided a more aesthetically pleasing surface that was less plastic in appearance and less shiny than Paraloid (Cano *et al*. 2010, 462). Overall Poligen® 91009 was found to be a promising coating for the protection of metal artifacts (copper, brass, and steel in these case studies).

Table 6.2 Physical Properties of Incralac® and Poligen® ES 91009

Properties	Incralac ®	Poligen® ES 91009
Chemical nature	ethyl methacrylate -butyl acrylate copolymer (Paraloid® B44) in toluene (40.1 wt.%), xylene (40.9 wt.%), methyl ethyl ketone (4 wt.%) with benzotriazole as corrosion inhibitor/UV protector*	polyethylene wax emulsion made from a polymer based on ethene in water
Color	Transparent	Transparent
Solids content (%)	15%	20-22
Tg	60˚ C (Paraloid® B44)	NA
pH	NA	8-9.5
Refractive Index	1.89 (Paraloid® B44)	NA
Viscosity (ISO 2431 cup 4 mm, 23˚ C)	NA	15-150 s
Flow time	NA	25-100 s (23˚ C)
LD-Wert/LT-value (%)(= lichtdurchlässigkeit/translucence)	NA	80-95
Freezing point (capillary tube method)	NA	0˚ C
Freeze-thaw stability	NA	Protect from frost
Average particle size	NA	NA
Density (g/cm^3) (23˚ C)	NA	0.98 - 1.0
Boiling Point	NA	100˚ C
Flash point	NA	> 100˚ C
Applications	Protective coatings for metals	1)Additive for coatings e.g. metal, glass; 2) additive for water-based adhesives; 3) resistance to corrosion: e.g. on metal
Boiling point/range	82-115˚ C	100˚ C
Vapour density	Heavier than air	NA
Evaporation rate	Slower than butyl acetate	NA
VOC content (wt.)	83.2 %	NA

NA = not available
Poligen® information obtained from BASF Safety Data Sheet Poligen® ES 91009 and online brochure FK/EVD 532 d/e Aug. 2006 (2006) from www.basf.com/detergents-formulators. Incralac® information obtained from MSDS for Incralac® manufactured by StanChem. Inc., East Berlin, CT 06023 and from Cameo for Paraloid® B44 (http://cameo.mfa.org).

6.5 Experimental

Testing the protective qualities of the two coatings on bronze involved exposure to the aggressive elements of volatile acetic acid and high relative humidity for an 8-week period. Two copper alloys were subjected to corrosion testing in high levels of acetic acid and relative humidity in Chapter 4 resulting in extensive corrosion. The coating tests in Chapter 6 are an extension of the corrosion tests in Chapter 4 since they were carried out on the same two alloys in the same test conditions. The goal was to test

the protectiveness of coatings under the same corrosive conditions in order to be able to recommend protective coatings for conservation. The tests were run by Dr. Emilio Cano in an environmental chamber in the certified laboratory of the Centro Nacional de Investigaciones Metalúrgicas (CENIM), CSIC, Madrid, Spain.

6.5.1 Aim

The aim of the corrosion test on bronze was to determine the protective qualities of two coatings against the aggressive nature of volatile emissions of acetic acid in high levels of relative humidity. The experimental conditions were chosen to simulate storage of bronze in wooden cupboards under accelerated corrosive conditions. The acceleration is required in order to produce results within the time frame of the test. The aim is to "induce the same mechanisms of degradation" as in the field (Jones 1996, 488). "…the protectiveness of coating systems can be compared in the conditions of an accelerated laboratory test…" but the ranking of coatings based on accelerated tests do not compare well with real time field tests (Jones 1996, 488).

These tests may be considered an extension of the corrosion tests reported in Chapter 4 based on replication of experimental conditions and copper alloy compositions. The experimental conditions of 4 ppm acetic acid and 86% RH reproduce those of test #10 of Test Series I: Part One in Chapter 4 (Table 4.4, Chapter 4). The same two copper alloys were used as well, tin bronze ASTM B584 (C91100) and leaded tin bronze ASTM B505 (C93400) (Table 4.1, Chapter 4).

6.5.2 Selection of Coatings used in Testing

The acrylic copolymer, Incralac®, and the ethylene copolymer (polyethylene) wax emulsion, Poligen® ES 91009, were chosen to test their protective qualities against acetic acid vapour concentrations on copper alloys. Incralac® was chosen since it has been used for decades by conservators for the protection of decorative and archaeological bronze, both indoors and outdoors, and continues to be used today. Incralac® consists 40% (wt.) Paraloid B44, an acrylic polymer commonly used in a 5 to 10% solution as a protective, barrier coating for archaeological metals (Table 6.2).

Poligen® was chosen for its hydrophobic properties since acetic acid is very reactive on metal in high levels of relative humidity and some acetate corrosion compounds have hydrophilic properties (Table 7.3; Appendix 7.2). Therefore Poligen® may protect uncorroded metal from acetic acid vapour attack and it may prevent ongoing chemical reactions in acetate corrosion on the surface of metals. Poligen® has produced promising results as a protective coating in tests by the European consortium PROMET (Innovative Conservation Approaches for Monitoring and Protecting Ancient and Historic Metals Collections from the Mediterranean Basin). Poligen® has not yet been accepted for use by conservators as a standard conservation material for metals.

Waxes have been applied on top of acrylic coatings such as Incralac® for both indoor and outdoor bronzes for years in the conservation of bronze (Plenderleith and Werner 1971). The hydrophobic wax offers protection by waterproofing the acrylic coating and by consolidating any defects in the barrier coating. In this study Incralac® and Poligen® were tested individually.

Incralac® as supplied (15% solution wt. to vol. in solvents) from Conservation Support Systems, P.O. Box 91746, Santa Barbara, CA 93190-1746 was used and Poligen® ES91009 (emulsion) was obtained from the manufacturer, BASF Corporation, 100 Campus Drive, Florham Park, NJ 07932.

6.5.3 Preparation of Test Coupons

6.5.3.1 Preparation of Metal for Coating

The tin bronze and leaded tin bronze were prepared in the same manner as those for the corrosion experiments in Chapter 4. The new test coupons were cut from a bar of ASTM metal with an electric saw and then wet-sanded with different grades of abrasive silicon carbide paper from grit size 240 down to 600 according to ASTM G1-03 (ASTM 2003a). The maximum dimensions were approximately 2 cm by 1.5 cm (varying in width somewhat, all narrowing at one end), and measured approximately 3 mm in thickness. They were very similar in shape and size, and therefore surface area, thereby rendering them suitable for direct comparison according to ASTM G54-84 (ASTM 1984). They were degreased with acetone prior to coating application according to ASTM G1-03 (ASTM 2003a). Removal of contaminants from the surface of metal by degreasing is

vital to prior to corrosion testing and before the application of coatings to metal objects following conservation cleaning. Residual contaminants may enhance unwanted corrosion in both cases.

6.5.3.2 Application of Coating

The coatings as supplied by the manufacture were applied with a natural bristle brush to replicate a common mode of conservation application: Incralac® as a 15% solution in solvents and Poligen® as an emulsion (Table 6.2). One coat only was applied to the central area of each test coupon avoiding the edges and was allowed to dry under average museum conditions (55% RH, 20° C) thereby avoiding accelerated drying. Approximately 0.25 ml. of coating material was applied to a surface area of approximately 0.5 x 0.5 cm. Determination of the thickness of the coatings applied was not possible due to irregularities from brush application, the meniscus phenomenon, and the unreported density of Incralac® (Table 6.2). A more controlled situation would have been required in Experimental Section 6.5 in order to calculate coating thickness. The thickness and application method of these coatings replicate conditions commonly found on museum objects. Cano *et al*. determined the thickness of two brushed layers of Paraloid B72 (an acrylate in the same family with Paraloid B44) and Poligen® ES91009 as 7μm and 1μm respectively (Table 6.1) (Cano *et al*. 2010). The diverse nature of solutions and emulsions is emphasized by the variation in thickness achieved with the Paraloid B72 (15% solids) and Poligen® (20% solids) coatings in spite of the similarity of their solids content (Cano *et al*. 2010, 455). The 1μm layer resulting from two brush coats of Poligen® in the Cano *et al*. (2010) project can be used as a rough estimate for the maximum thickness of the single brush coat of Poligen® in the Experimental work in Chapter 6 since Poligen® was used as supplied by the manufacturer in both cases. Although Incralac® contains a polymer from the Paraloid family (Paraloid B44), the Incralac® coating in the present study cannot be directly compared to the Paraloid B72 coating in the Cano *et al*. (2010) work since the polymers involved are not identical and since the solid contents of each differ considerably: the Paraloid B72 solution had a 15% (vol. to wt.) solids content and the Incralac® in the present study was a 15% solution (vol. to wt.) based on 44% wt. solids solution (Table 6.2).

6.5.3.3 Masking Areas of Exposed Metal

Approximately 8 weeks after application of the coatings all areas of exposed metal were masked with an epoxy resin according to ASTM G78-01 (ASTM 2001). The purpose of this was to avoid edge effects that can influence the performance of the coating by preferential attack during corrosion testing as specified in ASTM D1654-05 (ASTM 2005), ASTM G54-84 (ASTM 1984), ASTM D2803-03 (ASTM 2003b), and ASTM G85-02 (ASTM 2002).

Basic No-Blush transparent epoxy resin from the Progressive Epoxy Polymers, Inc. was used for this purpose (Appendix 19). The epoxy component consists of bisphenol-A-epichlorohydrin and benzyl alcohol. The hardener contains amine adduct, polyglycol diamine, and nonyl phenol (MSDS). Full curing is achieved in seven days.

6.5.3.4 Scribing of Coating

A test standard that involves scribing the coating, ASTM D1654-05, Standard Method of Evaluation of Painted or Coated Specimens Subjected to Corrosive Environments, was followed. This standard is used to evaluate coated test coupons in accelerated atmospheric exposure tests with respect to corrosion, blistering associated with corrosion, loss of adhesion at the scribe mark, and other film failure. It provides a means of comparing and evaluating the substrate and coating after exposure to corrosive environments. The coating on each test coupon was scribed with a scribing tool as described under Apparatus in D1654 after the epoxy masking resin was applied. The coatings had a total of 20 weeks to cure before being scribed. They were kept in low light levels during most of this time. The coupons were placed on Plexiglas racks during the exposure tests at an angle of 30º from the vertical so that the scratch was positioned vertically following ASTM B117-09 (ASTM 2009). This allows moisture droplets to run down along the length of the scribe during the test (ASTM D1654-05).

Filiform corrosion is known to initiate at the scribe in the temperature and relative humidity conditions used in this test and therefore presents itself as a likely corrosion candidate. Filiform corrosion “occurs under coatings on metal substrates that is characterized by a definite threadlike structure and directional growth” that initiates at the scribe according to ASTM D2803-03 (ASTM 2003b). Filiform corrosion usually

occurs between 20° and 35° C and 60 and 95% RH (ASTM D2803-03). Filiform corrosion is a "manifestation of differential aeration and crevice corrosion … under thin organic coatings" (Jones 1996, 224). Filiform corrosion moves laterally as 0.05 to 3 mm wide filaments under the coating (Jones 1996, 224). The filament is made up of an actively corroding head and an inactive tail. The head consumes oxygen while undergoing hydrolysis and acidification from 1 to 4 pH (Jones 1996, 224). "Filiform corrosion is enhanced by (soluble) atmospheric constituents … which assist acidification during differential aeration." (Jones 1996, 224). Oxygen and water migrate through defects in the coating to the corroding head of the filament.

6.5.4 Experimental Method

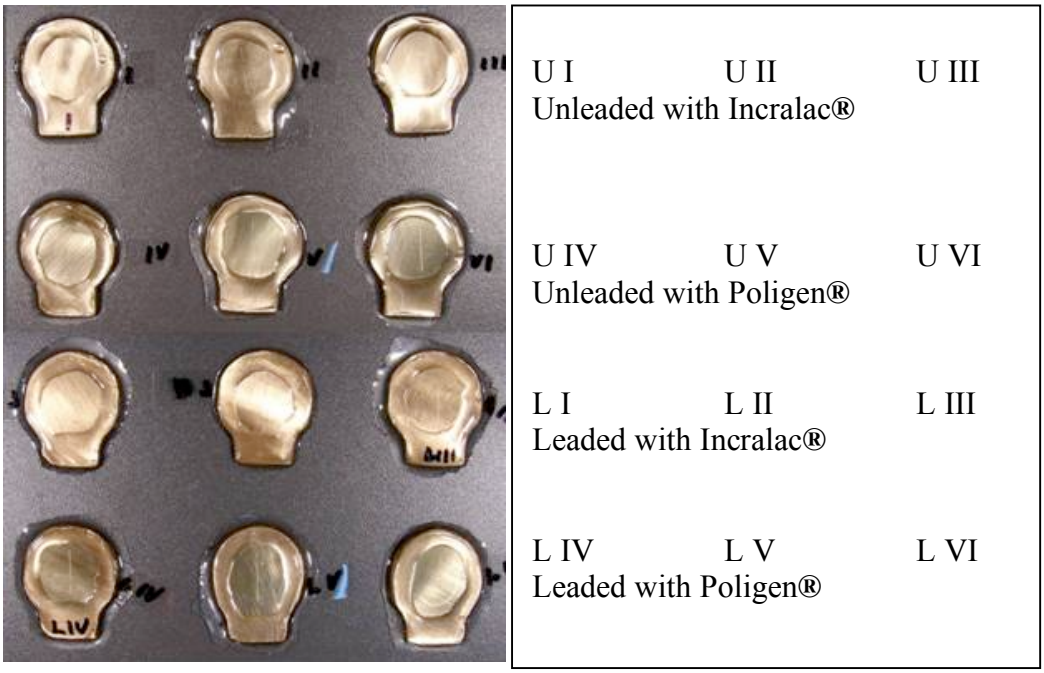

Figure 6.8 Coated coupons after scribing and prior to corrosion testing (field of view is approximately 12 cm across) (photo by Emilio Cano and Diana LaFuente)

Six leaded bronze coupons and six unleaded bronze coupons were coated with a 15% solution of Incralac® (Table 6.2). Six leaded bronze coupons and six unleaded bronze coupons were coated with Poligen® ES 91009 as supplied by the manufacturer (Table 6.2) (Figure 6.8). Half of the coupons were exposed to the corrosive conditions of acetic acid vapour in high humidity and the other half were controls exposed to high humidity without acid. The acid corrosive testing was carried out in Madrid by Dr. Emilio Cano of the Centro Nacional de Investigaciones Metalúrgicas (CENIM), CSIC, Avda. Gregorio del Amo 8, E-28040 Madrid, Spain. The control tests were carried out at the Getty Center in Los Angeles. The tests can be divided into two groups: leaded and

unleaded bronze coated with Incralac® in triplicate; leaded and unleaded bronze coated with Poligen® ES 91009 in triplicate (triplicate samples designated by ASTM G54-84). The test coupons were exposed to acetic acid vapour concentration of 4 ppm and 86% RH (±2%) at 30º C (±1º) for the duration of 8 weeks.

6.5.4.1 Generation of Controlled Humidity and Acidic Atmospheres

6.5.4.1.1 Selection of Acetic Acid Vapour Levels

Laboratory facilities at the Getty Conservation Institute were not available for the corrosion tests using acetic acid as explained in Section 4.2.2. in Chapter 4 thereby requiring the procurement of other facilities. Dr. Emilio Cano of the Centro Nacional de Investigaciones Metalúrgicas (CENIM), CSIC, offered to carry out the corrosion testing and subsequent interpretation of results in his certified laboratory. The highest level of acetic acid concentration obtainable in the laboratory's climate chamber was 4 ppm. Since this concentration represents approximately ten times that measured in museum storage on average (0.4 ppm) (Paterakis 2004) it establishes an accelerated condition that was deemed appropriate for a test of 8-week duration. 4 ppm was also chosen as it reproduces the acetic acid concentration of Test #10 of Test Series I: Part One (Section 4.2.1) and of Test Series I: Part Two (Section 4.2.2) in Chapter 4.

Figure 6.9 Test chamber (field of view is approximately 30 cm across, photo by Emilio Cano and Diana LaFuente)

6.5.4.1.2 Selection of Relative Humidity Levels

The highest level of RH used in the corrosion tests of Chapter 4 was chosen, 86% RH, to reproduce the conditions of Test #10 of Test Series I: Part One and Test Series I:

Part Two and to create extreme conditions in humidity in the absence of extreme conditions in acetic acid level. 40 ppm acetic acid in the Test Series I: Part One corrosion tests of Chapter 4 are considered extreme conditions. Since this corrosion test necessitates accelerating conditions on account of its brief duration, i.e. 8 weeks, it was important to expose the test coupons to extreme conditions. The highest level of RH (86%) was chosen since the highest acidic concentration (40 ppm) could not be obtained.

6.5.4.2 Test Chamber

The same test chamber that was used for Test Series I: Part Two (Section 4.2.2 in Chapter 4) was used to test the protective coatings. See Section 4.2.2.2.1 Test Chamber in Chapter 4 for a description of the chamber operation and Figure 4.37 for a diagram of the chamber.

The coupons were placed on Plexiglas racks during the exposure tests at an angle of 30º from the vertical so that the scratch was positioned vertically following ASTM B117-09, Standard Method of Salt Spray [Fog] Testing (Figure 6.9) (ASTM 2009). This allows moisture droplets to run down along the length of the scribe during the test (ASTM D1654-05).

The conditions were very uniform in the test chamber since the ratio of volume to exposed surface area of the test coupons was very high and because the test coupons were positioned away from the gas inlet and outlet (E. Cano pers comm. 2009).

The controls were run in a glass bell jar at room temperature using a saturated solution of sodium sulphate to maintain a RH of 86%. The bell jar remained unopened for the duration of the test at the Getty Center in Los Angeles.

6.5.4.3 Controlling and Monitoring Acidic Concentration and Relative Humidity during Testing

The means for controlling and monitoring the acid concentration and relative humidity during testing are identical with those given in Section 4.2.2.2.2 in Chapter 4.

6.5.5 Results after Corrosion Testing

Both coatings remained intact, well adhered to the metal substrate, and prevented corrosion of the underlying metal (Figure 6.10). Bulky, white corrosion formed on the exposed metal in the scribe of the leaded bronze coupons (Figures 6.11, Figure 6.12) (E. Cano pers comm. 2009). The protective films did not allow the infiltration of corrosion under these test conditions.

6.5.5.1 ASTM D1654-05

The evaluation of the scribed area of the test coupons was carried out according to Procedure A, 7.1 (Method 1, Air Blow-Off) of ASTM D1654-05, Standard Method of Evaluation of Painted or Coated Specimens Subjected to Corrosive Environments. Within 15 minutes of removing the test coupons from the test chamber they were rinsed with water. The scribed area was blasted with an air gun at a 45° angle with a pressure of 550 kPa (80 psi) to test the adhesion of the film to the metal surface. The evaluation resulted in a rating of 10 (zero creepage from the scribe) for all scribed coupons (ASTM D1654-05, Rating of Failure at Scribe Procedure A).

U I U II U III
Unleaded with Incralac®

U IV U V U VI
Unleaded with Poligen®

L I L II L III
Leaded with Incralac®

L IV L V L VI
Leaded with Poligen®

Figure 6.10 Coated coupons after testing (field of view is approximately 10 cm across). Scribed lines are a bit more evident than before corrosion testing in part due to corrosion build-up in the scribes. (Photo by Emilio Cano and Diana LaFuente).

An adjacent, unscribed area on each coated coupon was evaluated according to Procedure B of ASTM D1654-05. This procedure checks for "corrosion spots, blisters, and other types of failure". The evaluation resulted in a rating of 10 (no failure) for all test pieces (ASTM D1654-05, Rating of Unscribed Areas Procedure B).

6.5.5.2 Optical Microscopy

Optical microscopy was used to examine the condition of the films in the scribed areas before and after corrosion testing. Breaking and flaking of the Incralac® film (Figure 6.14) and deformation of the Poligen® film (Figure 6.13) were visible before the corrosion tests. These two morphologies were caused by the mechanical action of the scribe at the time of scribing and elucidate the difference in hardness between Poligen® ES 91009 and Incralac®. Numerous microscopic air bubbles are visible in the Poligen® film that formed during application of the coating by brushing (Figure 6.15).

These results compare favorably with the two case studies in which Poligen® was found to protect copper, brass, and steel from corrosion in various corrosive conditions (Section 6.4 Polymers). Incralac® provided equally successful results as a protective coating, in spite of the fact that Paraloid B44 in Incralac® is reported to be permeable to water and water vapour (DeWitte 1973/74; Rocca and Mirambet 2007, 310). Prolonged exposure to UV or thermal extremes, known to contribute to the mechanical failure of Incralac®, were not experimental variables in this test.

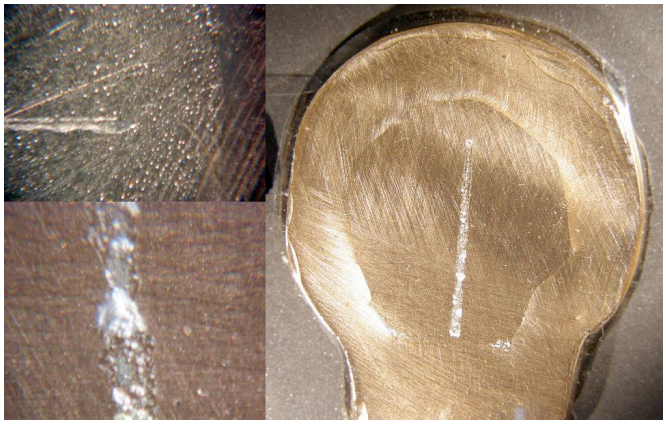

Figure 6.11 Pb-rich white corrosion in scribes of leaded coupons after corrosion testing: photo lower left (3 mm across) and right (2.5 cm across) is leaded coupon LII with Incralac®, photo upper left (10 mm across) is leaded coupon LIV with Poligen®, epoxy resin masking agent visible encircling Incralac® on leaded coupon LII (right), (photos by Emilio Cano and Diana LaFuente)

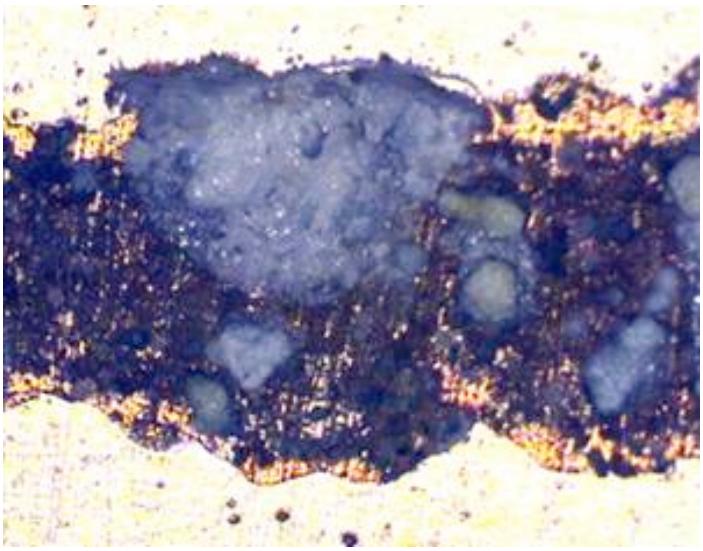

Figure 6.12 Detail of the scribe running horizontally, viewed from above, in leaded coupon LII coated with Incralac® after corrosion testing detailing Pb-rich white corrosion in top center of scribed groove (detail of righthand photo in Fig. 6.11). Upper and lower light colored horizontal borders are the unscribed, coated metal coupon surface (field of view from top to bottom is approximately 0.7 mm), (photo by Emilio Cano and Diana LaFuente)

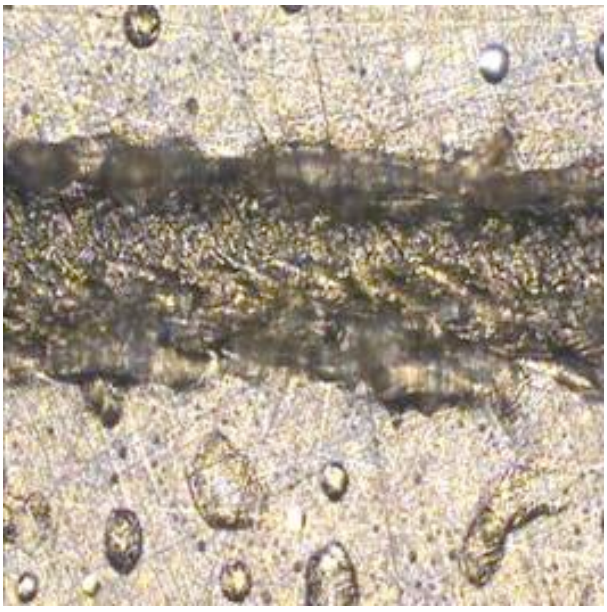

Figure 6.13 Scribe in Poligen® coating on unleaded coupon UIV before corrosion testing showing deformation of polymer layer at edges of scribed groove (field of view is approximately 1.5 mm across) (photo by Emilio Cano and Diana LaFuente)

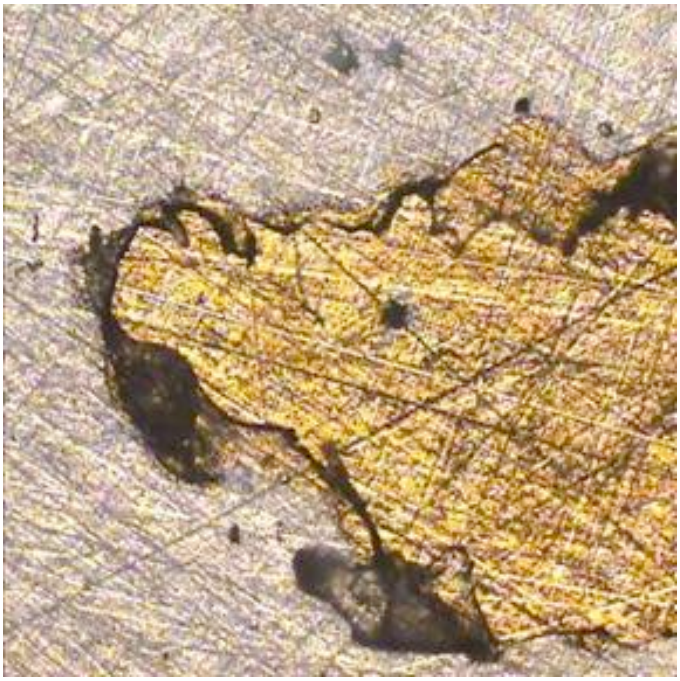

Figure 6.14 Incralac® coating chipped from scribing on unleaded coupon UI before corrosion testing, yellow area is uncoated metal coupon, scratching is below coating layer from coupon preparation (field of view is approximately 0.35 mm), (photo by Emilio Cano and Diana LaFuente)

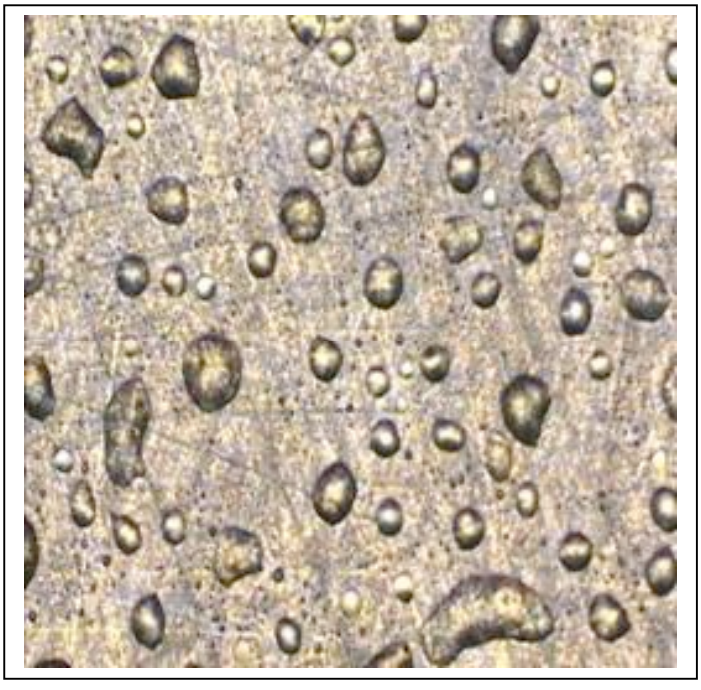

Figure 6.15 Air bubbles in Poligen® coating on unleaded coupon UIV before corrosion testing (field of view is approximately 1.5 mm), (photo by Emilio Cano and Diana LaFuente)

6.5.5.3 XRD

XRD was not carried out on the corrosion in the scribed areas. The XRD results of the corrosion on the coupons of the same alloys in Test Series I: Part Two (Chapter 4, Table 4.20), that were exposed to the same atmospheric conditions in the same test chamber for the same time period, may be used to estimate the corrosion identification on the scribed coupons. Hyrdrocerussite was found on the leaded alloy and cuprite was found on the unleaded alloy of the uncoated coupons in Chapter 4. Since the same alloys were used in the tests of coated coupons, we may assume that the bulky white corrosion in the scribed areas of the leaded coupons (Figures 6.11, 6.12) is hydrocerussite. From the formation of chlorides on all uncoated coupons in Test Series I: Part Two we know that an unidentified source of chloride contamination was present in the Madrid Test Chamber (E. Cano pers comm. 2009).

6.6 Conclusions

In the case of atmospheric corrosion, as was simulated in this corrosion test, ionic conduction through an electrolyte is the means by which corrosion occurs (Koehler 1981, 95). “Factors that play a role on corrosion and on method of coating detachment are 1) reactivity of the metal; 2) nature of the metal surface; 3) nature of the surface contaminants; 4) inhibitive pigments (in pigmented coatings); 5) coating discontinuities; 6) nature of the corrosive environment” (Koehler 1981, 94).

ASTM D1654-05 evaluation of the test coupons showed good adhesion of the coatings to the metal substrate and the prevention of corrosion of the underlying metal. Coatings swell as water is absorbed either from the vapour or liquid state resulting in less resistance to the passage of contaminants. Several factors that influence the water absorption by the coating are 1) length of exposure to water, 2) temperature, 3) coating thickness, and 4) polarization conditions (Schwenk 1981, 103). After an 8-week period of exposure to 86% relative humidity we may assume that the coatings absorbed water. We can also presume that water had been adsorbed at the oxide-coating interface but not to the point of permitting mechanical detachment of the coating (Section 6.3.2.2) (Koehler 1981, 94). Given longer exposure to the corrosive test conditions, corrosion would have infiltrated under the protective coatings from the scribed areas, most likely

taking the form of filiform corrosion or oxide lifting (Section 6.3.2.2.3) (Jones 1996, 491).

In spite of the presence of the chloride contaminant in the Madrid Test Chamber, and the fact that chloride ions may in some instances serve as a catalyst for corrosion, the coatings protected the underlying metal during the duration of the test.

Under these conditions, Poligen® ES 91009 and Incralac® performed very well as protective coatings on the two copper alloys in 4 ppm acetic acid vapour concentration and 86% RH. Given the mode of application of the coatings resulting in uneven layers the thickness of the coatings could not be determined. The irregular thickness of the brushed coatings was confirmed by Cano *et al*. (2010, 457). While it is tempting to state that a certain coating thickness on the smooth metal coupons provided adequate protection in the test conditions, this can not be readily applied to a corroded metal surface for the reasons explained in Section 6.4.1. Coating a corroded object presents many challenges not encountered with a smooth, uncorroded metal surface. An elaborate corrosion structure was determined for copper acetate by SEM and SEM-EDS analysis in Chapter 4 (Figure 4.13). This consisted of a raised and very irregular surface morphology that would prevent the application of a homogeneous and intact coating layer. The reduction or removal of this corrosion is to be recommended prior to applying a polymer coating for the protection of copper alloys contaminated by exposure to carbonyl compounds.

In spite of the fact that the acrylic polymer in Incralac® was found to be permeable to water (De Witte 1973/74, 144; Rocca and Mirambet 2007, 310), it protected the underlying metal for the duration of the test. The solubility of Incralac® is known to decrease upon aging whereas the solubility behavior of Poligen® ES 91009 has yet to be determined. For this reason Poligen® ES 91009 is to be considered an experimental polymer in the conservation field undergoing evaluation for its applicability as a conservation material. Solubility information for Poligen® ES 91009 was not available from the manufacturer. The determination of the means for its removal, whether mechanical, chemical, or both, will in large part influence the decision regarding its adoption as a conservation material. Conservators emphasize the reversibility of treatments and favor materials of low toxicity for reasons of health and safety.

For future research many other variables of protective coatings could tested including different coating thicknesses, degree of viscocity, degree of penetration into corrosion, efficacy of a coated corroded surface compared to a coated uncorroded surface, and multi-component coatings such as Poligen® on top of Incralac®.

Chapter 7 Recommendations for the Prevention and Treatment of Corrosion by Acetic Acid

Introduction

Extensive research into the effects of air pollutants on art and artifacts in collections and their control in museums has been carried out (Blades 1998; Blades *et al*. 2000; Blades *et al*. 2002; Cassar *et al*. 1999). This chapter first addresses the means of preventing the attack by acetic acid vapour and other Volatile Organic Compounds (VOCs) on objects in storage or display cases. Mitigation options are recommended for microclimates (museum cases) rather than macroclimates (the open air museum system). For this reason general heating, ventilating, and airconditioning systems (HVAC) and filtration systems are not included in the discussion. Two obvious options present themselves when one considers mitigation: 1) increase ventilation in the case thereby lowering the concentration of volatile organic compounds (VOCs) or 2) decrease ventilation in the case in order to facilitate control of the RH, oxygen content, and/or temperature within. Selection of the first option will depend on the contaminants initiating from within the case and the air quality of the macroclimate of the museum. The more tightly sealed the case the easier it will be to control the RH or oxygen levels within. Temperature is another consideration. The source and positioning of lighting for display cases must not contribute to increased temperature. In the choice of materials used for the construction of storage and display cases, while the negative aspects involving the off-gassing of VOCs from wood have been emphasized throughout this work, it should be kept in mind that the buffering capacity of wood is an advantage in the maintenance of a stable interior environment. Metal cases are recommended for the display and storage of metals but one must be aware that fluctuations in temperature and RH will more readily find their way into the interior of the cases since metal is a poor buffer and a good conductor. The maintenance of an appropriate and stable RH or temperature inside a metal case can be challenged by inappropriate and fluctuating conditions on the exterior that may be found in the museum environment overall.

The second part of this chapter addresses the conservation treatment of contaminated and corroded objects. Conservation treatment may be passive (control of the environment) or active (invasive cleaning). The options of mechanical (dry) cleaning, chemical (wet) cleaning, and a combination of these are considered. Examples of these cleaning options are presented.

According to Tetreault (Tetreault 2003a, 61), the protocol for addressing the gaseous contamination of metal objects in storage or display enclosures includes the following:

1) remove the object from the contaminated area
2) identify the contaminant(s)
3) identify the source(s) of contamination
4) reduce the gaseous pollutants by
    a) replacing the off-gassing products or applying barriers to their surfaces
    b) increasing the ventilation in the case and/or
    c) using adsorbents (in tightly sealed cases)
5) mitigate the effects of gaseous pollutants by reducing the reaction rates (in tightly sealed cases) by
    a) lowering the RH and/or
    b) lowering the oxygen content and/or
    c) lowering the temperature
6) monitor the level of pollution
7) return object to the case once improved conditions have been achieved.

7.1 Behavior of Contaminated Objects

Some researchers state that residual acetic acid remaining on the object can contribute to further corrosion once the object is returned to a humid environment (Donovan and Stringer 1971, 543; Tetreault *et al*. 1998, 27). Moving objects with sodium acetate corrosion from wooden storage to metal storage does not guarantee the halt of reactions since this compound provides ample sodium and acetate ions for further reactions in high humidities (Thickett 1998, 10). Metal storage cabinets have low buffering capabilities that can allow high levels of RH (Thickett 1998, 10).

Due to the sensitivity of lead to carbonyl acids leaded copper alloys been given much emphasis throughout this work. Regarding lead that has been damaged by acetic acid in a humid environment, the formation of more lead corrosion compounds will be inhibited and "acetic acid will be at least partly desorbed, and progressively fewer intermediates [e.g. lead acetate oxide hydrate] should be available for further carbonation [corrosion]" when removed from the humid, acidic environment (Tetreault *et al*. 1998, 27). One author states that residual organic acid on the surface of lead will probably

evaporate once the object is moved to an unpolluted environment (Selwyn 2004, 120). It is claimed that corrosion will cease if the concentration level in new surroundings is sufficiently low (Selwyn 2004, 120).

7.2 Acceptable Levels of Acetic Acid, Formic Acid and Formaldehyde

'Acceptable Damage Concentration' (ADC) is defined as the minimum level of pollutant that can be detected by the measurement method (Brokerhof and Van Bommel 1996). This was the precurser to NOAEL (No Observable Adverse Effect Level), which is defined as "the highest level of a pollutant that does not produce an adverse effect on a specific chemical or physical characteristic of a material in a particular experimental set-up (analytical method, exposure time, temperature, RH, etc.)." The NOAEL of acetic and formic acid on copper and lead are presented in Table 7.1 (Tetreault 2003a, 21).

Table 7.1 NOAEL of Acetic and Formic Acid on Copper and Lead

NOAEL	Acetic acid		Formic acid	
	μg m^{-3}	ppm	μg m^{-3}	ppm
Copper (color change)		0.5[3] (≥50%RH)		0.4[2] (75%RH)
Copper (weight change)			8000	3.0[2] (≥54%RH)
Lead (untarnished) (color change)				0.04[2] (≥54% RH)
Lead (untarnished) (weight change)	400	0.16[1]	200	0.1[2] (≥54%RH)
Lead (tarnished) (weight change)	3000	1.2[1]		

blank fields indicate no available information; [1]Tetreault 2003a, 26; [2]Tetreault *et al.* 2003, 244; [3]Thickett *et al.* 1998, 263

LOAED, the lowest observed adverse effect dose, "is the cumulative dose concentration [LOAEL x time] at which the first signs of adverse effects are observed." (Tetreault 2003a, 23). Recommendations of safe concentrations of acetic acid for the protection of bronze are based on the published LOAED figures by Thickett and Tetreault in Table 4.7 in combination with test results in Chapter 4. The recommended level for copper tin bronze falls just below the LOAED of acetic acid for copper (0.4 ppm yr) and the recommended level for leaded bronze falls just below the LOAED for lead (0.02 ppm yr). The doses can be adjusted according to the ambient RH and the preservation target, i.e. the desired length of protection in storage or exhibition (Tetreault

2003b). For example, to protect copper for 10 years a dose less than 0.04 ppm yr would be required in a RH of 50 to 60%. Recommended levels are discussed further in Chapter 8 under Guidelines for Curators and Conservators.

The range of acceptable levels of acetic and formic acid concentrations for materials reported in Table 7.1 (0.04 – 3 ppm) are lower than the TLVs (Threshold Limit Value) for human health and safety: 10 ppm acetic acid (Appendix 18.1) and 5 ppm formic acid (Appendix 18.2) (Chapter 2, section 2.3). For formaldehyde the LOAED 0.48 ppm (Table 7.1) exceeds the TLV (0.3 ppm) (Appendix 18.3). The Threshold Limit Value is the maximum permissible concentration of a material, generally expressed in parts per million in air for some defined period of time (often 8 hours, but sometimes for 40 hours per week over an assumed working lifetime) in the workplace (http://msds.chem.ox.ac.uk/glossary/tlv.html). TLV is an internationally adopted unit of measurement for health and safety. The OSHA (Occupational Safety and Health Administration) and NIOSH (National Institute for Occupational Safety and Health) are US-based organizations that have defined the following limits: PEL (permissible exposure limit), REL (recommended exposure limit), and IDLH (immediately dangerous to life or health concentration). The TLVs (Threshold Limit Values) are used in museums internationally.

7.3 Prevention

7.3.1 Monitoring Carbonyl Compounds

An important criterion for collections is preventive conservation. Preventive conservation involved maintaining a safe environment. Knowledge that the environment is safe involves measuring and monitoring the levels of VOC's in storage and display areas.

7.3.1.1 Sampling the Air

A few simple qualitative and semi-quantitative tests for volatile acids can be carried out either inside the storage case with the object or in test tubes with samples of materials for case/exhibit construction.

7.3.1.1.1 Volatile Acids

A test for volatile acids (non-specific) that may be run inside the storage case does not require the removal of a sample (Odegaard *et al*. 2000, 186,187). Filter paper or cotton string is dipped in a mixture of cresol red solution or cresol purple solution (indicator dye) with ethanol and methanol and is allowed to dry. The test paper or string is placed near (not touching) the object to be tested, ideally beneath the object (acidic vapours are heavier than air), for up to 5 days. In the case of cresol red a color change from yellow to reddish purple indicates acid (non-specific), in the case of cresol purple the color will change from yellow to purple (Odegaard *et al*. 2000, 186,187).

The iodide-iodate test for volatile organic acids is a colorimetric test for volatile acids (both acetic and formic) (Thickett and Lee 2004, 18). A colorless test solution of potassium iodide, potassium iodate, and starch is enclosed in small test chamber for 30 minutes with materials to be tested. "The iodate and iodide ions react with the hydrogen ions of the volatile acid to produce elemental iodine:

$$5I^- + IO_3^- + 6H^+ \rightarrow 3H_2O + 3I_2$$

The iodine subsequently reacts with the starch in the solution to produce a blue colour" (Thickett and Lee 2004, 18). The test can be influenced by carbon dioxide absorption from air over prolonged periods of time that produces a blue color.

The following test uses pH papers and lime water (Odegaard 2005, 182,183). A small sample of the material to be tested is placed in a sealed test tube with boiled distilled water and pH paper (0-14 pH) that has been wetted with lime water (calcium hydroxide solution) and kept at a temperature of 50° C for increments of 1 hours, 4 hours, 1 day, and several days. Acids released from the sample will neutralize the base (the lime water solution) causing the pH paper to change color. Color of the pH paper must be compared to a control (Odegaard 2005, 182,183).

A similar test for volatile organic acids uses pH papers and glycerol (Odegaard Odegaard *et al*. 2000, 183,184). A small sample of the material to be tested is placed in a sealed test tube with pH paper (0-14 pH) that has been wetted with a glycerol-water

solution and monitored everyday for a few weeks. Color of pH paper is compared to a control (Odegaard *et al*. 2000).

Many types of passive sampling devices (PSDs) exist (Grzywacz and Stulik 1992; Grzywacz 2006). They are small devices that are placed in storage or display areas for a designated period of exposure. They are designed to measure the concentrations of specific compounds. Passive sampling devices (PSDs) can be divided into the following categories: qualitative direct-reading PDSs; quantitative direct-reading PSDs; qualitative laboratory-analysed PSDs; quantitative laboratory-analysed PSDs (Grzywacz 2006). The quantitative direct-reading PSDs are also called "colorimetric direct-reading samplers and are available as diffusion tubes, badges, and test sticks." (Grzywacz 2006, 38). Diffusion tubes manufactured by Draeger and Gastec are examples of quantitative direct reading PSDs that were used in the experimental work in Chapter 4 (Appendix 19) (Figure 7.1). Quantitative laboratory-analysed PSDs are supplied as diffusion tubes or badges and the results are analysed in the laboratory. One example of quantitative laboratory-analysed diffusion tube samplers was designed in Scotland at the University of Strathclyde for measuring acetic and formic acid (Appendix 19) (Gibson *et al*. 1997a; Gibson *et al*. 1997 b; Gibson *et al*. 1997c). This sampler was used to measure the acetic acid concentration in storage cabinets in the Athenian Agora (Table 2.2) (Paterakis 2003). Another example of a laboratory-analysed passive sampling device is an environmental impact sensor, designed by the Fraunhofer Institute of Silicate Research (ISC), Germany (Mottner 2007). It has been used in many European countries since 1992. The environmental impact sensor after exposure is analysed by infrared spectroscopy (FTIR) (Mottner 2007). A diffusion tube sampler was designed for use in the museum that is analysed by ion chromatography for determination of acid concentration (Hodgkins 2008).

Figure 7.1 Gastec and Draeger Diffusion Tubes

In active samplers, the air to be tested is drawn through the diffusion tube with a pump. There are direct-reading active sampling devices (e.g. made by Draeger company), and laboratory-analysed active sampling devices. In a study carried out in the National Archaeological Museum and the Numismatic Museum of Athens in Greece laboratory-analysed active and laboratory-analysed passive sampling devices were compared (Dremetsika *et al*. 2005). The laboratory-analysed active sampling devices used were Supelco Orbo tubes with SKC pumps (Appendix 19). The laboratory-analysed passive sampling devices used were SKC charcoal passive samplers. Analysis was carried out with Reverse Phase High Performance Liquid Chromatography (HPLC). Acetic acid was found at 10 times the concentration of formic acid in cases constructed of wood or medium density fiberboard (MDF) (Dremetsika *et al*. 2005). The concentrations ranged from 0.02 to 2.42 μg m^{-3} (8 – 968 ppb) for acetic acid and from 0.03 to 0.18 μg m^{-3} (57 – 344 ppb) for formic acid (Dremetsika *et al*. 2005). These acetic acid levels are comparable with those found in the Athenian Agora and the British Museum (Chapter 2, Tables 2.2, 2.4) and these formic acid levels are comparable with those found in the British Museum (Chapter 2, Tables 2.3, 2.5).

More sophisticated computerized devices have been developed for environmental monitoring. Some are serially connected passive samplers (Butsugan 2006) and others involve real time monitoring (Prosek *et al.* 2008). A research project, "Automated Corrosion Sensors as On-Line Real Time Process Control Tools" (CORRLOG), was performed within the Sixth Framework Program of the European Commission (Hubert *et al*. 2008; Prosek *et al*. 2008). In this program environmental data were monitored and

logged by computer and automated corrosion loggers were tested. Another means of monitoring environmental conditions are piezoelectric quartz crystal (PQC)-based dosimeters (Odlyha *et al*. 2008). Lead coated PQC crystals with associated electronic components are connected to a computer for real time monitoring of the environment.

7.3.1.1.2 Acetic Acid Vapour

The simplest and least expensive means of determining levels of acetic acid are color indicating test papers (e.g. A-D papers for acetic acid) but these do not provide accurate, quantitative readings (Grzywacz 2006, 32). Passive sampling monitors that are shipped to a laboratory for analysis after exposure provide reliable and accurate readings but are costly (Grzywacz 2006, 69). The most accurate means of measurement involves the gas chromatograph that was reported in Chapter 4 to determine the level of acetic acid concentration in the test chambers. An intermediate means of monitoring that provides semi-quantitative analysis can be found in the relatively economic glass sampling tubes manufactured by Draeger and Gastec (Figure 7.1) (Grzywacz 2006, 36,39). These fall into the category of quantitative direct-reading PSDs (section 7.3.1.1.1). These sampling tubes can be recommended for museums and collections that cannot afford costly laboratory analysis and are suitable for 0.4 ppm acetic acid vapour thresholds.

7.3.1.2 Analyzing the Object

Acetates and formates may be present on an object without any outward visible signs. Ion chromatography has the potential to detect trace levels of acetate and formate efflorescence as well as adsorbed acetic and formic acid on objects not yet showing efflorescence or corrosion (Tennent *et al*.1992, 878). The low detection limits of ion chromatography can indicate acetates and formates when there are no visible signs of efflorescence on the surface of the object (Tennent *et al*. 1992, 870). It may alert conservators to the possibility of objects with adsorbed acetate and formate to "incipient efflorescence" (Tennent *et al*. 1992, 880). Detection limits were 0.01 mg 1^{-1} for Na^{+} and 0.02 mg 1^{-1} for CH_3COO^{-} and $HCOO^{-}$ (Tennent *et al*. 1992, 874). A case study by Tennent *et al*. (1992) of the detection of acetate and formate on objects with no visible signs were two bronzes in British Museum that were soaked in water and the water analysed by ion chromatography (Tennent *et al*.1992, 877). They had the same

provenance, one had been treated with sodium sesquicarbonate and the other had not. No carbonyl efflorescence was visible on either object. Acetate and formates were found on the treated object but not on the other object: acetate 75.8 ± 1.4 μg cm^2; formate 13.1 ± 0.6 μg cm^2 (the amount of acetate/formate analyte ions present per cm^2 of the surface of the artifact (Tennent *et al*. 1992, 877). The formation of sodium acetate trihydrate by the reaction of acetic acid vapour with sodium sesquicarbonate has been observed (Tennent *et al*. 1992, 878). Another case study by Tennent *et al*. (1992) of acetate and formates on objects with no outward visible signs were 3 bronze arrowheads from the Burrell Collection that had been stored for 9 years in wooden cabinets with an acetic acid level of 0.14 to 0.32 ppm (Tennent *et al*. 1992, 878). Nothing is mentioned regarding their conservation treatment. Acetate ranged from 15.4 ± 0.8 to 30.0 ± 2.1 μg cm^{-2}; formate ranged from 8.4 ± 0.1 to 36.6 ± 0.3 μg cm^{-2} (concentration expressed as μg cm^{-2} of the surface of the artifact) (Tennent *et al*. 1992, 879).

7.3.2 Controlling Exposure to Carbonyl Compounds

Four main strategies have been defined by Hatchfield (2002, 55) for the mitigation of pollutants in museums: 1) ventilation and filtration that address the general museum atmosphere; 2) selection of materials to use in proximity to objects; 3) improvement of existing materials that are problematic; 4) targeting the enclosure of the object, i.e. the application of coatings or barriers, the use of vapour-phase inhibitors or scavengers.

Different approaches can be taken to control the exposure of objects in storage or on display to carbonyl compounds to. One involves barriers to block the volatile emissions and another involves adsorbents or sacrificial sinks that absorb the volatile emissions. The use of adsorbents and sacrificial sinks is easier, less invasive, and is recommended over the application of barriers to acidic case materials or to the objects themselves and thus reduces the acidic concentrations in contact with the objects.

7.3.2.1 Means of controlling Emissions

7.3.2.1.1 Barriers and Sealers

Except for oxidative paints, most paints and varnishes may be used to coat wooden materials. Oxidative paints include oil-based, oil-based urethane, alkyds, and epoxy ester (Tetreault 2003a). Low VOC (Volatile Organic Compound) paints include water based and solvent based. Low VOC paints are classified in Canada as having less than 250g/l VOC content (Hatchfield 2002, 113).

Sometimes the objects themselves are coated with vapour barrier films such as cellulose nitrate, methacrylates and polyvinyl acetates (Hatchfield 2002, 113). Cellulose nitrate and polyvinyl acetates both display unfavorable attributes, the acrylates have been recommended for the protection of metals indoors (Hatchfield 2002, 113). Coatings on metal objects are protective for the short term only, such as the dilute solutions (5-15%) of various grades of Paraloid in acetone forming thin coatings (Section 7.3.6) (Hatchfield 2002, 113). These coatings are subject to irregularities and defects as seen in the 15% solution of Paraloid B72 in Figure 6.7. These thin coatings are preferred by museums to maintain a natural metal look by avoiding the plastic appearance or shine of thicker coatings.

Several commercial barriers layers are available on the market that may be applied permanently to seal the inside of display or storage cases. Commercial laminated aluminum foil, e.g. Marvelseal® 360, which is a polypropylene, polyethylene/aluminum/polyethylene film forms a successful barrier (Appendix 19) (Hatchfield 2002, 104; Tetreault 2003a). Home-made laminated aluminum foil barriers can be made by ironing aluminum to wood surface using a PE or LDPE polyethylene plastic sheet as the adhesive. The foil is then covered with fabric or acid-free matboard to protect the foil layer (Tetreault 2003a). Rosco-Cinefoil™ (epoxy-coated aluminum sheeting) can also be used (Appendix 19) (Hatchfield 2002). Two other types of effective barrier films for acetic and formic acid, formaldehyde and acetaldehyde are Moistop® 622, a polyester/aluminum/polyethylene film, and Melinex® 402, a polyester film (Appendix 19). Heat sealing and taping the overlapped edges provide a satisfactory seal (Hatchfield 2002, 104). Melinex® (polyester terephthalate) film used with activated charcoal cloth reduced offgassing to the same degree as did Moistop® and Marvelseal®

(Hatchfield 2002, 104). Calcium hydroxide nanoparticles have been applied to the surface of wood to neutralize the gaseous acids (Giorgi *et al.* 2009).

7.3.2.1.2 Adsorbents

Adsorbents and scavengers can be used effectively in enclosed spaces to remove impurities from gases or liquids (Cruz *et al*. 2008; Hatchfield 2002, 115). An "adsorbent removes one substance from another by adhering the substance to the surface of the adsorbent, primarily a physical rather than a chemical process…" (Hatchfield 2002, 115). Examples of adsorbents are activated carbon, activated clays, zinc compounds, silica gel, and lead coupons. Adsorbents act as sacrificial sinks. Once adsorbents become saturated they can re-emit the pollutants they adsorbed in a process called desorption (Hatchfield 2002, 115). There are three classes of adsorbents (Hatchfield 2002, 116): 1) hydrophobic adsorbents with no ionic surface charge such as graphitized carbon black; 2) hydrophilic adsorbents with positive surface charge such as activated silica gel; 3) adsorbents with negative surface charge such as activated charcoal that interact with specific adsorbates . Activated carbon can be very effective for scavenging volatile acids including acetic and formic acid (Tetreault 2003a, 56). Charcoal cloth reduced the concentration of these acids in a closed case by 50% over a six-month period (Gibson *et al*. 1997b, 17). Carbon impregnated with sodium hydroxide or potassium hydroxide undergoes a chemical reaction with the pollutant forming a new product and therefore does not re-emit the pollutants. These products manufactured by Purafil Inc. are reported to be effective for removing acetic acid (Hatchfield 2002, 119). "MicroChamber® products incorporate alkaline buffers, zeolite molecular trap and/or activated carbon into a variety of paper products." (Appendix 19) (Hatchfield 2002, 122). They can be used in display and storage to adsorb pollutants and are very effective for removing acetic acid and other acidic gases (Hatchfield 2002, 123; Vine and Hollinger 1993, 125). Static and Corrosion Intercept™ products of Engineered Materials, Inc. are reactive polymers that contain "finely divided, highly reactive copper in a polymer matrix." (Hatchfield 2002, 123) (Appendix 19). These products have been used successfully as a barrier over wooden panels preventing corrosion by acetic and formic acid (Engineered 1995, 4). The use of calcium carbonate as a buffer in paint or paper is rather controversial (Arney *et al*. 1979, 15), while it adsorbs acetic acid forming calcium acetate it is said that acetate is unstable and can liberate more acetic acid (Farmer 1962, 328). Lead is considered a hypersensitive material in the control strategies for preservation of materials in museums

(Tetreault 2003a, 62). Lead coupons are an inexpensive alternative to sacrificial sinks in display or storage cases but face many limitations. Their efficiency as scavengers depends on many factors: the material and surface area of the objects in the case, the capacity of the objects themselves to serve as sinks or scavengers (lead objects are more susceptible to acidic emissions than copper), extent of exposure to pollutants from within and from without the case, the ratio of the surface area of the lead scavengers to the objects themselves requiring protection, the degree of leakage of the case, the rate of air exchange in the case, and the circulation of air within the case with regard to the positioning of the lead coupon scavengers. The goal of the scavengers is to react with the acidic emissions before they reach the objects in the collection.

7.3.2.1.3 Testing Materials to be used in Storage or Display

A qualitative test used by conservators for determining the suitability of materials for use in the storage or display of metals is known as the Oddy Test. It was implemented in the British Museum by Andrew Oddy in the 1970s (Oddy 1973; Oddy 1975) and has undergone several alterations since (Green and Thickett 1993; Green and Thickett 1995). It involves enclosing the material to be tested with a metal coupon in moisture in a test tube and heating 60° C for 28 days (Green 1990; Thickett and Lee 2004, 13). This simple, non-specific test is now widely used in museums.

Table 7.2 Stable Materials Recommended for use in Storage or Display from the Museum of Fine Arts, Boston

Category	Material
Structural materials	Glass
	Metals including anodized aluminum, stainless steel
	Aluminum laminates (Alucobond®)
	High-pressure laminates (Formica®)
	Powder-coated metals
Support materials	Tycore® honeycomb paperboard
	Coroplast® (fluted polyethylene/ polypropylene
	Archival corrugated cardboard
Plastics	Teflon®
	Polyethylene
	Tyvek® spunbonded polyethylene
	Polypropylene
	Polyethylene terephthalate (MylarD)
	Acrylics
	Polystyrene
	Polycarbonate
	Polyester
	Nylon
Adhesives	Acrylic adhesives
	Hot-melt adhesives based on polyethylene/polypropylene
	Acrylic emulsion or dispersion adhesives
Gaskets, caulking	Neutral cure silicone caulk
	Polyethylene foam
	Silicone foam
	PFTE (polytetrafluoroethylene)
	Acrylic caulk
Paints and coatings	Acrylic paints
	Water-borne polyurethanes
Fabrics	Undyed, unbleached cotton or linen
	Polyesters
	Hollytex® or Ree may® spunbonded polyester
Paper products	Acid-free (neutral pH) paper
	Neutral pH tissue paper
	Microchamber paper products
Other materials	Aluminum laminate vapour-barrier sheeting (e.g. Marveseal®)
	Pacific Silvercloth®
	Corrosion Intercept®

(From Hatchfield 2002, Appendix 18.3 “Product Stability”, 157-158) (Appendix 19)

7.3.2.1.4 Materials that are Safe for use in Storage and Display

Table 7.2 lists materials free from contamination by acetic and formic acid that are stable and safe use in storage and display (Hatchfield 2002). The most stable materials, and therefore the most suitable for display or storage of metal objects, can be divided into the following categories: structural materials, support materials, plastics, adhesives, gaskets and caulking, paints and coatings, paper products, and other materials (Hatchfield 2002). A comprehensive list of materials known to off-gas these acids may

be found in Tetreault (2003), Apendix 1, “Sources and Levels of Various Pollutants” and in Grzywacz (2006), Appendix 18.1, “Major Gaseous Pollutants of Concern to Museums, Their Sources, and At-Risk Materials” (Grzywacz 2006, 101-103; Tetreault 2003a, 99-101).

7.3.3 Controlling Exposure to Moisture

7.3.3.1 Preventing the Electrochemical Reactions between the Carbonyl Compounds and the Metal by maintaining a Low RH

Increasing RH increases the emission rate of acetic acid from wood and formaldehyde from medium density fiberboard (MDF) (Thickett *et al*. 1998, 263). Silica gel is the most widespread absorbent used to maintain a low RH in closed cases. Silica gel will also absorb some pollutants such as formaldehyde (Hatchfield 2002), so it should be changed more frequently. Commercial brands of absorbents that incorporate silica gel are Rhapidgel, Artengel, and Art-Sorb (Tetreault 2003a) (Appendix 19).

7.3.3.2 Preventing the Migration of the Carbonyl Corrosion Compounds by maintaining them in the Crystalline State

The equilibrium relative humidities (eqRH) of a sodium copper carbonate acetate is approximately 65% eqRH and 75% eqRH for sodium acetate trihydrate (Thickett 1998, 9). The maintenance of a RH below these levels would stabilize these acetate compounds in the crystalline state and represent a safe level for objects afflicted by these acetate compounds in storage. Not until the eqRH is reached will they deliquesce. When deliquescence of these hydroscopic corrosion products occurs sodium and acetate ions may be released allowing them to spread and further contaminate the artefact (Thickett 1998, 9). Saturated salt or glycerol solutions may be used to maintain a specific level of RH in enclosures. The evolution of gaseous pollutants from saturated salt solutions can occur in some cases contributing to the corrosion products on metal (Hatchfield 2002, Piechota 1992). This was checked in my experiments in Chapter 4 (Test Series I: Part One) and was not found.

7.3.4 Controlling Exposure to Oxygen

Electrochemical reactions between the gaseous carbonyl compounds and metal are prevented in an anoxic environment. Techniques of removing oxygen are referred to

as “absorption, interception or scavenging.” (Hatchfield 2002, 120). Many of these have been developed for the food packing industry. Iron-based oxygen absorbers called Ageless™ were developed by the Mitsubishi Gas Chemica American, Inc., in 1977 (Appendix 19). The iron salts react with atmospheric moisture and oxygen forming ferric oxides. They are distributed in packets that are designed for specific volumes of air in well-sealed vapour barrier bags. Several grades are available for different conditions of oxygen and moisture content (Maekawa and Elert 2003). Another oxygen absorber designed by Mitsubishi is the RPSystem™ to be used in low RH conditions (Appendix 19). The RPSystem™ incorporates bags made of a vapour barrier polymer films. The absorbent packet is enclosed in the vapour barrier bag with the object and an oxygen eye that indicates the exhaustion of the oxygen absorber. The bags are heat-sealed protecting the object inside a film of very low oxygen-permeability. Atco™ and FreshPax™ are other brands of oxygen absorbers (Appendix 19) (Maekawa and Elert 2003). Several barrier polymer films are available with differing degrees of permeability and melting temperature (for heat-sealing) (Maekawa and Elert 2003, 20).

The author has used the RPSystem with ESCAL bags for the desiccated storage of metal artifacts in Kaman-Kalehoyuk, Turkey. “ESCAL is silica or siloxane-coated 0.11 mm film with water vapour permeability of 0.01 g/m^2/day and an oxygen transmission rate of only 0.05 cc/m^2/day.” (Maekawa and Elert 2003, 123). It is claimed to maintain an anoxic environment for much longer periods than the other oxygen-barrier films (Maekawa and Elert 2003, 123).

7.3.5 Controlling Exposure to High Temperature

By lowering the temperature we can discourage the off-gassing from wood and chemical reactions from taking place on the metal (Thickett *et al*. 1998, 263). The low temperatures required to inhibit chemical reactions, however, are not normally feasible for the storage and display of artifacts in most museums (Tetreault 2003a, 60).

7.3.6 Protective Coatings

The application of barrier coatings to the object may be considered an alternative to applying barrier films or coatings to the walls of the enclosure surrounding the object (Section 7.3.2.1.1). The acrylate polymers have been recommended for the protection of

metals indoors (Hatchfield 2002, 113). In Chapter 6 two polymers were tested as protective coatings for copper alloys against volatile acetic acid (4 ppm) in 86% RH: Incralac® (ethyl methacrylate -butyl acrylate copolymer) and Poligen® ES 91009 (polyethylene wax emulsion) (Appendix 19). Conservators look for the following properties in their selection of protective coatings: ease of solubility, ease of application, reversibility, delayed aging properties, moderate to high glass transition temperature (Tg), low toxicity of solvent carrier, versatility regarding range of solvents that may be used for purposes of controlling evaporation rate, coefficient of thermal expansion to correspond with the metal being coated, degree of transparency, and degree of luster when dry.

Regarding reversibility, periodic removal and reapplication of a coating is required to maintain a protective layer for the metal. Coatings and their applications are not considered to be permanent. We have seen in Chapter 6 that protectiveness does not depend entirely on the degree of permeability of the coating or on the adhesion of the coating to the metal. The most important criterion for protectiveness is the formation of an intact, uncompromised coating (i.e. one without holes or losses). A few major factors that influence the success of an intact, uncompromised protective coating include the "nature of the metal surface, the nature of the surface contaminants, and the nature of the corrosive environment" (Koehler 1981, 94). In general, the thicker the coating the more protection it will afford. Disadvantages of thicker coatings, however, include greater difficulty in reversibility, a plastic appearance, and shine.

7.4 Conservation Treatment

There are two basic approaches to the conservation treatment of metal objects that are contaminated and/or corroded by acetic acid vapour and other VOCs. A passive conservation approach involves the regulation of particular environmental variables of the storage or display area: RH or oxygen. Moisture and oxygen are the two factors that allow electrochemical reactions to occur. It is not sufficient to remove the contaminated objects from the source of the contamination to halt corrosion. The object must be immobilized in a process called passive stabilization. Various means of controlling the environmental factors of RH and oxygen were discussed in section 7.3 The corrosion compounds, specifically the sodium and acetate ions, may be immobilized by the maintenance of a RH lower than the equilibrium RH (eqRH) of the compound(s) present.

This will halt further progression of corrosion by preventing deliquescence. The removal of oxygen is another means with which to halt the corrosion process. An active conservation approach involves the removal of the contaminant(s) and/or corrosion products from the objects themselves (i.e. cleaning). Several examples of conservation treatment approaches on Saqqara bronzes in the British Museum and the Petrie Museum follow.

7.4.1 Saqqara Bronzes in the British Museum and the Petrie Museum

David Thickett while at the British Museum recommended the mechanical removal of the compounds containing sodium and acetate in cases of localized corrosion on the Egyptian bronzes (Thickett 1998, 10). For more widespread corrosion he recommended their removal by soaking or poulticing with distilled water. While sodium acetate trihydrate is water soluble, a sodium copper carbonate acetate first identified at the British Museum is only partially soluble in water (Appendix 7.2). The application of water involves the risk of accelerating corrosion reactions, however, and the "diffusion of ions through thick corrosion layers can be an extremely slow process" (Thickett 1998, 10).

A group of unregistered bronzes from Saqqara in the collection of the British Museum consisted of predominantly uncleaned and untreated objects (Wang *et al*. 2009). The greenish-blue corrosion on these objects was identified by XRD, SEM/EDX, and Raman Spectroscopy as a mixture of chalconatronite, copper sulphates, sodium acetate trihydrate, and a sodium copper carbonate acetate (Wang *et al*. 2009). Conservation approaches to the cleaning of archaeological bronze have shifted from very invasive to less invasive with a reduction in the use of chemicals. This trend is revealed at the British Museum in the treatment of this group of Saqqara bronzes (Wang *et al*. 2009). "Treatment of these Saqqara bronzes varied in degree according to their surviving physical condition and any intervention was balanced by an evaluation of the risk of loss of evidence contained in the residual corrosion." (Wang *et al*. 2009, 80). Passive means of stabilization by climate control are preferred instead of the active stabilization methods using chemical corrosion inhibitors (benzotriazole). Improvements in storage materials and conditions have been carried out at the British Museum by replacing unsuitable storage materials, such as wood cabinets and cotton wool padding, with metal cabinets and polyethylene foam. Preliminary examination of the objects consisted of

microscopic examination followed by investigative cleaning and radiography to determine extent of preserved detail.

The corrosion products identified on the Saqqara bronzes in the Petrie Museum were predominantly copper sodium formate acetate and chalconatronite with one instance of a sodium copper carbonate acetate. The objects have been stored in tightly sealed wooden cases since their arrival at the museum in the 1970s to the present. Plans are underway for their transfer to new cases of a more suitable material (S. Pancaldo pers comm. 2009).

7.4.1.1 Mechanical (Dry) Cleaning

Mechanical cleaning of the unregistered Saqqara bronzes in the British Museum was carried out by British Museum conservators with the use of small hand tools under magnification. Cleaning was carried out to the level of the original surface at the green copper carbonate or red cuprite layer (Figure 7.2) (Wang *et al*. 2009, 80). In some cases the corrosion was "softened by soaking in successive baths of distilled water" before mechanical removal (Wang *et al*. 2009, 80). Following cleaning some of these unregistered bronzes may be deemed eligible for cataloguing into the collections of the Department of Ancient Egypt and Sudan.

Figure 7.2 British Museum unregistered Saqqara situla before (left) and after (right) cleaning, (Wang *et al*. 2009, fig. 9, 80)

7.4.1.2 Chemical (Wet) Cleaning

In the consideration of the removal of carbonyl and associated corrosion (such as chalconatronite) it is appropriate to determine the solubility of the compounds. Solubility tests were carried out by the author on the corrosion products of two Petrie objects from Saqqara that were identified in Chapter 5: copper sodium formate acetate on UC 30660B (handle) and chalconatronite with a sodium copper carbonate acetate on UC 30669 (Ewer fragments). These solubility tests were carried out by the author prior to the publication of the cleaning of the Saqqara bronzes at the British Museum by Wang *et al*. (2009), referred to in Section 7.4.1.1. The solvents used were deionized water, acetone, industrial methylated spirits (IMS) (95% ethanol, 5% methanol), and petroleum spirit. Few grains of corrosion were removed from the object and placed on a glass slide. A drop of solvent was applied and the reaction (or lack thereof) was examined through the binocular microcope. Results are presented in Table 7.3. "Partially soluble" is considered more soluble than "slightly soluble".

Table 7.3 Solubility of Corrosion on Two Saqqara Bronzes in Petrie Museum (determined from solubility tests carried out by the author)

Solvent	Copper sodium formate acetate on UC 30660B (handle)	Chalconatronite with a sodium copper carbonate acetate on UC 30669 (Ewer fragments).
acetone	ins	ps
IMS	ss	ps
Petroleum spirit	ins	ss
Deionized water	ps	ps

Ins = insoluble; ss = slightly soluble; ps =partially soluble

These solubility tests confirmed the published information in Appendix 7.2 that chalconatronite and a sodium copper carbonate acetate are partially soluble in water (Table 7.3). Copper sodium formate acetate from Petrie object UC 30660B was also found to be partially soluble in water (Table 7.3).

7.4.1.3 Combination of Mechanical (Dry) and Chemical (Wet) Cleaning

The solubility tests carried out by the author on the corrosion of two Petrie objects described in Section 7.4.1.2 were taken a step further by introducing mechanical cleaning techniques: cotton swabs and scalpel. A combination of mechanical and chemical cleaning techniques were used to facilitate corrosion removal.

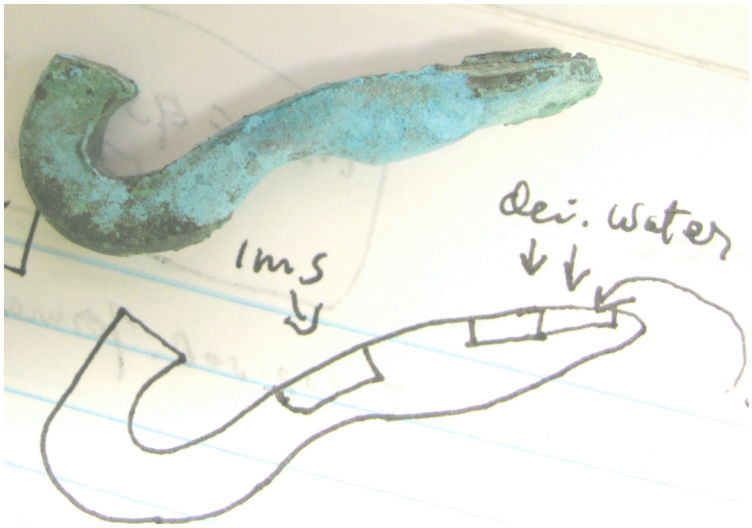

Figure 7.3 UC30660B side one with copper sodium formate acetate, test cleaning carried out with IMS and deionized water on swab showed greater cleaning action with water (for scale ruled paper in photo is 7 mm) (photo Alice Boccia Paterakis, copyright of the Petrie Museum of Egyptian Archaeology)

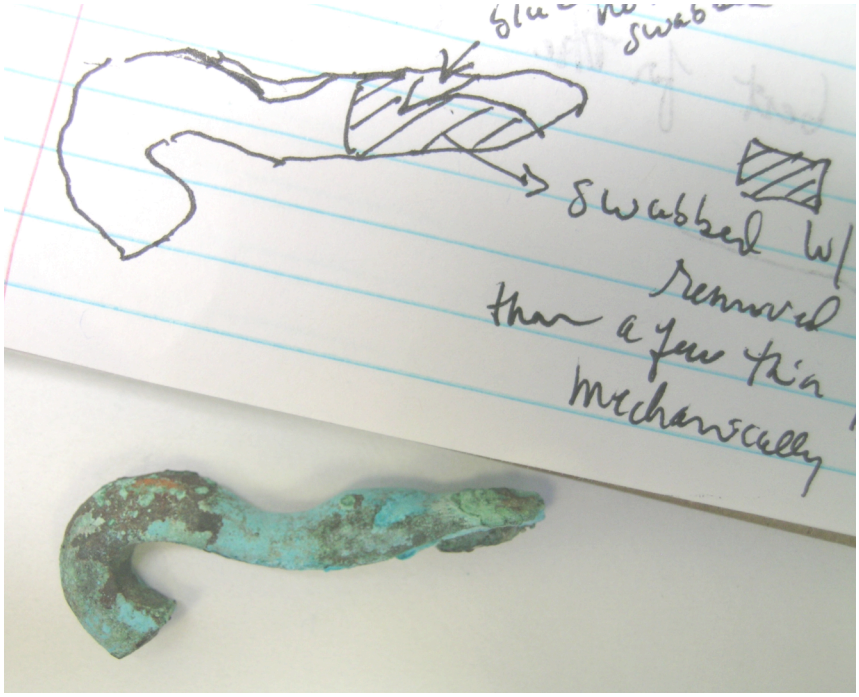

Figure 7.4 UC30660B side two with copper sodium formate acetate, test cleaning carried out with deionized water on swab (cross-hatched area in drawing) (for scale ruled paper in photo is 7 mm) (photo Alice Boccia Paterakis, copyright of the Petrie Museum of Egyptian Archaeology)

These cleaning tests were carried out by the author prior to the publication of the cleaning of the Saqqara bronzes at the British Museum by Wang *et al*. (2009), referred to in Section 7.4.1.1. Copper sodium formate acetate, found to be partially soluble in water, was removed with deionized water on a swab down to the metal susbstrate on UC 30660B (whereas IMS on a swab removed it only partially) (Figure 7.3 and Figure 7.4). Copper sodium formate acetate on UC 30660B did not form a hard crust and was easily removed from the smooth substrate with a swab and deionized water.

On UC 30669 chalconatronite was found to be quite hard in places and difficult to remove even with a scalpel, especially from rough, irregular surface areas. Swabbing with deionized water slowly softened and partially dissolved this corrosion. The areas of softer, more powdery blue corrosion on UC 30669 are attributed to a sodium copper carbonate acetate (identified by XRD by the author, Chapter 5) that was much easier to remove with swabs and deionized water (Figure 7.5). A combination of chemical and mechanical cleaning was an advantage in the removal of this sodium copper carbonate acetate and chalconatronite.

It is important to distinguish these carbonyl corrosion products from bronze disease. Copper chlorides form deep within the copper alloy object and erupt at the surface. Bronze disease is not water-soluble and requires other means for its removal and/or stabilization. Chemical desalination by soaking the object for extended periods in sodium sesquicarbonate does not guarantee complete removal of chlorides and subjects the object to further corrosion. Complete mechanical removal would necessitate carving large voids in the object in order to reach the chlorides below that surface constituting an unacceptable practice. Stabilization means using corrosion inhibitors or preventive conservation by controlling oxygen and RH levels are preferred today.

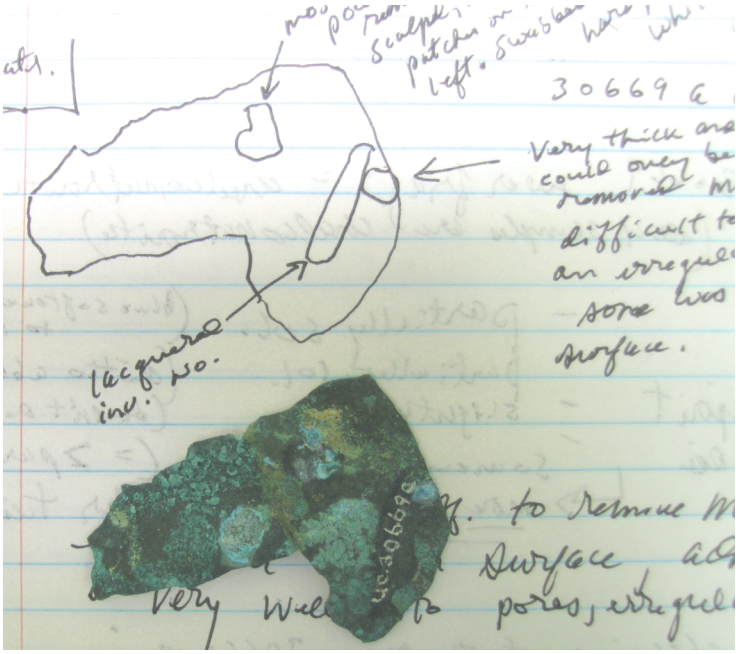

Figure 7.5 UC30669 with chalconatronite (area indicated with arrow on right) and a sodium copper carbonate acetate (area indicated with arrow at top), test cleaning carried out with deionized water, swab, and scalpel (for scale ruled paper in photo is 7 mm) (photo Alice Boccia Paterakis, copyright of the Petrie Museum of Egyptian Archaeology).

7.4.1.4 Preservation of the Corrosion

In some cases the preservation of contextual evidence is favored over the exposure of original detail in the metal by cleaning. The foot of an avian bronze statuette preserved mineralized textile on the surface and there were indications that the body may have been made of wood (Figure 7.6) (Wang *et al*. 2009, 78). In this case the metal corrosion was retained as was the mineralized textile as contextual evidence of original materials of manufacture and associated burial materials. The upper part of the foot, originally inserted into the body of the statuette (no longer extant), was covered with sodium acetate trihydrate and a sodium copper carbonate acetate (Wang *et al*. 2009, 78). These carbonyl corrosion products are considered strong evidence to support the theory that the body of the statue (no longer extant) was made of wood. The authors consider the influence of composite objects, wooden funerary items, and mass burials of mummified birds at the Sacred Animal Necropolis at Saqqara on the formation of corrosion on these bronzes (Wang *et al*. 2009).

Figure 7.6 Foot from unregistered Saqqara bird statuette in The British Museum, blue corrosion identified as sodium acetate trihydrate and a sodium copper carbonate acetate (scale unavailable) (Wang *et al*. 2009, Fig. 6, 78)

7.4.2 Lead

We have seen the important role lead plays in the corrosion behavior of leaded copper alloys. Regarding lead that has been damaged by acetic acid in a humid environment, "Cleaning may be necessary… to stop the active corrosion…" (Tetreault *et al*. 1998, 27). The implications and effectivness of cleaning will now be examined in this context.

7.4.2.1 Chemical (Wet) Cleaning

"Appropriate washing techniques are required to prevent impurities or chemical residues from re-initiating the corrosion process." (Tetreault *et al*.1998, 27). In Chapter 5 we saw that most lead corrosion products found on objects exposed to acetic acid are insoluble in water, with the exception of lead acetates that are rarely captured (Appendix 7.1). Lead acetate is a transient compound that readily forms lead carbonate. Therefore we can presume that the "impurities and chemical residues" referred to above consist almost entirely of the water-soluble ions of sodium and acetate (and lead acetate if present).

7.4.2.2 Mechanical (Dry) Cleaning

The mechanical cleaning method of airbrasive was applied successfully on lead and lead/tin inlays in Japanese lacquer objects to remove hydrocerrusite (water-insoluble) and lead formate (Heath and Martin 1988, 140). This mechanical method using aluminum oxide no. 16 and glass beads no. 9 was chosen to protect the organic materials of the composite objects from liquid cleaning agents (Heath and Martin 1988, 140). It was carried out under magnification to remove all corrosion products from pits and cavities (Heath and Martin 1988, 141). Airbrasive is considered a rather harsh option due to the impact on the soft surface of lead. Respiration protection is important when removing lead corrosion by mechanical means.

7.4.2.3 Preservation of the Corrosion

In the case of contaminated storage conditions, the stripping of lead may not be a solution since the removal of lead carbonate corrosion (resulting from exposure to carbonyl acids) strips away the protective passivating carbonate patina (Lane 1987, 150). Likewise, the removal of conservation protective coatings exposes the vulnerable surface of lead to further attack (Lane 1987, 150). One must consider the possibility of residual sodium or acetate ions trapped between the carbonate corrosion crust and metal substrate and the degree to which the overlying carbonate layer will nullify their reactivity.

Conclusion

The carbonyl corrosion products containing sodium and acetate and associated copper corrosion products vary in degree of water-solubility and therefore in their hygroscopic behavior (Thickett 1998, 9). The formation of water on the surface of metal from moisture in the air may influence the solubility of the corrosion products (Figure 6.1). These are important criteria that must be taken into account when making decisions regarding mitigation and treatment of affected objects. Objects without hygroscopic corrosion products are not as sensitive to RH fluctuations, are not threatened by the spread of sodium or acetate ions through deliquescence, and therefore may be easier to maintain in a stable state without resorting to active conservation treatments. Another factor that may dissuade the conservator from removing non-hygroscopic corrosion (i.e.

water-insoluble) is the greater challenge posed by harder and more tenacious crusts that are well bonded to the metal surface. Objects with hygroscopic corrosion compounds stand a higher risk of continued deterioration given fluctuations in RH that reach the equilibrium RH (eqRH) of the compounds thereby allowing the migration of corrosive ions through deliquescence. Their increased solubility in water, however, can facilitate their removal through wet cleaning procedures. Some of the carbonyl compounds containing acetate and sodium in this study were found to be partially water-soluble which may dictate a combination of wet and dry mechanical cleaning techniques for their removal.

This leads to the conclusion that the identification of the corrosion present and the determination of the degree of its response to moisture (i.e. hygroscopic nature), its solubility characteristics and its eqRH level(s) (if hygroscopic), are vital pieces of information required by the conservator in order to make an informed decision regarding treatment of the contaminated objects. Two basic approaches that the conservator may consider are 1) passive conservation by controlling the environment in which the contaminated object is housed, or 2) active conservation treatment of the object (i.e. cleaning) to remove some or all of the corrosion compounds/corrosive ions present or the application of a barrier coating. Hydrophobic wax would help prevent the formation of corrosion. Very little investigation of conservation treatments targeting copper alloys with carbonyl corrosion has been carried out to date. Other Egyptian copper alloy objects in the Petrie Collection carry corrosion products needing attention. Plans are currently underway for the examination, cleaning, and stabilization of a group of Egyptian copper alloy amulets from the Petrie Museum (S. Pancaldo pers comm. 2010). This is an area for future research warranting extensive cleaning trials combined with analytical monitoring to determine the most suitable treatments. Elemental mapping of sodium with SEM-EDS during washing and removal of corrosion can monitor the distribution of sodium and the effectiveness of removal.

Chapter 8 Conclusions

Introduction

The corrosion and conservation challenges of ancient bronze (copper-tin and copper-tin-lead) artifacts in archaeological collections have inspired this project. Acetic acid has been identified as the cause of acetate corrosion on archaeological bronze that can be accentuated by uncontrolled climatic conditions. A gap was identified by the meager number of corrosion studies on bronze under the corrosive influence of acetic acid vapour and high relative humidity. Emphasis in the literature has been placed on the testing of pure copper and brass (copper-zinc alloy). Only two studies have been located and cited from the literature regarding the corrosion of leaded bronze by acetic acid vapour (Bastidas *et al*. 1995, López-Delgado *et al*. 1997). These studies focused on the protective qualities of a patina (copper sulphide). The present study has filled this void in the study of copper-tin and leaded copper-tin corrosion in acetic acid vapour in indoor enclosures by subjecting new and ancient bronze to accelerated corrosion tests. This project has been designed with the goal of aiding conservators and curators in the treatment, storage, and display indoors of archaeological copper alloys. The project has been streamlined to address unsuitable storage conditions commonly found in museums and archaeological collections by testing various levels of acetic acid vapour and relative humidity in a closed environment. It has also been designed to address conservation treatment questions regarding the influence of residual conservation chemicals (sodium sesquicarbonate) and the protective qualities of coatings (Incralac® and Poligen® ES 91009). For ease of reference, specific figures, tables, and appendices are cited again to highlight specific evidence or test results.

The novelty of this research rests on seven accomplishments: 1) this is the first project to study the corrosive effects of volatile acetic acid on unleaded bronze; 2) this is the first project to produce acetate corrosion on copper tin bronze and on leaded copper tin bronze (without artificial patina); 3) these are the first corrosion tests of volatile acetic acid on unleaded and leaded bronze while monitoring the development of corrosion with SEM and SEM-EDS; 4) this is the first case of the formation of acetate on authentic, naturally corroded archaeological bronzes under test conditions; 5) this is the first case of the transformation of corrosion typical to archaeological bronzes (i.e. carbonates) to

acetate (after removing the corrosion from the object); 6) this is the first study to target carbonyl corrosion on bronzes from the same archaeological site and dates of excavation; 7) this study presents the first documented conservation cleaning tests to be carried out of carbonyl corrosion on bronze.

Corrosion testing was carried out in three levels of RH and acetic acid vapour concentration. A limitation of the research lies in these experimental parameters that did not permit the determination of the minimum levels of RH and acid concentration in which acetates form on the copper alloys. Recommendations for corrosion prevention are offered based on the results of this research combined with those of other researchers on copper and lead.

This study has successfully answered the research questions posed in Chapter One as follows:

1. Acetate corrosion forms on bronzes in museums and archaeological collections from exposure to carbonyl emissions from wooden cases in combination with moisture and contaminants that can act as catalysts;
2. Oxides, carbonates, chlorides, sulphates, sulphides, and phosphates of copper and lead, in order of prevalence, form on ancient bronzes in addition to acetates;
3. The factors that contribute to acetate corrosion on bronzes in museums and archaeological collections are exposure to volatile acetic acid, inappropriate storage/display materials that off-gas, and conservation treatments with inappropriate materials such as acetic acid, acetate, and sodium compounds;
4. The formation of acetate and formate corrosion on bronzes can be prevented by removing the source(s) of acid emissions and by not introducing acetates and formates from conservation treatments;
5. The most suitable conservation treatments for bronzes contaminated with acetate corrosion include the removal of the source of contamination, removal of the acetate corrosion, and maintainence a low RH to prevent mobilization of the acetate ions and ongoing corrosion;
6. Acetate compounds have been studied predominantly on Egyptian bronzes by the author and other researchers but have been found on artifacts from other areas of the world as well. It is not a phenomenon that is restricted to ancient Egyptian or Greek artifacts although the salinity of soil in these regions may be a contributing factor.

Each research objective listed in Chapter One will be addressed in answer to the research questions beginning with the processes of acetate formation on copper alloys followed by the influence of alloy composition, RH, acid concentration, patina, and conservation materials on these corrosion processes.

Processes of Acetate Formation on Copper Alloys

The examination of the processes of acetate formation on copper alloys involves several influential variables: alloy elements, RH, acid vapour concentration, patina, and conservation materials. Water is adsorbed on the surface of the metal from moisture in the air. The thickness of the water layer depends on many factors including chemical composition of the metal, roughness of the surface, RH, and temperature (Kleber and Schreiner 2003). This water layer serves as an electrolyte in the corrosion of the copper alloy.

The first corrosion to typically form on copper in unleaded bronze is cuprite. When acetic acid vapour is introduced it is adsorbed onto the wetted surface and corrosion occurs on the adsorbed water film. Cuprite forms first followed by copper hydroxide, copper acetate hydroxide, and finally copper acetate. Once the surface is covered with cuprite the acetic acid vapour travels through the aborescent cuprite crystals reaching the copper core of the test pieces (Figure 4.8). The crystal formations in Figure 4.13 may be attributed to the development of copper acetate hydroxide analogous to a tree trunk branching out into copper acetate, as described by López-Delgado. The final components forming the patina are copper acetate and cuprite as found in Test Series I Part One (Table 4.16) and by Lopez-Delgado on pure copper (Table 3.2) (Lopez-Delgado *et al.* 1998). The lowest dose of acetic acid vapour which caused the formation of copper acetate on pure copper was 0.5 ppm yr (40%, 80% RH) (Cano and Bastidas 2002) and of copper hydroxy acetate was 2.8 ppm yr (100% RH) (Table 3.2) (Lopez-Delgado *et al.* 1998). In the Chapter 4 tests copper acetate formed on unleaded bronze in 6.3 ppm yr at 86% RH. There are no other studies on copper tin bronze available for comparison.

The formation of acetate on leaded bronze differs considerably from unleaded bronze and depends on many factors one of the most important being the percentage of Pb in the leaded bronze. Other factors that influence the corrosion of leaded bronze by

acetic acid vapour are pre-existing lead patina, concentration of the acid, RH, surface roughness of the metal, and temperature. The corrosion process of lead involves the formation of an adsorbed layer of water on the surface from moisture that acts an an electrolyte followed by the formation of Pb oxide. Lead encourages the formation of a thicker water layer on the leaded coupons than on the unleaded coupons as witnessed by the author in Test Series I Part One and by Wadsak (Wadsak *et al.* 2002). Pb oxide and CO_2 form lead hydroxy carbonate (hydrocerussite). Lead oxide or lead hydroxide patina on leaded bronze has been found to protect the bronze from corrosion in moisture and to retard the corrosion of the bronze compared to pure copper (Wadsak *et al.* 2002). When acetic acid vapour is introduced acetate ions form lead hydroxy acetate, lead hydroxy carbonate, lead acetate oxide, and lead acetate. All four compounds are in the hydrated state and vary in degrees of water-solubility. Researchers differ in opinion regarding the order of the formation of these compounds (Tetreault *et al.* 1998; Niklasson *et al.* 2005). One species of lead acetate oxide formed at 54% RH that was insoluble in water (Tetreault *et al.* 1998). This compound may have contributed to the reduction in weight gain shown by the leaded coupons in 52% RH in Test Series I Part One (Table 4.10)

SEM imaging and SEM-EDS analysis of the leaded test coupons during the testing in Chapter 4 revealed the order and intensity of corrosion development of the various elements of the alloy. After one week a wet surface is visible with prismatic crystals interspersed most likely of cuprite (Figure 4.15). After 2 weeks three corrosion morphologies were evident: large prismatic crystals of high Cu content, fine crystals of high Cu content covering the surface, and long, flat crystals of predominantly Pb (Figure 4.17). After 2 weeks the Cu-rich phases accounted for the majority of surface area whereas by 8 weeks the Pb-rich phase had covered considerably more surface area (Figure 4.19). The corrosion products identified by XRD after 8 weeks were cuprite, hydrocerussite , and copper acetate hydrate. After 8 weeks the corrosion morphology of the copper compounds on the leaded coupons is completely different from those on the unleaded coupons. There are no arborescent or branch-like corrosion products. Instead, the copper acetate has a finer, low-lying crystalline structure. The long sheaths covering much of the surface are hydrocerussite.

In the Chapter 4 tests copper acetate formed on leaded bronze in 6.3 ppm yr at 86% RH. The dose below 6.3 ppm yr that was tested by the author, 0.6 ppm yr, did not produce acetate.The lowest dose of acetic acid vapour tested by Bastidas, 2 ppm yr at

100% RH, caused the formation of copper acetate on leaded bronze (5% Pb) with a copper sulphide patina (Bastidas *et al.* 1995). There are no other studies on leaded bronze that fall within the dose range tested in Chapter 4 for comparison. The lowest dose of acetic acid to cause acetate (lead acetate oxide) to form on pure lead was 0.4 ppm yr (Table 3.7) (Tetreault *et al.* 1998). Lead acetate was not identified by the author after 8 weeks of corrosion testing most likely because of its transitional nature that readily forms the more stable lead hydroxy carbonate (hydrocerussite).

The degree of protection provided by lead oxide or lead hydroxide from acetic acid vapour depends on the morphology and solubility of the lead compounds, the homogeneity of the corrosion layer and impurities in the lead, such as chloride and sulphur, the acid concentration, and the RH (Tetreault *et al.* 1998). Overall the leaded coupons gained more weight than the unleaded coupons with the exception of those coupons in 0.4 ppm yr at 52% RH (Table 4.10). The formation of an insoluble lead acetate oxide may have inhibited corrosion of these coupons. In the 0.6 ppm yr tests at 86% RH acetate was not identified, only hydrocerussite. This dose exceeds the doses reported to cause the formation of acetate on pure copper (0.5 ppm yr at 40% RH) and pure lead (0.4 ppm yr at 54% RH) (Cano and Bastidas 2002; Tetreault *et al.* 1998). The absence of acetate may be attributed to one of two alternative factors: hydrocerussite succeeded in protecting the copper and lead from attack by acetic acid or lead acetate formed during the testing but transformed into hydrocerussite by week 8. Given the exposure dose 0.6 ppm yr, that exceeds the dose required for the formation of acetate on copper and lead, the lead component may have protected the copper in the bronze from attack by acetic acid. The SEM images record the gradual covering of the surface by lead sheaths over the course of the 8-week test (Figure 4.19).

Alloy Composition

Leaded bronze is prone to greater damage by acetic acid attack than unleaded bronze due to the cyclical corrosion process between lead and acetate ions in the presence of moisture. The higher the lead content the greater the risk for attack and extent of damage by acetic acid. The acetate ion can be introduced into the object by corrosion of the lead in leaded bronze. For this reason leaded bronze is more vulnerable to attack by acetic acid than unleaded bronze. Since lead corrodes in lower

concentrations of acetic acid than does copper the copper may be unaffected until a higher concentration is reached.

Relative Humidity and Acetic Acid Concentration

The relative humidity and acid concentration play a crucial role in the development of acetate corrosion. After the 8-week duration of the corrosion tests reported in Table 4.16, Table 4.17, and Table 4.18, acetate was identified on leaded and unleaded bronze at the highest RH level tested, 86%, but not at 54% or 32%. 32% RH prevented all corrosion up to 0.4 ppm yr and prevented acetate formation up to 4.6 ppm yr of acetic acid. Acetates were detected from 6.3 ppm yr acetic acid but not from 0.6 ppm yr or 0.06 ppm yr at 86% RH. It is possible transitional acetate formed on the leaded bronze that transformed into hydrocerussite by the end of these tests. For this reason the recommended doses for the prevention of corrosion in the following Guidelines for Conservators and Curators error on the side of caution. An increase in RH and/or acetic acid promotes increased corrosion. There is an inverse relationship between RH and carbonyl concentrations: the higher the RH the lower the acid concentration required for carbonyl corrosion to occur and vice versa.

Patina (Pre-Existing Corrosion)

Pre-existing corrosion necessarily complicates the chemical reactions that take place on bronze when exposed to acetic acid vapour, as opposed to a polished test coupon. Oxides, carbonates, chlorides, and sulphates, commonly found on archaeological bronze, may react with the acetic acid forming acetate in addition to or in place of a pre-existing compound such as carbonate. This was illustrated in Chapter 4 with the conversion of chalconatronite (sodium copper carbonate) to a sodium copper carbonate acetate (Appendix 10.7) and malachite (copper carbonate) to copper acetate (Appendix 10.9). The corrosion tests in Chapter 4 produced copper acetate (Table 4.19) on archaeological coin #5 with the pre-existing corrosion products of tenorite and cuprite (Table 4.5).

Theories regarding the development and conversion of copper corrosion on bronze by volatile acetic acid have been posed by researchers. In this study these hypotheses have been tested and non-carbonyl corrosion products (without acetate) have

been successfully converted into compounds containing acetate. This study shows that objects with residual sodium from conservation treatments (with sodium-based chemical compounds) or from burial are prone to form corrosion compounds containing sodium and acetate in which the sodium acts as a catalyst in their formation. This would suggest that all the objects identified with carbonyl corrosion in the case studies (Appendix 16) were contaminated with sodium. Pre-existing corrosion on bronze, such as chalconatronite and malachite, can be converted into acetate compounds by exposure to acetic acid vapour. Therefore these patinas are not protective against attack by acetic acid. The hypothesis that conservation chemicals such as sodium sesquicarbonate, when combined with copper corrosion such as malachite, will produce a sodium copper carbonate acetate under the influence of acetic acid has been proven. Residual sodium sesquicarbonate from conservation treatment of bronze can form sodium acetate.

Conservation Materials

In this discussion of the processes of acetate formation on copper alloys the role of alloy elements, RH, acid concentration, and patina have been examined. Additional variables that may contribute to acetate formation include certain conservation materials and treatments. Materials and treatments involving acetic acid and acetate are to be avoided. Vinegar, acetic acid, and EDTA have been used to clean bronze which can leave residual acetate ions. Adhesives and consolidants containing acetate should also be avoided.

Sodium sesquicarbonate, commonly used in the past for the stabilization of bronze, can tarnish unleaded bronze and can promote faster corrosion of leaded bronze by acetic acid vapour as evidenced in the Madrid tests (Test Series I Part Two). Sodium sesquicarbonate was found to encourage acid attack on copper in leaded bronze in the tests at 86% RH and 52% RH (Test Series I Part One). Sodium from sodium sesquicarbonate contributed to the formation of sodium copper carbonate acetate and sodium acetate trihydrate in Test Series II. The adoption of sodium sesquicarbonate and other chemical compounds containing sodium are best avoided in conservation as residual sodium forms hygroscopic salts that encourage corrosion. Conservators should be aware that residual sodium from burial will increase the vulnerability of the artifacts to attack by acetic acid emissions and therefore they must take extra care in the removal

of all residual sodium by washing or choose means of preventive conservation for these artifacts through controlled environment or with protective coatings.

While sodium appears to promote carbonyl corrosion, sodium is not a necessary prerequisite as carbonyl corrosion products can also form in the absence of sodium. The corrosion test results in Table 4.16 illustrate that sodium was not necessary for the formation of copper acetate. Copper acetate formed at a very high concentration of acetic acid vapour, 40 ppm, a level that exceeds most storage and display case conditions. It would appear that sodium is not required to catalyze reactions forming carbonyl compounds at such high concentration levels (40 ppm).

Case Studies and New Corrosion Compounds

The case studies consist of 42 objects in total and consist of bronzes that are predominantly Egyptian from various sites and periods. Artifacts found in Egypt make up 76% of the objects analysed, Greece 21.5%, and Italy 2.5%. The case studies represent the first study to target carbonyl corrosion on bronzes from the same archaeological site (Saqqara Sacred Animal Necropolis, Egypt), historical period, and dates of excavation that are distributed amongst several museum collections. These Saqqara bronzes were excavated from 1964 to 1976 and acquired by several museums in the UK. The Saqqara bronzes (22 objects) represent 52% of the total number of objects in the case studies. The goal with the Saqqara bronzes was to compare the effects of conservation treatments (when documented) and storage conditions on a coherent group of Egyptian bronzes in various museum collections.

Carbonyl corrosion compounds were identified on 79% of the 42 objects analysed. Copper sodium formate acetate represents 23% of the carbonyl compounds found on the 22 Saqqara bronzes and 21% of the carbonyl compounds found on the total of 42 objects analysed. The remaining 54% of carbonyl corrosion on the 22 Saqqara bronze objects and the remaining 57% of carbonyl corrosion on all 42 objects analysed is predominantly a sodium copper carbonate acetate and/or sodium acetate in a few cases.

The identifications of corrosion made in the case studies will form part of an international compendium of carbonyl corrosion in museum collections. This compendium will form a database on the internet for access by conservators,

conservation scientists and curators. A few corrosion samples in this study could not be identified by XRD and, in many samples, I have discovered corrosion compounds in association with carbonyl corrosion on archaeological bronzes that are absent from the International Centre for Diffraction Data (ICDD). Mixtures of compounds, intermediate compounds, non-stoichiometric compounds, and non-crystalline compounds present difficulties in their identification by XRD. Extensive data analysis of non-stoichiometric compounds is required for their characterization by XRD. Included in these unidentified compounds are likely to be other multiple-component carbonyl compounds, in addition to sodium copper carbonate acetate and copper sodium formate acetate, requiring further analysis and characterization for their identification.

Speculation regarding the influence of wood from original statue parts or bases, or wooden shrines enclosing the statues at Saqqara, Egypt, (Chapter 5, sections 5.1.3, 5.2.1.2, 5.4.1.2) has been clarified by findings at the British Museum (Wang *et al*. 2009). Acetate corrosion was identified on the leg of a bronze bird statue from Saqqara, Egypt, that was originally inserted into a wooden body (not extant) (Figure 7.7). Acetate corrosion developed on the leg inserted into the wood but not on the exposed foot of the statue. This finding lends credence to the possibility that acetate compounds could have developed before and during burial by contextual wood and that they can withstand centuries of burial.

The influence of conservation materials on the development of acetate corrosion could not be determined with reliability in the case studies. This was due to two factors: lack of object-specific conservation treatment records and similar storage conditions in all the museums (wooden cabinets without climate control). The importance of conservation documentation can not be overemphasized.

Guidelines for Conservators and Curators

Results of the corrosion tests in Chapter 4 reflect the published LOAED figures for corrosion by acetic acid on copper (0.4 ppm yr, 50-60% RH) and lead (0.02-0.03 ppm yr, 50-75% RH) (Tetreault *et al.* 1998). They also demonstrate that copper tin bronze and leaded (8% Pb) bronze have higher LOAEDs than pure copper and pure lead for the formation of acetate corrosion in 52% and 86% RH. The alloyed elements increase the resistance of the metal to acetate corrosion.

The recommended minimum doses of acetic acid for the prevention of corrosion on leaded (8% Pb) and unleaded bronze in this study are based on the corrosion results in Chapter 4 in conjunction with published LOAED figures for acetic acid on copper and lead (Table 4.7) (Tetreault 2003a; Tetreault *et al.* 2003; Thickett *et al.* 1998). Although copper tin bronze and leaded (8% Pb) bronze demonstrated higher LOAEDs than pure copper and pure lead for the formation of acetate corrosion in 52% and 86% RH in the Chapter 4 tests, the doses recommended for the prevention of corrosion error on the side of caution. The formation of transitional acetate on leaded bronze that may go undetected complicates the determination of LOAED for acetate on leaded bronze. The recommended dose for copper tin bronze falls just below the LOAED of acetic acid for copper (0.4 ppm yr) and the recommended dose for leaded (8% Pb) bronze falls just below the LOAED for lead (0.02 ppm yr) above 50% RH. The doses can be adjusted according to the ambient RH and the preservation target, i.e. the desired length of protection in storage or exhibition (Tetreault 2003b). For example, to protect unleaded bronze for 1 year a dose less than 0.4 ppm yr is recommended and for 10 years a dose less than 0.04 ppm yr is recommended in RH 52% to 86%. For leaded bronze a dose less than 0.02 ppm yr for 1 year and less than 0.002 ppm yr for 10 years is recommended in RH 52% to 86%. A dose less than 0.4 ppm yr for 1 year and less than 0.04 ppm yr for 10 years is recommended for the protection of leaded bronze in 32% RH. Bronze with a lead content exceeding 8% will require a lower dose.

Recommended dose levels for the prevention of all corrosion for a period of 1 year:

- <0.4 ppm yr acetic acid for unleaded bronze in 52% to 86% RH
- <0.02 ppm yr acetic acid for leaded (8% Pb) bronze in 52% to 86% RH
- <0.4 ppm yr acetic acid for leaded (8% Pb) bronze in 32% RH

Recommended Actions for the Prevention of Corrosion

- Avoid storage/display of copper alloys in materials that emit volatile acetic acid
- Avoid conservation treatments using sodium compounds, acetic acid, or acetates
- Determine the composition and the lead content of bronze artifacts
- Identify the corrosion present
- Measure the level of carbonyl emissions in storage/display

- Measure RH in storage/display
- Maintain a low RH, the lower the RH the less provocation of corrosion
- The higher the lead content of the bronze, the lower the RH and acid concentration necessary for prevention of corrosion

Treatment of Objects with Acetate Corrosion

- Removal of contaminated object from storage/display area with volatile acetic acid emissions is not adequate for protection
- RH must be kept low in new storage/display location to inactivate the acetate ions on the contaminated object or acetate corrosion should be removed through cleaning
- A combination of wet and dry cleaning has been shown to be effective for the removal of acetates in preliminary cleaning tests
- Application of coatings may be an alternative means of protection for uncontaminated objects

Future Conservation

The conservation treatment of bronze with carbonyl corrosion is a new and unexplored field. Until now the focus of bronze conservation has been the prevention and treatment of bronze disease. Often blue, green, and blue-green corrosion on bronze is mistakenly identified by visual inspection and attributed to bronze disease, a species entirely different from carbonyl corrosion. The mistaken identification of carbonyl corrosion as bronze disease by visual assessment with the naked eye was discussed in Chapter 1. Two main characteristics may be used to distinguish carbonyl corrosion containing copper from bronze disease: the carbonyl compounds containing copper are blue or blue-green and form on the surface whereas bronze disease is usually pale green in color erupting from below the surface of the metal. Microchemical tests for acetate may be found in Appendix 17. Failure to detect acetates does not rule out their presence in initial stages of formation, however. Acetates in trace quantities have been detected by IC that went undetected by other analytical means (Tennent *et al.* 1992).

This study has revealed a preponderance of carbonyl corrosion in archaeological bronze collections. This work stresses the importance of the identification of carbonyl

corrosion and the determination of its solubility properties and equilibrium relative humidity (eqRH). Armed with this knowledge the conservator may make an informed decision regarding treatment. The conservator may select preventive or active means of conservation. Preventive means of conservation include control of the environment while active means include cleaning to remove corrosion.

This project offers the first documentation of cleaning tests of archaeological bronze artifacts with acetate and other carbonyl corrosion. Approaches to the cleaning of bronze artifacts with carbonyl corrosion are little addressed in the literature. Suitable cleaning methods for removal of corrosion are based on the degree of solubility. As part of this project two carbonyl corrosion compounds were subjected to solubility testing with four solvents and were determined to be partially soluble in deionized water. A sodium copper carbonate acetate and copper sodium acetate formate were determined to be partially soluble in water requiring a combination of wet and dry cleaning methods for their removal. Swabbing with deionized water provided the best results and is a method that can be recommended for the removal of these compounds.

The hygroscopic nature of many carbonyl compounds renders them sensitive to relative humidity and each of these compounds is characterized by a particular equilibrium relative humidity (eqRH) at which the crystals pass from the crystalline to the liquid state (deliquescence) and vice versa. The eqRH of these compounds may be used as a guide for controlling the RH (or RH range) in display and storage cases. The eqRH of sodium acetate and a sodium copper carbonate acetate have been published (75% and 65% respectively) (Thickett 1998, 9) but those of copper sodium formate acetate and copper acetate hydrate have yet to be determined. The sodium and acetate ions may be rendered inactive by the maintenance of a RH lower than that of the eqRH of the compound(s) present. The presence of multiple corrosion compounds necessarily complicates their mitigation due to differences in solubility and eqRH.

Conservators may adopt either preventive or active means of conservation. Preventive means of conservation consist in controlling the environmental factors of volatile acid concentration, RH, oxygen level, and the application of protective coatings. Recommended doses of acetic acid for storage and display are included in the Guidelines for Conservators and Curators. Bronze without lead may withstand somewhat higher concentrations. Sorbents may be placed in storage and display cases that protect the

artifacts from acetic acid attack. The maintenance of a desiccated or anoxic environment will prevent the occurrence of carbonyl corrosion.

The history of the study of coatings for bronze has concentrated on the protection against bronze disease (a form of corrosion caused by the chemical reaction of moisture with chlorides in the metal). The relatively few bronze artifacts in this study with conservation treatment records have confirmed that the protective qualities of the corrosion inhibitor Benzotriazole and coatings such as Incralac® have a finite duration and cannot be expected to serve beyond a certain number of years. It is well known that these materials must be reapplied periodically. Corrosion tests to assess the protective qualities of two coatings on bronze against acetic acid vapour were carried out in Chapter 6. Figure 6.10 illustrates the first documented test results of coatings on bronze against corrosive attack by volatile acetic acid.

New leaded and unleaded bronze coupons were coated with the acrylate solution, Incralac®, and with the polyethylene emulsion, Poligen® ES 91009, and subjected to high levels of acetic acid vapour and relative humidity constituting accelerated test conditions. Satisfactory results of corrosion protection on bronze were achieved with Incralac® as well as Poligen®. Incralac® has been used for decades to protect bronze from moisture, handling, and bronze disease. I have demonstrated the additional protective properties of Incralac® on bronze recommending it as a protective coating against acetic acid attack. Poligen® is a polymer recently introduced as a potential protective, hydrophobic coating material for the conservation of metal. This is the first study of its application as a protective coating on new, polished bronze. Poligen® has yet to be assessed on ancient bronze artifacts. Coating a rough, corroded surface is much more challenging and poses difficulties in achieving a homogeneous, coherent, and intact film. These challenges should be kept in mind when considering coating a corroded archaeological artifact. Initial test results with Poligen® as a protective coating for bronze are positive and mirror the promising results obtained by other researchers on copper, brass, and steel. The next step in the determination of its suitability as a conservation material will be to perform solubility tests for removability (reversibility). Poligen® requires further testing before it can be recommended as a protective coating on bronze.

It is my intention to compile a database of acetate corrosion products (by identifying artifacts in collections and including conservation treatments and storage history when available) that other conservators, conservation scientists, and researchers may refer to and build upon as a tool for the identification of carbonyl corrosion in collections. This will be carried out after the completion of my degree research.

Bibliography

Aastrup, T., Wadsak, M., Schreiner, M. and Leygraf, C., 2000. Experimental in situ studies of copper exposed to humidified air. *Corrosion Science* 42, 957-967.

Agora Excavations, American School of Classical Studies, Athens, Greece, unpublished and undated conservation treatment records.

Arney, J.S., Jacobs, A.J. and Newman, R., 1979. The influence of calcium carbonate deacidification on the deterioration of paper. In: *Preprints of papers presented at the seventh annual meeting: Toronto, Canada, 30 May-1 June 1979*. Toronto: American Institute for Conservation of Historic and Artistic Works, 10-17.

Arni, P., Gray, J. and Scougall, R., 1961. The emission of corrosive vapours by wood. I. Survey of the acid-release properties of certain freshly felled hardwoods and softwoods. *Journal of Applied Chemistry* 11, 305-313.

Arni, P., Cochrane, G. and Gray, J., 1965. The emission of corrosive vapours by wood, II. The analysis of the vapours emitted by certain freshly felled hardwoods and softwoods by gas chromatography and spectrophotometry. *Journal of Applied Chemistry* 15, 463-468.

Ashley-Smith, J. (ed.), 1987. *Science for Conservators. Book 1 An Introduction to Materials, Book 2 Cleaning, Book 3 Adhesives and Coatings.* London: the Conservation Unit, Museums and Galleries Commission.

ASM, 1990. *Binary Alloy Phase Diagrams, Vol 2*. Materials Park, Ohio: ASM International.

ASM, 2004. *ASM Handbook, Vol. 9, Metallography and Microstructures*. Materials Park, Ohio: ASM International.

ASTM, 1984. ASTM G54-84, *Standard Practice for Simple Static Oxidation Testing.* Philadelphia: American Society for Testing and Materials.

ASTM, 2001. ASTM G78-01, *Standard Practice for Conducting Moist SO_2 Tests.* Philadelphia: American Society for Testing and Materials.

ASTM, 2002. ASTM G85-02, *Standard Practice for Modified Salt Spray (Fog) Testing.* Philadelphia: American Society for Testing and Materials.

ASTM, 2003a. ASTM G1-03, *Standard Practice for Preparing, Cleaning, and Evaluating Corrosion Test Specimens.* Philadelphia: American Society for Testing and Materials.

ASTM, 2003b. ASTM D2803-03, *Standard Test Method for Filiform Corrosion Resistance of Organic Coatings on Metal.* Philadelphia: American Society for Testing and Materials.

ASTM, 2005. ASTM D1654-05, *Standard Method of Evaluation of Painted or Coated Specimens Subjected to Corrosive Environments.* Philadelphia: American Society for Testing and Materials.

ASTM, 2009. ASTM B117-09, *Standard Method of Salt Spray [Fog] Testing*. Philadelphia: American Society for Testing and Materials.

Baines, J. and Málek, J., 1989. *Atlas of Ancient Egypt.* New York: Facts on File, Inc.

BASF, 2004. *Poligen® ES 91009 Data Sheet*. Ludwigshafen: BASF.

BASF, 2006. *Luwax®, Poligen®, Waxes and Wax Emulsions for Many Industrial Applications*, on-line brochures EVD 0 108 e 08.2005 (2005) and FK/EVD 532 d/e. Retrieved 12 August 2006 from www.basf.com/detergents-formulators

Bastidas, J.M., Alonso, M.P., Mora, E.M. and Chico, B., 1995. Corrosion of bronze by acetic and formic acid vapours, sulphur dioxide and sodium chloride particles. *Materials and Corrosion* 46, 515-519.

Bastidas, J., Lopez-Delgado, A., Cano, E., Polo, J. and Lopez, F., 2000. Copper corrosion mechanism in the presence of formic acid vapour for short exposure times. *Journal of the Electrochemical Society* 147, 3, 999-1005.

Beldjoudi, T, Bardet, F, Lacoudre, N, Andrieu, S, Adriaens, A., Constantinides, I. and Brunella, P., 2001a. Surface modification processes on European Union bronze reference materials for analytical studies of cultural artifacts. *Revue de métallurgie: cahiers d'informations techniques* 98, 9, 803-808.

Beldjoudi, T., Bardet, F., Lacoudre, N., Andrieu, S., Adriaens, A., Constantinides, I. and Brunella, P., 2001b. Surface modification processes on European Union bronze reference materials for analytical studies of cultural artifacts. *Surface Engineering* 17, 3, 231-235.

Bhuvanesh, Nattamai (undated). *Bruker D8 Advanced GADDS Instrument, a Tutorial for Beginners, X-ray Diffraction Laboratory.* College Station, Texas: Department of Chemistry, Texas A&M University (pdf).

Bisht, A.S. (ed.), 2003. *Conservation Science*. Delhi [India]: Agam Kala Prakashan.

Blades, N., 1998. Gaseous pollution in the museum environment: the uses and abuses of monitoring campaigns. *The Conservator* 22, 44-48.

Blades, N., Cassar, M., Oreszczyn, T. and Croxford, B., 2000. Preventive conservation strategies for sustainable urban pollution control in museums. In: R. Ashkok and P. Smtih (eds.), *Tradition and Innovation: Advances in Conservation: Contributions to the Melbourne Congress, 10-14 October 2000*. London: International Institute for Conservation of Historic and Artistic Works, 24-28.

Blades, N., Kruppa, D. and May, C., 2002. Development of a Web-based software tool for predicting the occurrence and effect of air pollutants inside museum buildings. In: R. Vontobel (ed.), *ICOM Committee for Conservation 13th Triennial Meeting, Rio de Janeiro, 22-27 September 2002: Preprints*. London: Earthscan Ltd., 9-14.

Bowker, M., Rowbotham, E., Leibsle, F. and Haq, S., 1996. The adsorption and decomposition of formic acid on Cu{110}. *Surface Science* 349, 97 - 100.

Bowker, M., Bennett, R., Poulston, S. and Stone, P., 1998a. Insights into surface reactivity: formic acid oxidation on Cu(110) studied using STM and a molecular beam reactor. *Catalysis Letters* 56, 77-83.

Bowker, M., Poulston, S., Bennett, R., Stone, P., Jones, A., Haq, S., Hollins, P., 1998b. A combined STM/molecular beam study of formic acid oxidation on Cu(110). *Journal of Molecular Catalysis A: Chemical* 131,185-197.

Brokerhof, A.W. and Van Bommel, M., 1996. Deterioration of calcareous materials by acetic acid vapour: a model study. In: J. Bridgland (ed.), *ICOM Committee for Conservation 11th Triennial Meeting, Edinburgh, Scotland, 1-6 September, 1996, Preprints.* London: Earthscan Ltd., 769-775.

Brown, B.F., 1977. *Corrosion and Metal Artifacts: A Dialogue between Conservators and Archaeologists and Corrosion Scientists.* NBS Special Publication 479. United States: National Institute of Standards and Technology.

Bruker Advanced X–ray Solutions, 1998. *Diffraction Solutions for Material Research – D8 Discover.* Karlsruhe, Germany: Bruker.

Brunnert, S., 1985. Die Anwendung von Schwefelwasserstoff bei der Bleirestaurierung (The use of hydrogen sulphide for the restoration of lead). *Arbeitsblätter für Restauratoren 18*, 2, 161-168.

Brunoro, G., Laguzzi, G., Luvidi, L. and Chiavari, C., 2001. Corrosion evaluation of artificially aged 6 wt-% tin bronze. *British Corrosion Journal* 36, 3, 227-232.

Buckingham, J. (ed.), 1985. *Dictionary of Organic Compounds*. (5th edition). New York: Chapman and Hall.

Butsugan, M., 2006. *Measurement of Volatile Organic Compounds in Indoor Air of Museum by Serially Connected Passive Samplers, Paper prepared for the 7th Indoor Air*

Quality 2006 Meeting (IAQ 2006). Retrieved on 30 October 2009 from World Wide Web: http://iaq.dk/iap/iaq2006/2006_contents.htm

Byne, L.S., 1899. The corrosion of shells in cabinets. *J. Conchology* 9, 172 - 178, 253 - 254.

Caley, E.R., 1941. The corroded bronze of Corinth. *Journal of the American Philosophical Society* 84, 5, 689-761.

Caley, E.R., 1964. *Analysis of Ancient Metals*. New York: The Macmillan Company.

Cano, E., López, M.F., Simancas, J. and Bastidas, J.M., 2001a. X-Ray photoelectron spectroscopy study on the chemical composition of copper tarnish projects formed at low humidities. *Journal of the Electrochemical Society* 148, 1, E26-E30.

Cano, E., Torres, C.L. and Bastidas, J.M., 2001b. An XPS study of copper corrosion originated by formic acid vapour at 40% and 80% relative humidity. *Materials and Corrosion* 52, 667-676.

Cano, E. and Bastidas, J.M., 2002. Effect of relative humidity on copper corrosion by acetic and formic acid vapours. *Canadian Metallurgical Quarterly* 41, 3, 327-336.

Cano, E., Bastidas, D. M., Argyropoulos, V. and Siatou, A., 2007. Electrochemcial techniques as a tool for testing the efficiency of protection systems for historical steel objects. In V. Argyropoulos (ed.), *Strategies for Saving Our Cultural Heritage, papers presented at the international conference on conservation strategies for saving indoor metallic collections, 25 Feb-1 March 2007, Cairo.* Athens: TEI, 121-126.

Cano, E., Bastidas, D.M., Argyropoulos, V., Fajardo, S., Siatou, A., Bastidas, J.M. and Degrigny, C., 2010. Electrochemical characterization of organic coatings for protection of historic steel artifacts. *J. Solid State Electrochemistry* 14, 453-463. DOI 10.1007/s10008-009-0907-1

Carley, A., Davies, P. and Mariotti, G., 1998. The oxidation of formic acid to carbonate at Cu(110) Surfaces. *Surface Science* 401,400-411.

Cassar, M., Blades, N. and Oreszczyn, T., 1999. Air pollution levels in air-conditioned and naturally ventilated museums: a pilot study. In: J. Bridgland (ed.), *ICOM Committee for Conservation 12th triennial meeting, Lyon, 29 August-3 September 1999, Preprints.* London: Earthscan Ltd., 31-37.

Chaplin, T., Clark, R. and Scott, D., 2006. Study by Raman Microscopy of nine variants of the green-blue pigment verdigris. *Journal of Raman Spectroscopy* 37, 1-3, 223 – 229.

Clarke, S.G. and Longhurst, E.E., 1961. The corrosion of metals by acid vapours from wood. *Journal of Applied Chemistry* 11, 435-443.

Coles, E., Gibson, J. and Hinde, R., 1958. The corrosion of lead by dilute aqueous organic acids. *Journal of Applied Chemistry* 8, 5, 341-348.

Considine, D.M. (ed.), 1984. *Van Nostrand Reinhold Encyclopedia of Chemistry*. New York: Van Nostrand Reinhold Company.

Craddock, Paul T., 1976. The composition of copper alloys used by the Greek, Etruscan and Roman civilizations. 1. The Greeks before the Archaic period. *Journal of Archaeological Science* 3, 2, 93-113.

Craddock, Paul T., 1977. The composition of the copper alloys used by the Greek, Etruscan and Roman civilizations. 2. The Archaic, Classical and Hellenistic Greeks. *Journal of Archaeological Science* 4, 2, 103-123.

Craddock, Paul T., 1978. The composition of the copper alloys used by the Greek, Etruscan and Roman civilizations. 3. The origins and early use of brass. *Journal of Archaeological Science* 5, 1, 1-16.

CRC, 1998-1999. *Handbook of Chemistry and Physics.* (79th edition). Boca Raton: CRC Press.

Cronyn, J., 1990. *The Elements of Archaeological Conservation*. London: Routledge.

Cruz, A.J., Pires, J., Carvalho, A.P. and Brotas de Carvalho, M., 2008. Comparison of adsorbent materials for acetic acid removal in showcases. *Journal of Cultural Heritage* 9, 3, 244-252.

Dawson, J., 1988. Ulick Evans and the treatment of bronze disease in the Fitzwilliam Museum, 1948-1980. In V. Daniels (ed.), *Early Advances in Conservation.* London: British Museum. British Museum Occasional Paper 65, 71-80.

Degrigny, C., Le Gall, R. and Guilminot, E., 1996. Faciès de corrosion développés sur des poids en plomb du Musée du CNAM de Paris. In: J. Bridgland (ed.), *ICOM Committee for Conservation 11th Triennial Meeting, Edinburgh, Scotland, 1-6 September, 1996, Preprints.* London: Earthscan Ltd., 865-869.

De Witte, E., 1973/1974. The protection of silverware with varnishes, *Bulletin Institut Royal du Patrimoine Artistique*, 140-151.

Dillmann, P. (ed.), 2007. *Corrosion of Metallic Heritage Artefacts: Investigation, Conservation and Prediction for Long-term Behaviour.* Cambridge: Woodhead Publishing Limited. European Federation of Corrosion Publications no. 48.

Donovan, P.D., 1986. *Protection of Metals from Corrosion in Storage and Transit*. Chichester: Ellis Horwood Limited.

Donovan, P.D. and Stringer, J., 1971. The corrosion of metals by organic acid vapours. In N.E. Hamner (ed.), *Proceedings of the Fourth International Congress on Metallic Corrosion held in Amsterdam in 1969*, 537-544.

Down, J., MacDonald, M.A., Tétreault, J. and Williams, R. S., 1996. Adhesive testing at the Canadian Conservation Institute - an evaluation of selected poly(vinyl acetate) and acrylic adhesives. *Studies in Conservation* 41, 1, 19-44.

Dremetsika, A.V., Siskos, P.A. and Bakeas, E.B, 2005. Determination of formic and acetic acid in the interior atmosphere of display cases and cabinets in Athens Museums by Reverse Phase High Performance Liquid Chromatography. *Indoor Built Environment* 14, 51-58.

Dubus, M. and Laurent, A., 2009. Tout ce que vous devez savoir sur les vitrines en bois (Everything you should know about wooden showcases). *Technè: la science au service de l'histoire de l'art et des civilisations* 29, 101-108.

Eagleson, M. (trans.), 1994. *Concise Encyclopedia Chemistry*. Berlin: Walter de Gruyter.

Elbourne, R. and Buchanan, G. A., 1970a. Chronopotentiometric study of complexes of tin (II) with some carboxylic acids. *Journal of Inorganic and Nuclear Chemistry* 32, 493-499.

Elbourne, R. and Buchanan, G. A., 1970b. Potentiometric study of complexes of tin (II) with some carboxylic acids. *Journal of Inorganic and Nuclear Chemistry* 32, 3359-3567.

Ellingson, L.A., Shedlosky, T.J., Bierwagen, G.P., de la Rie, E.R. and Brostoff, L.B., 2004. The use of electrochemical impedance spectroscopy in the evaluation of coatings for outdoor bronze. *Studies in Conservation* 49, 53-62.

Engineering Materials, Inc. 1995. *Corrosion Intercept. Paper Preservation.* Technical Bulletin 29. Buffalo Grove, Ill.: Engineered Materials, Inc.

Eremin, K. and Wilthew, P., 1998. Monitoring concentrations of organic gases within the National Museums of Scotland. *SSCR Journal* 9, 15-19.

Erhardt, D., Hopwood, W., Padfield, T. and Veloz, N.F., 1984. The durability of Incralac: examination of a ten year old treatment. In D. de Froment (ed.), *ICOM Committee for Conservation 7th Triennial Meeting in Copenhagen, 10-14 September 1984, Preprints.* Paris: ICOM, 84.22.1-84.22.3.

European Commission, 1998. RTDinfo, Retreived on 14 September 2009 from http://ec.europa.eu/research/rtdinf19/19e07.html

Evans, U.R., 1951. The corrosion situation: past, present and future. *Chemistry and Industry* 706-711.

Evans, U.R., 1961. *The Corrosion and Oxidation of Metals: Scientific Principles and Practical Applications.* London: Edward Arnold publishers Ltd.

Faltermeier, R., 1995. *The Evaluation of Corrosion Inhibitors for Application to Copper and Copper Alloy Archaeological Artifacts.* Unpublished PhD thesis, University College London.

Faltermeier, R. B., 1999. A corrosion inhibitor test for copper-based artifacts. *Studies in Conservation* 44, 2,121-128.

Farmer, R.H., 1962. Corrosion of Metals in Association with Wood: I. Corrosion by Acidic Vapours from Wood: II. Corrosion of Metals in Contact with Wood. *Wood* (August, November) 326-328, 443-446.

Feigl, F. and Anger, V., 1972. *Spot Tests in Inorganic Analysis.* Amsterdam: Elsevier Publishing Company.

Fink, C. and Eldridge, C., 1925. *The Restoration of Ancient Bronzes and Other Alloys.* New York: Metropolitan Museum of Art.

Fink, C.G. and Polushkin, E.P.,1936. Microscopic study of ancient bronze and copper. *Transactions of the American Institute of Mining and Metallurgy 122*, 90-117.

Fitzhugh, E.W. and Gettens, R.J., 1971. Calclacite and other efflorescent salts on objects stored in wooden museum cases. In R. Brill (ed.), *Science and Archaeology*, Cambridge (MA): MIT Press, 91-102.

Frondel, C. and Gettens, R.J., 1955. Chalconatronite, a new mineral from Egypt. *Science, New Series* 122, 3158, 75-76.

Fulton, J.W., 2002. *Dehydrogenation* . Retrieved 18 March 2006 from http://www.accessscience.com, DOI 10.1036/1097-8542.184100

Garrels, R. M. and Christ, C. L., 1965. *Solutions, Minerals and Equilibria*. New York: Harper and Row.

Gauthier, J. 1958. *Etude de quelques propriétés des sels neutres er basiques de cuivre des acides formique, acétique, propionique & Propositions données par la Faculté.* Ph.D. diss. Procede Sertic. Lyons: l'Université de Paris

Gettens, R.J. and Frondel, C., 1955. Chalconatronite: an alteration product of some ancient Egyptian bronzes. *Studies in Conservation* 2, 64-75.

Gettens, R.J., 1963. Mineral alteration products on ancient metal objects. In: G. Thomson (ed.), *Recent Advances in Conservation, Contributions to the IIC Rome Conference 1961*. London: Butterworths, 89-92.

Gibson, L., Cooksey, B., Littlejohn, D. and Tennent, N., 1997a. Determination of experimental diffusion coefficients of acetic acid and and formic acid vapours in air using a passive sampler. *Analytica Chimica Acta* 341, 1-10.

Gibson, L.T., Cooksey, B.G., Littlejohn, D. and Tennent, N.H., 1997b. A Diffusion tube sampler for the determination of acetic acid and formic acid vapours in museum cabinets. *Analytica Chimica Acta* 341, 11-19.

Gibson, L.T., Cooksey, B.G., Littlejohn, D. and Tennent, N.H., 1997c. Determination of acetic acid and formic acid vapour concentrations in the museum environment by passive sampling. *European Cultural Heritage Newsletter on Research*, 10 (Jun), 108-112.

Gibson, L.T. and Watt, C.M., 2010. Acetic and formic acids emitted from wood samples and their effect on selected materials in museum environments. *Corrosion Science* 52, 1, 172-178.

Gill, H. and Leygraf, C., 2007a. Quantitative in situ analysis of initial atmospheric corrosion of copper induced by acetic acid. *Journal of the Electrochemical Society* 154, 5, C272-C278.

Gill, H. and Leygraf, C., 2007b. Initial atmospheric corrosion of copper induced by carboxylic acids, a comparative in situ study. *Journal of the Electrochemical Society* 154, 11, C611-C617.

Giorgi, R., Chelazzi, D., Fratini, E., Langer, S., Niklasson, A., Rådemar, M., Svensson, J. and Baglioni, P., 2009. Nanoparticles of calcium hydroxide for wood deacidification: decreasing the emissions of organic acid vapors in church organ environments. *Journal of cultural heritage* 10, no. 2, 206-213.

Gong, H., Wang, Y., Teo, S. and Huang, L., 1999. Interaction between thin-film tin oxide gas sensor and five organic vapours. *Sensors and Actuators* B54, 232 – 235.

Gosling, J., Manti, P. and Nicholson, P.T., 2004. *Discovery and Conservation of a Hoard of Votive Bronzes from the Sacred Animal Necropolis at North Saqqara.* Retrieved October 2008 from www.PalArch.nl, archaeology of Egypt/Egyptology, 2, 1.

Graedel, T.E., 1987. Copper patinas formed in the atmosphere - II. A qualitative assessment of mechanisms. *Corrosion Science* 27, 7, 721-740.

Graedel, T.E., 1994. Chemical mechanisms for the atmospheric corrosion of lead. *Journal of the Electrochemical Society* 141, 922-927.

Green, C.I., 1987. *The Temple Furniture from the Sacred Animal Necropolis at North Saqqara 1964-1976.* London: Egypt Exploration Society.

Green, L.R., 1990. *Selection of Materials and Methods for Display*. Unpublished British Museum Report 1990/1. London: The British Museum.

Green, L.R. and Thickett, D., 1993. Interlaboratory comparison of the Oddy test. In: N. Tennent (ed.), *Conservation Science in the UK*. London: James and James Science Publishers Ltd, 111-116.

Green, L.R. and Thickett, D., 1995. Testing materials for the storage and display of artifacts – a revised methodology. *Studies in Conservation* 40, 145-152.

Greenspan, L., 1977. Humidity fixed points of binary saturated aqueous solutions. *Journal of Research of the National Bureau of Standards -A. Physics and Chemistry* 81A, 1, 89-96.

Grzywacz, C.M. and Stulik, D.C., 1992. Passive monitors for the detection of pollutants in museum environments. In Pamela Hatchfield (ed.), *AIC Objects Specialty Group Postprints 1991, Vol. 1.* Washington, D.C.: American Institute for Conservation, 33-41.

Grzywacz, C. and Tennent, N., 1994. Pollution monitoring in storage and display cabinets: carbonyl pollutant levels in relation to artifact deterioration. In A. Roy and P. Smith (eds.), *Preventive Conservation Practice, Theory and Research: Preprints of the Contributions to the Ottawa Congress, 12-16 September 1994*. London: International Institute for Conservation, 164-170.

Grzywacz, C., 2006. *Monitoring for Gaseous Pollutants in Museum Environments.* Los Angeles: Getty Conservation Institute.

Halsbergh, L., Erhardt, D., Gibson, L. and Zehnder, K. 2005. Simple methods for the identification of acetate salts on museum objects. In J. Bridgland (ed.), *Preprints of the ICOM Committee for Conservation 14th Triennial Meeting in The Hague, 12-16 September, 2005*. London: James and James Scientific Publishers, 639-647.

Harch, A., Robbiola, L., Fiaud, C. and Santrot, M.H., 1993. Caractérisation des principaux types d'altération des objects anciens en plomb. In: S. Pennec and L. Robbiola (eds.), *Actes de la 7e Rencontre Annuelle du Groupe de Travail: Draguignan, 23 avril 1993, Laboratoire de Conservation-Restauration de Draguignan.* Draguignan: ICOM Committee for Conservation, 15-31.

Hastings, E.A., 1997. *The Sculpture from the Sacred Animal Necropolis at North Saqqara 1964-1976.* London: Egypt Exploration Society.

Hatchfield, P. B., 2002. *Pollutants in the Museum Environment.* London: Archetype Publications.

Hawley, G., 1981. *The Condensed Chemical Dictionary*. (10th edition). New York: Van Nostrand Reinhold Company.

Hawley, G., 2001. *The Condensed Chemical Dictionary*. (14th edition). New York: John Wiley and Sons.

Heath, D. and Martin, G., 1988. The corrosion of lead and lead/tin alloys occurring on Japanese lacquer objects. In: J.S. Mills, P. Smith, K. Yamasaki (eds.), *The Conservation of Far Eastern Art: Preprints of the Contributions to the Kyoto Congress, 19-23 September 1988.* London: IIC, 137-141.

Heitz, E., Henkhaus, R. and Rahmel, A., *Corrosion Science, an Experimental Approach*. New York: Ellis Horwood Ltd., 1992.

Hemming, D., 1977. The production of artificial patination on copper. In: B.F.Brown (ed.), *Corrosion and Metal Artifacts: a Dialogue between Conservators and Archaeologists and Corrosion Scientists.* NBS Special Publication 479. Washington, D.C.: U.S. Department of Commerce, 93-102.

Hiers, G.O., 1948. Lead and lead alloys. In: H.H. Uhlig (ed.). *The Corrosion Handbook*, New York: John Wiley and Sons, Inc., 207-216.

Hodgkins, R., 2008. *Detection of Acetic and Formic Acids in Storage Environments using Museum Diffusion Tubes and Ion Chromatography, and Identification of Efflorescence on Fossils from the Natural History Museum of Los Angeles County.* Unpublished Master of Chemistry Thesis, University of California, Los Angeles.

Holsworth, R.M., 1982. Overview – on the weathering of organic coatings. In: *Permanence of Organic Coatings*. Philadelphia: ASTM. ASTM Special Technical Publication 781, 3-9.

Holtzberg, F., Post, B. and Fankuchen, I. 1953. The crystal structure of formic acid. *Acta Crystallogr.* 6, 127-130.

Horie, C.V. and Vint, J.A., 1982. Chalconatronite: a by-product of conservation? *Studies in Conservation* 27, 185-186.

Horie, C.V., 2003. *Materials for Conservation*. Oxford: Butterworth-Heinemann.

Hromatka, O. and Ebner, H., 1959. Vinegar by submerged oxidative fermentation. *Ind. Eng. Chem.* 51, 10, 1279-1280.

Hsu, C., McCullen, E. and Tobin, R., 2003. Unusual adsorption kinetics of formic acid on Cu(100) studied by dc resistance and nonresonant infrared reflectance changes. *Surface Science* 542,120 - 128.

http://cameo.mfa.org (August 14, 2006)

http://chemistry.about.com (April 11, 2010)

http://course1.winona.edu/sberg/ChemStructures/Formic.gif (April 11, 2010)

http://electrochem.cwru.edu/ed/dict.htm (January 16, 2009)

http://msds.chem.ox.ac.uk/glossary/tlv.html (September 5, 2009)

http://www.dac.neu.edu/cammp/x-ray.htm (June 3, 2009)

http://www.petrie.ucl.ac.uk/index2.html (May 23, 2009)

http://www.shodor.org/appstchem/advanced/redox/index.html (April 9, 2010)

Hubert, V., Hunger, K. and Philippe, L., 2008. *Monitoring Indoor Air Quality in the New Collections Centre of the Swiss National Museums, paper prepared for the 8th Indoor Air Quality 2008 Meeting (IAQ 2008).* Retrieved on 30 October 2009 from World Wide Web: http://iaq.dk/iap/iaq2008/2008_contents.htm

Irwin, J., Prime, A., Hardman, P., Wincott, P. and Thornton, G., 1996. The interconversion of SnO_2(110) reduced phases by reaction with formic acid. *Surface Science* 352-354, 480-484.

Jaeschke, R. and Jaeschke, H., 1988. Early conservation techniques in the Petrie Museum. In: S. Watkins, C. Brown (eds.), *Conservation of Ancient Egyptian Materials:*

Preprints of the Conference organised by the United Kingdom Institute for Conservation, Archaeology Section, held at Bristol, 15-16 December 1988. London: UKIC, 17-23.

Johnson, G.E., Bair, H.E. and Anderson, E.W., 1981. The states of water in polymer films. In: H. Leidheiser (ed.), *Corrosion control by Organic Coatings*. Houston: National Association of Corrosion Engineers, 4-11.

Jones, R.E. and Templeton, D.H. 1958. The crystal structure of acetic acid. *Acta Crystallogr*. 11, 484-487.

Jones, D.A. 1996. *Principles and Prevention of Corrosion*. Upper Saddle River: Prentice Hall.

Kinloch, A.J., 1987. *Adhesion and Adhesives: Science and Technology*. New York: Chapman and Hall.

Kirk-Othmer Encyclopedia of Chemical Technology, 2004. (5th edition). Vol. 1, "acetic acid", 115-136; Vol. 5, "carboxylic acid", 27-77. New York: John Wiley & Sons, Inc.

Kleber, C., Schreiner, M., 2003. In situ TM-AFM investigations of the influence of zinc and tin as alloy constituents of copper to the early stages of corrosion. *Applied Surface Science* 217, 294-301.

Klein, S., 1999. Iron Age leaded tin bronzes from Khirbet Edh-Dharih, Jordan. *Journal of Archaeological Science* 26, 1075-1082.

Koehler, E.L., 1981. Underfilm corrosion currents as the cause of failure of protective organic coatings. In: H. Leidheiser (ed.), *Corrosion Control by Organic Coatings*. Houston: National Association of Corrosion Engineers, 87-96.

Kugler, W., 2003. X-ray diffraction analysis in the forensic science: the last resort in many criminal cases. *Advances in X-ray Analysis* 46, 1-16.

Laguzzi, G., Tommesani, L., Luvidi, L., Bucci, R. and Brunoro, G., 1999. Thin layer activation technique application in bronze corrosion monitoring. *Corrosion Science* 41, 197-202.

Lane, H., 1975. The reduction of lead. In: P. Smith (ed.), *Conservation in Archaeology and the Applied Arts: Preprints of the Contributions to the Stockholm Congress, 2-6 June 1975.* London: International Institute for Conservation, 215-217.

Lane, H., 1980. Some comparisons of lead conservation methods, including consolidative reduction. In: *The Conservation and Restoration of Metals, Proceedings of the Symposium held in Edinburgh, 30-31 March, 1979.* Edinburgh: Scottish Society for Conservation and Restoration, 50-60.

Lane, H. 1987. The conservation and storage of lead coins in the department of coins and medals, British Museum. In: J. Black (ed.), *Recent Analysis in the Conservation and Analysis of Artifacts, Jubilee Conservation Conference Papers, London, 6-10 July 1987.* London: Summer Schools Press, 149-153.

Lang, R., 1995. *The Corrosion of Metal Antiquities by Pollutants from Wooden Storage Materials: A Case Study at N.M.G.M.* Unpublished report for the Diploma in Archaeological Conservation, University College London.

Lang, R., 1996. Corrosion of copper-alloy antiquities in wooden storage boxes. *Conservation News* (UKIC) 61, 57-58.

Lange's Handbook of Chemistry, 2005. (16th edition). Speight, J. (ed.), New York: McGraw-Hill.

López-Delgado, A., Bastidas, J.M., Alonso, M.P. and López, F.A., 1997. Influence of acetic and formic vapours on patinated artistic bronze. *Journal of Materials Science Letters* 16, 776-779.

López-Delgado, A., Cano, E., Bastidas, J.M. and López, F.A., 1998. A laboratory study of the effect of acetic acid vapour on atmospheric copper corrosion. *Journal of Electrochemical Society* 145, 12, 4140-4147.

López-Delgado, A., Cano, E., Bastidas, J.M. and López, F.A., 2001. A comparative study on copper corrosion originated by formic and acetic acid vapours. *Journal of Materials Science* 36, 5203-5211.

Lucas, A., 1932. *Antiques, Their Restoration and Preservation.* London: Edward Arnold & Co.

Mabille, I., Bertrand, A., Sutter, E.M.M. and Fiaud, C., 2003. Mechanism of dissolution of a Cu-13Sn alloy in low aggressive conditions. *Corrosion Science* 45, 855-866.

Maekawa, S. and Elert, K., 2003. *The Use of Oxygen-Free Environments in the Control of Museum Insect Pests.* Los Angeles: Getty Conservation Institute.

Manti, P. and Gosling, J., 2007. *Challenges on the Conservation of Decorated Bronzes from the Sacred Animal Necropolis at North Saqqara, Egypt.* Poster prepared for Decorated Surfaces of Ancient Egyptian Objects: Technology, Deterioration and Conservation Conference, ICON Archaeology Group and the Fitzwilliam Museum, University of Cambridge, 7-8 September, 2007, Cambridge, England. (PDF retrieved from the authors)

Mattias, P., Maura, G. and Rinaldi, G., 1984. The degradation of lead antiquities from Italy. *Studies in Conservation* 18, 87-92.

Maxwell-Hyslop, K.R. and Williams, A.R., 1976. Ancient steel from Egypt. *Journal of Archaeological Science* 3, 4, 283-305.

May, E. and Jones, M. (eds.), 2006. *Conservation Science: Heritage Materials*. Cambridge: Royal Society of Chemistry.

Miles, C., 1986. Wood coatings for display and storage cases. *Studies in Conservation* 31, 114-126.

Mills, D.J. and Mayne, J.E.O., 1981. The inhomogeneous nature of polymer films and its effect on resistance inhibition. In: H. Leidheiser (ed.), *Corrosion Control by Organic Coatings*. Houston: National Association of Corrosion Engineers 12-17.

Moffatt, W.G., 1984. *The Handbook of Binary Phase Diagrams, Schenectady, Vol. 2.* New York: Genium Publishing Corporation.

Moncrieff, A., 1966. Protecting silver from tarnishing. *IIC News* 4, 6-7.

Mottner, P., 2007. Early warning dosimeters for monitoring indoor museum climate: environmental impact sensors and LightCheck™. In: V. Argyropoulos (ed.), *Strategies for saving our Cultural Heritage, Papers presented at the International Conference on Conservation Strategies for Saving Indoor Metallic Collections, 25 Feb-1 March 2007, Cairo.* Athens: TEI, 53-57.

Nicholls, J.R., 1934. Deterioration of shells when stored in oak cabinets. *Chemistry and Industry* 53, 1077-1078.

Nicholson, P. and Smith, H., 1996. An unexpected cache of bronzes. *Egyptian Archaeology* 9, 18.

Nicholson, P., 2004. Conserving bronzes from north Saqqara. *Egyptian Archaeology* 25, Autumn, 7-9.

Nicholson, P., 2005. The Saqqara bronzes project, 2004. *The Journal of Egyptian Archaeology* 91,12-15.

Nicholson, P., 2006. The Saqqara bronzes project, 2005. *The Journal of Egyptian Archaeology* 92, 19-21.

Niklasson, A., Johansson, L. and Svensson, J., 2005. Influence of acetic acid vapour on the atmospheric corrosion of lead. *Journal of the Electrochemical Society* 152, 12, B519-B525.

Niklasson, A., Johansson, L. and Svensson, J., 2007. Atmospheric corrosion of lead, the influence of formic acid and acetic acid vapours. *Journal of the Electrochemical Society* 154, 11, C618-C625.

Nockert, M. and Wadsten, T., 1978. Storage of archaeological textile finds in sealed boxes. *Studies in Conservation* 23, 38-41.

Norman, M., 1988. Early conservation techniques and the Ashmolean. In: *Conservation of Ancient Egyptian Materials: Preprints of the Conference organised by the United Kingdom Institute for Conservation, Archaeology Section, held at Bristol, 15-16 December 1988.* London: UKIC, 7-16.

Oddy, W.A. and Hughes, M.J., 1970. The stabilization of "active" bronze disease and iron antiquities by the use of sodium sesquicarbonate. *Studies in Conservation* 15, 183-189.

Oddy, W.A., 1973. An unsuspected danger in display. *Museums Journal* 73, 27-28l.

Oddy, A., 1975. The corrosion of metals on display. In P. Smith (ed.), *Conservation in Archaeology and the Applied Arts: Preprints of the Contributions to the Stockholm Congress, 2-6 June 1975.* London: International Institute for Conservation, 235-237.

Odegaard, N., Carroll, S. and Zimmt, W.S., 2000. *Material Characterization Tests for Objects of Art and Archaeology.* London: Archetype Publications Ltd.

Odlyha, M., Jakiela, S., Theodorakopoulos, C., Slater, J.M., Caviccioli, A. and de Faria, D.L.A., 2008. *The Application and Further Development of Piezoelectric Quartz Crystal (PQC)-based Dosimeters for Monitoring Microclimates, paper prepared for the 8th Indoor Air Quality 2008 Meeting (IAQ 2008).* Retrieved 30 October 2009 from http://iaq.dk/iap/iaq2008/2008_contents.htm

Orchin, M. (ed.), 2005. *The Vocabulary and Concepts of Organic Chemistry*. (Second edition). Hoboken: John Wiley and Sons, Inc.

Organ, R.M., 1970. The Conservation of Bronze Objects. In: S. Doringer et al. (eds.), *Art and Technology: A Symposium on Classical Bronzes.* Cambridge: MIT Press, 73-84.

Otiena-Alego, V., Heath, G., Hallam, D. and Creagh, D., 1998a. Electrochemical evaluation of the anti-corrosion performance of waxy coatings for outdoor bronze conservation. In: W. Mourey (ed.), *Metal 98, Proceedings of the International Conference on Metals Conservation, Draguignan-Figanieres, France, 27-29 May, 1998.* London: James & James (Science Publishers) Ltd., 309-314.

Otiena-Alego, V., Hallam, D., Viduka, A., Heath, G. and Creagh, D., 1998b. Electrochemical impedance studies of the corrosion resistance of wax coatings on artificially patinated bronze. In: W. Mourey (ed.), *Metal 98, Proceedings of the International Conference on Metals Conservation, Draguignan-Figanieres, France, 27-29 May, 1998.* London: James & James (Science Publishers) Ltd., 315-319.

Padfield, T., Erhardt, D. and Hopwood, W., 1982. Trouble in store. In: N. Brommelle and G. Thomson (eds.), *Science and Technology in the Service of Conservation: Preprints of the Contributions to the Washington Congress, 3-9 September 1982.* London: International Institute for Conservation, 24-27.

Paterakis, A.B. 1998. Archaeological metals in the ancient Athenian Agora. In: W. Mourey and L. Robbiola (eds.), *Metal 98: Proceedings of the International Conference on Metals Conservation: Draguignan-Figanières, France, 27-29 May, 1998.* London: Earthscan Ltd., 60-63.

Paterakis, A.B., 1999. A conservation survey of Bronze Age metals in the Athenian Agora. In P.P. Betancourt, V. Karageorghis, R. Laffineur, and W. Niemeier (eds.), *Meletemata, Studies in Aegean Archaeology Presented to Malcolm H. Weiner as He enters his 65th Year. Aegaeum* 20, 651-659.

Paterakis, A.B., 2000a. Two gilded bronze sculptures from the Athenian Agora. In: T.D.Weisser (ed.), *Gilded Metals – History, Technology, Conservation.* London: Archetype Publications Ltd., 97-107.

Paterakis, A.B., 2000b. Athenian gilded bronzes from a conservation perspective. In: C. C. Mattusch (ed.), Acta of the 13th International Bronze Congress, held at Cambridge, Massachusetts, May 28-June 1, 1996. *Journal of Roman Archaeology, Supplementary Series* no. 39, I, 173-177.

Paterakis, A.B., 2003. The influence of conservation treatments and environmental storage factors on corrosion of copper alloys in the ancient Athenian Agora. *Journal of the American Institute for Conservation* 42, 2, 313-339.

Paterakis, A.B., 2004. The hidden secrets of copper alloy artifacts in the Athenian Agora. In: I. D. MacLeod (ed.), *Metal 2001: Proceedings of the ICOM Committee for Conservation Metals Working Group*. Perth: Western Australian Museum, 232-236.

Paterakis, A.B., 2007. The corrosion of archaeological bronzes by acetic acid – recommendations. In: C. Degrigny (ed.), *Metal 07: Interim Meeting of the ICOM-CC Metal WG Amsterdam, 17-21 September, 2007.* Amsterdam: Rijksmuseum, 94-99.

Petrie, W.F., 1904. *Methods and Aims in Archaeology*. London: Macmillan.

Petrie Museum Website, 2009. Retrieved June 2009 from http://www.petrie.ucl.ac.uk/ online catalogue.

Piechota, D., 1992. Humidity control in cases: buffered silica gel versus saturated salt solutions. *Western Association for Art Conservation Newsletter* 15, 19-21.

Plenderleith, H.J., 1934. *The Preservation of Antiquities*. London: The Museums Association.

Plenderleith, H.J., 1956. *The Conservation of Antiquities and Works of Art*. London: Oxford University Press.

Plenderleith, H.J. and Werner, A.E.A., 1971. *The Conservation of Antiquities and Works of Art.* Oxford: Oxford University Press.

Pollard, A.M., Thomas, R.G. and Williams, P.A., 1990. Mineralogical changes arising from the use of aqueous sodium carbonate solutions for the treatment of archaeological copper objects. *Studies in Conservation* 35, 148-152.

Poulston, S., Jones, A., Bennett, R. and Bowker, M., 1997. An STM investigation of formic acid adsorption on oxygen precovered Cu(110). *Surface Science* 377-379, 66-70.

Pourbaix, M., 1974. *Atlas of electrochemical equilibria in aqueous solutions.* Houston: National Association of Corrosion Engineers (NACE).

Pourbaix, M., 1976. Some applications of potential-pH diagrams to the study of localized corrosion. *Journal of the Electrochemical Society* 123, 2, 25c-35c.

Pourbaix, M., 1977. Electrochemical corrosion and reduction. In: B.F. Brown (ed.), *Corrosion and Metal Artifacts: A Dialogue between Conservators and Archaeologists and Corrosion Scientists.* Washington, D.C.: U.S. Department of Commerce, National Bureau of Standards. NBS Special Publication 479, 1-16.

Price, C. and Brimblecombe, P., 1994. Preventing salt damage in porous materials. In: *Preventive Conservation: Practice, Theory and Research. Preprints of the contributions to the Ottawa Congress, 12-16 September 1994.* London: International Institute for Conservation, 90-93.

Price, C., Hallam, D., Heath, G., Creagh, D. and Ashton, J., 1995. An electrochemical study of waxes for bronze sculpture. In: I. MacLeod (ed.), *Metal 95: Proceedings of the International Conference on Metals Conservation: Semur en Auxois, 25-28 September. 1995*. London: Earthscan Ltd., 223-241.

Price, C. (ed.), 2000. An expert chemical model for determining the environmental conditions needed to prevent salt damage in porous materials. In: *Protection and Conservation of the European Cultural Heritage.* Research report N. 11, European Commission. London: Archetype Books.

PROMET, 2009. Retrieved 3 October 2009 from http://www.eng.um.edu.mt/~met/inter_promet.html

Prosek, T., Kouril, M., Degres, Y., Thierry, D. and Doubravova, K., 2008. *Automated Atmospheric Corrosion Sensors for Real Time Monitoring: Sensitivity and First Practical Experiences, paper prepared for the 8th Indoor Air Quality 2008 Meeting (IAQ 2008).* Retrieved 30 October 2009 from http://iaq.dk/iap/iaq2008/2008_contents.htm

Rahn-Koltermann, G., Buss, D.H., Fuchs, R. and Glemser, O., 1991. Zur Kenntnis basischer Kupferacetate. *Zeitschrift für Naturforschung* 46b, 1020-1024.

Rathgen, F., 1905. *The Preservation of Antiquities.* Cambridge: University Press.

Raychaudhuri, M.R. and Brimblecombe, P., 2000. Formaldehyde oxidation and lead corrosion. *Studies in Conservation* 45, 226-232.

Redmore, F.H., 1979. *Fundamentals of Chemistry.* Englewood Cliffs: Prentice-Hall, Inc.

Rigaku, 2008. *D/MAX-RAPID II Rigaku/Curved IP X-ray Diffractometer System.* Tokyo: Rigaku Corporation. Retrieved 12 October 2008 from http://www.rigaku.com/downloads/brochures/

Robbiola, L., Blengino, J.M. and Fiaud, C., 1998. Morphology and mechanisms of formation of natural patinas on archaeological Cu-Sn Alloys. *Corrosion Science* 40, 12, 2083-2111.

Rocca, E. and Mirambet, F., 2007. Corrosion inhibitors for metallic artifacts: temporary protection. In: P. Dillmann, G. Béranger, P. Piccardo, and H. Matthiesen (eds.), *Corrosion of Metallic Heritage Artefacts: Investigation, Conservation and Prediction for Long-term Behaviour.* Cambridge (UK): Woodhead Publishing Ltd. European Federation of Corrosion Publications no. 48, 308-334.

Schweitzer, P.A., 2004. *Encyclopedia of Corrosion Technology*. New York: Marcel Dekker, Inc.

Schweizer, F., 1994. Bronze objects from lake sites: from patina to “biography”. In: D.A. Scott (ed.), *Ancient and Historic Metals, Conservation and Scientific Research.* Los Angeles: Getty Conservation Institute 33-50.

Schwenk, W. 1981. Adhesion loss of organic coatings: causes and consequences for corrosion protection. In: H. Leidheiser (ed.), *Corrosion Control by Organic Coatings.* Houston: National Association of Corrosion Engineers, 103-110.

Scott, A., 1926. *The Cleaning and Restoration of Museum Exhibits, Third Report.* London: H.M.S.O.

Scott, D., 1990. Bronze disease: A review of some chemical problems and the role of relative humidity. *Journal of the American Institute for Conservation* 29, 2, 193-206.

Scott, D. (ed.), 1994. *Ancient and Historic Metals: Conservation and Scientific Research.* Los Angeles: Getty Conservation Institute.

Scott, D., Taniguchi, Y. and Koseto, E., 2001. The verisimilitude of verdigris: a review of the copper carboxylates. *Reviews in Conservation* 2, 73-91.

Scott, D., 2002. *Copper and Bronze in Art: Corrosion, Colorants, Conservation*. Los Angeles: Getty Conservation Institute.

Scott, D., 2004. *Metallography of Metals*. Unpublished course book. University of California, Los Angeles.

Selwyn, L., 2004. *Metals and Corrosion: A Handbook for the Conservation Professional.* Ottawa: Canadian Conservation Institute.

Shreir, L., 1978. *Corrosion: Metal/Environment Reactions.* 1. London: Butterworths.

Siatou, A., Argyropoulos, V., Charalambous, D., Polikreti, K. and Kaminari, A., 2007. Testing new coating systems for the protection of metal collections exposed in uncontrolled museum environment. In: V. Argyropoulos (ed.), *Strategies for Saving our Cultural Heritage, Papers presented at the International Conference on Conservation*

Strategies for saving Indoor Metallic Collections, 25 Feb-1 March 2007, Cairo. Athens: TEI, 115-120.

Sim, J.H., Kamaruddin, A.H., Long, W.S. and Najafpour, G., 2007. Clostridium aceticum-a potential organism in catalyzing carbon monoxide to acetic acid: application of response surface methodology. *Enzyme and Microbial Technology* 40, 5, 1234-1243.

Skale, S., Doleček,V. and Slemnik, M., 2007. Substitution of the constant phase element by Warburg impedance for protective coatings. *Corrosion Science* 49, 1045-1055.

Stambolov, T., 1985. *The Corrosion and Conservation of Metallic Antiquities and Works of Art.* Amsterdam: Central Research Laboratory for Objects of Art and Science.

Stone, P., Poulston, S., Bennett, R.A., Price, N.J. and Bowker, M., 1998. An STM, TPD and XPS investigation of formic acid adsorption on the oxygen-precovered c(6x2) surface of Cu(110). *Surface Science* 418, 71-83.

Taboury, K.F., 1931. Des modifications chimiques de certaines substances calcaires conservees dans des meubles en bois. *Bull. de la Soc. Chim. de France* 49, 1289 - 1293.

Tanter, G. and Jull, S., 1987. *An Infrared Spectroscopic Examination of Corrosion Samples for the Science Museum.* unpublished report, Science Museum of London.

Tennent, N. (ed.), 1979. *The Conservation and Restoration of Metals: Proceedings of the Symposium held in Edinburgh 30-31 March 1979*. Edinburgh: Scottish Society for Conservation & Restoration.

Tennent, N.H. and Baird, T., 1985. The deterioration of Mollusca collections: identification of shell efflorescence. *Studies in Conservation* 30, 73-85.

Tennent, N.H. and Baird, T., 1992. The identification of acetate efflorescence on bronze antiquities stored in wooden cabinets. *The Conservator* 16, 39-43, 47.

Tennent, N.H., Cooksey, B.G., Littlejohn, D. and Ottaway, B. J., 1992. Some applications of ion chromatography to the study of the deterioration of museum artifacts.

In: Vandiver, P., Druzik, J., Wheeler, G. and Freestone, I. (eds.), *Materials Issues in Art and Archaeology III: Symposium held April 27-May 1, 1992, San Francisco, California, USA.* Materials Research Society symposium proceedings, 267. Warrendale: Materials Research Society, 869-882.

Tennent, N. (ed.), 1993. *Conservation Science in the UK. Preprints of the Meeting held in Glasgow, May 1993.* London: James and James Science Publishers Ltd.

Tennent, N.H., Cooksey, B. G., Littlejohn, D., Ottaway, B. J., Tarling, S. E. and Vickers, M., 1993a. Unusual corrosion and efflorescence products on bronze and iron antiquities stored in wooden cabinets. In: N.H. Tennent (ed.), *Conservation Science in the UK*. London: James and James (Science Publishers) Ltd., 60-66.

Tennent, N.H., Tate, J. and Cannon, L., 1993b. The corrosion of lead artifacts in wooden storage cabinets. *SSCR Journal* 4, 8-11.

Tetreault, J. and Stamatopoulou, E., 1997. Determination of concentrations of acetic acid emitted from wood coatings in enclosures. *Studies in Conservation* 42, 141-156.

Tetreault, J., Sirois, J. and Stamatopoulou, E., 1998. Studies of lead corrosion in acetic acid environments. *Studies in Conservation* 43, 17-32.

Tetreault, J., 2003a. *Airborne Pollutants in Museums, Galleries, and Archives: Risk Assessment, Control Strategies, and Preservation Management.* Ottawa: Canadian Conservation Institute.

Tétreault, J., 2003b. Guidelines for pollutant concentrations in museums, *CCI Newsletter* 31, June.

Tetreault, J., Cano, E., Van Bommel, M., Scott, D., Dennis, M., Barthés-Labrousse, M., Minel, L. and Robbiola, L., 2003. Corrosion of copper and lead by formaldehyde, formic and acetic acid vapours. *Studies in Conservation* 48, 4, 237-250.

Thickett, D. and Lee, L.R., 1994. *The Selection of Materials for the Storage or Display of Museum Objects.* London: British Museum. The British Museum Occasional Paper No. 111.

Thickett, D., 1996. *Analysis of Blue Corrosion on Copper Alloy Dagger EA 65263.* Report CA1996/55, Department of Conservation, Conservation Research Group. London: The British Museum, London, unpublished.

Thickett, D. and Lee, L., 1996. *Analysis of Corrosion Products from Four Egyptian Bronzes: EA 22164, 22667, 63574, 71434.* Report CA1996/25, Department of Conservation, Conservation Research Group. The British Museum, London, unpublished.

Thickett, D., 1997. *Relative Effects of Formaldehyde, Formic and Acetic Acids on Lead, Copper and Silver.* Report No. 1997/12, Department of Conservation, Conservation Research Group. London: The British Museum, unpublished.

Thickett, D., 1998. *Investigation of an Unusual Pale Blue Corrosion occurring on Egyptian Copper Alloy Artifacts.* Report no. 1998/18, Department of Conservation, Conservation Research Group. The British Museum, London, 15 pages, unpublished.

Thickett, D., Bradley, S. and Lee, L., 1998. Assessment of the risks to metal artifacts posed by volatile carbonyl pollutants. In W. Mourey and L. Robbiola (eds.), *Metal 98: Proceedings of the International Conference on Metals Conservation: Draguignan-Figanières, France, 27-29 May, 1998.* London: Earthscan Ltd., 260-264.

Thickett, D. and Odlyha, M., 2000. Note on the identification of an unusual pale blue corrosion product from Egyptian copper alloy artifacts. *Studies in Conservation* 45, 63-67.

Thickett, D. and Lee, L., 2004. *The Selection of Materials for the Storage or Display of Museum Objects*. London: The British Museum. British Museum Occasional Paper No. 111.

Thickett, D., Fletcher, P., Calver, A. and Lambarth, S., 2007. The effect of air tightness on RH buffering and control. In: T. Padfield, K. Borchersen, and M. Christensen (eds.), *Museum Microclimates: Contributions to the Copenhagen Conference, 19-23 November 2007.* Copenhagen: Nationalmuseet, 245-251.

Thickett, D., 2008. Presentation in original contexts via microclimates. In: D. Saunders, J. Townsend, and S. Woodcock (eds.), *Conservation and Access: Contributions to the London Congress 15-19 September 2008.* London: International Institute for Conservation of Historic and Artistic Works, 98-103.

Townsend, J.H. (ed.), 2002. *Conservation Science 2002: Papers from the Conference held in Edinburgh, Scotland, 22-24 May 2002*. London: Archetype Books.

Townsend, J.H. (ed.), 2008. *Conservation Science 2007: Papers from the Conference held in Milan, Italy 10-11 May 2007.* London: Archetype Publications.

Trentelman, K., Stodulski, L., Scott, D.A., Back, M., Stock, S., Strahan, D., Drews, A.R., O'Neill, A., Weber, W.H., Chen, A.E. and Garrett, S.J., 2002. The characterization of a new pale blue corrosion product found on copper alloy artifacts. *Studies in Conservation* 47, 4, 217-227.

Tsatsouli, K., 2004. *"Bronze disease": The Influence of Relative Humidity on Cuprous Chloride.* Unpublished Master's Thesis. Cardiff University. School of History and Archaeology, Cardiff, United Kingdom.

Turgoose, S., 1985. The corrosion of lead and tin: before and after excavation. In: G. Miles (ed.), *Lead and Tin: Studies in Conservation and Technology.* UKIC Occasional Papers no. 3, 15-26.

Ulmann, 2003. *Ullmann's Encyclopedia of Industrial Chemistry*. Vol. 1, Vol. 15. Weinheim: WILEY-VCH Verlag GmbH & Co.

Vander Voort, G.F. (ed.), 2004. *ASM Handbook Metallography and Microstructures, 9.* Materials Park, Ohio: ASM International.

Van Tasssel, R., 1945. Une Efflorescence d'Acetatochlorure de Calcium sur des Roches Calcaires dans des Collections. *Bulletin du Musee royal d'Histoire naturelle de Belgique,* 21, 26 (Dec.), Brussels, 11 pages.

Vine, M.G. and Hollinger, W.K., 1993. Active archival housing. *Restaurator* 14, 123-130.

Wadsak, M., Aastrup, T., Wallinder, I.O., Leygraf, C. and Schreiner, M., 2002. Multianalytical in situ investigation of the initial atmospheric corrosion of bronze. *Corrosion Science* 44, 4, 791-802.

Wang, Q., Huang, H. and Shearman, F., 2009. Bronzes from the sacred animal necropolis at Saqqara, Egypt: a study of the metals and corrosion. *The British Museum Technical Research Bulletin*, 3, 73-82.

Watson, R., 1789. *Chemical Essays,* 5. London.

Webster, 1949. *Webster's New International Dictionary of the English language*. Springfield (MA): G. and C. Merriam Company, Publishers.

Weierter, V. and Tate, J., 1993. The corrosion of "lead" communion tokens. In N.H. Tennent (ed.), *Corrosion Science in the United Kingdom*. London: James & James Science Publishers Ltd., 57-59.

Werner, A.E., 1967. Two problems in the conservation of antiquities: corroded lead and brittle silver. In: W.J. Young (ed.), *Application of Science in Examination of Works of Art: Proceedings of the Seminar, September 7-16, 1965.* Boston: Museum of Fine Arts, 96-99.

Werner, G. 1987. Corrosion of metal caused by wood in closed spaces. *Recent Advances in the Conservation and Analysis of Artifacts: Jubilee Conservation Conference Papers London 6-10 July 1987.* London: Summer Schools Press, 185-188.

Wheeler, G. S. and Wypyski, M., 1993. An unusual efflorescence on Greek ceramics. *Studies in Conservation* 38, 1, 55-62.

Wu, C., Yin, M., O'Brien, S. and Koberstein, J.T., 2006. Quantitative analysis of copper oxide nanoparticle composition and structure by X-ray Photoelectron Spectroscopy. *Chemistry of Materials* 18, 25, 6054–6058.

www.basf.com/detergents-formulators (Retrieved 12 August 2006)

Yaseen, M., 1981. Permeation properties of organic coatings in the control of metallic corrosion. In: H. Leidheiser (ed.), *Corrosion Control by Organic Coatings*. Houston: National Association of Corrosion Engineers, 24-27.